Synthesis and Reactivity of Cyclometallated Complexes containing Nitrogen Donor Ligands

Thesis Submitted for the Degree of

Doctor of Philosophy

By

Omar Khalid AL-Duaij

in the Department of Chemistry

at the

University of Leicester

June 2005

ProQuest LLC
789 East Eisenhower Parkway
P.O. Box 1346
Ann Arbor, MI 48106-1346

Title: Synthesis of Reactivity of Cyclometallated Complexes

Containing Nitrogen Donor Ligands

Author: Omar Khalid AL-Duaij

ABSTRACT

This thesis describes the synthesis and reactivity of cyclometallated complexes containing nitrogen donor ligands.

Chapter One introduces the general chemistry of cyclometallated complexes containing C,N-bidentate ligands, then describes the mechanism of cyclometallated complexes. This is followed by an overview of the applications of cyclometallated complexes.

Chapter Two provides an introduction to hemilability and reviews the synthesis of cyclopalladated complexes containing C,N,X tridentate ligands (X = N, S, O). The synthesis of new cyclopalladated imines containing oxygen-functionalised tethers is described. Coordination of the oxygen is shown to depend on i) the nature of the oxygen donor, ether, alcohol or phenol. ii) the length of the linker. iii) whether the complexes are neutral or cationic.

Chapter Three establishes the scope of acetate-assisted C-H activation for the synthesis of arene ruthenium and Cp*M (M = Ir, Rh) half-sandwich cyclometallated complexes with nitrogen-donor ligands *via* imine, amine, oxazoline and pyridine and with $P(OPh)_3$. The method can activate sp^2 C-H bonds of phenyl, pyrrole and thiophene, and one example of an sp^3 C-H bond. The method also allows N-H activation of a pyrrole-imine. Preliminary investigations of the mechanism are also described.

Chapter Four reports the reactivity of the cyclometallated half-sandwich complexes (synthesised in chapter three). Alkenes and CO provide simple substitution products. Alkynes are shown to insert regioselectivity into the M-C bond. In some cases subsequent C-C or C-N bond formation occurs to form carbocyclic or heterocyclic products. With PhC≡CH, insertion of two molecules can occur to give novel products. Throughout the thesis X-ray crystallography has been used to verify or identify some of the products (>40 structures).

This thesis is dedicated

To

My parents

Statement

This thesis is based on work conducted by the author, in the Department of Chemistry of the University of Leicester, during the period between October 2001 and September 2004.

All the work described in the thesis is original unless otherwise stated in the text or in the references. This work is not being presented for any other degree.

Signed:_____ Date:15/06/2005

Omar Khalid AL-Duaij

ACKNOWLEDGEMENTS

I wish to express my sincere gratitude to everyone who helped to make this thesis possible. First, my grateful appreciation is extended to my supervisor Dr. David Davies, for his invaluable supervision and advice throughout my study. His guidance and instruction made this study possible.

Second, I would like to thank Dr G.A. Griffith for the variable temperature and 2D NMR spectra and Dr G.A. Eaton for the mass spectra. Special thanks are due to Dr J. Fawcett for the X-ray structure determinations and doing some proof reading throughout the thesis' chapters. I really value his sincerity and patience.

Third, I would like to convey my sincerest gratitude to all friends in the Department of Chemistry at the University of Leicester.

Finally, I would like to express my deepest gratitude to my wife and children for their support during my study. I promise to compensate them for the intermittent periods when they went without husband and father.

Abbreviations and Symbols

General and Physical

Atm	=	Atmosphere
br s	=	broad singlet
COSY	=	correlated spectroscopy
d	=	doublet
dd	=	doublet of doublets
dt	=	doublet of triplets
δ	=	chemical shift
°	=	degrees
ES-MS	=	electrospray mass spectrometry
FAB-MS	=	fast atom bombardment mass spectrometry
h	=	hour
hυ	=	Irradiation
Hz	=	Hertz
IR	=	Infrared
K	=	Kelvin
m	=	multiplet
min	=	minute
nOe	=	nuclear Overhauser enhancement
NOESY	=	nuclear Overhauser enhancement spectroscopy
NMR	=	nuclear magnetic resonance
ppm	=	parts per million
q	=	quartet
RT	=	room temperature
s	=	singlet
sept.	=	septet
t	=	triplet
UV	=	Ultraviolet

Chemical

AcOH	=	Acetic Acid
BF_4	=	Tetrafluoroborate

Bn	=	benzyl
bipy	=	2,2'-bipyridine
^{n}Bu	=	n-Butyl
^{t}Bu	=	t-Butyl
C_2H_4	=	Ethene
CH_2Cl_2	=	Dichloromethane
CO	=	Carbon monoxide
COD	=	cyclooctadiene
Cp	=	cyclopentadienyl anion
CpH	=	cyclopentadiene
Cp*	=	pentamethyl-cyclopentadienyl anion
DMSO	=	Dimethylsulphoxide
dba	=	Dibenzylideneacetone
dpa	=	1,2-diphenylethylenediamine
dppe	=	1,2-bis(diphenylphosphino)ethane
dppp	=	1,2-bis(diphenylphosphino)propane
d.e.	=	diastereomeric excess
e.e.	=	enantiomeric excess
Et	=	Ethyl
EtCN	=	Propionitrile
Et_3N	=	Triethylamine
EtOH	=	Ethanol
$HC{\equiv}CCO_2Et$	=	Ethyl propiolate
LiCl	=	Lithium Chloride
m	=	meta
Me	=	methyl
MeCN	=	acetonitrile
MeOH	=	methanol
mes	=	1,3,5-trimethylbenzene (mesitylene)
$MgSO_4$	=	Magnesium sulphate
o	=	Ortho
OAc	=	acetate
OMe	=	Methoxy
OTf	=	triflate

oxaz	=	oxazoline
p	=	Para
PF_6	=	Hexafluorophosphate
Ph	=	Phenyl
$PhC{\equiv}CCO_2Et$	=	Ethyl phenylpropiolate
$PhC{\equiv}CH$	=	Phenylacetylene
$PhC{\equiv}CPh$	=	Diphenylacetylene
PhCN	=	Benzonitrile
$P(Me)_3$	=	Trimethylphosphine
$P(OPh)_3$	=	Triphenylphosphite
PPh_3	=	Triphenylphosphine
^{i}Pr	=	isopropyl
py	=	pyridine
p-cy	=	4-isopropyl-toluene
p-TSA	=	Toluene sulphonic acid
SbF_6	=	Hexafluoroantimonate
THF	=	tetrahydrofuran

List of Contents

Chapter One:

General Introduction

Chapter One – General Introduction

1.1 Cyclometallated Complexes

The chemistry of cyclometallated complexes is one of the most advanced areas of modern organometallic chemistry. Cyclometallated complexes have attracted much attention in the past two decades because of their use in such diverse areas as catalysis, organic synthesis, asymmetric synthesis and photochemistry (see **Section 1.5**), and the area has been the subject of several reviews.[1-8]

The term "cyclometallation" was introduced by Trofimenko[9] to describe those reactions of transition metal complexes in which a ligand undergoes an intramolecular metallation with formation of a chelate ring containing a metal-carbon bond and a metal-donor atom bond (**Fig. 1.1**). This chapter describes the synthesis, mechanism and application of cyclometallated compounds, concentrating on those with X = N (**Fig. 1.1**).

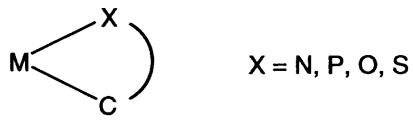

Fig. 1.1

In 1963 Kleinman and Dubeck[10] reported the first cyclometallated complex (**1.1**) formed by the reaction of azobenzene with nickelocene. This compound was found to be monomeric, soluble in organic solvents and stable in air. Subsequently azobenzene has been extensively employed in the formation of other metal aryl σ-bonds, thus, Cope and Siekman described the dimer (**1.2**).[11] Related compounds (**1.3**) have been formed from N,N-dimethylbenzylamine.[12, 13]

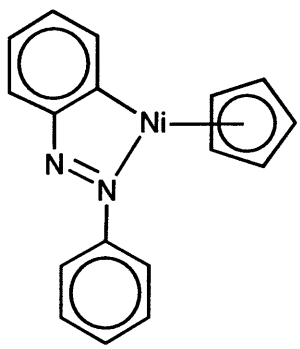

(1.1)

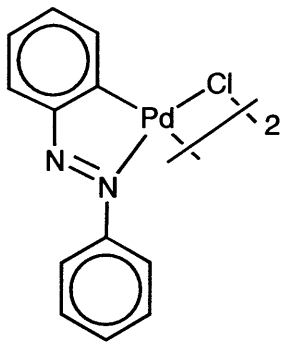

(1.2)

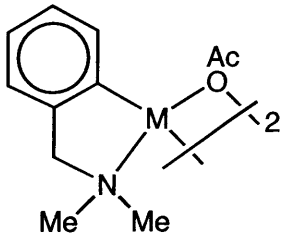

M = Pd, Pt

(1.3)

1.2 Methods of synthesis of cyclometallated complexes with C,N-bidentate ligands

Cyclometallated complexes containing C,N-bidentate ligands can be obtained by a variety of methods.[1-5, 7, 8, 14, 15] the most common of which are C-H activation, oxidative addition and transmetallation. However ligand exchange,[16-18] nucleophilic attack[19] and insertion reactions[20-22] have also been used. The insertion method will be considered under reactivity of cyclometallated complexes (see **Chapter 4**), the other methods are summarised below.

C–H Activation

The most attractive and fundamental route to cyclometallated compounds is direct activation of C–H bonds[7]; an example of a C,N-bidentate cyclometallated complex formed via C-H bond activation is shown in **Scheme (1.1)**.[23] Further examples of N-donor ligands that can form cyclometallated compounds by C-H bond activation are described in **Section 1.3**.

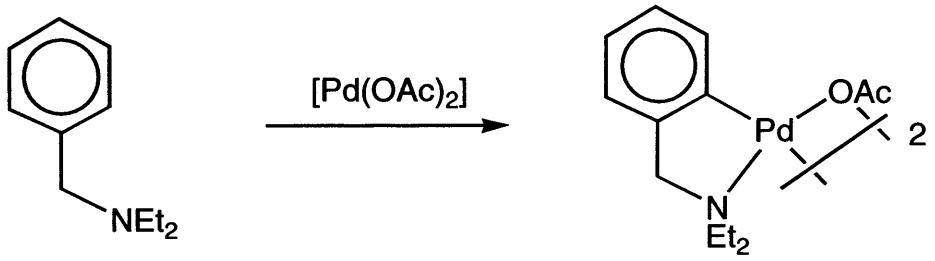

(Scheme 1.1)

Oxidative Addition

Activation of carbon-halogen bonds by low-valent metal species such as Ir^{I}, Ni^{0}, Pd^{0} and Pt^{0} provides a good method to synthesize cyclometallated complexes. For example, the oxidative addition of 2-chlorobenzylideneaniline **(1.4)** to $Pd(dba)_2$ gives cyclometallated complex **(1.5)**, as shown in **Scheme (1.2)**.[24]

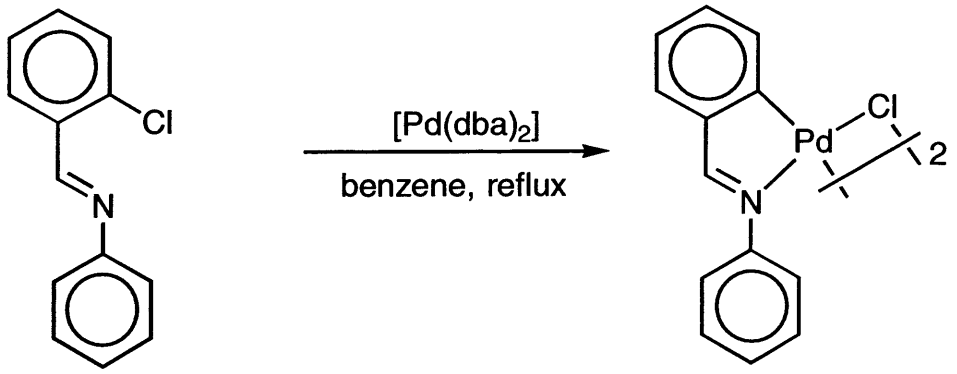

(1.4) **(1.5)**

(Scheme 1.2)

This method of synthesising C,N-cyclometallated complexes works mainly with d^{10}, d^8, or d^6 metal precursors such as $[Pd_2(dba)_3]$[25], $M_3(CO)_{12}$,[26] (M = Ru, Fe) and $[W(CO)_3(EtCN)_3]$[27] respectively. The reaction of $[W(CO)_3(EtCN)_3]$ with fluorinated ligand **(1.6)** yields cyclometallated complex **(1.7)** **(Scheme 1.3)**.

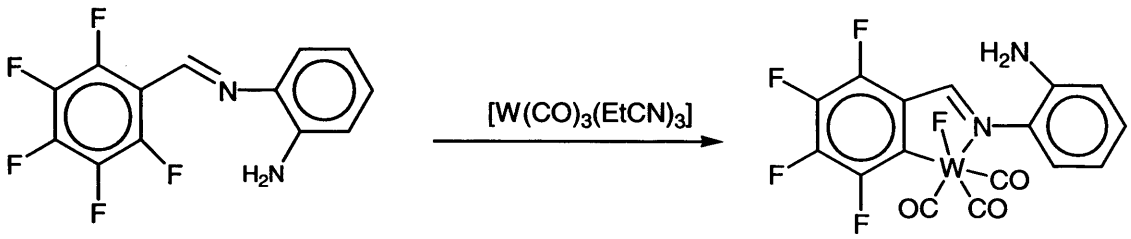

(1.6) **(1.7)**

(Scheme 1.3)

Transmetallation

The transmetallation reaction is one of the most powerful methods to synthesize cyclometallated compounds that cannot be obtained by direct cyclometallation.[8] In this method, an organometallic compound of lithium, tin, zinc, mercury or manganese reacts with a metal halide to form a cyclometallated complex. Examples of transmetallation reactions using an organomercury[28] or organolithium[29] reagent are shown in **Scheme 1.4**.

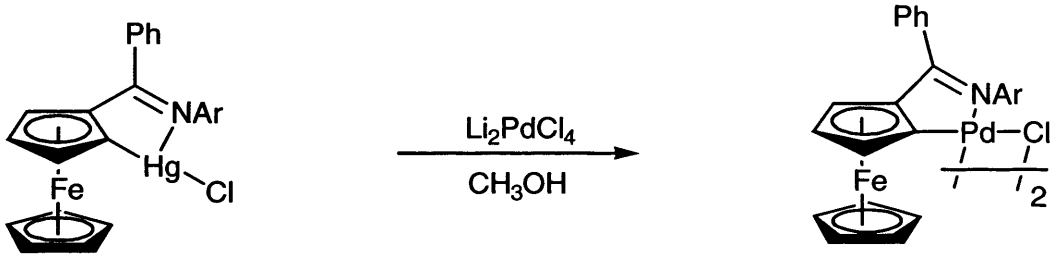

(1.8) **(1.9)**

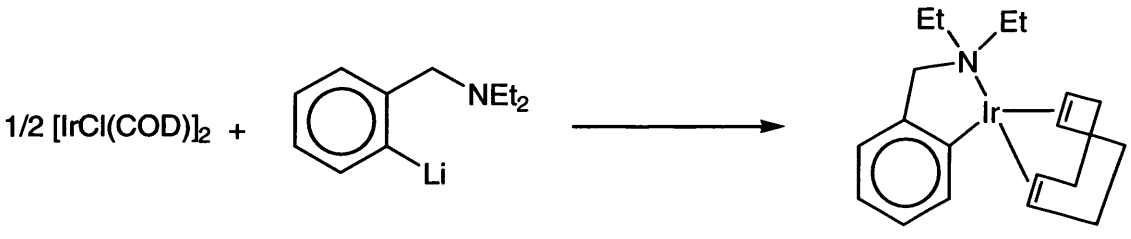

(1.10)

(Scheme 1.4)

Ligand exchange

Some cyclometallated complexes have been generated via ligand exchange, including cyclopalladated derivatives of azobenzene, benzylideneaniline, 8-methylquinoline (**Scheme 1.5**).[15], benzylpyridine (**Scheme 1.6**),[14] as well as N, N-dimethyl-4-nitrobenzylamine which is not available by other methods.[13]

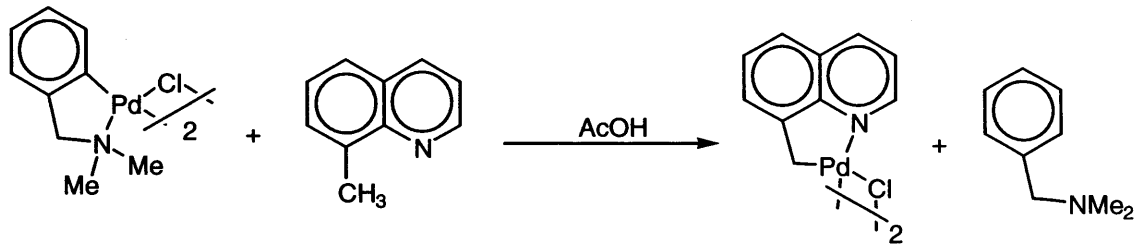

(1.11) **(1.12)**

(Scheme 1.5)

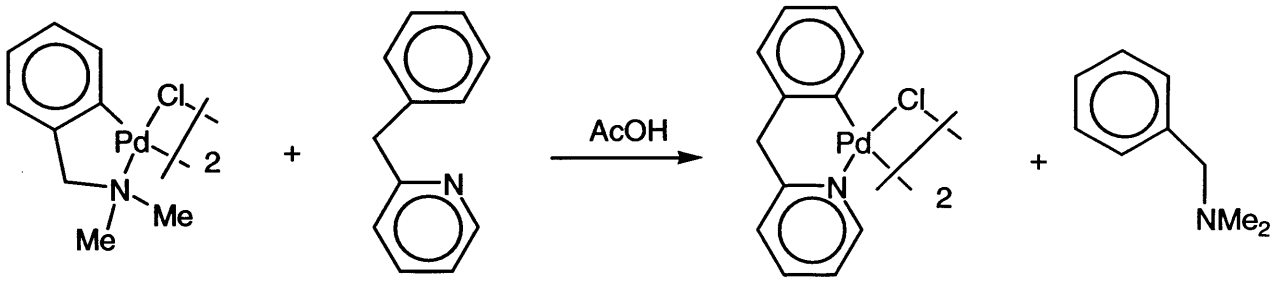

(1.11) **(1.13)**

(Scheme 1.6)

Nucleophilic attack on coordinated alkene

Holton and Kjonaas[19] have synthesized a five-membered ring palladacycle (**1.15**) by nucleophilic attack on a coordinated olefin (**Scheme 1.7**).

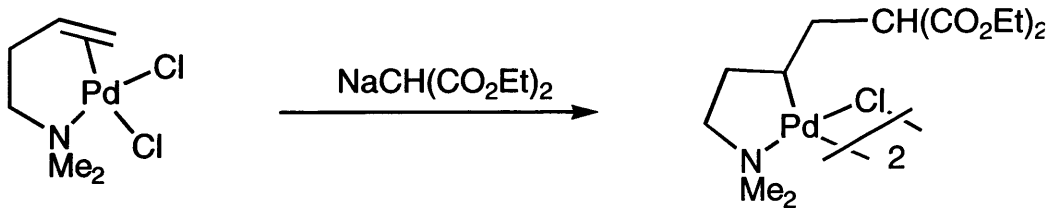

(1.14) **(1.15)**

(Scheme 1.7)

1.3 C,N-bidentate Cyclometallated Complexes formed by C-H activation

A wide variety of cyclometallated complexes containing C,N-bidentate ligands with different metals and forming different ring sizes have been made by C-H activation. These can be classified into groups based on the type of nitrogen donor atoms.

1.3.1 Amines

A large number of cyclometallated amine complexes have been reported the vast majority involve activation of an aromatic C-H bond.[1-7] Examples containing a five **(1.11)**[30] and a six-membered ring **(1.16)**[30] are shown in **Scheme 1.8**. Activation of sp^3 C-H bonds is also possible *e.g.* formation of **(1.17)**[31] **(Scheme 1.9)**.

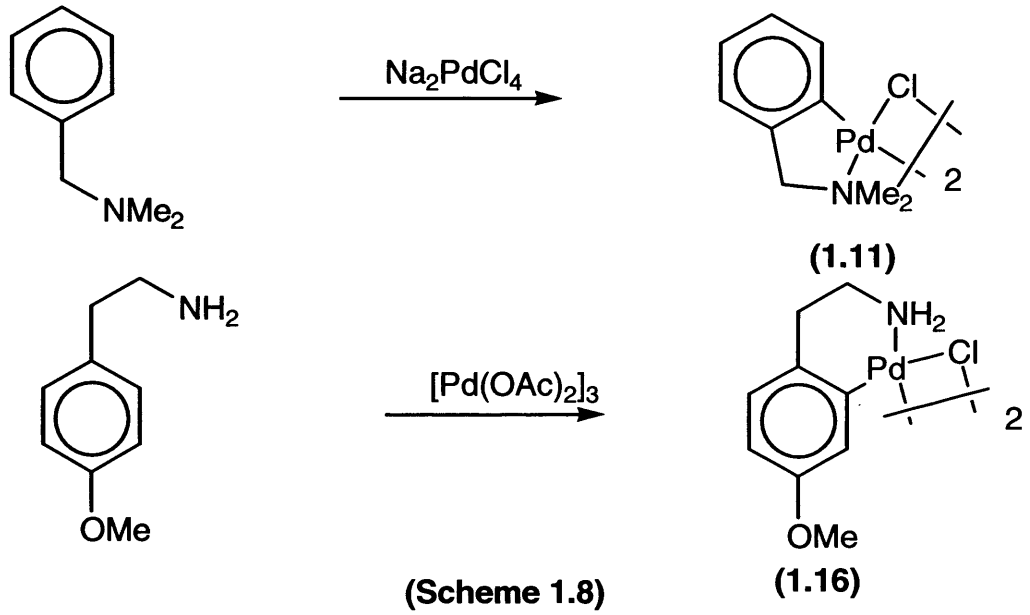

(Scheme 1.8)

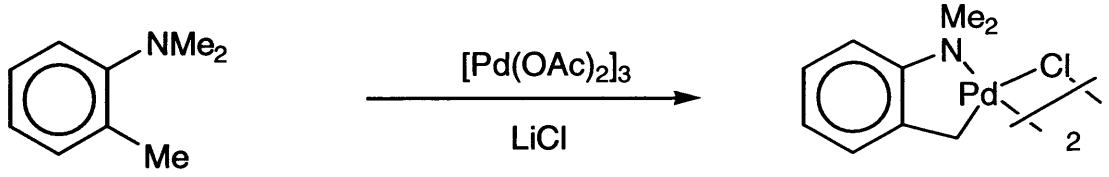

(1.17)

(Scheme 1.9)

Ferrocenylamine ligands can also react to give C,N-bidentate cyclometallated complexes in high yield[8], e.g. synthesis of **(1.19)** as shown in **Scheme 1.10**.[32]

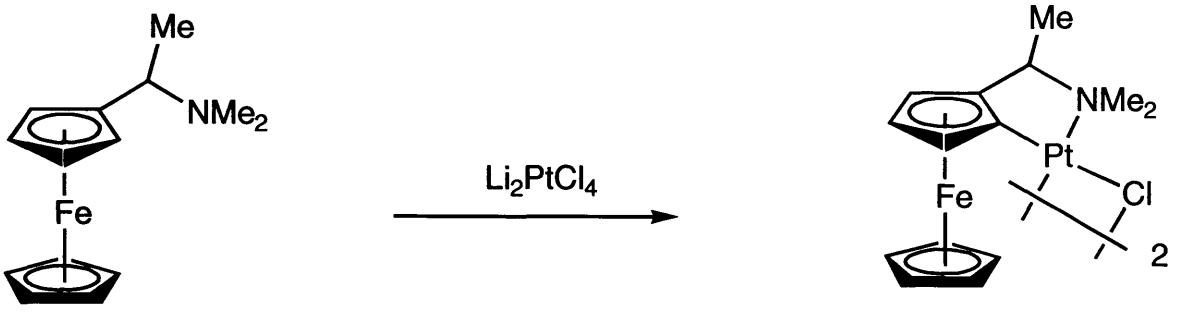

(1.18) **(1.19)**

(Scheme 1.10)

Dimeric palladacyclic complexes may exist as *syn* or *anti* isomers as shown in **Fig. 1.2.**

anti **X = OAc, Cl, Br** ***syn***

(Fig. 1.2)

Early work suggested these complexes exist only as the anti isomer, however, Ryabov *et al.*[33] reported that the dimers **(1.11)** and **(1.20)** are a mixture of *anti* and *syn* isomers as determined by ^{1}H NMR spectroscopy (see **Chapter 2**).

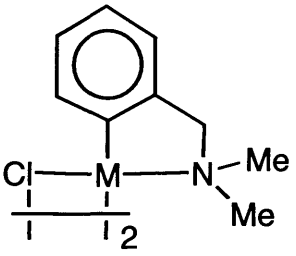

(1.11) M = Pd
(1.20) M = Pt

1.3.2 Imines

Imines derived from benzaldehyde afford many kinds of C,N-bidentate cyclometallated complexes, having five or six-membered rings, by C-H activation of an aromatic or aliphatic C-H bond. Molnar and Orchin[34] first reported the reaction of imine **(1.21)** with $PdCl_2(PhCN)_2$ to form **(1.5)** in 1969 **(Scheme 1.11).**

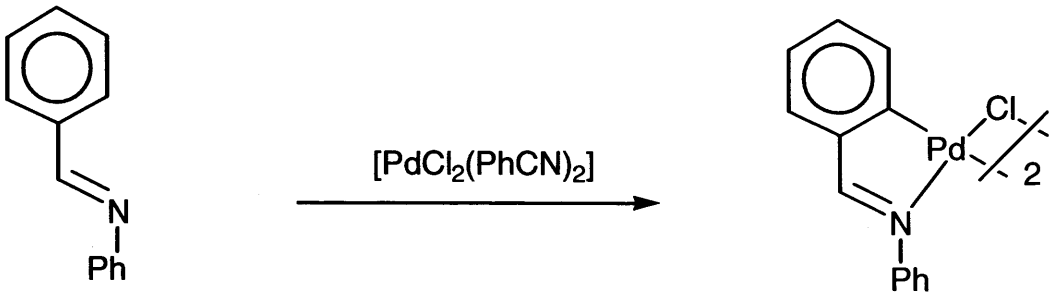

(1.21) **(1.5)**

(Scheme 1.11)

Benzaldehyde imines also react with $[Pd(OAc)_2]_3$ to give acetate-bridged dimers (**1.23**) which can be converted to the corresponding chloro- and bromo-bridged dimers (**1.24**) by addition of NaX (X = Cl, Br) (**Scheme 1.12**).[12]

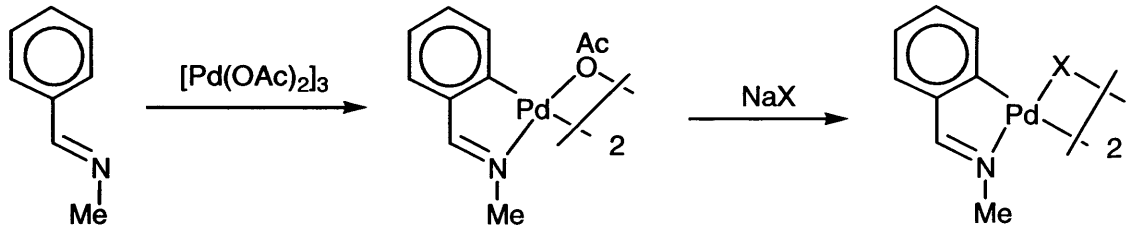

(1.22) **(1.23)** **X = Cl, Br** **(1.24)**

(Scheme 1.12)

In general, a strong tendency to form five-membered metallacycles and preferential activation of aromatic (ortho aryl position) over aliphatic C-H bonds is widely accepted[2, 4, 6, 7], an example is shown in **Scheme 1.13**.[35] However, if the ortho aryl position is blocked aliphatic C-H bond activation can occur to form a six-membered ring cyclometallated complex (**1.28**) as shown in **Scheme 1.14**.[35]

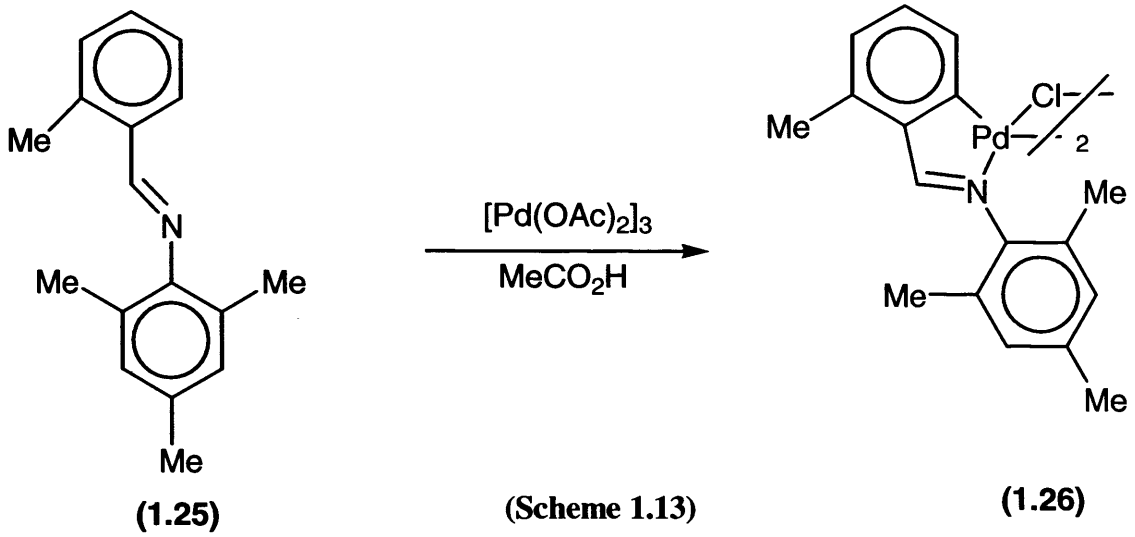

(1.25) (Scheme 1.13) (1.26)

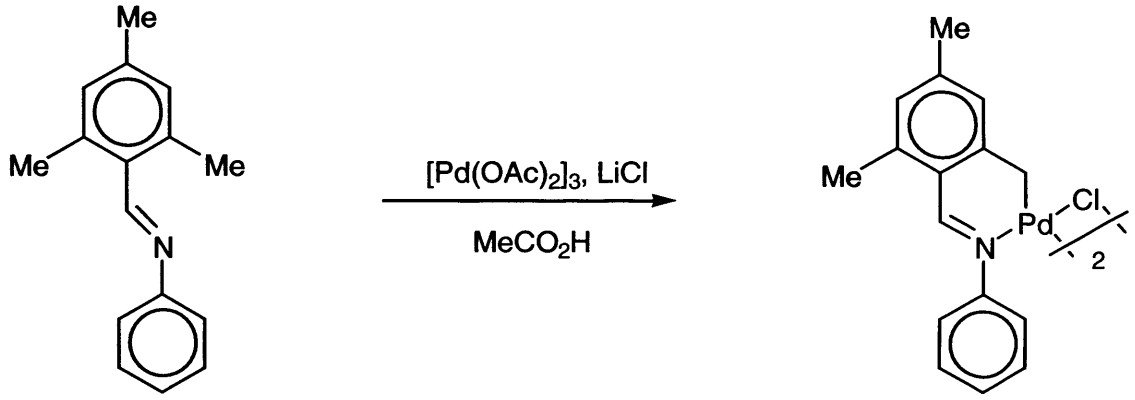

(1.27) (1.28)

(Scheme 1.14)

Imines can have two isomeric forms (E or Z), which can give rise to different cyclometallated derivatives as shown in **Fig. 1. 3**.

(E-form) (Z-form)

(Fig. 1. 3)

Both *endo* and *exo* cyclometallated compounds can be obtained from the E-form whereas only *exo* derivatives are possible from the Z-form. In the case of the E-isomer, the *endo* cyclometallated complexes are preferred;[36-39] for example formation of **(1.30)**[35] **(Scheme 1.15)**. Substituent groups on the aromatic rings can also control *exo* and *endo* selectivity. Thus, *exo* complexes can be obtained from an E imine if the ortho positions to form an *endo* ring are blocked in the E form *e.g.* **(1.31) (Scheme 1.15)**.[35]

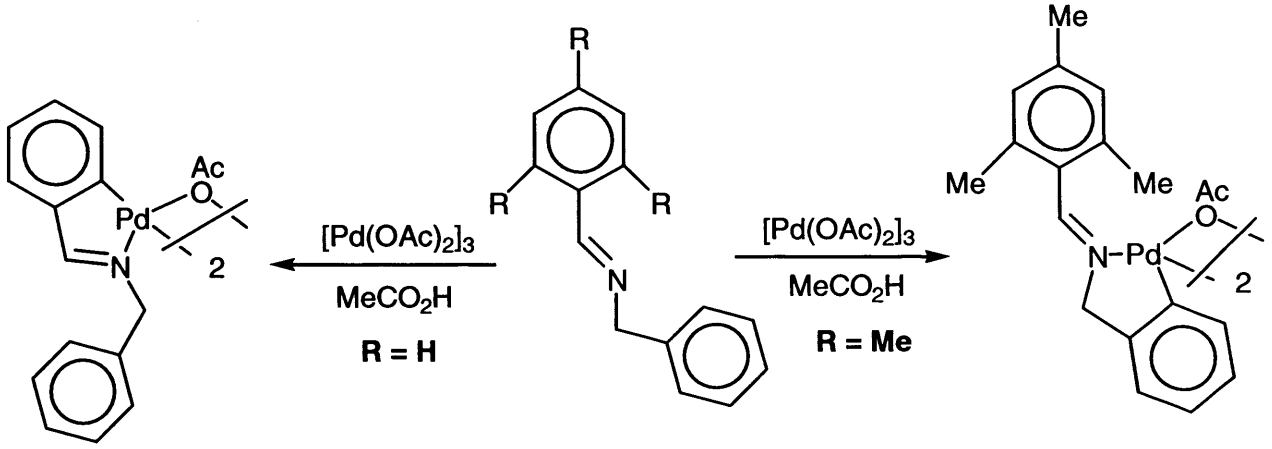

(1.30) **(1.29, R = H, Me)** **(1.31)**

(Scheme 1.15)

Examples of cyclometallated ferrocene derivatives *e.g.* **(Scheme 1.16)**[40] have increased considerably during the last two decades due to the wide variety of interesting and novel applications.

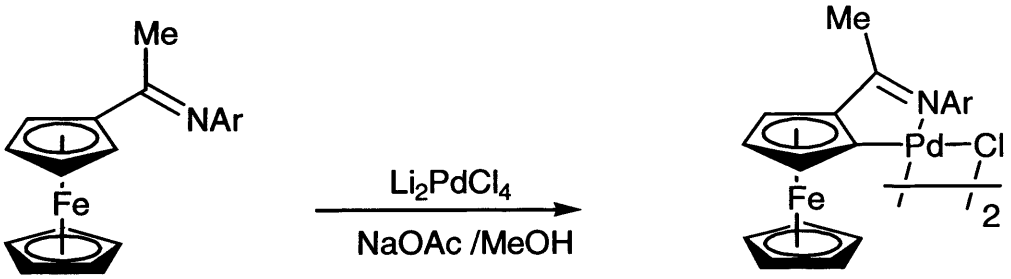

(1.32) **(Scheme 1.16)** **(1.33)**

Diimines can afford double cyclometallation, thus, diimine with $[Pd(OAc)_2]_3$ to gives the double cyclometallated complex **(1.34)**.[41]

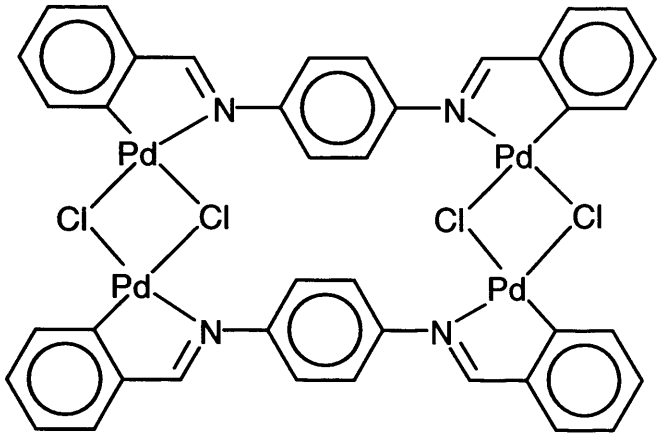

(1.34)

1.3.3 Oxazolines

As found in imines, oxazoline ligands have a C=N bond, which can form *endo* and *exo* metallacycles and the *endo* metallacycle is favoured. Thus, cyclometallation of **(1.35, R = Ph)** gives *endo* metallacycle **(1.36)**. However for **(1.35, R = Me)**, formation of an *endo* metallacycle is not possible and cyclometallation requires harsher condition to form the *exo* product **(1.47)** **(Scheme 1.17)**.[42]

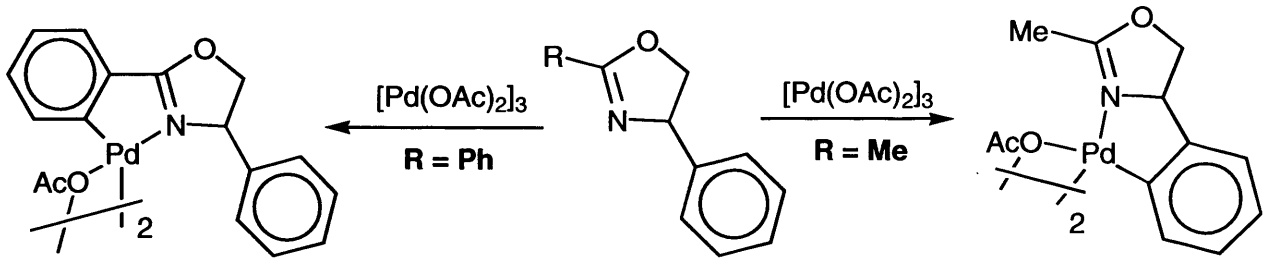

(1.36) **(1.35, R= Ph, Me)** **(1.37)**

(Scheme 1.17)

Cyclopalladation of ozaxolines can also occur via activation of an aliphatic C-H bond in the formation of **(1.38)**[43]. Ferrocenyloxazolines also undergo cyclometallation in good yield *e.g.* **(1.39)** which contains both planar and carbon-based chirality and has been used as a enantioselective catalyst for rearrangement of allylic N-aryl benzimidates.[44]

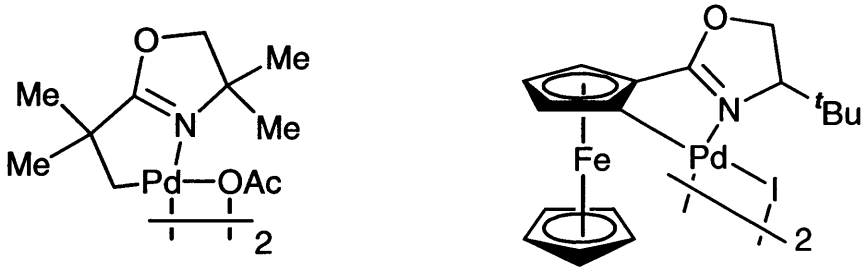

(1.38) **(1.39)**

1.3.4 Pyridine derivatives

Five-membered ring bidentate (**1.40**) and C,N,C-tridentate (**1.41**) cyclometallated complexes can be formed from 2,6-diphenylpyridine (**Scheme 1.18**).[45]

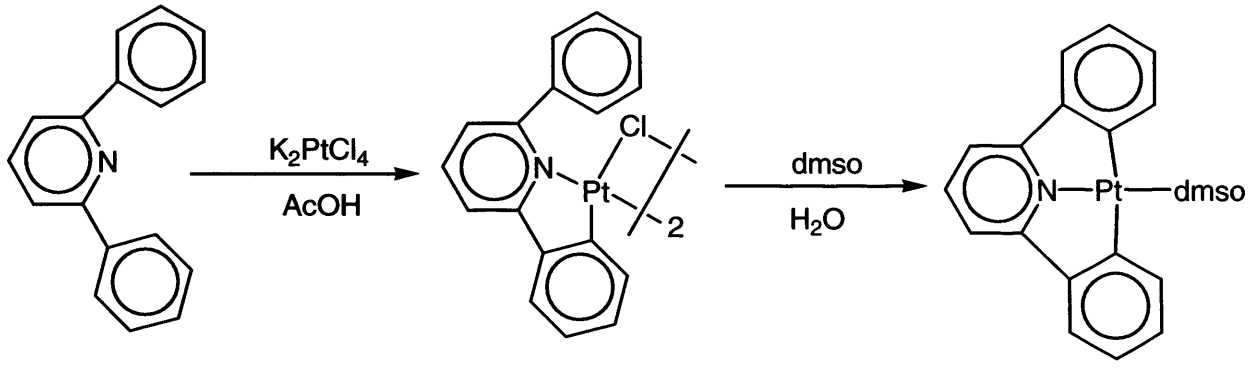

(1.40) **(1.41)**

(Scheme 1.18)

Tridentate cyclometallated complexes with a monoanionic NNC coordination can also be made *e.g.* (**1.42**).[46] Substituted pyridines have also been used as a chelates for activation of sp^3 atoms *e.g.* (**1.43**).[47]

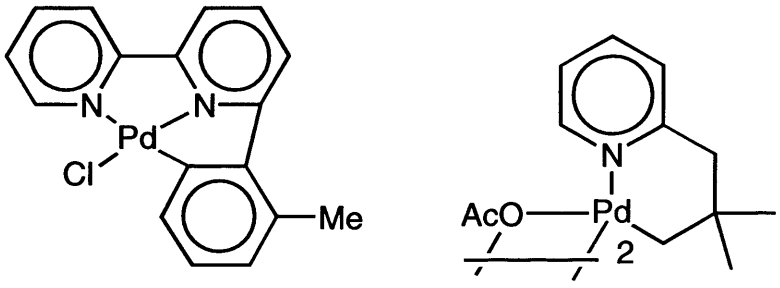

(1.42) **(1.43)**

1.3.5 Other C, N-bidentate cyclometallated complexes

Cyclometallated complexes of other N-donor ligands include azobenzenes (**1.44**),[23] oximes (**1.45**),[48] and hydrazones (**1.46**)[49] as shown in (**Fig. 1.4**).

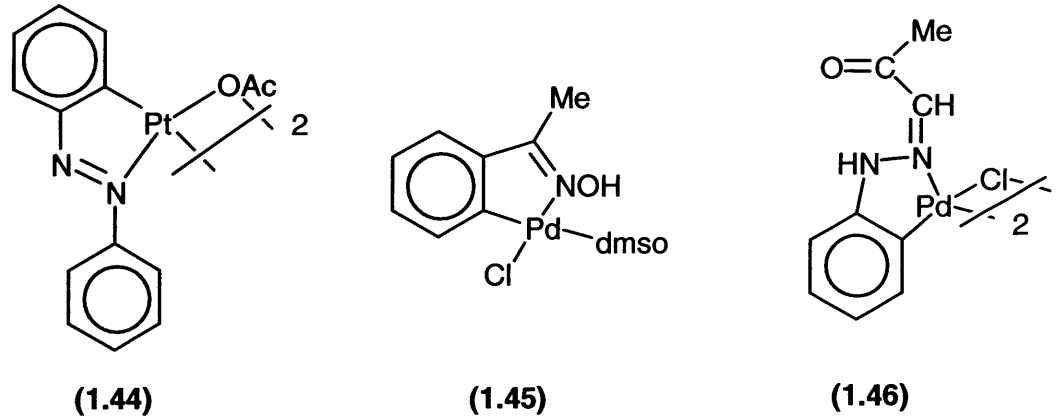

(1.44) **(1.45)** **(1.46)**

(Fig. 1.4)

1.3.6 C, N-bidentate complexes from cyclometallation of heterocyclic rings

So far all the examples discussed have involved activation of a phenyl C-H or an aliphatic C-H bond, heterocyclic sp^2 C-H bonds can also be activated *e.g.* pyrrole (**1.47**)[50] and thiophene (**1.48**)[51] and (**1.49**).[52]

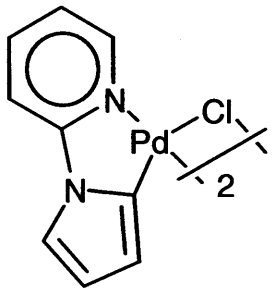

(**1.47**)

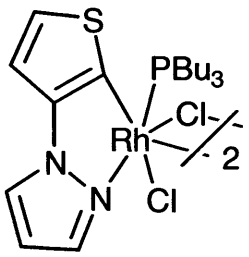

(**1.48**)

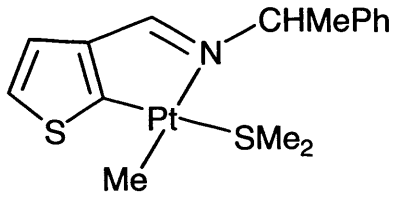

(**1.49**)

1.4 Mechanism of Activation of the C-H bond

As mentioned above (**Section 1.2**) cyclometallated complexes can be made by many different methods, however this thesis will focus on the C-H activation method. C-H activation by metal complexes is an area of much current interest,[53, 54] and there are three generally accepted mechanisms, nucleophilic (oxidative addition), electrophilic activation and σ-bond metathesis. Ryabov[7] suggested that if the metal ends up σ bonded to the carbon of highest electron density, the cyclometallation is an electrophilic mechanism, but if it is to the most electron-deficient, the pathway is nucleophilic *i.e.* oxidative addition and he said "generally, the discrimination between the mechanistic pathways (nucleophilic and electrophilic pathways) appears to be rather complicated and is also a problem in cyclometallation" .[7]

1.4.1 Nucleophilic mechanism

Bergman *et al.*[55, 56] have demonstrated intermolecular oxidative addition (Ir^I to Ir^{III}) (**Scheme 1.19**). Thus, irradiation of [$IrH_2(PMe_3)Cp^*$] led to rapid loss of H_2 *via* (**1.50**), which was proposed to undergo oxidative addition of the C-H bond, via a three-centre transition state (**1.51**), to give the Ir^{III} product (**1.52**).[57]

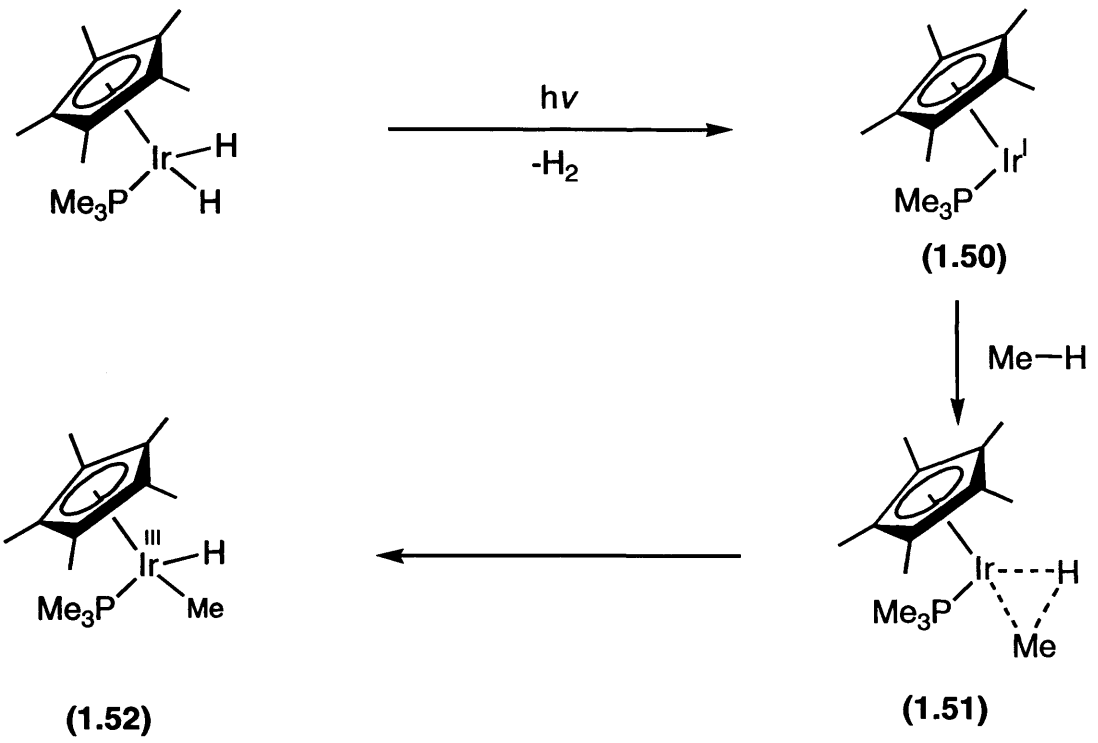

(Scheme 1.19)

The electron-donating Cp* and PMe_3 group provide the electron-rich metal centre necessary for oxidative addition. In early work, many metal complexes were shown to activate the strong arene C-H bond (110 Kcal/mol) but not the weaker alkane C-H bond (96-102 Kcal/mol).[58] However, oxidative addition of alkanes has been reported, *e.g.* Bergman *et al.*[59] demonstrated activation of cyclohexane **(Scheme 1.20)**.

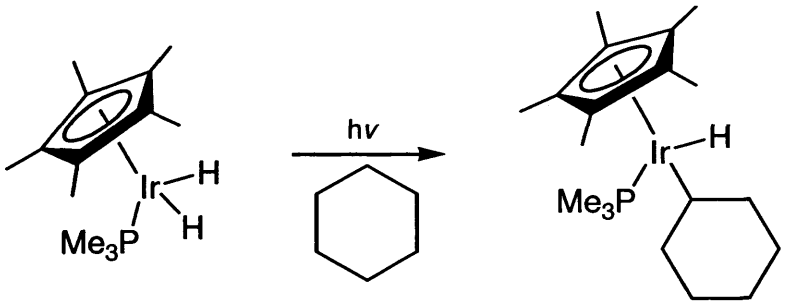

(Scheme 1.20)

In later work, Bergman *et al.* described the C-H activation reactions of [IrMe(PR$_3$)(OTf)Cp*] **(1.53)** with alkanes under mild conditions,[60] and proposed two possible mechanisms **(Scheme 1.21)**, **(a)** a nucleophilic pathway via oxidative addition, proceeding through Ir(V) intermediate **(1.54)**, then reductive elimination; or pathway **(b)** σ-bond metathesis through intermediate **(1.55)**, then elimination of methane to form **(1.56)**. Both mechanisms require dissociation of OTf to create a 16-electron species **(A)** with a vacant site on the metal. Theoretical studies support an oxidative addition mechanism.[61]

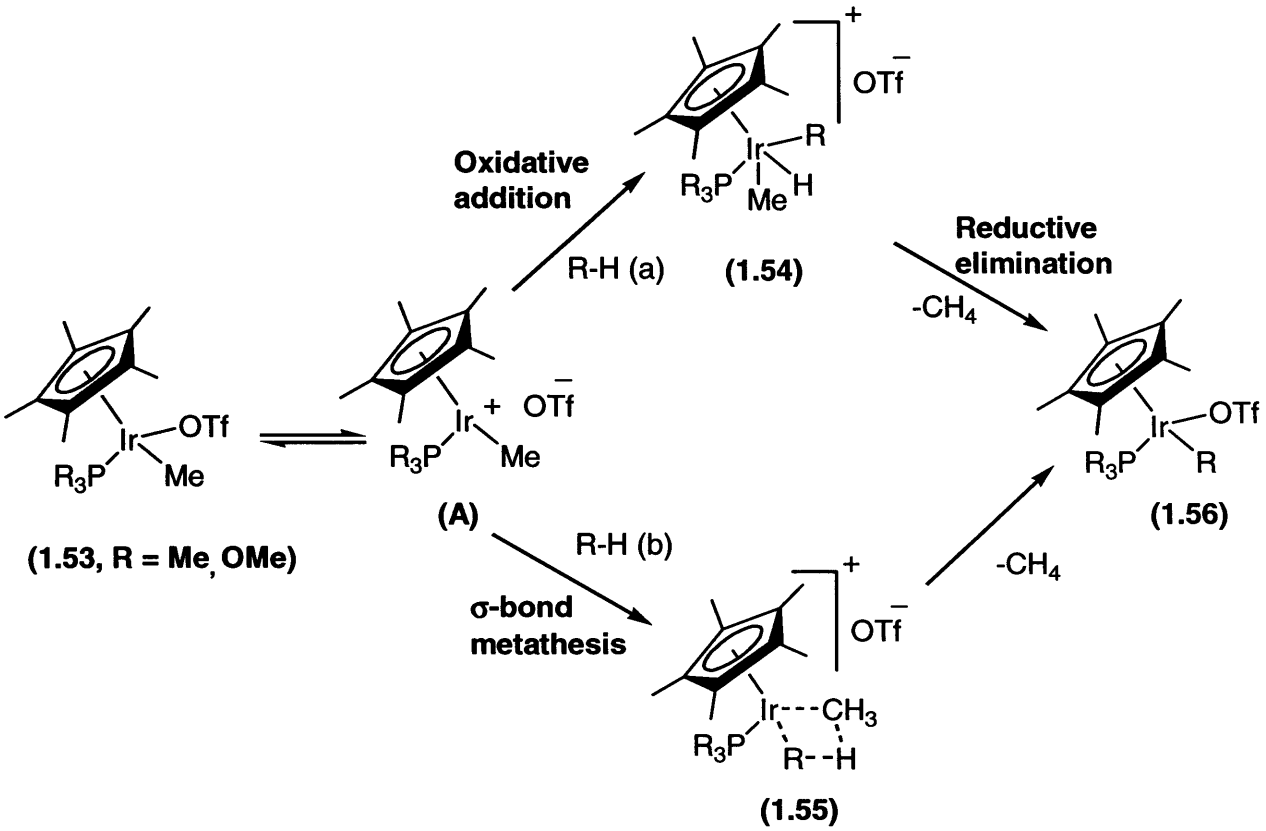

(Scheme 1.21)

Bergman[62] also showed that cationic Ir^{III} and Rh^{III} complexes **(1.57-1.60),** formed by reaction of $[M(Me)(PR_3)ClCp^*]$ (M = Ir, Rh, R = Me, OMe) with $NaBAr_4$ [Ar = 3,5-$C_6H_3(CF_3)_2$] in CH_2Cl_2. These contain a weakly bonded CH_2Cl_2, which dissociates more easily than triflate from **(1.53),** to form a 16-electron species **(B)** which undergoes C-H activation with benzene **(Scheme 1.22).**[63]

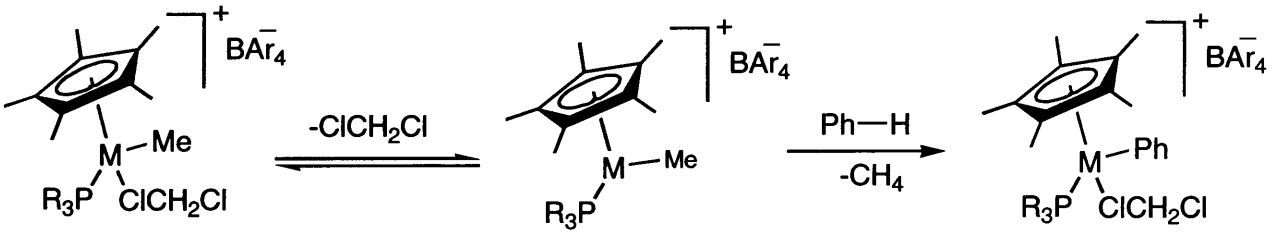

(1.57, M = Ir, R=Me)
(1.58, M = Ir, R= OMe)
(1.59, M = Rh, R= Me)
(1.60, M = Rh, R= OMe)

(B)

(Scheme 1.22)

A kinetic study of these reactions showed that Ir-complex (**1.58**) with the electron-withdrawing $P(OMe)_3$ on the metal reacts (30 times) slower than the more electron-rich PMe_3-containing complex (**1.57**). However for the corresponding Rh complexes (**1.59**) and (**1.60**) the rates are about the same and about 10^3 times slower than (**1.57**). Tolualdehyde easily displaces CH_2Cl_2 from (**1.59**) and (**1.60**) to form (**1.61**) and (**1.62**) which are more stable to dissociation, hence show lower rates of C-H bond activation (**Scheme 1.23**). Treatment of (**1.60**) with excess tolualdehyde (25-50 equivalents) results in immediate formation of (**1.62**) which after 4 days gives C-H activation product (**1.63**) as the major species.

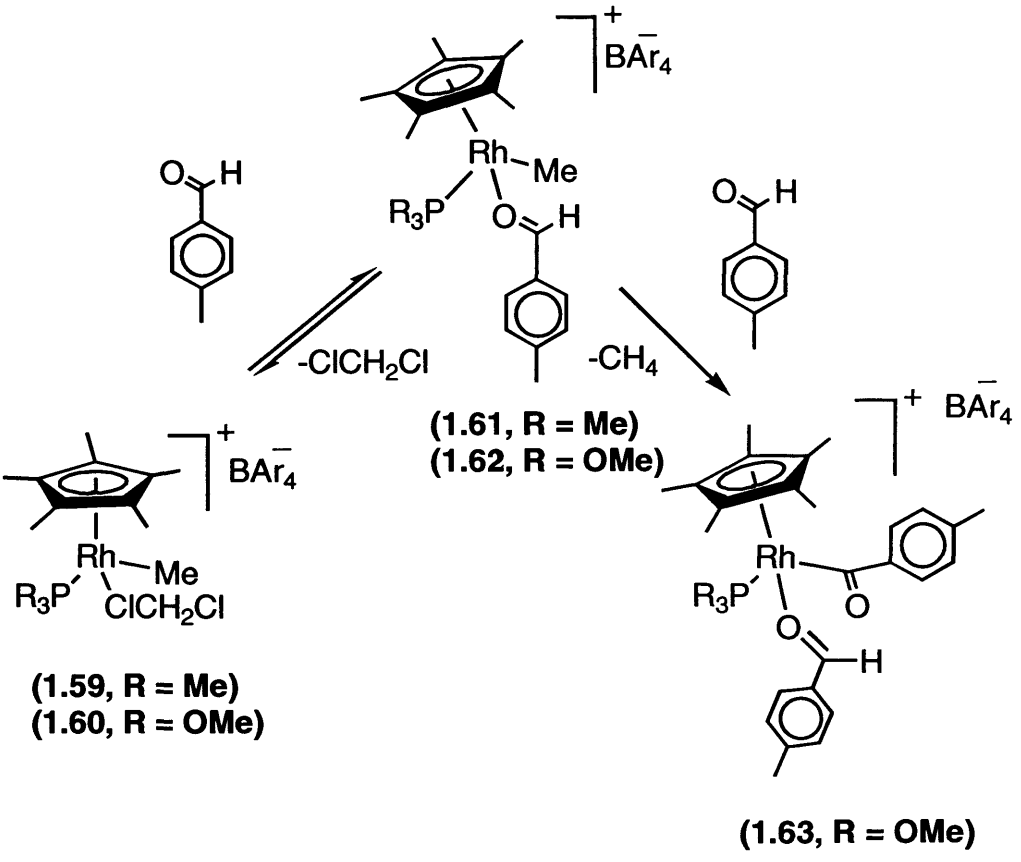

(Scheme 1.23)

Overall, Bergman's results show that the rate of C-H activation reactions of Ir^{III} and Rh^{III} complexes depends on:

1) Creation of a vacant site by dissociation of OTf^-, CH_2Cl_2 or aldehyde. Dissociation of CH_2Cl_2 is easier than OTf^- or an aldehyde groups and leads to an increase in the rate of C-H bond activation.

2) The donor properties of the PR_3 ligand; an electron-donating group (PMe_3) increases the rate compared with an electron-withdrawing $P(OMe)_3$ group with iridium. This may be due to making the dissociation step easier (see above) and / or making oxidative addition easier if the C-H activation step is nucleophilic. The donor properties of PR_3 seem to have little effect in the Rh case. Note, if the dissociation is the rate determining step the effect of PR_3 on rate gives no information about the C-H activation step.

3) The nature of the metal; the Ir complexes have a faster rate than the Rh complexes.

Examples of some cyclometallated complexes formed via a nucleophilic pathway are shown in **Scheme 1.24.**[57, 64]

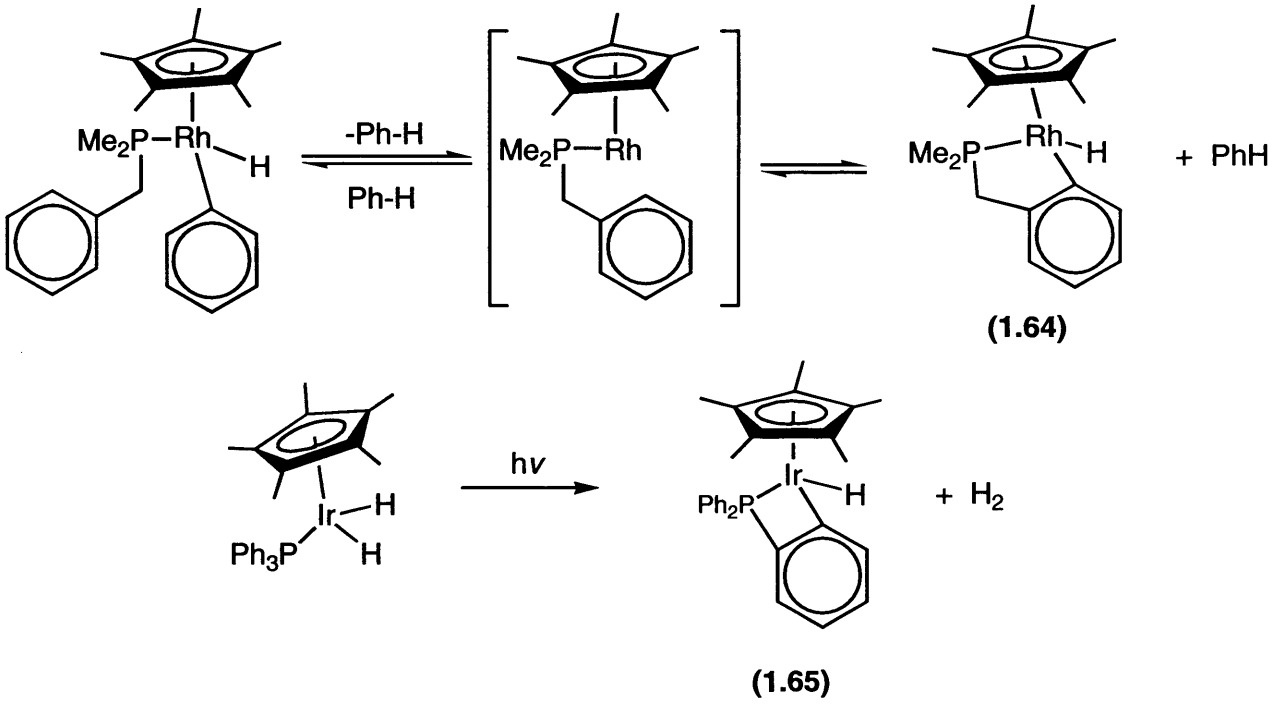

(Scheme 1.24)

1.4.2 Electrophilic mechanism

As mentioned by Ryabov, the electrophilic mechanism is thought to occur when an electron-poor metal ends up bound to the carbon of highest electron density. Most cyclopalladations with Pd^{2+} starting materials are believed to go via this mechanism. The proposed mechanism for electrophilic C-H activation of N,N-dimethylbenzylamine by $[Pd(OAc)_2]_3$ is shown in **(Scheme 1.25).** [65, 66]

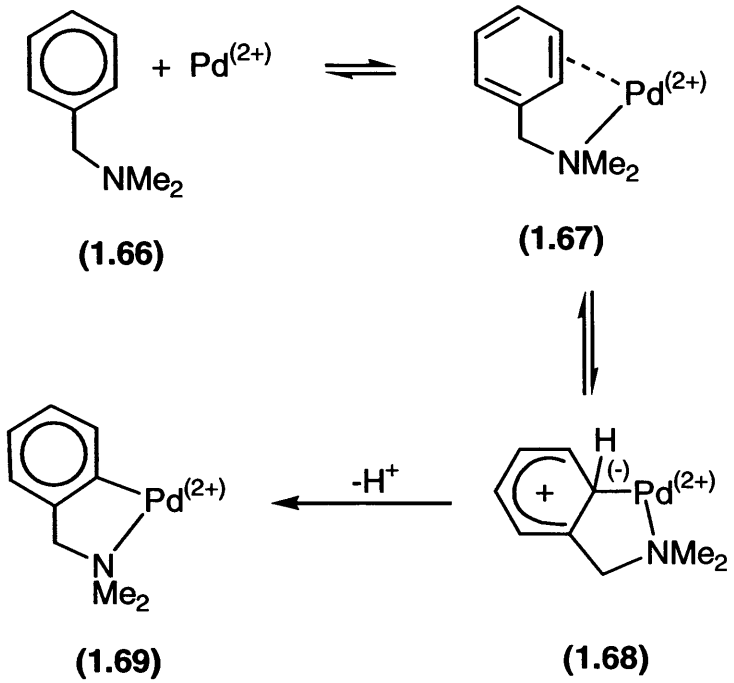

(1.66) **(1.67)** **(1.68)** **(1.69)**

(Scheme 1.25)

Electrophilic attack on the arene may be initiated *via* an η^2-interaction **(1.67)** to give the areneonium species **(1.68)**, followed by loss of H^+ to afford **(1.69)**. Ryabov[66] made a detailed kinetic study of the reaction and suggested a sterically congested transition state **(1.70)** involving acetate-assisted intramolecular deprotonation. Ryabov found that kinetically this step is electrophilic since the rate constants progressively increase as the donor strength of the ring substituents in N,N-dimethylbenzyl amines increases (*e.g.* 4-Cl < 4-OMe < 4-H < 4-Me < 3,4-$(OMe)_2$). Gomez[35] studied the mechanism of the cyclometallation of imines by $[Pd(OAc)_2]_3$ and suggested a similar process but with a four-membered transition state **(1.71).**

(1.70) **(1.71)**

1.4.3 σ-Bond metathesis mechanism

As mentioned before, oxidative addition requires an electron-rich metal, while σ-bond metathesis tends to be observed with highly electrophilic (d^0) metal centres which are unable to undergo oxidative addition. Watson *et al.*[67] described the σ bond metathesis mechanism for the exchange of $^{13}CH_4$ with the methyl group of **(1.72)** **(Scheme 1.26)**.

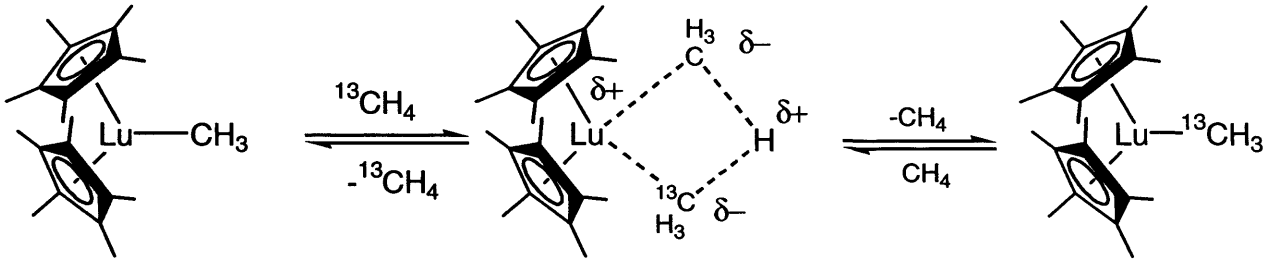

(1.72) **(1.73)** **(1.74)**

(Scheme 1.26)

The methyl may coordinate very weakly to the electrophilic Lu centre via a C-H bond. This is followed by an electrocyclic rearrangement with proton transfer via transition state **(1.73)** which results in methyl group exchange to give **(1.74)**. Initially these transformations were believed to involve highly polar transition states, however Bercaw *et al.* have suggested that the transition state may be relatively non-polar and suggested the term "σ bond metathesis".[68]

1.5 Applications of Cyclometallated complexes

1.5.1 Catalysts (or Catalyst precursors)

The earliest demonstration that palladacyclic catalysts could show higher activity than non-cyclometallated analogues was by Lewis *et al.*[69] who found that the orthometallated complex $[PdCl\{k^2\text{-}P,C\text{-}P(OC_6H_4)(OPh)_2\}\{P(OPh)_3\}]$ formed from $[PdCl_2\{P(OPh)_3\}_2]$ could be used as an active precatalyst for the hydrogenation of alkenes and alkynes. Palladacycle catalysts are considered to be amongst the most active catalysts for C-C and C-heteroatom bond formation.[70, 71] Herrmann *et al.*[72] reported that the palladacyclic complex **(1.75)** and related species showed very high activity in the Heck coupling of aryl halides with simple alkenes **(Scheme 1.27)**, with turn-over numbers (TONs) of up to 1,000,000 for the coupling of n-butylacrylate with aryl bromide.

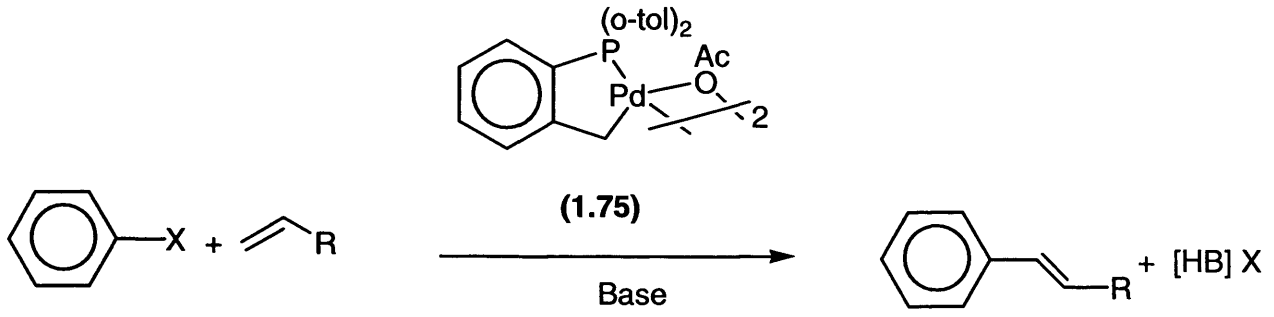

(Scheme 1.27)

The application of **(1.75)** is not limited to the Heck reaction. For example **(1.75)** catalysed the Suzuki reaction of phenylboronic acid with 4-bromoacetophenone **(Scheme 1.28)** with TON's of up to 74000.[72]

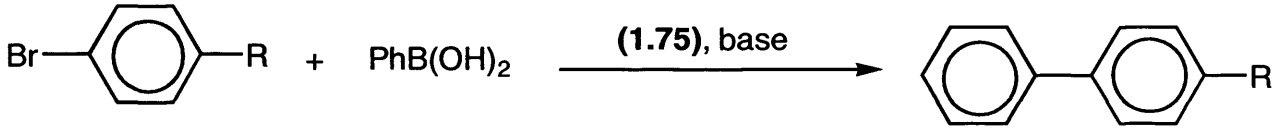

(Scheme 1.28)

Catalytic activity is by no means limited to phosphorus-containing palladacycles. Complexes obtained by cyclopalladation of imines *e.g.* **(1.76)**,[73, 74] oxazolines *e.g.* **(1.77)**[73, 74] or amines *e.g.* **(1.78)** ,[75-77] have been reported and described to be good catalysts in Heck and Suzuki coupling with TON's of greater than $1x10^6$ in the best cases.

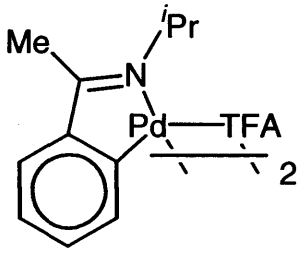

(1.76)

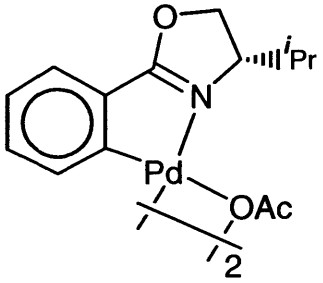

(1.77)

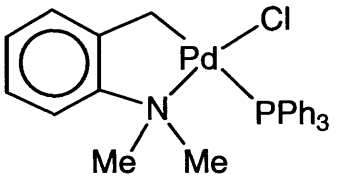

(1.78)

Recyclability of palladacyclic catalysts has also been investigated. For example, Bergbreiter *et al.* synthesised the polymer-modified catalyst **(1.79)** containing a tridentate cyclometallated ligand, which was recycled three times in the Heck coupling reaction of iodobenzene with methylacrylate or styrene.[78] However, for bidentate cyclometallated complexes, many papers showed no recyclability. For example, Bedford *et al.*[79] have found that the silica-supported palladacycle imine **(1.80)** show only poor recyclability in the Suzuki reaction. In this case, Pd(0) species was formed indicating that imine-based palladacyclic catalysts are unstable.

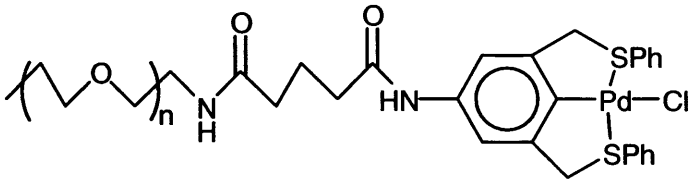

(1.79)

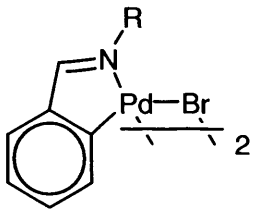

R = $(CH_2)_3Si(OEt)_3$

(1.80)

1.5.2 Catalytic Intermediates

As well as being catalyst precursors cyclometallated complexes can be intermediates in several catalytic processes particularly ones involving C-H activation and subsequent C-C coupling. For example, the hydroiminoacylation of an alkene with aldimine **(1.81)** catalysed by $[Rh(PPh_3)_3Cl]$ **(Scheme 1.29)**.[80] The mechanism involves the oxidative addition of a C-H bond to form the intermediate cyclometallated species **(1.82)**, followed by alkene insertion and reductive elimination to produce ketimine **(1.83)**.

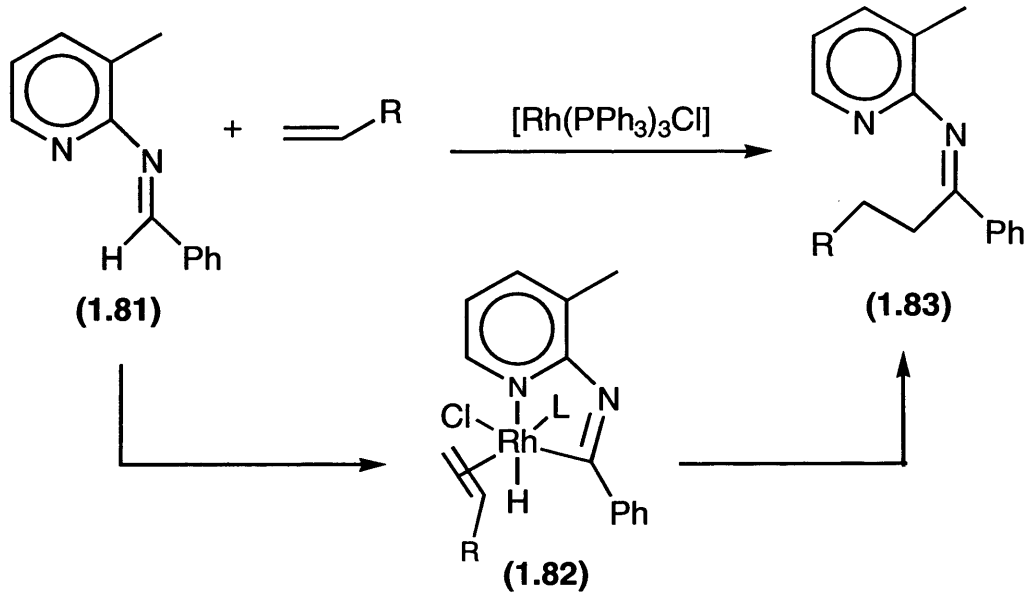

(Scheme 1.29)

A ruthenium phosphine complex can also be used as catalyst for addition of a C-H bond of an aromatic ketone **(1.84)** to an alkene through an intermediate cyclometallated complex **(1.85)** as shown in **scheme 1.30**.[81]

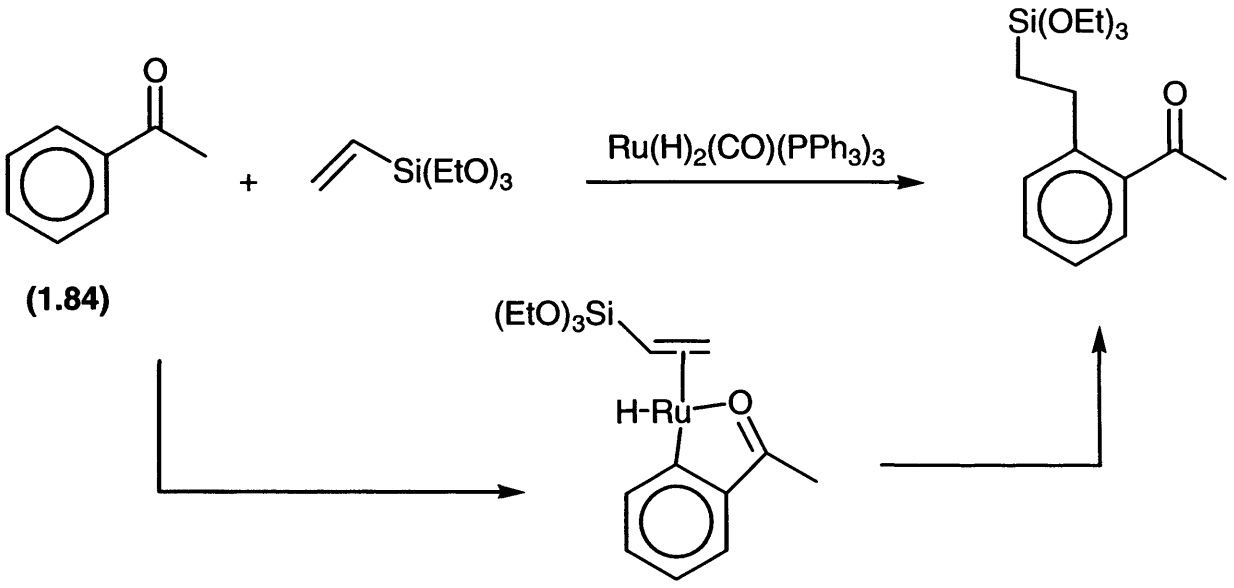

(Scheme 1.30)

1.5.3 In organic synthesis.

Cyclometallated complexes can also be used as starting materials in organic synthesis. Palladacycles undergo insertion of alkynes or alkenes; an example is shown in **scheme 1.31**.[82] The insertion of alkyne into the Pd-C presumably forms **(1.86)**, which undergoes reductive elimination to give heterocyclic compound **(1.87)**.[82] Some examples of ruthenium half-sandwich complexes, which show similar reactivity are discussed in **Chapter 4**.

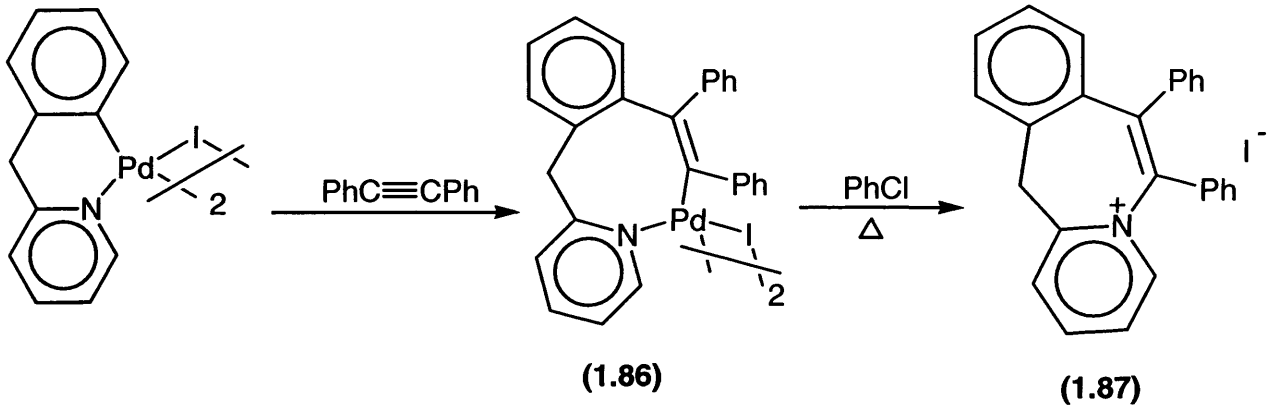

(Scheme 1.31)

The Heck type reaction of palladacycle complexes with alkenes also leads to C-C bond formation in **(1.88)** **(Scheme 1.32)**.[83]

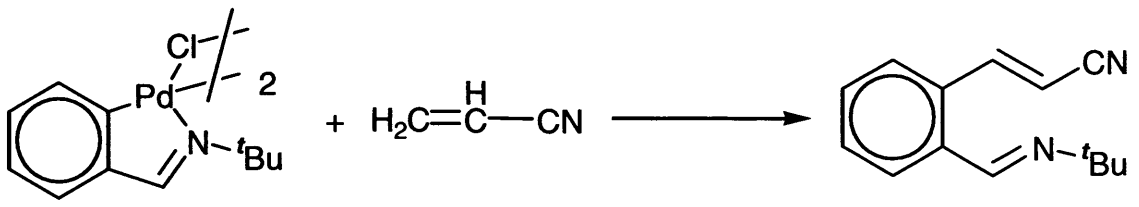

(1.88)

(Scheme 1.32)

Pfeffer *et al.* described the formation of cationic heterocyclic products by reaction with an allene **(Scheme 1.33)**.[84] Two isomeric products **(1.90)** and **(1.91)** were formed from the intermediate **(1.89)** which was observed by ^{1}H NMR spectroscopy.

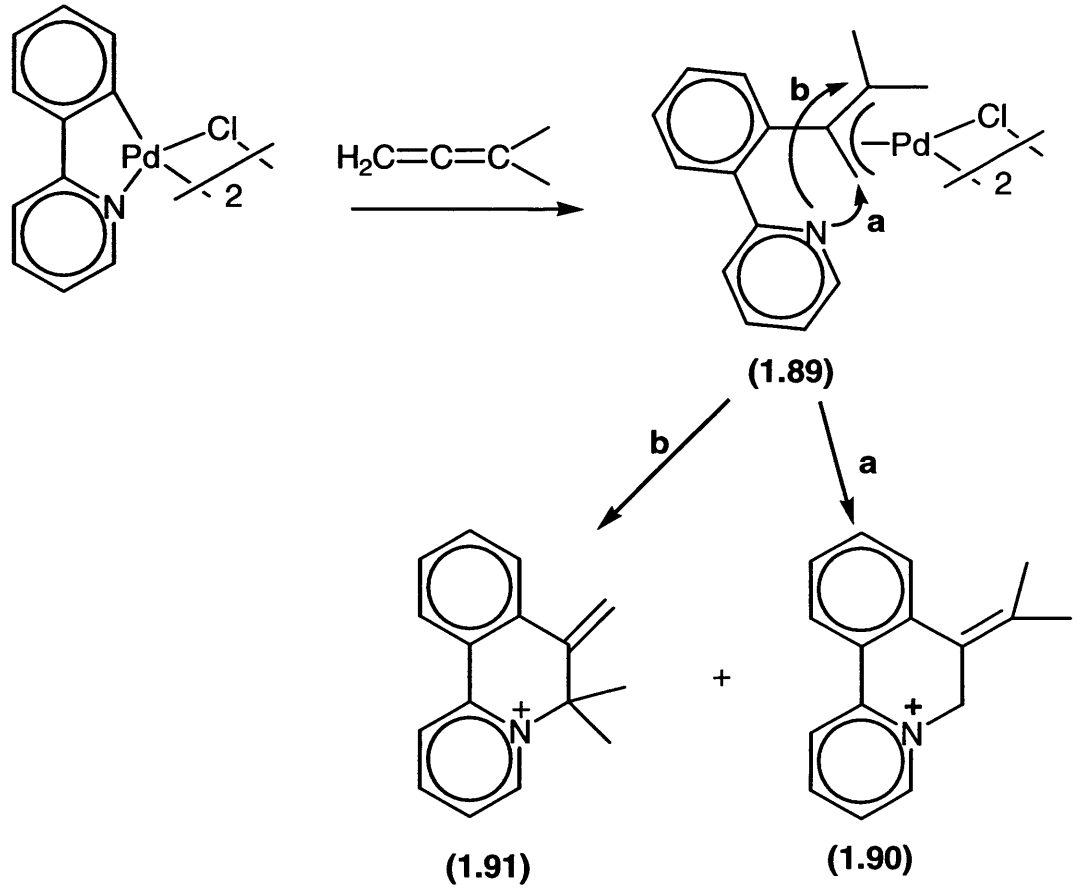

(Scheme 1.33)

1.5.4 Chiral derivatising agents:

Enantiomerically pure cyclometallated compounds are of great interest as a consequence of their application in the determination of enantiomeric excess[85, 86] and the resolution of Lewis bases.[87, 88] Leung *et al.*[85] found that an efficient NMR determination of the enantiomeric excess

of 1,2-diamines can be achieved by coordination to cyclometallated complex **(1.92)** to form (R,R,R) and (R,S,S) diastereomers **(1.93)** (**Scheme 1.34**).

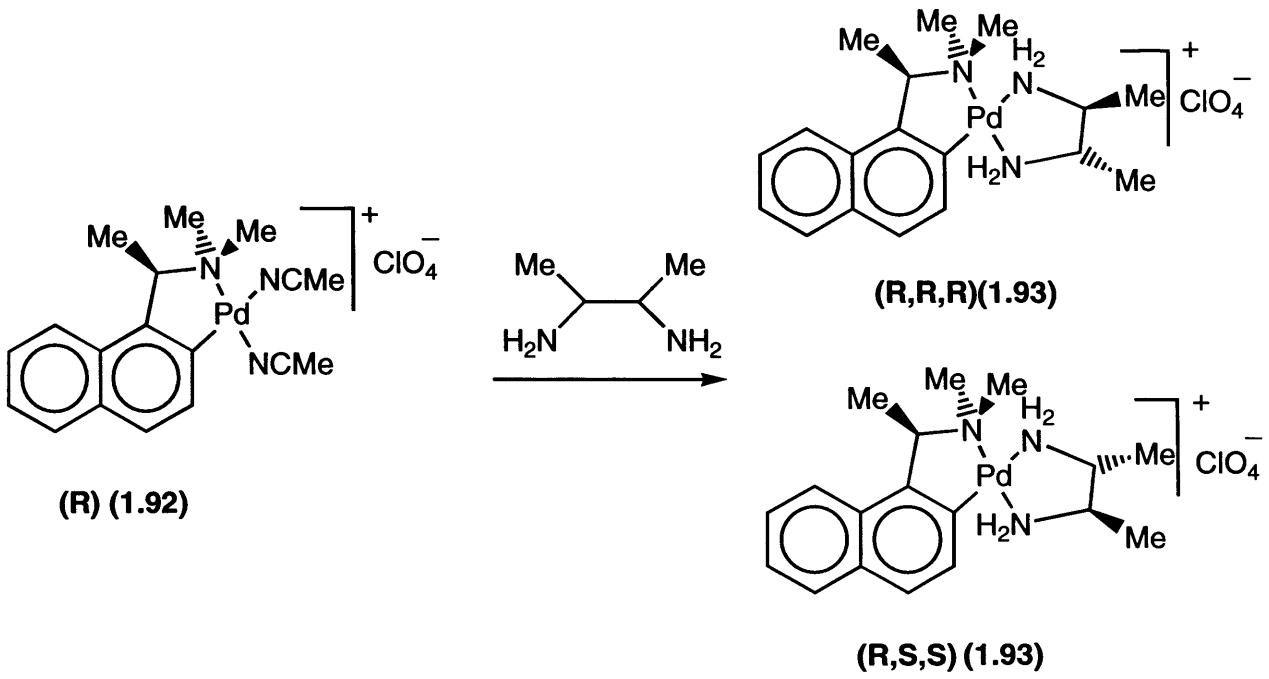

(Scheme 1.34)

More recently Granell *et al.*[89] have described that use of the optically pure palladacycle **(1.94)** to resolve the P-Chiral phosphines **(Scheme 1.35)**. Reaction of **(1.94)** with $[NiCl_2(PBzCyPh)_2]$ (used as an air-stable source of the chiral phosphine) gave two diastereomers which could be separated by chromatography or recrystallisation. Reaction with dppe liberated the free chiral phosphine.

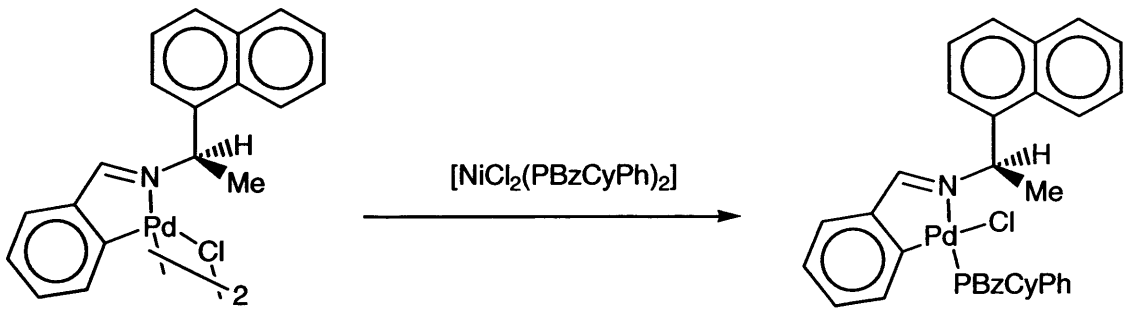

(1.94)

(Scheme 1.35)

(1.95, Rc, Sp)
(1.95`, Rc, Rp)

1.5.5 Liquid crystals

Cyclometallated complexes are also attractive in thermotropic mesomorphism (*i.e.* liquid-crystal behavior).[90] Ghedini *et al.*[91] described the first example of liquid-crystalline

cyclopalladated azobenzene complexes (**1.96**) and (**1.97**), both complexes are nematic liquid crystals.

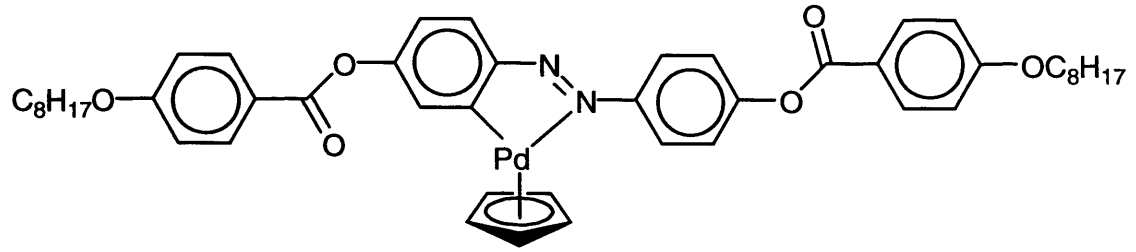

(1.96)

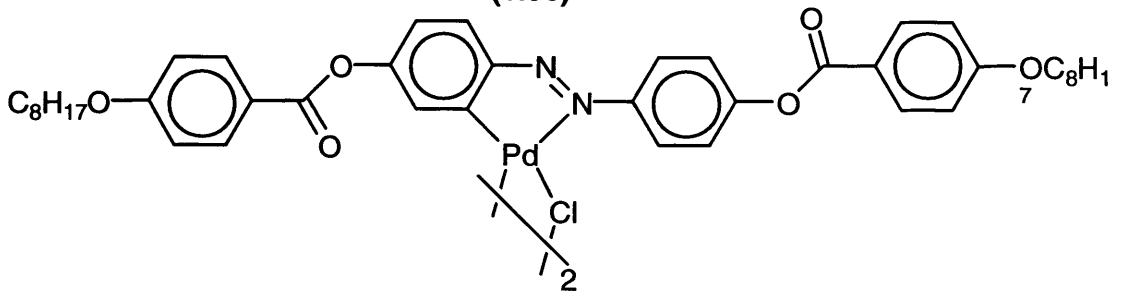

(1.97)

Rourke *et al.* found that cyclopalladated Schiff base complexes such as (**1.98**) form mesophases at > 200° C giving an isotropic liquid at around 250° C at which temperature they decompose.

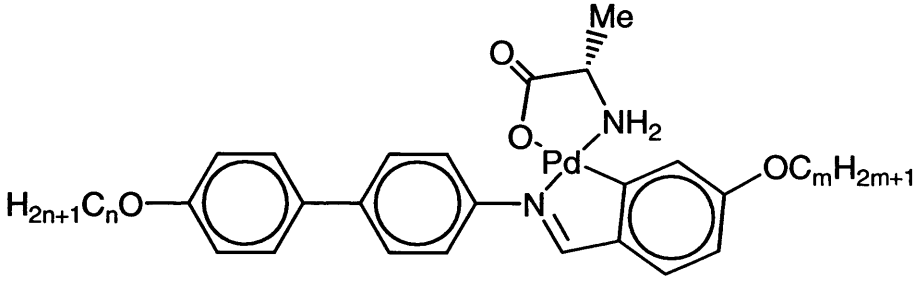

(1.98)

1.5.6 Fluorescent complexes

Luminescent Pd(II) and Pt(II) cyclometallated complexes have attracted much attention recently because of their potential applications in sensors and photochemical and electroluminescent devices. Complexes (**1.99**)[92] and (**1.100**)[92] are luminescent, the latter even at room temperature; the character of the emissive state is mainly MLCT.

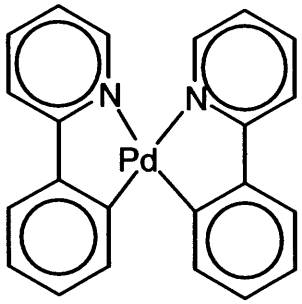

(1.99)

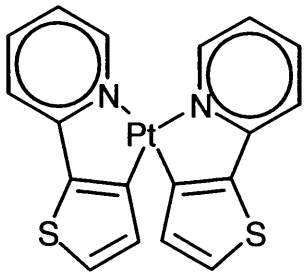

(1.100)

Thompson *et al.*[93] reported that Rh and Ir cyclometallated complexes can have exited state lifetimes of the order of microseconds. Complex **(1.101)** has high phosphoresce efficiency and microsecond excited state lifetime, which make it ideal for OLED applications.

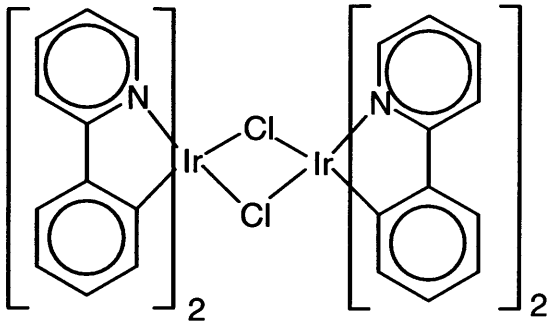

(1.101)

1.5.7 Electrochemical applications

More recently Ryabov *et al.*[94] found that cycloruthenated complex **(1.102)** and **(1.103)** can be used as mediators of electron transfer (electron shuttles) to or from oxidized or reduced active sites of redox enzymes.

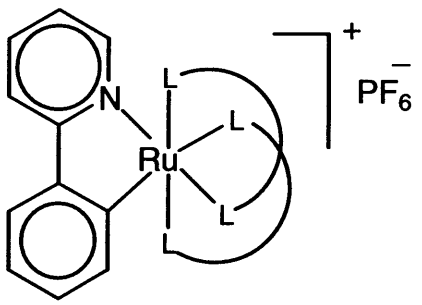

(LL = bpy)

(1.102)

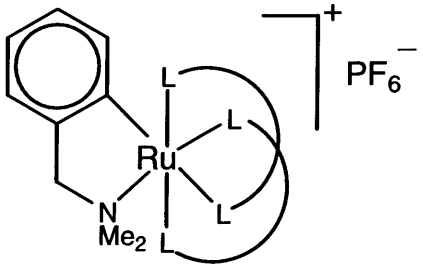

(LL = bpy)

(1.103)

Bibliography

1 J. Dehand and M. Pfeffer, *Coord. Chem. Rev.*, 1976, **18**, 327.

2 M. I. Bruce, *Angew. Chem., Int. Ed. Engl.*, 1977, **16**, 73.

3 I. Omae, *Chem. Rev.*, 1979, **79**, 287.

4 G. R. Newkome, W. E. Puckett, V. K. Gupta, and G. E. Kiefer, *Chem. Rev.*, 1986, **86**, 451.

5 E. C. Constable, *Polyhedron*, 1984, **3**, 1037.

6 I. Omae, *Coord. Chem. Rev.*, 1988, **83**, 137.

7 A. D. Ryabov, *Chem. Rev.*, 1990, **90**, 403.

8 Y. Wu, S. Huo, J. Gong, X. Cui, L. Ding, K. Ding, C. Du, Y. Liu, and M. Song, *J. Organomet. Chem.*, 2001, **637-639**, 27.

9 S. Trofimenko, *Inorg. Chem.*, 1973, **12**, 1215.

10 J. P. Kleiman and M. Dubeck, *J. Am. Chem. Soc.*, 1963, **85**, 1544.

11 A. C. Cope and R. W. Siekman, *J. Am. Chem. Soc.*, 1965, **87**, 3272.

12 H. Onoue and I. Moritani, *J. Organomet. Chem.*, 1972, **43**, 431.

13 A. C. Cope and E. C. Friedrich, *J. Am. Chem. Soc.*, 1968, **90**, 909.

14 A. D. Ryabov and G. M. Kazankov, *J. Organomet. Chem.*, 1984, **268**, 85.

15 A. D. Ryabov and A. K. Yatsimirsky, *Inorg. Chem.*, 1984, **23**, 789.

16 A. D. Ryabov, V. A. Polyakov, and A. K. Yatsimirsky, *J. Chem. Soc. Perkin Trans.*, 1983, **2**, 1503.

17 H. Horino and N. Inoue, *J. Org. Chem.*, 1981, **46**, 4416.

18 A. D. Ryabov, *Inorg. Chem.*, 1987, **26**, 1252.

19 R. A. Holton and R. A. Kjonaas, *J. Organomet. Chem.*, 1977, **142**, C15.

20 R. F. Heck, *J. Am. Chem. Soc.*, 1968, **90**, 313.

21 H. Osser and M. Pfeffer, *J. Chem. Soc. Chem. Commun*, 1985, 1540.

22 F. Maassarani, M. Pfeffer, and G. Le Borgne, *J. Chem. Soc. Chem. Commun*, 1986, 488.

23 J. M. Thompson and R. F. Heck, *J. Org. Chem.*, 1975, **40**, 2667.

[24] J. Albert, J. Barro, and J. Granell, *J. Organomet. Chem.*, 1991, **408**, 115.

[25] J. M. Vila, M. Gayoso, M. T. Pereira, M. L. Torres, J. J. Fernandez, A. Fernandez, and J. M. Ortigueira, *J. Organomet. Chem.*, 1997, **532**, 171.

[26] M. I. Bruce, M. Z. Iqbal, and F. G. A. Stone, *J. Organomet. Chem.*, 1971, **31**, 275.

[27] T. G. Richmond, C. E. Osterberg, and A. M. Arif, *J. Am. Chem. Soc.*, 1987, **109**, 8091.

[28] Y. J. Wu, Y. H. Liu, K. L. Ding, H. Z. Yuan, and X. A. Mao, *J. Organomet. Chem.*, 1995, **505**, 37.

[29] I. C. M. Wehman-Ooyevaar, I. F. Luitwieler, K. Vatter, D. M. Grove, W. J. J. Smeets, E. Horn, A. L. Spek, and G. van Koten, *Inorg. Chim. Acta*, 1996, **252**, 55.

[30] J. Vicente, I. Saura-Llamas, J. Cuadrado, and M. C. Ramirez de Arellano, *Organometallics*, 2003, **22**, 5513.

[31] C. Mutet and M. Pfeffer, *J. Organomet. Chem.*, 1979, **171**, C34.

[32] V. I. Sokolov, L. L. Troitskaya, and O. A. Reutov, *J. Organomet. Chem.*, 1977, **133**, C28.

[33] A. D. Ryabov, L. Kuzmina, V. A. Polyakov, G. M. Kazankov, E. S. Ryabova, M. Pfeffer, and R. van Eldik, *J. Chem. Soc., Dalton Trans.*, 1995, 999.

[34] S. P. Molnar and M. Orchin, *J. Organomet. Chem.*, 1969, **16**, 196.

[35] M. Gomez, J. Granell, and M. Martinez, *J. Chem. Soc., Dalton Trans.*, 1998, 37.

[36] M. Crespo, X. Solans, and M. Font-Bardia, *Organometallics*, 1995, **14**, 355.

[37] J. Albert, M. Gomez, J. Granell, J. Sales, and X. Solans, *Organometallics*, 1990, **9**, 1405.

[38] M. Crespo, M. Martinez, J. Sales, X. Solans, and M. Font-Bardia, *Organometallics*, 1992, **11**, 1288.

[39] J. Albert, J. Barro, and J. Granell, *J. Organomet. Chem.*, 1991, **115**, 115.

[40] S. Q. Huo, Y. J. Wu, C. X. Du, Y. Zhu, H. Z. Yuan, and X. A. Mao, *J. Organomet. Chem.*, 1994, **483**, 139.

[41] J. M. Vila, M. Gayoso, M. T. Pereira, M. Camino Rodriguez, J. M. Ortigueira, and M. Thornton-Pett, *J. Organomet. Chem.*, 1992, **426**, 267.

[42] O. N. Gorunova, K. J. Keusemen, B. M. Goebel, N. A. Kataeva, A. V. Churakov, L. G. Kuz`mina, V. V. Dunina, and I. P. Smoliakova, *J. Organomet. Chem.*, 2004, **689**, 2382.

[43] G. Balavoine and J. C. Clinet, *J. Organomet. Chem.*, 1990, **390**, C84.

[44] Y. Donde and L. E. Overman, *J. Am. Chem. Soc.*, 1999, **121**, 2933.

[45] G. W. V. Cave, F. P. Fanizzi, R. J. Deeth, W. Errington, and J. P. Rourke, *Organometallics*, 2000, **19**, 1355.

[46] S. Stoccoro, B. Soro, G. Minghetti, A. Zucca, and M. A. Cinellu, *J. Organomet. Chem.*, 2003, **679**, 1.

[47] A. Zucca, S. Stoccoro, M. A. Cinellu, G. Minghetti, and M. Manassero, *J. Chem. Soc., Dalton Trans.*, 1999, 3431.

[48] A. D. Ryabov, G. M. Kazankov, A. K. Yatsimirsky, L. G. Kuz'mina, O. Y. Burtseva, N. V. Dvortsova, and V. A. Polyakov, *Inorg. Chem.*, 1992, **31**, 3083.

[49] J. Albert, A. Gonzalez, J. Granell, R. Moragas, C. Puerta, and P. Valerga, *Organometallics*, 1997, **16**, 3775.

[50] M. Nonoyama, *J. Organomet. Chem.*, 1984, **262**, 407.

[51] M. Nonoyama, *J. Organomet. Chem.*, 1982, **229**, 287.

[52] C. Anderson, M. Crespo, M. Font-Bardia, and X. Solans, *J. Organomet. Chem.*, 2000, **604**, 178.

[53] A. E. Shilov and G. B. Shul'pin, *Chem. Rev.*, 1997, **97**, 2879.

[54] B. A. Arndtsen, R. G. Bergman, T. A. Mobley, and T. H. Peterson, *Acc. Chem. Res.*, 1995, **28**, 154.

[55] S. R. Klei, J. T. Golden, P. Burger, and R. G. Bergman, *J. Mol. Catal. A.*, 2002, **189**, 79.

[56] B. A. Arndtsen and R. G. Bergman, *J. Organomet. Chem.*, 1995, **504**, 143.

[57] A. H. Janowicz and R. G. Bergman, *J. Am. Chem. Soc.*, 1983, **105**, 3929.

[58] W. D. Jones and F. J. Feher, *Acc. Chem. Res.*, 1989, **22**, 91.

[59] A. H. Janowicz and R. G. Bergman, *J. Am. Chem. Soc.*, 1982, **104**, 352.

[60] S. R. Klei, T. D. Tilley, and R. G. Bergman, *J. Am. Chem. Soc.*, 2000, **122**, 1816.

[61] D. M. Tellers and R. G. Bergman, *Organometallics*, 2001, **20**, 4819.

[62] B. K. Corkey, F. L. Taw, R. G. Bergman, and M. Brookhart, *Polyhedron*, 2004, **23**, 2943.

[63] D. M. Tellers, C. M. Yung, B. A. Arndtsen, D. R. Adamson, and R. G. Bergman, *J. Am. Chem. Soc.*, 2002, **124**, 1400.

[64] W. D. Jones and F. J. Feher, *J. Am. Chem. Soc.*, 1985, **107**, 620.

[65] A. J. Canty and G. V. Koten, *Acc. Chem. Res.*, 1995, **28**, 406.

[66] A. D. Ryabov, I. K. Sakodinskaya, and A. K. Yatsimirsky, *J. Chem. Soc. Dalton Trans.*, 1985, 2629.

[67] P. L. Watson and G. W. Parshall, *Acc. Chem. Res.*, 1985, **18**, 51.

[68] M. E. Thompson, S. M. Baxter, A. R. Bulls, B. J. Burger, M. C. Nolan, B. D. Santarsiero, W. P. Schaefer, and J. E. Bercaw, *J. Am. Chem. Soc.*, 1987, **109**, 203.

[69] L. N. Lewis, *J. Am. Chem. Soc.*, 1986, **108**, 743.

[70] R. B. Bedford, *Chem. Commun.*, 2003, 1787.

[71] J. Dupont, M. Pfeffer, and J. Spencer, *Eur. J. Inorg. Chem.*, 2001, 1917.

[72] W. A. Herrman, V. P. W. Bohm, and C.-P. Reisinger, *J. Organomet. Chem.*, 1999, **576**, 23.

[73] M. Ohff, A. Ohff, and D. Milstein, *Chem. Commun.*, 1999, 357.

[74] H. Weissman and D. Milstein, *Chem. Commun.*, 1999, 1901.

[75] S. Iyer and C. Ramesh, *Tetrahedron*, 2000, **41**, 8981.

[76] I. P. Beletskaya, A. N. Kashin, and N. B. Karlstedt, *J. Organomet. Chem.*, 2001, **622**, 89.

[77] F. Yang, Y. Zhang, R. Zheng, J. Tie, and M. He, *J. Organomet. Chem.*, 2002, **651**, 146.

[78] D. E. Bergbreiter, P. L. Osburn, and Y.-S. Liu, *J. Am. Chem. Soc.*, 1999, **121**, 9531.

[79] R. B. Bedford, C. S. J. Cazin, M. B. Hursthouse, M. E. Light, K. J. Pike, and S. Wimperis, *J. Organomet. Chem.*, 2001, **633**, 173.

[80] C. Jun, C. W. Moon, and D. Lee, *Chem. Eur. J.*, 2002, **8**, 2423.

[81] F. Kakiuchi, S. Sekine, Y. Tanaka, A. Kamatani, M. Sonoda, N. Chatani, and S. Murai, *Bull. Chem. Soc. Jpn.*, 1995, **68**, 62.

[82] F. Maassarani, M. Pfeffer, and G. L. Borgne, *Organometallics*, 1987, **6**, 2043.

[83] I. R. Girling and D. A. Widdowson, *Tetrahedron Lett.*, 1982, **23**, 4281.

[84] J. Chengebroyen, M. Linke, M. Robitzer, C. Sirlin, and M. Pfeffer, *J. Organomet. Chem.*, 2003, **687**, 313.

[85] S. Y. M. Chooi, P. H. Leung, C. C. Lim, K. F. Mok, G. H. Quek, and K. Y. Sim, *Tetrahedron Asymmetry*, 1992, **3**, 529.

[86] J. Albert, J. Granell, G. Muller, D. Sainz, M. Font-Bardia, and X. Solans, *Tetrahedron Asymmetry*, 1995, **6**, 325.

[87] S. B. Wild, *Coord. Chem. Rev.*, 1997, **166**, 291.

[88] F. Robin, F. Mercier, L. Ricard, F. Mathey, and M. Spagnol, *Chem. Eur. J.*, 1997, **8**, 1365.

[89] J. Albert, J. M. Cadena, J. R. Granell, X. Solans, and M. Font-bardia, *Tetrahedron Asymmetry*, 2000, **11**, 1943.

[90] R. W. Date, E. F. Iglesias, K. E. Rowe, J. M. Elliott, and D. W. Bruce, *J. Chem. Soc. Dalton Trans.*, 2003, 1914.

[91] M. Ghedini, F. Neve, and D. Pucci, *Eur. J. Inorg. Chem.*, 1998, 501.

[92] A. Zelewsky, P. Belser, P. Hayoz, R. Dux, X. Hua, R. Suckling, and H. Stoeckli-Evans, *Coord. Chem. Rev.*, 1994, **132**, 75.

[93] S. Lamansky, P. Djurovich, D. Murphy, F. Abdel-Razzaq, R. Kwong, I. Tsyba, M. Bortz, B. Mui, R. Bay, and M. E. Thompson, *Inorg. Chem.*, 2001, **40**, 1704.

[94] A. D. Ryabov, V. S. Sukharev, L. Alexandrova, R. Le Lagadec, and M. Pfeffer, *Inorg. Chem.*, 2001, **40**, 6529.

Chapter Two:

Cyclopalladated Imines Containing an O-Functionalised Tether; Factors Controlling Coordination Of the Oxygen

Chapter Two - Cyclopalladated Imines Containing an O-Functionalised Tether; Factors Controlling Coordination Of the Oxygen

There has been much interest recently in C,N-bidentate cyclometallated complexes. This chapter describes the study of compounds derived from potentially (C,N,O)-tridentate ligands. The aim is to assess what factors control coordination of an oxygen donor ligand tethered to a C,N-chelate and to establish whether this interaction can be hemilabile.

2.1 Introduction

Imines derived from benzaldehyde afford many kinds of C,N-cyclometallated complexes. However, the vast majority involve ligands which are only bidentate, complexes with tri- or tetradentate cyclometallated ligands are much rarer. C,N-bidentate cyclometallated ligands with pendant donor atoms can in principle act as tridentate ligands, examples **(2.1-2.3)**[1-3] are shown in **Scheme 2.1**.

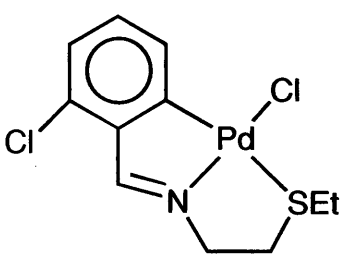

(2.1)

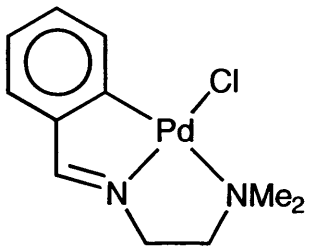

(2.2)

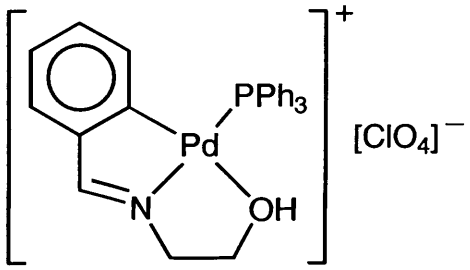

(2.3)

(Scheme 2.1)

2.1.1 Hemilability

Ligands that contain two different donor atoms may bind in a hemilabile way, *i.e.* one end may bind strongly while the other may bind weakly and hence dissociate easily.[4-6]

Functionalised phosphines with soft and hard donor groups *viz.* phosphorus and oxygen, represent the most studied class of hemilabile ligands.[5] Ethers and alcohols are weak donors, particularly to soft metals. Hence, the phosphorus binds strongly to soft metals whilst the oxygen may dissociate to leave a vacant site for other ligands, as can be observed in **Scheme (2.2)**.[7]

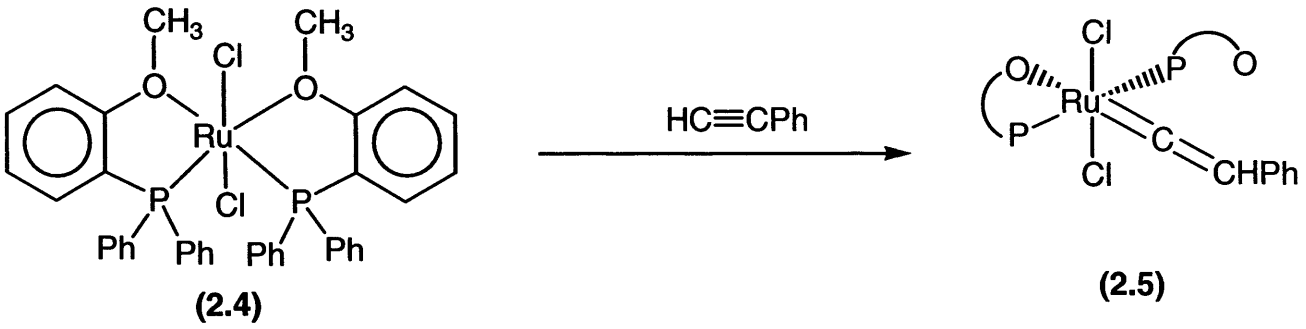

(2.4) **(2.5)**

(Scheme 2.2)

Thus, in **(2.4)** one of the P,O-ligands acts as a hemilabile chelate and promotes the reaction with HC≡CPh to form **(2.5)**. The corresponding reaction with the related complex $[RuHCl(CO)(P^iPr_3)_2]$, for example, does not convert HC≡CPh into the corresponding [Ru=C=CHPh].

Metal complexes containing hemilabile ligands are catalytically active in a range of reactions, including hydrogenation, carbonylation and epoxidation.[4-6] The hemilabile ligand can help stabilise coordinatively unsaturated species yet the ready dissociation of one donor allows further reaction. An example of a catalytic cycle involving a hemilabile P,O-ligand is shown in **Scheme 2.3**.[5]

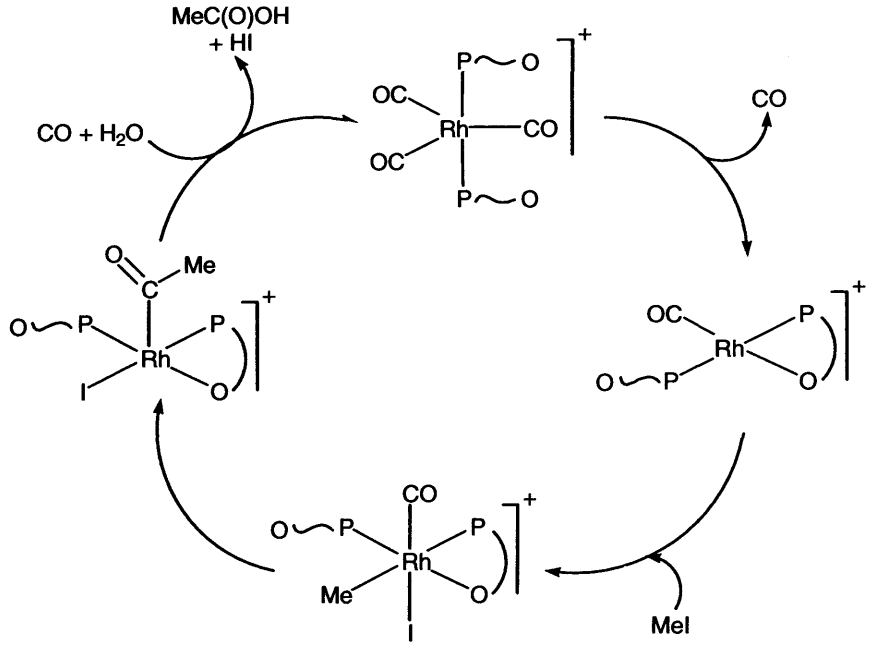

(Scheme 2.3)

2.1.2 Late-Transition metal alkoxide

Complexes containing bonds between oxygen and late transition metals have been implicated as reactive intermediates in numerous important catalytic systems.[8] A variety of late-metal alkoxide complexes, including parent hydroxide species have now been synthesised.[9, 10]

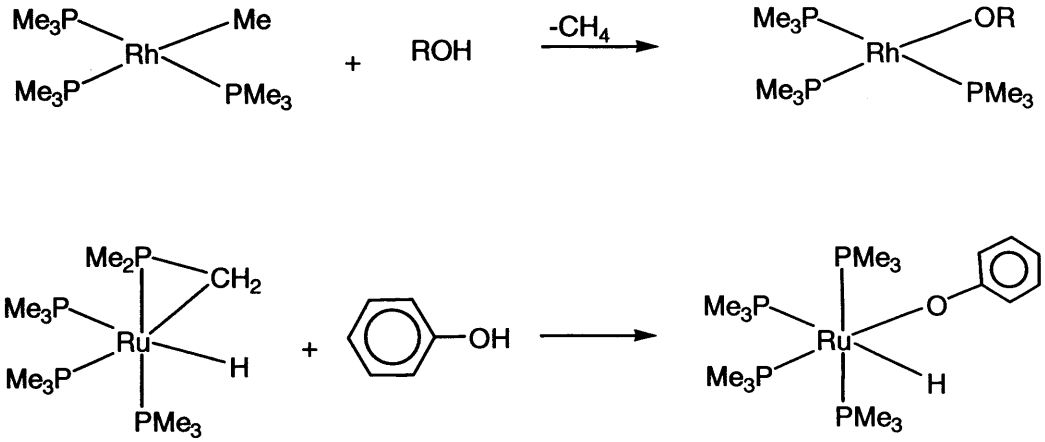

(Scheme 2.4)

Addition of alcohols to metal alkyls can yield metal alkoxides **(Scheme 2.4)**.[10, 11] Late-transition metal alkoxides react with electrophilic organic compounds such as acid chlorides and also deprotonate a variety of weak acids such as alcohols and amines.[12]

2.1.3 Cyclometallated Complexes Containing Tridentate Ligands

The majority of tridentate cyclometallated complexes involve symmetrical XCX (X = S, P, N), donor sets,[13-17] and have been shown to give some highly stable catalyst systems.[15, 18, 19] Examples of the synthesis of SCS **(2.6)** and PCP **(2.7)** tridentate complexes by C-H activation are shown in **Scheme 2.5**. [18, 19]

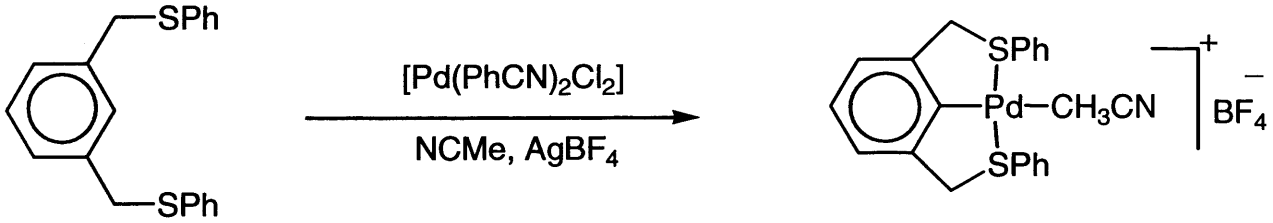

(2.6)

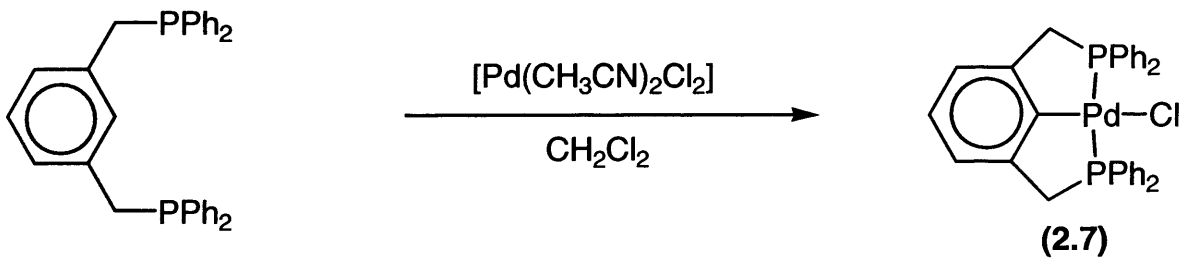

(2.7)

(Scheme 2.5)

Similar N,C,N tridentate complexes **(2.8)**[20] and **(2.9)**[21] may be synthesised by oxidative addition or by transmetallation respectively **(Scheme 2.6)**.

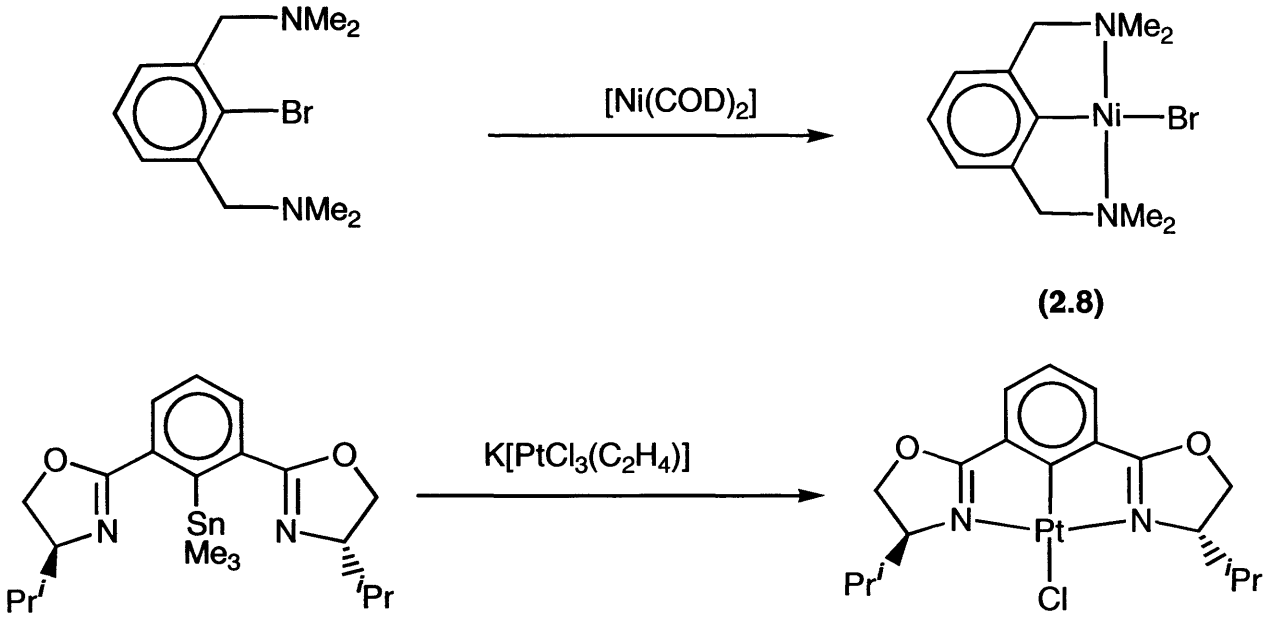

(Scheme 2.6)

Similar cyclometallated complexes with unsymmetrical C,N,N tridentate ligands have been described;[22-26] for example, reaction of **(2.10)** with $[Pd_2(dba)_3]$ gives **(2.11)** **(Scheme 2.7)**.[2]

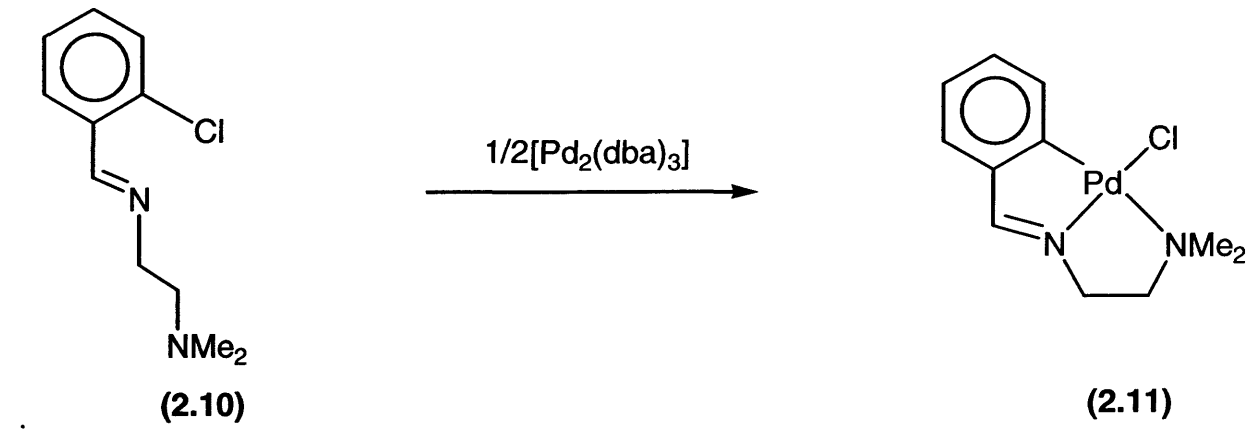

(Scheme 2.7)

Complex **(2.11)** is easily converted to bidentate C,N coordination by reaction with phosphines **(Scheme 2.8)**.[2] Vila *et al.* have shown that the coupling of the imine and (H^6) proton resonances to the phosphorus atom can be used to determine the stereochemistry of the complex. Thus, when the P is *trans* to N **(2.13)**, coupling to the imine proton and the (H^6) proton is observed but no coupling is observed when P is *trans* to C **(2.12)**.

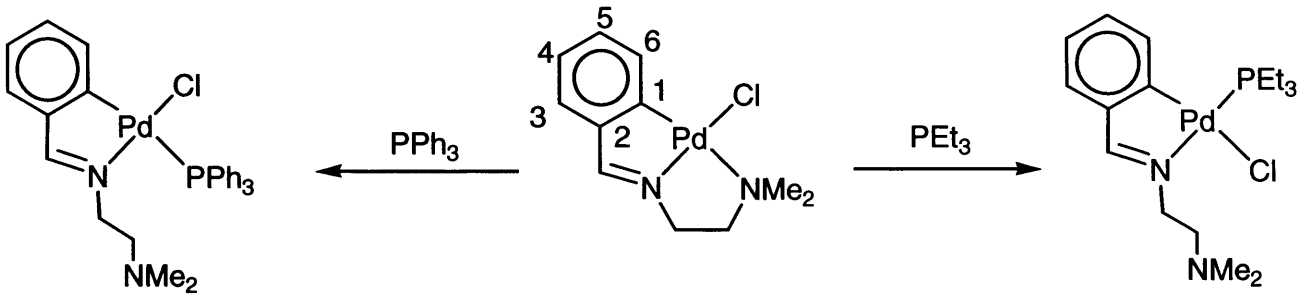

(2.12) **(2.11)** **(2.13)**

(Scheme 2.8)

They suggest that the phosphine ligand cleaves the Pd-NMe_2 bond with coordination of the phosphorus atom to the vacant site at palladium, *cis* to the imine. This coordination prevails with the less basic phosphine (PPh_3),[2] whilst the more basic PEt_3 gives the P *trans* to imine product.[1, 26-28] However, similar reactions described by Fernandez *et al*[26] show that the PPh_3 can also coordinate *trans* to the imine **(Scheme 2.9).**

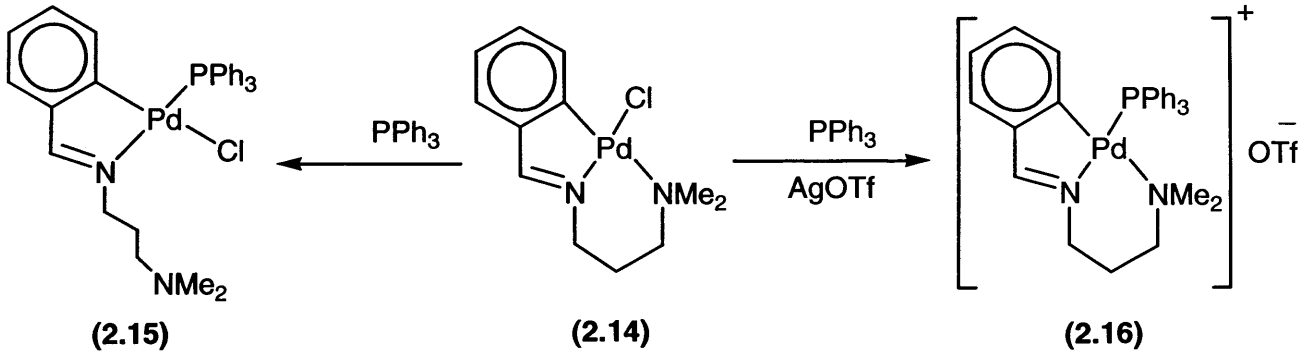

(2.15) **(2.14)** **(2.16)**

(Scheme 2.9)

Treatment of **(2.14)** with PPh_3 leads to cleavage of the Pd-NMe_2 bond to form **(2.15)** with the PPh_3 *trans* to the imine. In the reaction of **(2.14)** with PPh_3 and Ag^+, the NMe_2 is not displaced from coordination to the palladium, rather coordination of PPh_3 occurs after abstraction of chloride to give **(2.16)**. Tetradentate ligands with a C,N,N,C donor set are also known, an example is shown in **Scheme (2.10)**.[29]

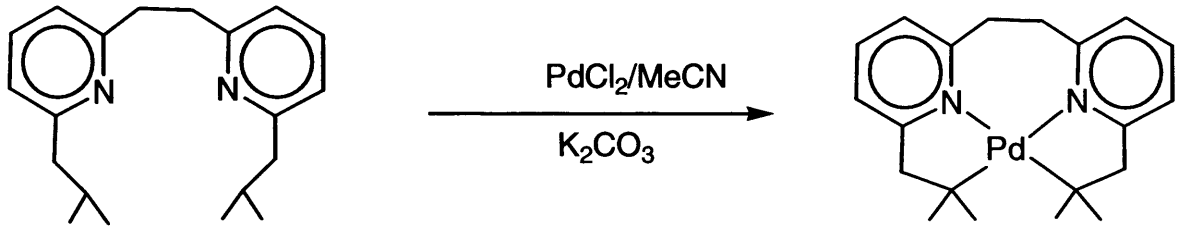

(Scheme 2.10)

In contrast with N,C,N and C,N,N ligands there are relatively few reports of C,N,S tridentate[1, 27, 30-39] or C,N,O[3, 28, 40-45] tridentate ligands. Reaction of the thioether functionalised imine **(2.17)** with Na_2PdCl_4 leads to complex **(2.18)**, with an N,S-bidentate chelate. Treatment of **(2.18)** with NaOAc leads to C-H activation and provides the C,N,S-tridentate complex **(2.19)** **(Scheme 2.11)**.[31, 32] Notably the imine isomerises from the Z-conformation in **(2.18)** to the E-isomer in order for cyclometallation to occur to give **(2.19)**. Presumably elimination of HOAc is easer than HCl as found previously (see **Scheme 1.9 Ch. 1**).

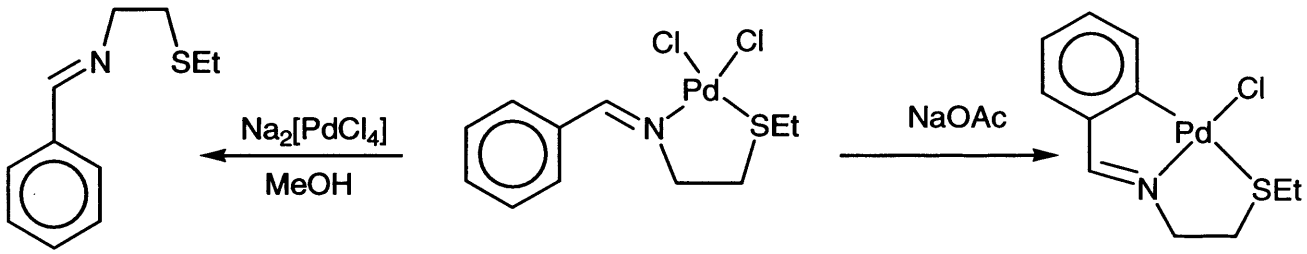

(2.17) **(2.18)** **(2.19)**

(Scheme 2.11)

Addition of an equimolar amount of PPh_3 to **(2.19)** leads to the cleavage of the Pd-S bond and coordination of PPh_3 **(Scheme 2.12)**. Notably, in **(2.20)**, the PPh_3 ends up *trans* to N rather than occupying the site vacated by the sulphur atom. Use of excess PPh_3 leads to cleavage of the Pd-N bond and formation of **(2.21)**.[31]

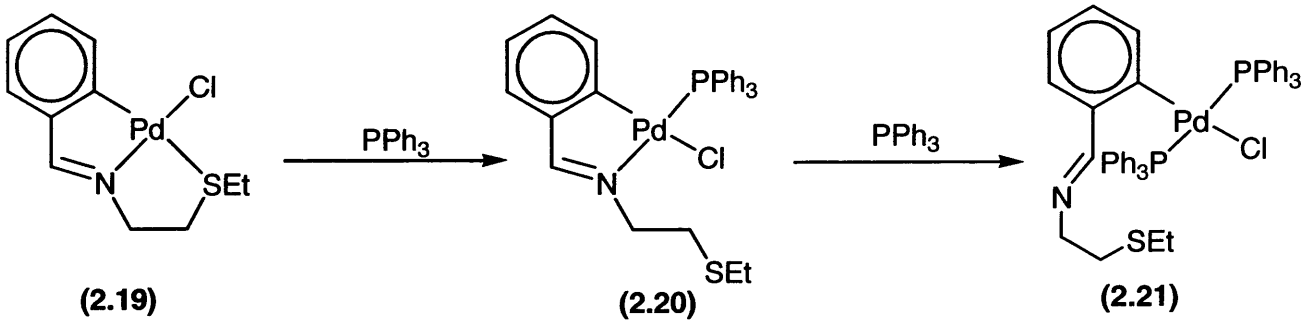

(2.19) **(2.20)** **(2.21)**

(Scheme 2.12)

Cationic cyclometallated complexes **(2.22)** with a C,N,S-tridentate ligand can be formed from either **(2.19)** or **(2.20)** by reaction with AgOTf **(Scheme 2.13)**.[1, 31]

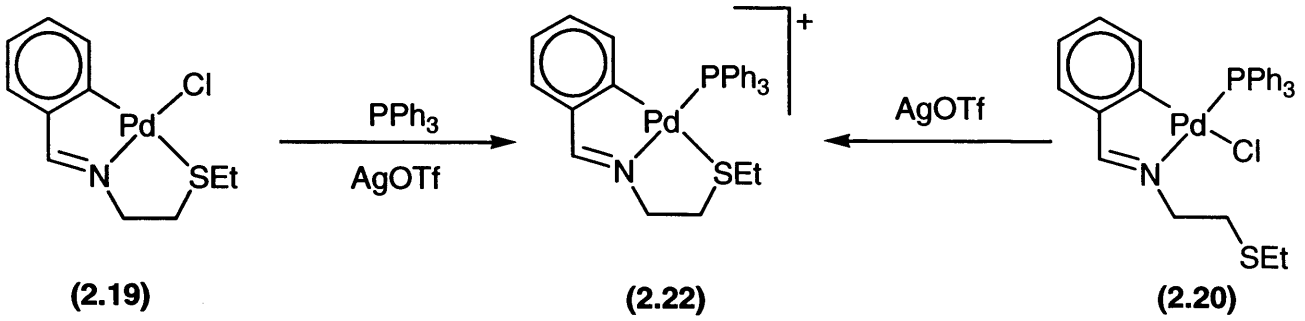

(2.19) **(2.22)** **(2.20)**

(Scheme 2.13)

Another C,N,S-tridentate complex was made by Vila *et al.*[30, 36] **(Scheme 2.14)**. Reaction of thiosemicarbazone **(2.23)** with K_2PdCl_4 gave the first example of a tetrameric C,N,S-cyclometallated complex **(2.24)** with deprotonation of the NH group as shown by X-ray diffraction. The Pd-S bridge bonds in tetramer **(2.24)** were cleaved when reacted with PPh_3, giving **(2.25)**. In this case, the C,N,S- ligand remained tridentate even when a large excess of PPh_3 was used.

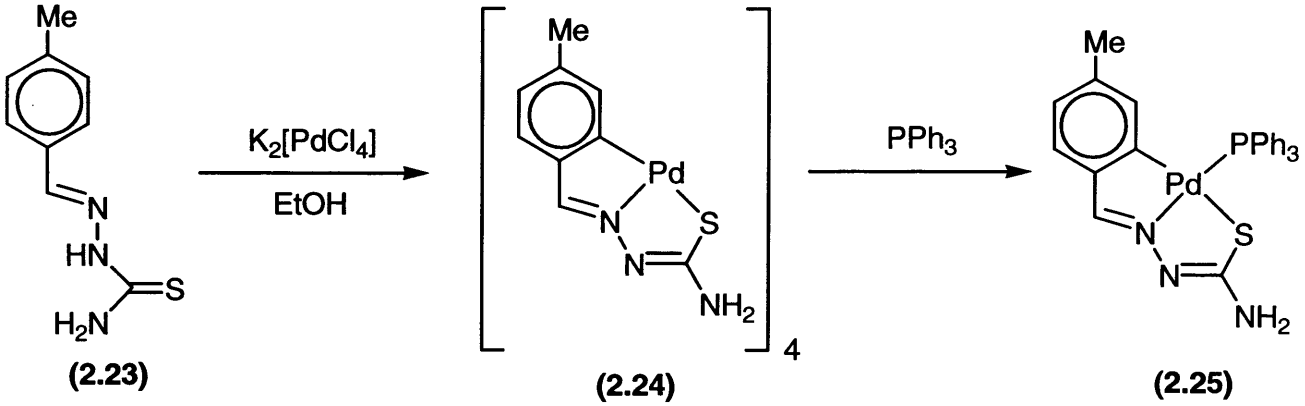

(2.23) **(2.24)** **(2.25)**

(Scheme 2.14)

This chapter will focus on C,N-cyclometallated ligands having a pendant oxygen-containing group which may coordinate to form a tridentate ligand. These are discussed in the next section.

2.1.4 Synthesis and Reactivity of Palladium Complexes containing C,N,O Ligands

Our interest is in C,N-cyclometallated systems with an O-functionalised tether which may, in principle, act as tridentate ligands. These may exhibit hemilability, or in the case of alkoxides, show novel reactivity. Relatively few C,N,O derivatives are known[28, 40, 41, 46-50] and some examples are discussed below. Different routes to C,N,O tridentate complexes have been reported depending on the nature of the O-donor. Palladium complex **(2.28)** is easily made by C-

H activation of **(2.26)** with $[Pd(OAc)_2]_3$ to give **(2.27)** then anion exchange with LiCl as shown in **Scheme 2.15**.[3]

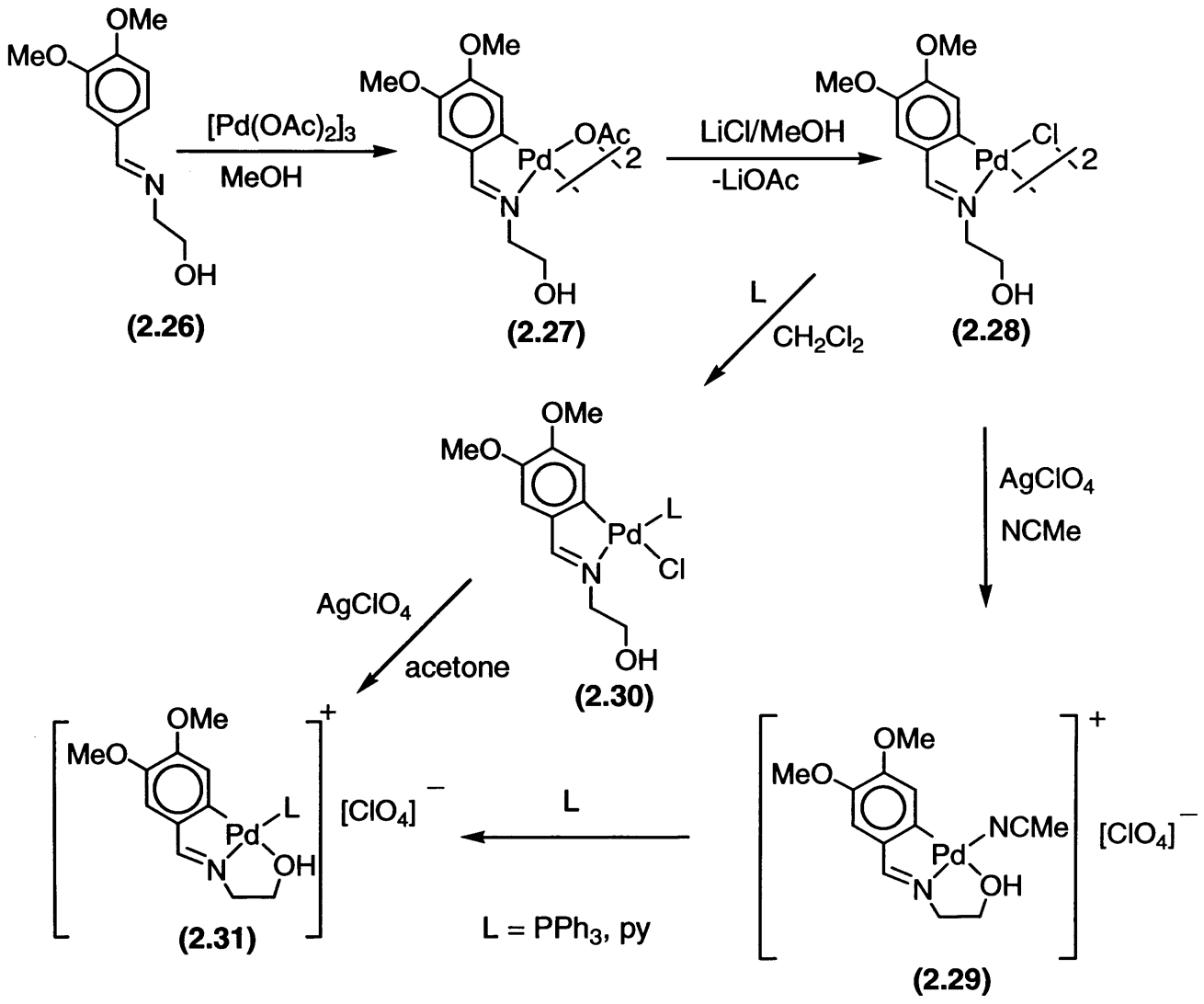

(Scheme 2.15)

Reaction of **(2.28)** with Ag^+ leads to abstraction of chloride and coordination of the alcohol making the ligand tridentate, with an acetonitrile completing the coordination sphere. The acetonitrile in **(2.29)** is easily displaced by PPh_3 or pyridine to give **(2.31)**. However, the oxygen atom in **(2.31)** is not substituted even by the addition of excess PPh_3 or pyridine. It is noteworthy that coordination of the alcohol tether only occurs in the cations. Thus, in complex **(2.28)**, the palladium achieves a 16-electron configuration by dimerisation through halide bridges rather than by coordination of the alcohol. Complex **(2.31)** can also be obtained by the reaction of **(2.28)** with a donor ligand such as PPh_3 or pyridine to give **(2.30)** then treatment with Ag^+. The imine and H^6 protons are coupled to the phosphorus atom, indicating the *trans* arrangement of the phosphine ligand and the imine in **(2.30, L = PPh_3)**.

If the oxygen donor is a phenol, as in **(2.32)**, the lower pK_a, can lead to deprotonation. During the course of our work, Fernandez *et al.*[42] reported the reaction of **(2.32)** with $[Pd(OAc)_2]_3$ to give tetramer **(2.33)** containing a dianionic C,N,O tridentate ligand (**Scheme 2.16**). The tetramer was reacted with PPh_3 giving **(2.34)**.

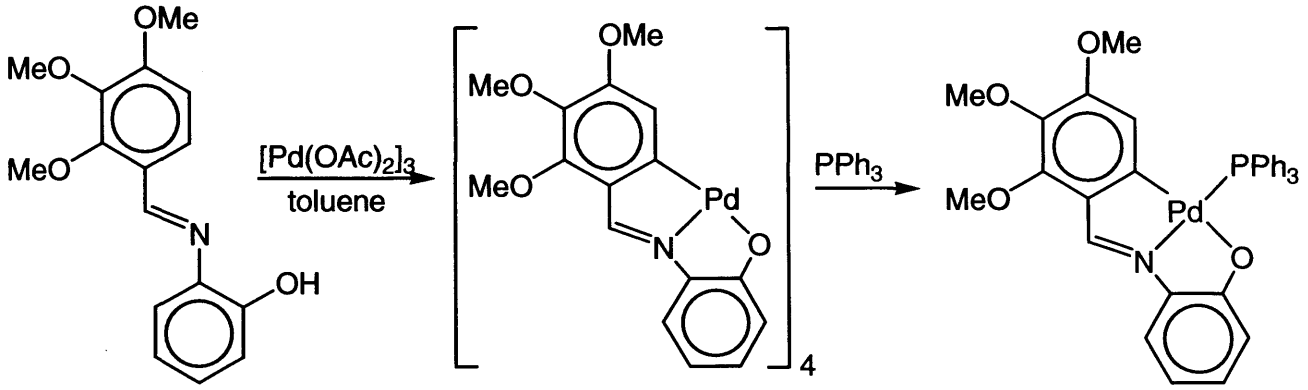

(2.32) **(2.33)** **(2.34)**

(Scheme 2.16)

The oxygen donor can also be an ether rather than an alcohol, *e.g.* **(2.36)** in **Scheme (2.17)**.[43] As in **Scheme 2.15**, the oxygen does not coordinate until the chloride is removed with AgOTf .

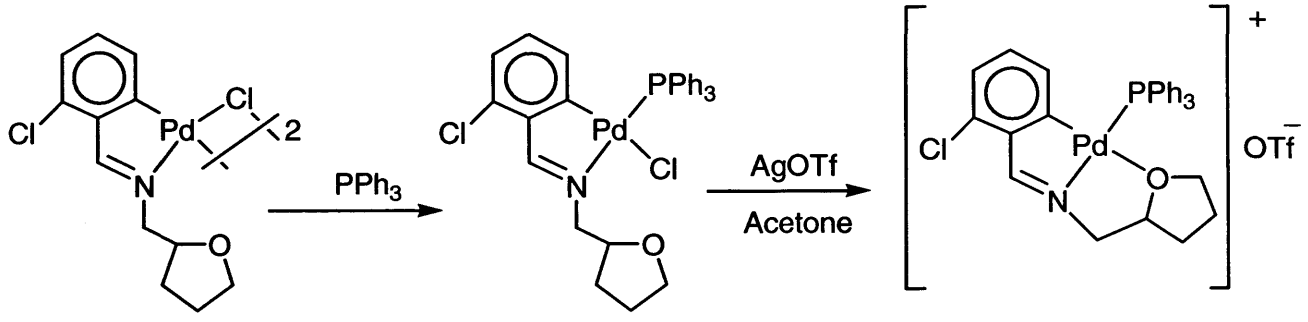

(2.35) **(2.36)**

(Scheme 2.17)

The oxygen donor can also be a semicarbazone. Unlike the thio analogue (**Scheme 2.14**) which reacts with $PdCl_4^{2-}$ to form a dianionic C,N,S ligand, **(2.37)** reacts to form a monoanionic C,N,O complex **(2.38)** (**Scheme 2.18**).[40] This is rare example of oxygen coordination in a neutral

complex rather than a cationic one. Treatment of **(2.38)** first with Ag^+ then PPh_3, leads to removal of the chloride ligand and replacement by the phosphine **(2.39)**. However, direct reaction of **(2.38)** with PPh_3 (1 equivalent) leads to cleavage of the O-Pd bond and formation of **(2.40)**, whilst reaction with excess PPh_3 leads to cleavage of N-Pd and O-Pd bonds to form **(2.41)**. Hence the stability of the Pd-O bond may be greater in cationic complexes than in neutral ones.

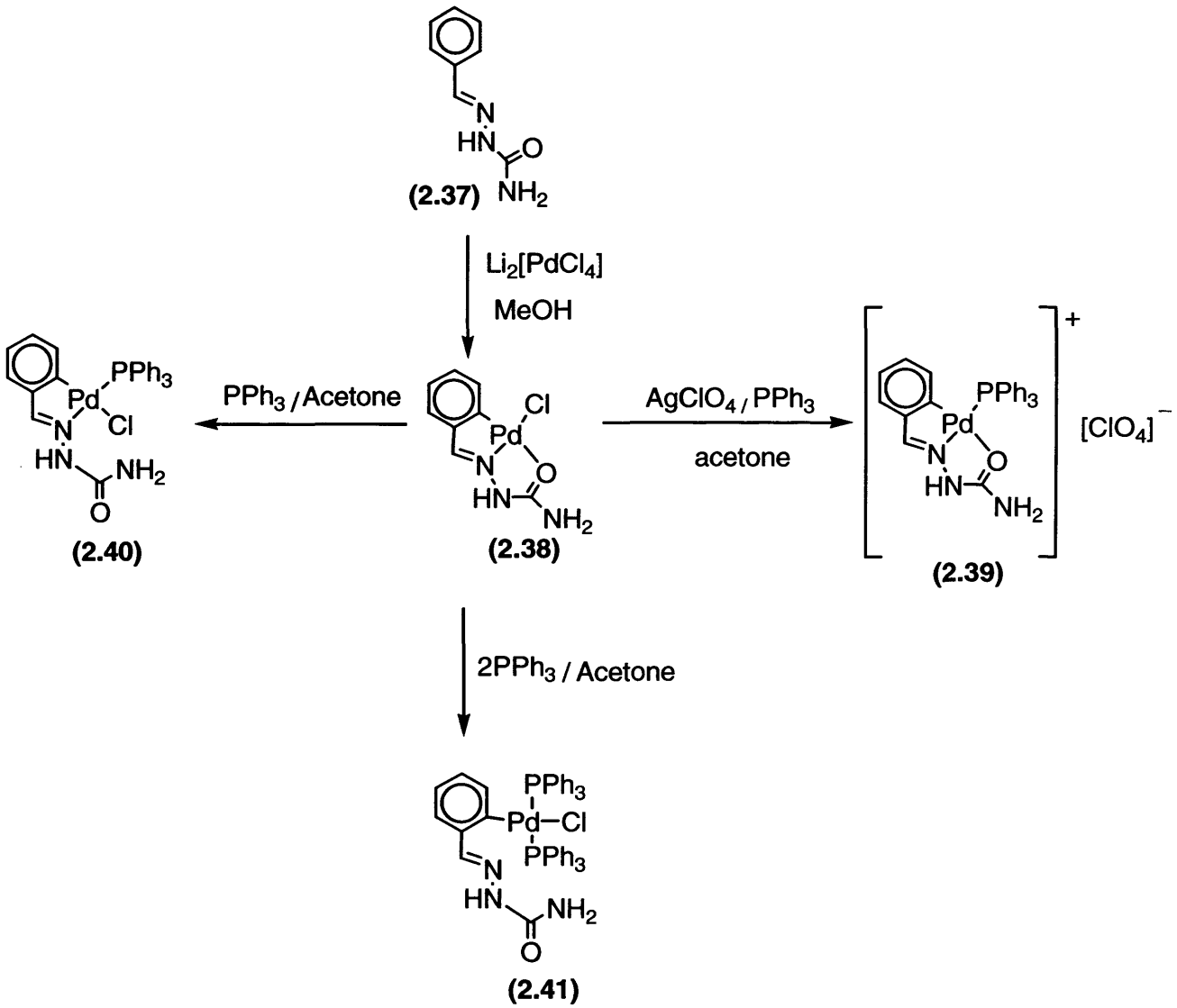

(Scheme 2.18)

This chapter will describe the synthesis of cyclometallated imines containing an alcohol or ether functionality. The reaction of these complexes and factors affecting coordination of the oxygen will be discussed.

2.2 Results and Discussion

2.2.1 Preparation of Imines

The imines **(a-h)** were synthesised by stirring equimolar amounts of an amine and the appropriately substituted benzaldehyde at room temperature in dichloromethane or ethanol as described by Navarro *et al.*[3]

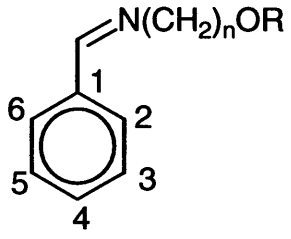

(a, n = 2, R = CH_3)
(b, n = 3, R = CH_3)
(c, n = 2, R = H)
(d, n = 3, R = H)

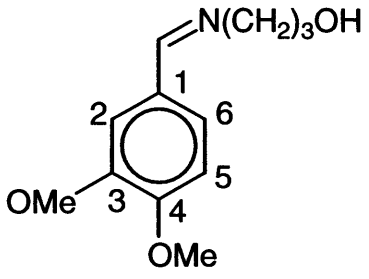

(e)

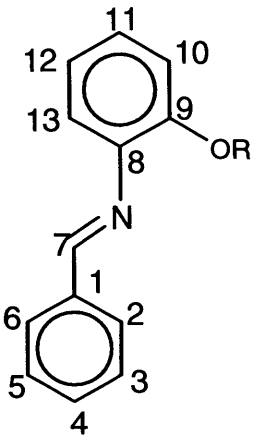

(f, R = CH_3)
(g, R = Ph)
(h, R = H)

In some cases, particularly those which have an OH group, anhydrous $MgSO_4$ was added to remove the water produced. In all cases ^1H and $^{13}C\{^1H\}$ NMR spectroscopy proved that the imines were pure, with the exception of **(d)** and **(e)** (see below) and **(f)**, which showed a mixture of starting material and product. In this case, excess benzaldehyde was added to leave a mixture of **(f)** and excess benzaldehyde, the latter does not affect the cyclometallation reactions. The imines **(a-h)** were obtained either as solids, which were purified by washing with hexane and filtration, or liquids which were used directly.

The ^1H NMR spectra of the imines show a characteristic singlet at δ 8.10-8.70 due to the imine proton (HC=N). Imines **(a, b, e and f)** containing OMe groups, also gave rise to singlets in the range δ 3.26 to 4.00. The OH group gave a broad peak at 3.92 for **(c)** but was not observed in **(d)** or **(e)**, the phenol OH in **(h)** was observed at δ 7.50. In the $^{13}C\{^1H\}$ NMR spectra the imine carbon was observed at δ 161-164 for **(a-f)** and at δ 157.38 for **(h)** with (C^1) of all the imines at *ca.* δ 136. The IR spectra of the imines showed the υ(C=N) at δ 1644-1648 cm^{-1} for **(a-e)** and at δ 1625-1629 cm^{-1} for **(f-h)**.

The ^1H NMR spectra of **(d)** and **(e)** showed the presence of two species in a ratio 2:1 for **(d, d`)** and 6:1 for **(e, e`)**. In each case, the major species showed a signal characteristic of the imine

proton, at δ 8.20 for **(d)** and δ 8.16 for **(e)**, however, this signal was absent from the minor isomer. The presence of isomers was also detected in the ^{13}C -{^{1}H} NMR spectra. For **(d)**, which is an oil, the mixture could not be separated by crystallisation. Hence, the mixture was reacted with $Pd(OAc)_2$ and the structure of one of the products from the reaction was determined by X-ray diffraction (see **Fig. 2.4** later). This showed that the ligand was derived from the minor component of **(d)** which has structure **(B)** **(Fig. 2.1)**. With this information it has been possible to assign peaks for both isomers (see Experimental)

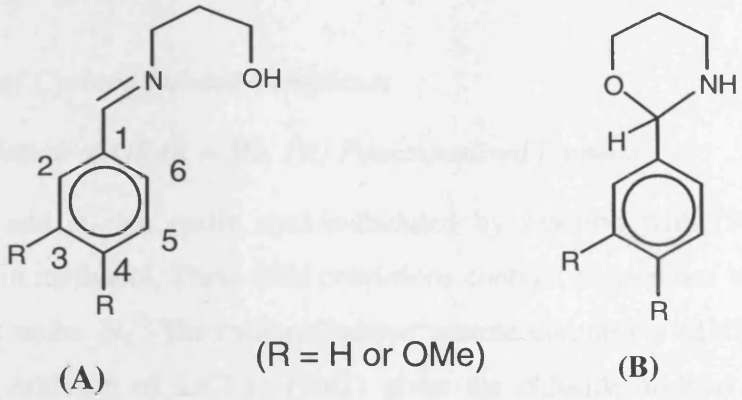

Fig. 2.1 Isomers of ligands **(d** and **e)**

Ligand **(e)** is a solid and crystallisation gave a crystal that was suitable for X-ray crystallography. This showed that the crystal was the major isomer **(A)**, with E configuration (see **Fig 2.2**). Selected bond lengths and angles are shown in **Table 2.1.**

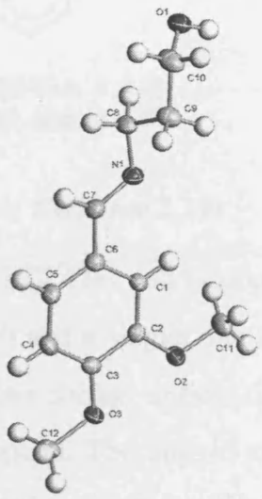

Fig. 2.2 Molecular structure of isomer A of ligand **(e)**

Table 2.1 Selected bond distances [Å] and bond angles [°] for imine (**e**).

Bond distances/[Å]			
C(6)-C(7)	1.465(2)	N(1)-C(7)	1.271(2)
C(6)-C(1)	1.406(2)	N(1)-C(8)	1.463(2)
Bond angles/ [°]			
C(1)-C(6)-C(7)	122.50(10)	C(7)-N(1)-C(8)	117.59(10)
C(5)-C(6)-C(7)	118.56(11)		

2.2.2 Preparation of Cyclopalladated Complexes

2.2.2a Cyclopalladation of OR (R = Me, Ph) Functionalised Ligands

The imines (**a** and **b**) are easily cyclopalladated by reaction with $[Pd(OAc)_2]_3$ at room temperature for 2h in methanol. These mild conditions contrast to previous work which reported refluxing overnight under N_2.[3] The cyclopalladated acetate complexes (**2.42a, b**) were isolated and characterised. Addition of LiCl to (**2.42**) gives the chloride-bridged dimers, $[Pd(L)Cl]_2$ (**2.43**), which precipitate from solution in good yield (**Scheme 2.19**). All the complexes were characterised by ^1H and $^{13}C\text{-}\{^1H\}$ NMR spectroscopy, FAB mass spectrometry, IR, elemental analysis and in some cases X-ray crystallography.

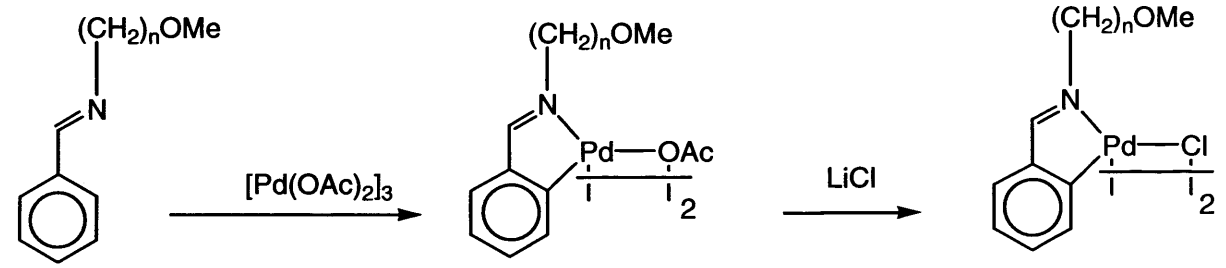

(a, n = 2) **(2.42a, n = 2)** **(2.43a, n = 2)**
(b, n = 3) **(2.42b, n = 3)** **(2.43b, n = 3)**

(Scheme 2.19)

The ^1H NMR spectra of complexes (**2.42a**) and (**2.43a**), with a C_2H_4 linker, show a singlet due to the methoxy group at *ca.* δ 3.30 and a singlet due to the imine proton (N=CH) at δ 7.29 (**2.42a**) or δ 7.83 (**2.43a**), these latter are shifted upfield 0.9 ppm (**2.42a**) and 0.36 ppm (**2.43a**) respectively compared with the free ligand. The upfield shift of the imine proton suggests that the imine is in the *E*-isomer as expected for cyclometallation to occur. In the aromatic region, there are four different multiplets each integrating to 1H. This confirms that one of the *ortho* protons has been replaced by the palladium. Orthometallation was confirmed by the $^{13}C\text{-}\{^1H\}$

NMR spectra, which showed only four aromatic carbons having protons attached and two quaternary aromatic carbons. The two acetate groups in (**2.42a**) are observed as a 6H singlet at δ 2.13. The equivalence of the acetate groups means the complex is an *anti*-isomer rather than *syn* (**Fig. 2.3**) or that the isomers are exchanging fast on the NMR timescale.

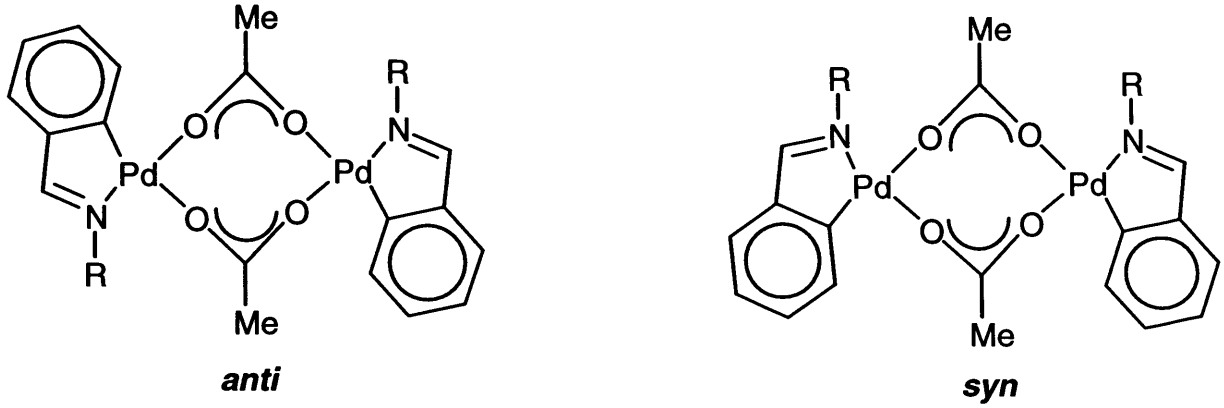

(Fig. 2.3)

Fernandez *et al.* showed that both the *syn* and *anti* isomers are present in acetate dimer (**2.44**). [28] Three resonances were observed for the OAc groups in the ^{1}H NMR spectrum; one for the *anti* isomer and two for the *syn* isomer. Similar observations were made by Ryabov *et al*, for complex (**1.3**).[51] Balavoine *et al* reported that the *syn* and *anti* isomers of (**1.85**) interconvert fast on the NMR timescale at ambient temperature, hence a sharp singlet is seen for the acetate protons.[52]

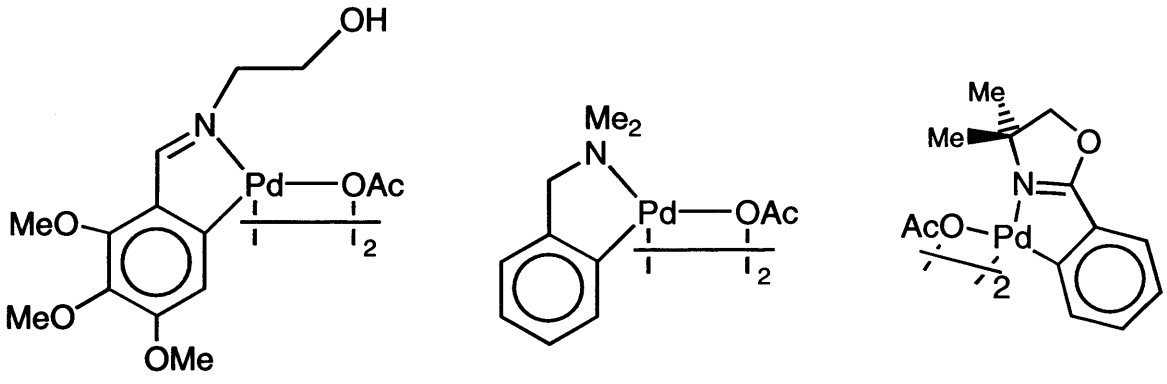

(2.44) **(1.3)** **(1.85)**

The ^{13}C-{^{1}H} NMR spectra of (**2.42a**) and (**2.43a**) show the expected peaks, the signals for (OMe) were observed at *ca* δ 59 ppm with the imine carbon at δ 173.82 (**2.42a**) and δ 176.21 (**2.43a**). The signals for (OAc) in (**2.42a**) were found at δ 24.67 and 181.36 ppm, suggesting that only one isomer (*anti*) is present in the solution. The IR spectra show strong absorptions at 1610 (**2.42a**) and 1613 cm^{-1} (**2.43a**) due to the C=N stretch which are at lower energy than the free ligand (1646 cm^{-1}), consistent with coordination of nitrogen to the metal. Strong absorption

bands at 1565 and 1413 cm^{-1} confirmed the presence of bridging acetate in **(2.42a)**, this is consistent with related acetate-bridged dimers.[53] FAB mass spectrometry confirmed that **(2.42a)** and **(2.43a)** are dimers, molecular ions being observed at *m/z* 655 due to $[M-H]^+$ and 608 $[M]^+$ respectively and fragment ions at *m/z* 597 $[Pd_2L_2(OAc)]^+$ **(2.42a)**, and 573 $[Pd_2L_2Cl]^+$ **(2.43a)**.

The ^1H NMR spectra of **(2.42b)** and **(2.43b)** with a C_3H_6 linker, show singlets due to the imine protons at δ 7.19 and 7.81, upfield shifts compared to the free ligand of 0.49 and 1.11 ppm respectively, confirming the *E*-configuration of the imine. In **(2.42b)** and **(2.43b)**, a singlet at *ca.* δ 3.28 is assigned to the OMe group, and the number of protons in the aromatic region confirms the orthometallation. In **(2.42b)**, the (OAc) protons give rise to a singlet at δ 2.13 consistent with the *anti* isomer, or the isomers could be exchanging fast on the NMR timescale. In the $^{13}C-\{^1H\}$ NMR spectra, four signals in the aromatic region due to CH carbons and two signals for quaternary carbons are seen for each complex, the imine carbon is observed at δ 172.54 **(2.42b)** and δ 174.97 **(2.43b)**. IR spectra of **(2.42b)** and **(2.43b)** are similar to those of **(2.42a)** and **(2.43a)**, with υ(C=N) at *ca.* 1610 cm^{-1}confirming coordination of the imine; in **(2.42b)**, bands due to bridging acetate are observed at 1570 and 1410 cm^{-1}. FAB mass spectrometry confirmed that **(2.42b)** and **(2.43b)** are dimers, molecular ions being observed at *m/z* 684 and 636 respectively and fragment ions at *m/z* 625 $[Pd_2L_2(OAc)]^+$ **(2.42b)** and 601 $[Pd_2L_2Cl]^+$ **(2.43b)**.

The related ether-functionalised ligands **(f)** and **(g)** were reacted in a similar way to **(a)** and **(b)**, however the acetate complexes were converted, directly to the chloride- bridged dimers **(2.43f)** and **(2.43g)** **(Scheme 2.20)**. The cyclometallations were confirmed by ^1H NMR spectroscopy, IR spectroscopy, FAB mass spectra and X-ray diffraction.

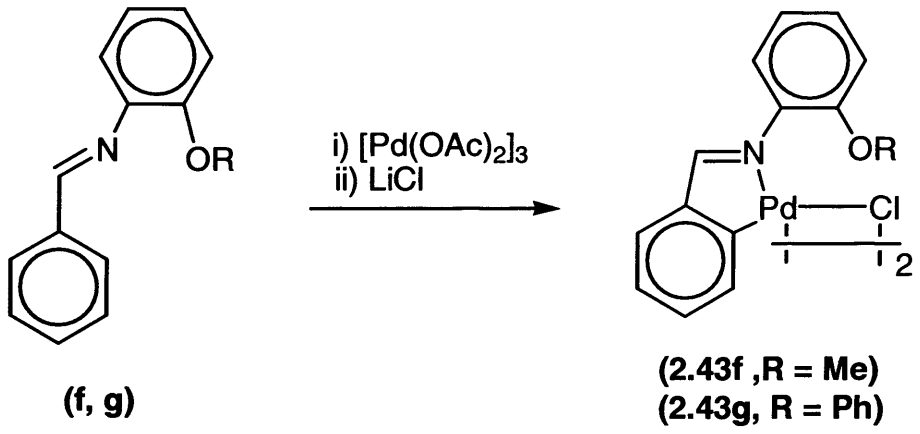

(f, g)

(2.43f ,R = Me)
(2.43g, R = Ph)

(Scheme 2.20)

The ^1H NMR spectra of **(2.43f)** and **(2.43g)** show only one set of signals, suggesting that the compounds exist in $CDCl_3$ solutions as a single geometrical isomer (*anti* or *syn* geometry), or the isomers are exchanging quickly on the NMR timescale. The imine proton is observed as a singlet

at δ 7.90 or δ 8.00 respectively, shifted upfield 0.3 ppm compared to the free ligands, confirming that the imine has the E configuration and is coordinated to the metal. FAB mass spectrometry showed ions at *m/z* 669 **(2.43f)** and 792 **(2.43g)** due to $[Pd_2L_2Cl]^+$. The IR spectra of **(2.43f)** and **(2.43g)** show a υ(N=C) absorption at 1602 and 1598 cm^{-1} compared to 1628 and 1629 cm^{-1} respectively in the free ligands.

Crystals of **(2.43b)**, **(2.43f)** and **(2.43g)** suitable for X-ray determination were obtained from dichloromethane/hexane. The structures are shown in **Fig. 2.4**, **Fig. 2.5** and **Fig. 2.6**. All three complexes are *anti* isomers of chloride-bridged dimers, in none of the complexes is there any interaction of the OR (R = Me, Ph) with the metal. Selected bond distances and angles are listed in **Table 2.2**.

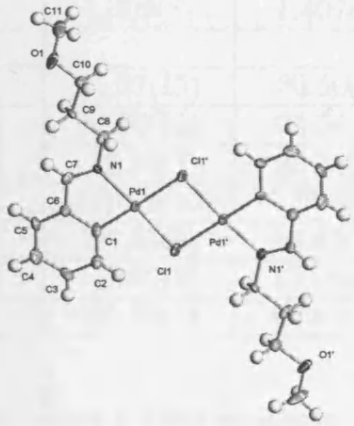

Fig. 2.4 Molecular structure of **2.43b**

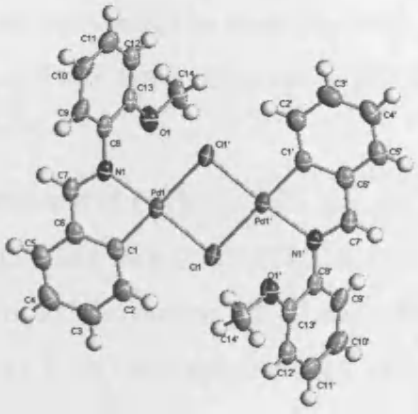

Fig. 2.5 Molecular structure of **2.43f**

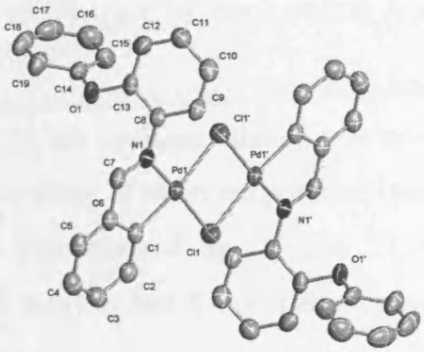

Fig. 2.6 Molecular structure of **2.43g**

Table 2.2 Selected bond distances [Å] and bond angles [°]

for complex **2.43b, 2.43f and 2.43g.**

Bond distances/[Å]	**2.43b**	**2.43f**	**2.43g**
Pd(1)-C(1)	1.979(4)	1.980(3)	1.975(3)
Pd(1)-N(1)	2.028(3)	2.035(2)	2.035(2)
Pd(1)-Cl(1)	2.3237(9)	2.3340(7)	2.3263(8)
N(1)-C(7)	1.281(5)	1.285(3)	1.287(3)
Pd(1)-Cl(1`)	2.4549(9)	2.4736(7)	2.4681(8)
C(6)-C(7)	1.437(5)	1.429(4)	1.435(1)
C(1)-C(6)	1.409(5)	1.407(4)	1.405(4)
Bond angles/ [°]			
C(1)-Pd(1)-N(1)	81.27(13)	80.50(10)	80.95(10)
C(1)-Pd(1)-Cl(1)	94.80(11)	95.54(8)	95.10(8)
Cl(1)-Pd(1)-Cl(1)`	86.10(3)	85.33(3)	86.64(3)
C(1)-Pd(1)-Cl(1)`	179.09(10)	178.68(8)	172.60(8)
N(1)-Pd(1)-Cl(1)`	97.83(8)	98.62(7)	97.89(7)
N(1)-Pd(1)-Cl(1)	176.07(8)	175.96(6)	173.79(6)
Pd(1)-Cl(1)-Pd(1)`	93.90(3)	94.67(3)	93.36(3)

In each case the palladium atom adopts a distorted square-planar geometry with the distortion most noticeable in the cyclometallated chelate angle C(1)-Pd(1)-N(1) of *ca* 81°, the sum of angles about the palladium atom is 360° **(2.43b)**, 360° **(2.43f)** and 360.6° **(2.43g)**. The Pd-Cl bonds *trans* to C range from 2.4549(9) to 2.4736(7) Å, whereas those *trans* to nitrogen range from 2.3237(9) to 2.3340(7) Å in accordance with the relative *trans* influences of C and N. The bond lengths are similar to those reported previously for chloride-bridged dimer complexes e.g the Pd-C and Pd-N bond distances in $[Pd\{C_6H_4C(H)=NPh\}(\mu\text{-}Cl)]_2$ are 1.965(2) Å and 2.022(1) Å respectively.[54]

The influence of the palladium starting material on the cyclometallation was investigated by reacting ligand **(a)** with $[PdCl_2(PhCN)_2]$ in dichloromethane at room temperature **(Scheme 2.21)**. This led to the formation of **(2.45)** which was characterised by ^1H and $^{13}C\text{-}\{^1H\}$ NMR spectroscopy, FAB mass spectrometry, IR, elemental analysis and X-ray crystallography.

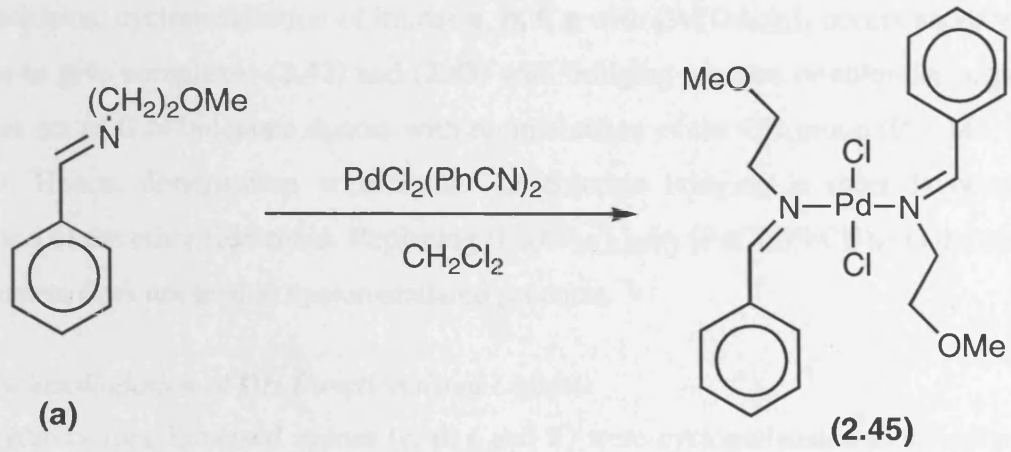

(a) (2.45)

(Scheme 2.21)

The ^{1}H and ^{13}C-{^{1}H} NMR spectra show two isomers in a 3:1 ratio, the major isomer showed two multiplets integrating to 5H in the aromatic region due to the phenyl ring, indicating that cyclometallation had not occurred. The mass spectrum showed ions corresponding to $[L_2PdCl]^+$ at *m/z* 467 and fragment at 431 due to further loss of HCl. The structure of **(2.45)** was determined by X-ray crystallography **(Fig. 2.7)**, and confirmed that the major isomer is a simple *trans* bis imine complex. Thus, acetate is necessary for facile cyclometallation in this case.

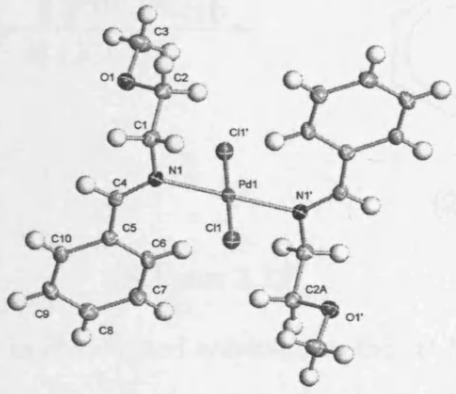

Fig. 2.7 Molecular structure of **2.45**

Table 2.3 Selected bond distances [Å] and bond angles [°] for complex **(2.45)**.

Bond distances/[Å]			
Pd-Cl(1)	2.3023(4)	N(1)-C(4)	1.277(2)
Pd-N(1)	2.016(2)	C(4)-C(5)	1.459(2)
Bond angles/ [°]			
N(1)-Pd-Cl(1)	91.34(4)	N(1)-Pd-N(1`)	180.00(8)

In conclusion, cyclometallation of imines **a, b, f, g** with $[Pd(OAc)_2]_3$ occurs under very mild conditions to give complexes **(2.42)** and **(2.43)** with bridging-acetates or chlorides respectively. The imines act as C,N-bidentate donors with no interaction of the OR group (R = Me, Ph) with the metal. Hence, dimerisation with acetate or chloride bridging is more favourable than coordination of the ether side chain. Replacing $[Pd(OAc)_2]_3$ by $[PdCl_2(PhCN)_2]$ in the absence of sodium acetate does not lead to cyclometallated products.

2.2.2b Cyclopalladation of OH Functionalised Ligands

The hydroxy-functionalised imines (**c, d, e** and **h**) were cyclopalladated in a similar manner to (**a, b, f** and **g**). Thus, imine (**c**) was reacted with $[Pd(OAc)_2]_3$ followed by LiCl leading to formation **(2.43c)** **(Scheme 2.22)**. A similar reaction was reported by Navarro *et al.*[3] as discussed earlier **(Scheme 2.15)**.

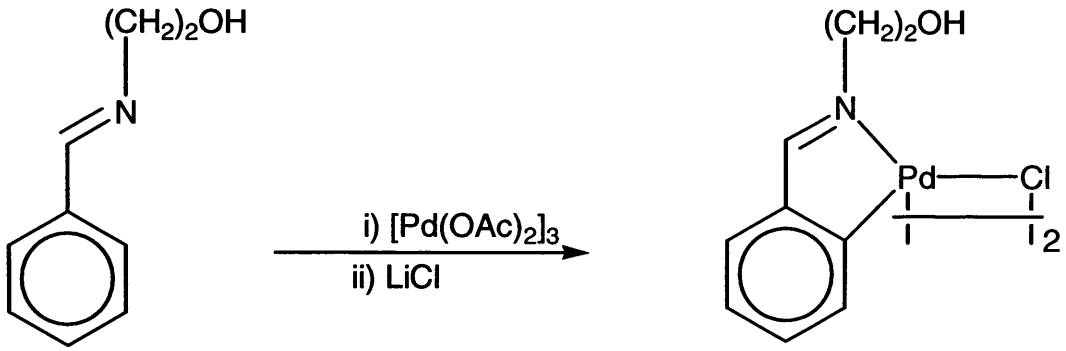

(c) **(2.43c)**

(Scheme 2.22)

Complex **(2.43c)** is insoluble in chlorinated solvents, so the ^1H NMR spectrum was recorded in d^6-DMSO however, some peaks were broad, and no signals could be observed in the $^{13}C-\{^1H\}$ NMR spectrum. The ^1H NMR spectrum of **(2.43c)** showed four inequivalent protons (as broad peaks) in the aromatic region as expected for the orthometallated product. The imine proton was observed at δ 7.90, approximately 0.3 ppm upfield from the corresponding signals in the free ligands, as expected for the E-isomer. The OH proton was observed at δ 4.55, close to that (δ 4.77) observed by Navarro *et al.* in **(2.28)**,[3] suggesting that the OH group is not coordinated and a chloride-bridged dimer structure is more stable. The υ(N=C) stretch is observed at 1613 cm^{-1}, about 30 cm^{-1} less than the free ligand, as expected for coordination of the imine. The FAB mass spectrum of **(2.43c)** shows a cluster of ions with a maximum at *m/z* 545 corresponding to $[Pd_2L_2Cl]^+$ and fragment ions at *m/z* 254 due to $[PdL]^+$. The elemental analysis is also consistent with the formulation **(2.43c)**.

As mentioned previously, ligand **(d)** exists as isomers **(d, d`)**, and this mixture was reacted with $[Pd(OAc)_2]_3$ to give a green crystalline precipitate, which was insoluble in chlorinated solvents. The ^1H NMR spectrum was recorded in d^6-DMSO, however, no signals were observed. FAB mass spectrometry shows ions at *m/z* 596 corresponding to the dimeric species $[Pd_2L_2(OAc)]^+$ and another cluster at 268 corresponding to the monomeric fragment $[PdL]^+$. The IR spectrum of the product from **(d, d`)** showed the band at 1563 and 1413 cm^{-1}, suggesting a bridging acetate, and bands at 1605 $cm^{-1}$and 3396 cm^{-1} assigned to (N=C) and (OH) respectively, suggesting the presence of the imine isomer **(d)**. However, the precise identity of the compound(s) formed from **(d)** cannot be ascertained from this data.

Recrystallisation from MeOH/ether gave crystals suitable for X-ray diffraction. The X-ray structure of the crystals showed an acetate-bridged dimer **(2.42d')**, containing a cyclometallated aminal **(Fig. 2.8)**. Selected bond distances and angles are listed in **Table 2.3**. The complex adopts the *anti* geometry, and the coordination geometry around each palladium atom is approximately square-planar. The Pd(1)-C(1) and Pd(1)-N(1) bond distances [1.952(5) and 2.047(4) Å] are similar to the values [1.96(2) and 2.022(12) Å] in $[Pd(\mu\text{-}OAc)(C_6H_4\text{-}^i\text{Pr-oxaz})]_2$.[55] The *trans* influence of the σ-bonded carbon is illustrated by the lengthening of the Pd-O bond *trans* to carbon [2.143(3) and 2.130(3) Å] relative to those *trans* to nitrogen atoms [2.049(3) and 2.053(3) Å]. The long distance between both palladium [3.123(3) Å] confirms that these is no interaction between them.

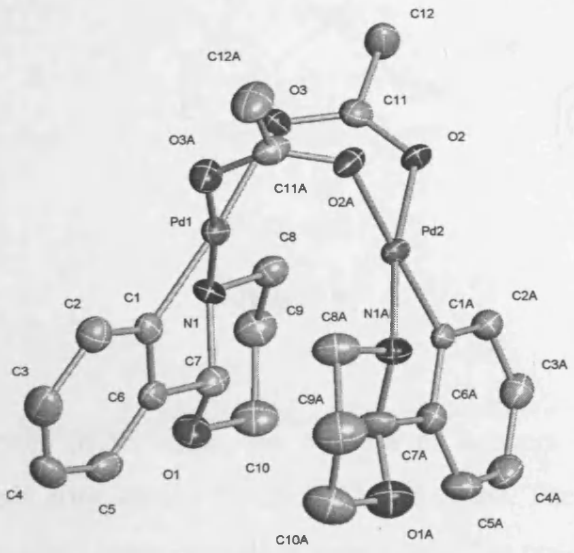

Fig. 2.8 Molecular structure of **2.42d`**(All hydrogen atoms have been omitted).

Table 2.4 Selected bond distances [Å] and bond angles [°] for complex **2.42d`**

Bond distances/[Å]			
Pd(1)-C(1)	1.952(5)	C(1)-C(6)	1.399(6)
Pd(1)-N(1)	2.047(4)	Pd(2)-O(2)	2.053(3)
Pd(1)-O(3)	2.143(3)	N(1)-C(7)	1.473(6)
Pd(1)-O(3A)	2.049(3)	O(1)-C(7)	1.399(5)
Pd(2)-O(2A)	2.130(3)	C(6)-C(7)	1.494(6)
Bond angles/ [°]			
N(1)-Pd(1)-O(3A)	172.57(14)	C(1)-Pd(1)-O(3A)	93.20(17)
C(1)-Pd(1)-O(3)	172.68(15)	O(3A)-Pd(1)-O(3)	90.68(13)
C(1)-Pd(1)-N(1)	80.78(17)	N(1)-Pd(1)-O(3)	94.85(13)

The complex was formed from the minor component of the ligand (**d`**), the product from the major imine isomer could be a mononuclear complex (**2.46d**) or the acetate-bridged dimer (**2.42d**) as shown in **Fig. 2.9**.

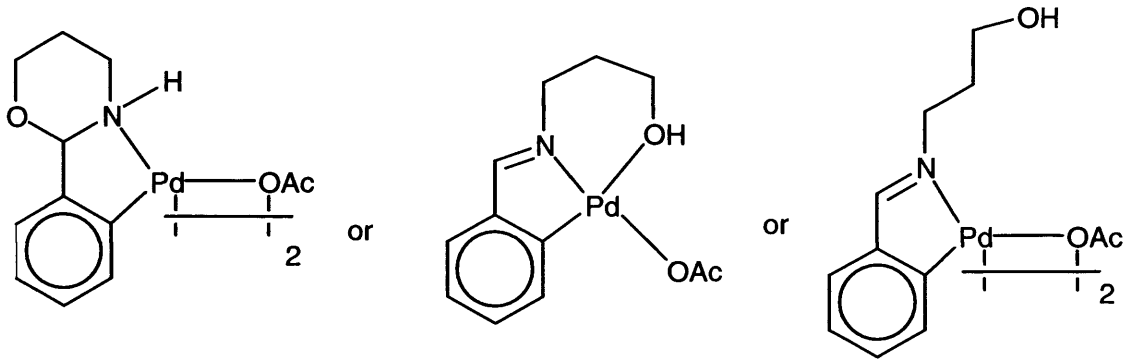

(2.42d') **(2.46d)** **(2.42d)**

(Fig. 2.9)

To try and gain further information, the mixture of isomers (**d, d`**) was reacted with $[Pd(OAc)_2]_3$ in MeOH, then after stirring for 2h, LiCl was added. The solution was concentrated and hexane was added to give a green crystalline precipitate. The possible products are shown in **Scheme 2.23**.

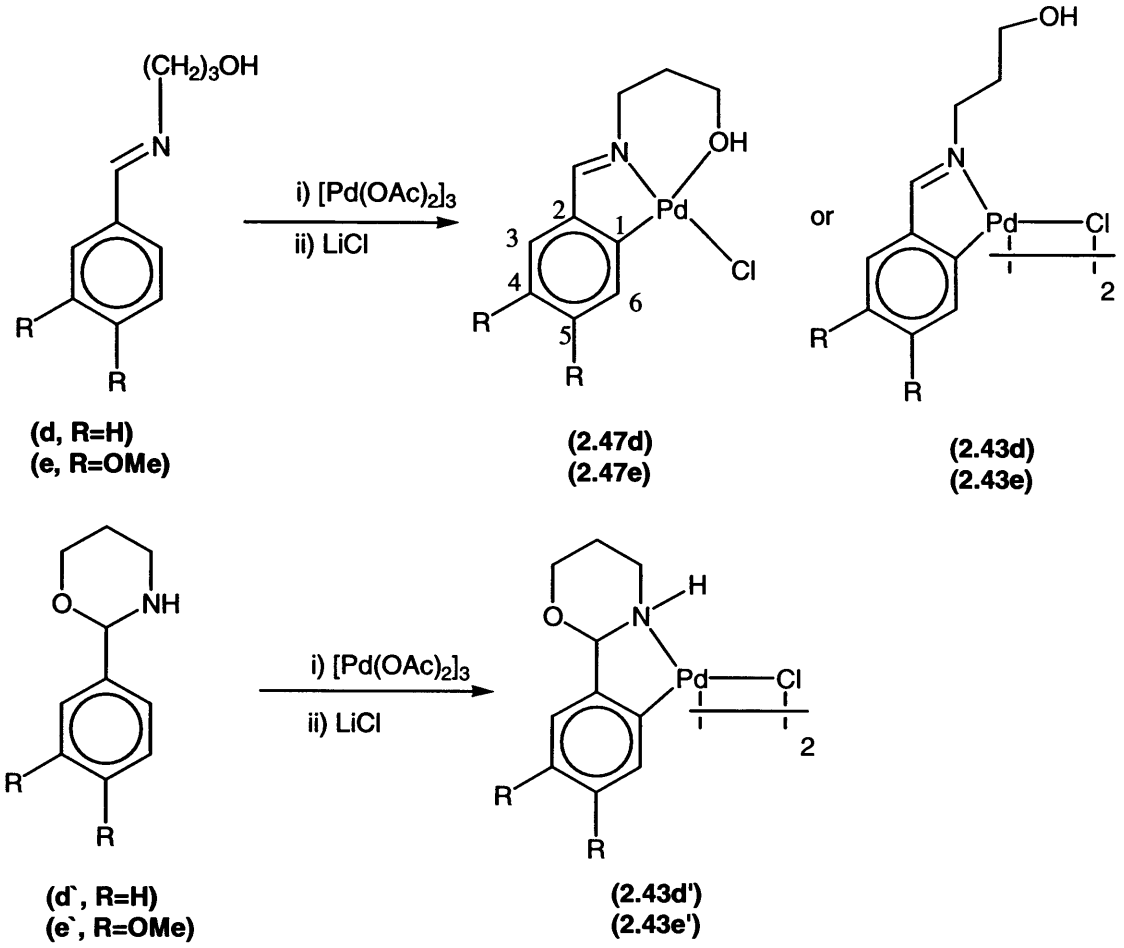

(Scheme 2.23)

The green precipitate formed from (**d, d`**) was insoluble in chlorinated solvents and the $^{1}H$ and $^{13}C$-{$^{1}H$} NMR spectra of the mixture in $d^{6}$-DMSO showed no signals at all. The FAB mass spectrum of the product from (**d, d`**) showed ions at *m/z* 268 $[Pd(L)]^{+}$, and no sign of dimeric species (**2.43d**) or (**2.43d`**). The IR spectrum of the precipitate showed a band assigned to N=C at 1585 $cm^{-1}$, about 60 $cm^{-1}$ less than the free ligand as expected for coordination of the imine isomer (**d**). A band assigned to υ(O-H) is seen at 3118 $cm^{-1}$ (*c.f.* 3282 $cm^{-1}$ for free OH in (**d, d`**)). The low energy possibly suggesting coordination of the OH.

Crystals were obtained from the mixture suitable for X-ray diffraction, the structure showed that the crystal was derived from the imine isomer with the oxygen coordinated to palladium to form a mononuclear (C,N,O) tridentate complex. The structure is shown in (**Fig. 2.10**) with selected bond distances and angles in **Table 2.5**. Hence, the coordination of the oxygen tether occurs to form (**2.47d**) rather than dimerisation through chloride bridges to form (**2.43d**). Since the chloride complex (**2.47d**) exists as C,N,O tridentate ligand it may be that the precursor acetate complex exists as (**2.46d**) rather than (**2.42d**) (**Fig. 2.9**). The fate of the minor isomer (**d`**) in this reaction is not known. For further discussion of the structure see later.

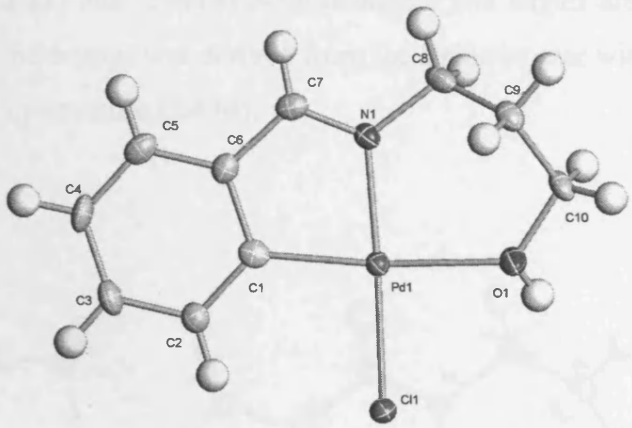

Fig. 2.10 Molecular structure of **2.47d**

Table 2.5 Selected bond distances [Å] and bond angles [°] for complex **2.47d**

Bond distances/[Å]		Bond angles/ [°]	
Pd(1)-C(1)	1.963(5)	C(1)-Pd(1)-O(1)	172.58(14)
Pd(1)-N(1)	2.008(3)	C(1)-Pd(1)-N(1)	81.03(16)
Pd(1)-O(1)	2.168(3)	N(1)-Pd(1)-O(1)	93.35(13)
Pd(1)-Cl(1)	2.320(2)	O(1)-Pd(1)-Cl(1)	89.40(9)
C(1)-C(6)	1.416(6)	C(1)-Pd(1)-Cl(1)	96.21(13)
N(1)-C(7)	1.272(5)	N(1)-Pd(1)-Cl(1)	177.23(10)
C(6)-C(7)	1.445(6)		

The reaction of **(e, e`)** with $[Pd(OAc)_2]_3$ followed by LiCl was carried out and the corresponding products are also shown in **Scheme 2.23**. The precipitate from **(e, e`)** was more soluble in chlorinated solvents than that from **(d, d`)** and the ^{1}H NMR spectrum showed a mixture of products. The FAB mass spectrum of the solid showed of ions at *m/z* 728 and 693 corresponding to dimeric species $[Pd_2L_2Cl_2]^+$ and $[Pd_2L_2Cl]^+$ and another cluster at 365 corresponding to the monomeric fragment $[Pd(L)Cl]^+$. Attempted separation of the mixture by column chromatography led to isolation of only one product.

The ^{1}H NMR spectrum of the isolated product shows two singlets at δ 3.81 and 3.90 due to two methoxy groups and a singlet at δ 7.72 due to the imine, confirming the presence of isomer **(e)**, an upfield shift of 0.4 ppm on coordination, as expected for the E-isomer. A broad singlet at δ 4.53 is assigned to the OH group, consistent with the imine isomer **(e)** since **(e`)** does not contain an OH group. In the aromatic region there are only two singlets at δ 6.76 (H^3) and δ 7.18 (H^6) each integrating to 1H. This confirms that one of the *ortho* protons has been replaced by the palladium. The υ(N=C) stretch is observed at 1633 cm^{-1}, about 15 cm^{-1} less than the free ligand, as expected for coordination of the imine. The structure of **(2.47e)** has been determined by X-ray

crystallography **(Fig. 2.11)** and selected bond distances and angles are listed in **Table 2.6**. The structure showed that the crystal was derived from the imine isomer with the oxygen coordinated to palladium as found in structure **(2.47d)**.

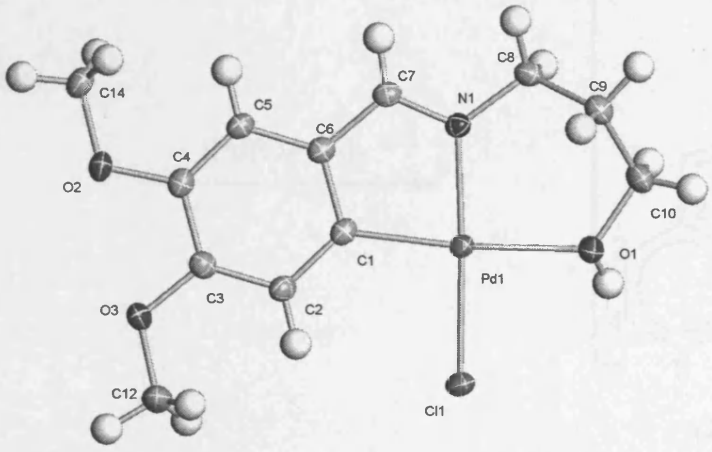

Fig. 2.11 Molecular structure of **2.47e**

Table 2.6 Selected bond distances [Å] and bond angles [°] for complex **2.47e**

Bond distances/[Å]		**Bond angles/ [°]**	
Pd(1)-C(1)	1.983(3)	C(1)-Pd(1)-O(1)	173.89(9)
Pd(1)-N(1)	2.014 (2)	C(1)-Pd(1)-N(1)	81.48(10)
Pd(1)-O(1)	2.167(2)	N(1)-Pd(1)-O(1)	93.04(8)
Pd(1)-Cl(1)	2.3103(7)	O(1)-Pd(1)-Cl(1)	89.30(5)
C(1)-C(6)	1.408(4)	C(1)-Pd(1)-Cl(1)	96.17(8)
N(1)-C(7)	1.291(3)	N(1)-Pd(1)-Cl(1)	177.65(6)
C(6)-C(7)	1.439(4)		

The palladium atoms in **(2.47d, e)** adopt a distorted square-planar geometry. In both structures, the N(1)-Pd(1)-O(1) chelate bite angle [93.35(13) and 93.04(8)° respectively] is larger than that for the C(1)-Pd(1)-N(1) [81.03(16) and 81.48(10)°], which is expected because of the larger chelate ring size (six-membered ring rather than five-membered ring). The Pd-C(1) bond distances [1.963(5) and 1.983(3) Å respectively] and Pd-N(1) bond distances [2.008(3) and 2.014(2) Å] are similar in both complexes.

Reaction of phenol-containing ligand **(h)** with $[Pd(OAc)_2]_3$ at room temperature gave a dark red precipitate **(2.48h)** **(Scheme 2.24)**. Repeating the reaction with addition of LiCl gave the same result. During the course of this research, this compound has been made and reported by Lopez *et al.*[44] by refluxing the reagents overnight. Complex **(2.48h)** was characterised by ^1H and

^{13}C-{H} NMR spectroscopy, FAB mass spectrometry, IR spectroscopy, elemental analysis and X-ray crystallography and the results are in agreement with those of Lopez *et al.*[44]

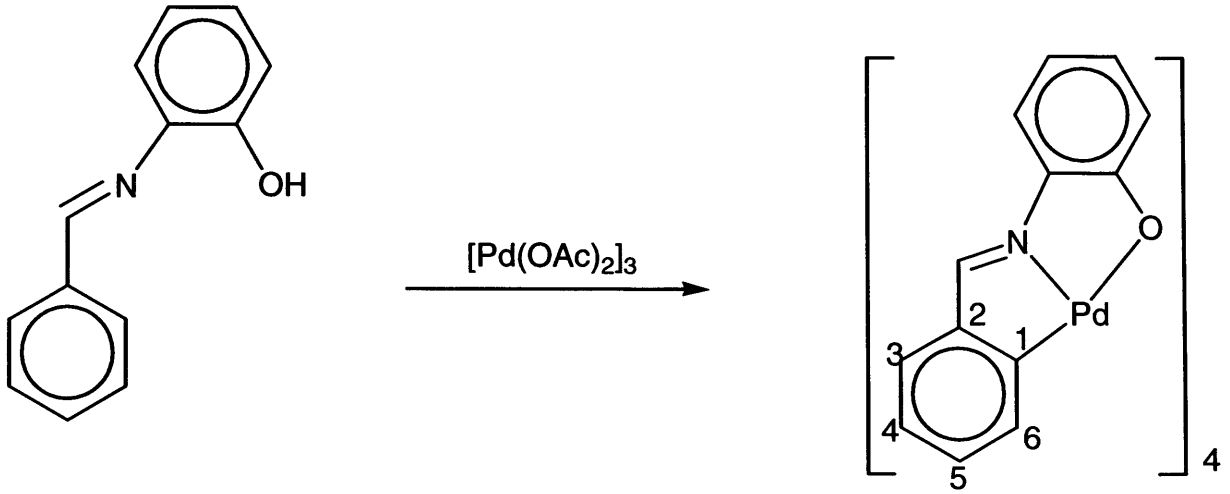

(h) **(2.48h)**

(Scheme 2.24)

The ^{1}H NMR spectrum of the product shows a singlet due to the imine proton at δ 7.12 shifted upfield (1.56 ppm) from the starting ligand. Four multiplets each integrating to 1H are observed in the aromatic region, confirming the cyclometallation. The proton (H^6) is also shifted upfield (1.36 ppm) due to the shielding effect of the phenyl rings of a neighbouring metallated ligand. The complex is only slightly soluble in $CHCl_3$, hence in the ^{13}C-{^{1}H} NMR spectrum only eight signals were observed in the aromatic region with a signal at δ 157.6 due to (HC=N).

The FAB mass spectrum showed a cluster of ions with a maximum at *m/z* 1207 corresponding to $[Pd(L)]_4$ (LH_2 = imine) and the isotopic pattern is in good agreement with a tetramer. The IR spectrum shows a υ(N=C) absorption at 1591 cm^{-1} compared to 1625 cm^{-1} in the free ligand, and there is no υ(OH) band consistent with the loss of the OH proton.

A crystal suitable for X-ray diffraction was obtained, and the structure in **Fig. 2.12** confirms that the complex **(2.48h)** is a tetramer. Selected bond distances and angles are listed in **Table 2.7**. In contrast to the alcohol containing ligands **(d)** and **(e)**, the phenol **(h)** is deprotonated on coordination, consistent with the greater acidity of phenol giving a dianionic CNO-tridentate ligand, each oxygen also bridges to another palladium atom.

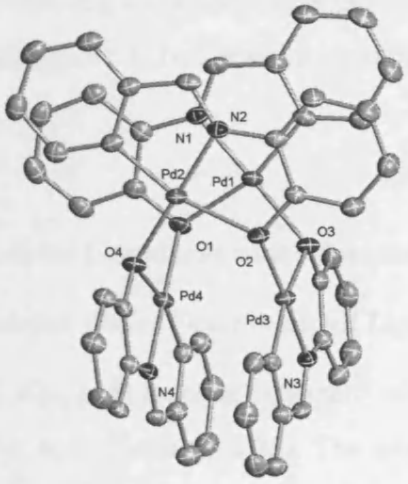

Fig. 2.12 Molecular structure of **2.48h** (All hydrogen atoms have been omitted).

Table 2.7 Selected bond distances [Å] and bond angles [°] for complex **2.48h**

Bond distances/[Å]		**Bond angles/ [°]**	
Pd(1)-C(1)	1.960(3)	N(1)-Pd(1)-O(1)	81.47(9)
Pd(1)-N(1)	1.952(3)	C(1)-Pd(1)-N(1)	82.39(12)
Pd(1)-O(1)	2.146(2)	C(1)-Pd(1)-O(1)	163.47(11)
Pd(1)-O(3)	2.053(2)	O(3)-Pd(1)-O(1)	98.65(8)
N(1)-C(7)	1.297(4)	N(1)-Pd(1)-O(3)	175.66(9)
C(1)-C(6)	1.413(4)	C(1)-Pd(1)-O(3)	97.72(11)
C(6)-C(7)	1.440(5)		
O(1)-C(13)	1.352(4)		

The Pd-O chelate bond length [2.146(2) Å] (*trans* to C) is longer than the Pd-O bridge bond [2.053(2) Å] (*trans* to N); due to the different influence of the ligand in the *trans* position, as reported by Lopez *et al* [2.132(11) and 2.029(7) Å respectively][44]. The Pd_4O_4 eight-membered ring has Pd.....Pd distances that are all greater than those found in the dimeric complexes, thus suggesting that there is no direct interaction between the Pd atoms.

In conclusion, hydroxy-functionalised imines **(c, d, e)** undergo orthometallation under very mild conditions. Coordination of the pendant oxygen to the metal to give a C,N,O-tridentate ligand complex depends on the length of the chain and the nature of the O-donor group. Thus for imine **(c)** containing a $(CH_2)_2OH$ group, dimerisation via chloride bridges in **(2.43c)** is more favourable than coordination of the OH as found previously for the related complex **(2.28)**.[3] In contrast, the $(CH_2)_3OH$-functionalised imines **(d, e)** prefer to form monomeric cyclometallated complexes with C,N,O-tridentate coordination **(2.47d, e)** rather than dimeric species. If the

oxygen donor is the more acidic phenol (**h**) coordination of O is accompanied by deprotonation to form the tetramer (**2.48h**) containing a dianionic C,N,O-tridentate ligand. A similar tetrameric complex (**2.24**) containing a dianionic C,N,S-phenylbenzothiazoline ligand has been reported previously.[39]

2.2.3 Reaction of Cyclopalladated Complexes with Monodentate Ligands

2.2.3a Reaction of Cyclopalladated OMe- Functionalised Ligands with PPh_3

Chloride-bridged dimers (**2.43a, b, f**) react as expected[3] with two equivalents of PPh_3 to give mononuclear derivatives (**2.49a, b, f**) (**Scheme 2.25**). The products were obtained in high yield and were characterised by ^1H, $^{13}C\{^1H\}$ and $^{31}P\{^1H\}$ NMR spectroscopy, FAB mass spectrometry, IR spectroscopy and microanalysis.

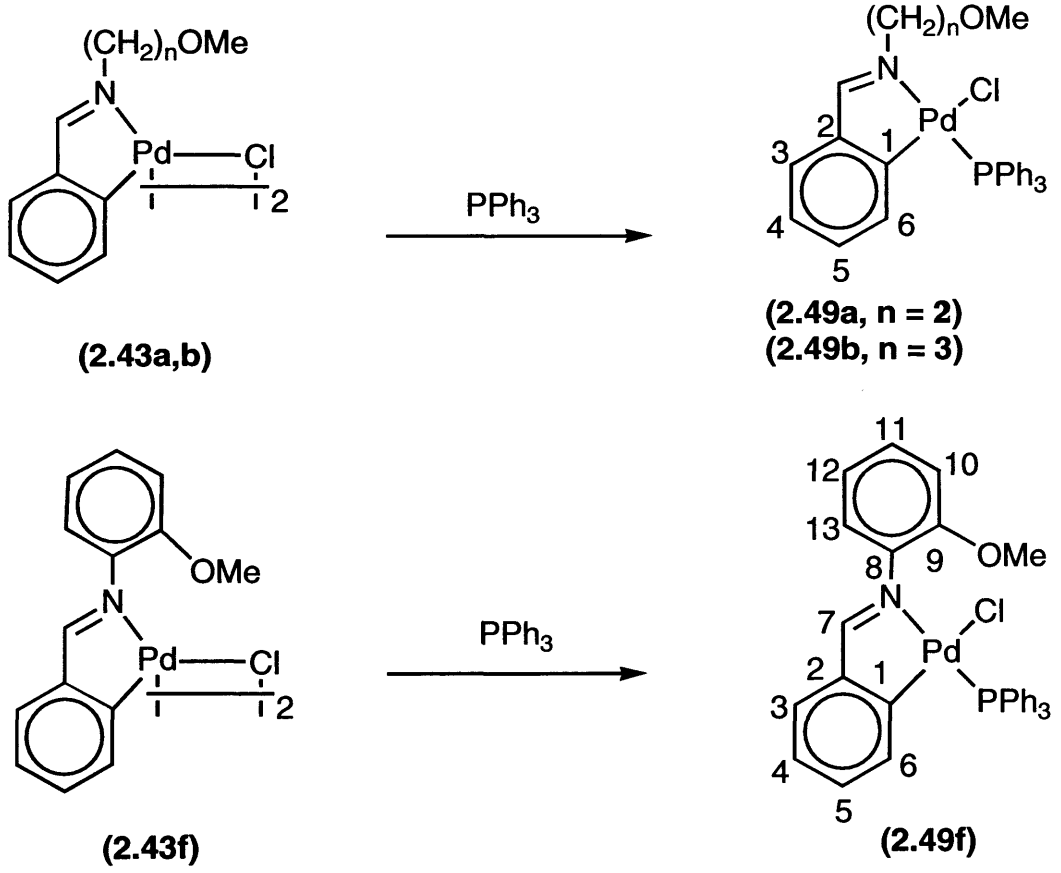

(Scheme 2.25)

The $^{31}P\{^1H\}$ NMR spectra of (**2.49a, b, f**) each show a singlet, at δ 39.5 (**2.49a**), 42.5 (**2.49b**) and 42.9 (**2.49f**) respectively, suggesting that only one isomer is present in solution. The ^1H NMR spectra of (**2.49a, b, f**) show four (1H) multiplets in the aromatic region due to the cyclometallated ligand, and one PPh_3 ligand. The imine protons are observed as doublets at δ

8.13 **(2.49a)**, δ 8.12 **(2.49b)** and δ 8.25 **(2.49f)**. The doublet coupling is to phosphorus (J_{PH} = 8 Hz) indicating the *trans* arrangement of the phosphine ligand and imine nitrogen.[3] The resonances due to (H^6) and (H^5) are shifted upfield, (0.74 to 1 ppm) and (0.37 to 0.52 ppm) respectively compared to the starting dimers, this is due to a ring-current of the adjacent PPh_3 ligand, confirming the P *trans* to N stereochemistry as found previously (e.g **(2.30)**).[3] Singlets at *ca* δ 3.36 **(2.49a, b)** and δ 3.87 **(2.49f)** are assigned to the OMe group. These chemical shifts are very similar to those of the starting compounds, suggesting that the OMe still has no interaction with the metal centre.

The ^{13}C-{^1H} NMR spectra of **(2.49a, b, f)** show signals corresponding to all the expected carbons, in particular the imine carbon is observed at δ 177.25 **(2.49a)**, 175.91 **(2.49b)** and 178.08 **(2.49f)** respectively, and OMe at δ 59.05 **(2.49a)**, 58.67 **(2.49b)** and 56.28 **(2.49f)**. In the aromatic region, (C^3, C^4, C^5) are observed at similar shifts to the starting dimers however the resonance for (C^1) is shifted downfield about 5 ppm after coordination of PPh_3. In each case, the PPh_3 ligand gives rise to two doublets at *ca.* δ 128 (C_m) and δ 135 (C_o) [d, *J* 12 Hz] and two singlets at δ 130 (C_p) and δ 131(C_i). The FAB mass spectra of **(2.49a), (2.49b)** and **(2.49f)** show ions at *m/z* 530, 544 and 578 respectively corresponding to $[M\text{-}Cl]^+$.

Careful recrystallisation of **(2.49b)** from dichloromethane/ether gave crystals suitable for X-ray diffraction. The X-ray structure is shown in **Fig. 2.13** with selected distances and angles in **Table 2.8**. The structure, confirms the coordination of PPh_3 *trans* to N and the bidentate nature of the cyclometallated imine.

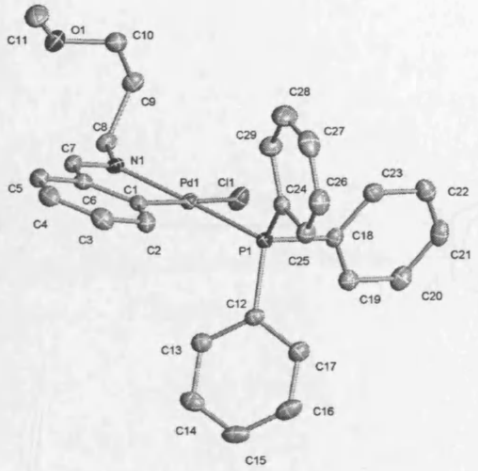

Figure 2.13 Molecular structure of **2.49b** (All hydrogen atoms have been omitted).

Table 2.8 Selected bond distances [Å] and bond angles [°] for complex **2.49b**.

Bond distances/[Å]		Bond angles/ [°]	
Pd(1)-C(1)	2.032(2)	C(1)-Pd(1)-N(1)	81.35(7)
Pd(1)-N(1)	2.102(2)	C(1)-Pd(1)-P(1)	93.94(6)
Pd(1)-P(1)	2.2493(6)	N(1)-Pd(1)-Cl(1)	92.05(5)
Pd(1)-Cl(1)	2.3691(6)	P(1)-Pd(1)-Cl(1)	92.64(2)
N(1)-C(7)	1.280(3)	N(1)-Pd(1)-P(1)	175.28(5)
C(1)-C(6)	1.415(3)	C(1)-Pd(1)-Cl(1)	172.94(6)
C(6)-C(7)	1.445(3)		

The palladium atom in **(2.49b)** is located in a slightly distorted square-planar environment. The Pd(1)-C(1) [2.032(2) Å] and Pd(1)-N(1) [2.102(2) Å] bond distances of the chelate ring are similar to those in [PdCl{C_6H_2-4,5-$(OMe)_2$-2-C(H)=N-CH_2CH_2OH}PPh_3] **(2.30, L = PPh_3)** [2.025(2) and 2.103(2) Å respectively][3], and slightly longer than those found in the chloride-bridged dimer **(2.43b)** [1.979(4) and 2.028(3) Å respectively].

2.2.3b Reaction of Cyclopalladated OH- Functionalised Ligands with PPh_3

Similar reactions were investigated with the alcohol-functionalised complexes. Thus, the dimer **(2.43c)** reacted easily with PPh_3 at room temperature and the product was characterised by ^1H, ^{13}C-{^1H} and ^{31}P-{^1H} NMR spectroscopy and FAB mass spectrometry, IR spectroscopy and microanalysis **(Scheme 2.26)**.

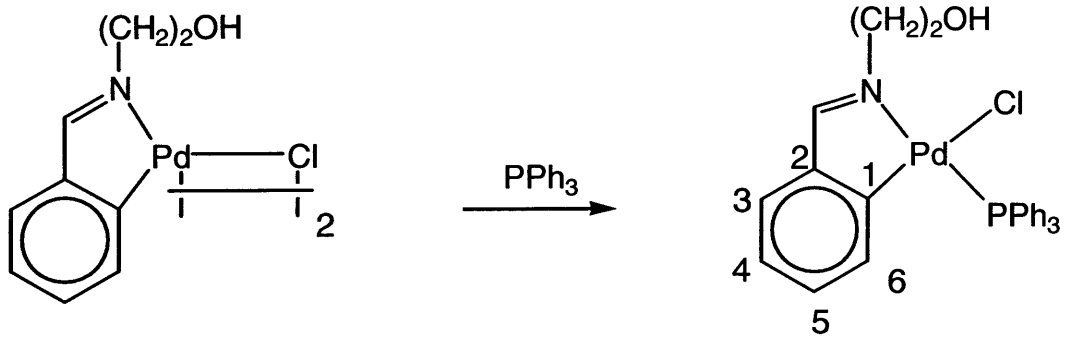

(2.43c) **(2.49c)**

(Scheme 2.26)

The ^{31}P-{^1H} NMR spectrum of **(2.49c)** shows a singlet at δ 41.14, suggesting the coordination of PPh_3 and appropriate resonances for PPh_3 are seen in the ^1H and ^{13}C-{^1H} NMR spectra. The ^1H NMR data is similar to that for [PdCl{C_6H_2-4,5-$(OMe)_2$-2-C(H)=N-

$CH_2CH_2OH\}PPh_3$] (**2.30, L = PPh_3**) reported by Navarro *et al.*.[3] The ^1H NMR spectrum of (**2.49c**) shows a broad signal at δ 2.59 due to the uncoordinated hydroxy group (*c.f.* δ 3.25 in **2.30**), this proton is expected to be further downfield if coordinated (see later in **2.53e, d**). The imine proton appears as a doublet coupling to P at δ 8.18 and the resonance for H^6 is observed at δ 6.41 ppm, shifted upfield due to shielding by the PPh_3 ligand, both these observations confirming the P *trans* to N stereochemistry. The $^{13}C-\{^1H\}$ NMR spectrum shows the expected signals. The FAB mass spectrum shows ions with maxima at *m/z* 551 and 516 corresponding to $[M]^+$ and $[M-Cl]^+$ respectively. The IR spectrum of (**2.49c**) shows the imine absorption at 1624 cm^{-1} and the OH stretch at 3430 cm^{-1}, the latter suggesting the OH group does not interact with the Pd as found by Navarro *et al* (*c.f.* 3459 cm^{-1} in **2.30**).[3]

The reaction of the C,N,O-tridentate complexes, (**2.47d**) and (**2.47e**) with PPh_3 was also investigated. Since (**2.47e**) was more easily obtained as a pure compound this is explained first. In this case, the reaction with PPh_3 could proceed by substitution of the alcohol, the orthometallated ligand being converted to bidentate coordination (two isomers possible), or by substitution of the chloride to form a cationic species. The possible products are shown in **Scheme 2.27**. The product was characterised by ^1H, $^{13}C-\{^1H\}$ and $^{31}P-\{^1H\}$ NMR spectroscopy, FAB mass spectrometry, IR spectroscopy and microanalysis.

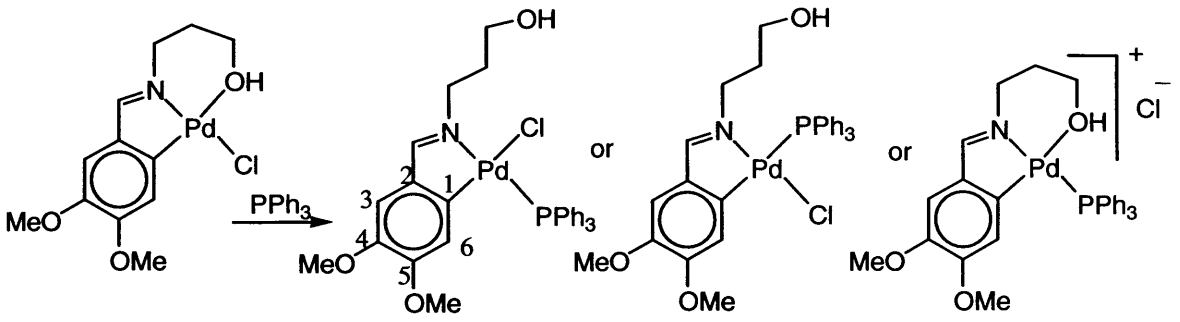

(**2.47e**) (**2.49e**) (**2.49e[a]**) (**2.49e[b]**)

(Scheme 2.27)

The $^{31}P-\{^1H\}$ NMR spectrum of the product showed a singlet, at δ 43.14, indicating a single product. The ^1H NMR spectrum is similar to those for (**2.49a**) and (**2.49b**). Thus, the imine proton was observed at δ 8.06 as a doublet due to coupling to phosphorus, suggesting the imine is *trans* to the PPh_3. The resonances due to (H^6) and the 5-OMe are both shifted upfield 1.5 and 1.09 ppm respectively compared to the starting material (**2.47e**) due to shielding by the PPh_3 providing further confirmation that the PPh_3 is adjacent to the metallated carbon and *trans* to the

nitrogen (*ie.* not **2.49e**[a]). The OH proton is observed at δ 2.99, compared to δ 4.53 in **(2.47e)** consistent with cleavage of the Pd-OH bond and formation of **(2.49e)** rather than (**2.49e**[b]). The ^{13}C-{^{1}H} NMR spectrum of **(2.49e)** shows the imine carbon resonance at δ 175.45 and the metallated carbon (C^1) at δ 151.08, 3 ppm downfield from the starting compound. The FAB mass spectrum shows ions at *m/z* 590 due to $[M-Cl]^+$. The IR spectrum of **(2.49e)** shows the imine stretch at 1620 cm^{-1}, similar to that (1633 cm^{-1}) in the starting compound, suggesting the imine is still coordinated. The OH stretch is observed at 3436 cm^{-1}, the higher shift suggests that the OH is not coordinated to the Pd atom. This value is consistent with the OH stretch (3459 cm^{-1}) found in the complex with a C_2H_4 linker, **(2.30, L = PPh_3)**.[3] A crystal of **(2.49e)** was suitable for X-ray diffraction and the structure is shown in **Fig. 2.14** with selected distances and angles in **Table 2.9**.

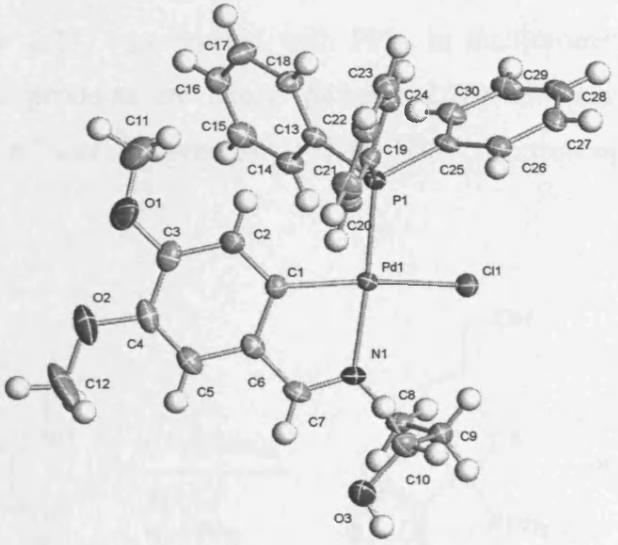

Fig. 2.14 Molecular structure of **2.49e**

Table 2.9 Selected bond distances [Å] and bond angles [°] for complex **2.49e**

Bond distances/[Å]		Bond angles/ [°]	
Pd(1)-C(1)	2.017(3)	C(1)-Pd(1)-N(1)	81.01(13)
Pd(1)-N(1)	2.096(3)	C(1)-Pd(1)-P(1)	94.16(10)
Pd(1)-P(1)	2.2583(9)	N(1)-Pd(1)-Cl(1)	92.23(8)
Pd(1)-Cl(1)	2.3766(9)	P(1)-Pd(1)-Cl(1)	92.97(3)
N(1)-C(7)	1.273(4)	N(1)-Pd(1)-P(1)	174.45(8)
C(1)-C(6)	1.401(5)	C(1)-Pd(1)-Cl(1)	168.76(10)

The structure confirms that displacement of the OH group from palladium has occurred and that the PPh_3 is *trans* to nitrogen. The crystal structure shows that the Pd has a slightly distorted square-planar coordination geometry. The Pd(1)-C(1) and Pd(1)-N(1) bond distances [2.017(3) and 2.096(3) Å respectively] are similar to those in **(2.49b)** [2.032(2) and 2.102(2) Å].

Complex **(2.49e)** arises from cleavage of the Pd-O bond and coordination of PPh_3. However, if the PPh_3 simply displaced the chelated oxygen it would be *cis* to nitrogen. Since the product has PPh_3 *trans* to nitrogen either the initially formed product isomerises or the reaction occurs *via* an associative 5-coordinate mechanism. The displacement of the O-donor by PPh_3 is not surprising given that Pd^{II} has a preference for coordination of relatively soft nucleophiles. It is consistent with displacement of NMe_2- and SEt-functionalised tethers by PPh_3 in complexes **(2.14)**[2] and **(2.20)**[31] (**Scheme 2.9** and **Scheme 2.12** respectively).

Having identified the product from **(2.47e)**, the mixture of compounds formed from the ligands **(d, d`)** (**Scheme 2.23**) was reacted with PPh_3 in dichloromethane. By analogy with **(2.47e)** and **(2.43c)**, two products are likely (**Scheme 2.28**). However, only one compound, showing a singlet at δ 42.67 was observed by $^{31}P-\{^1H\}$ NMR spectroscopy.

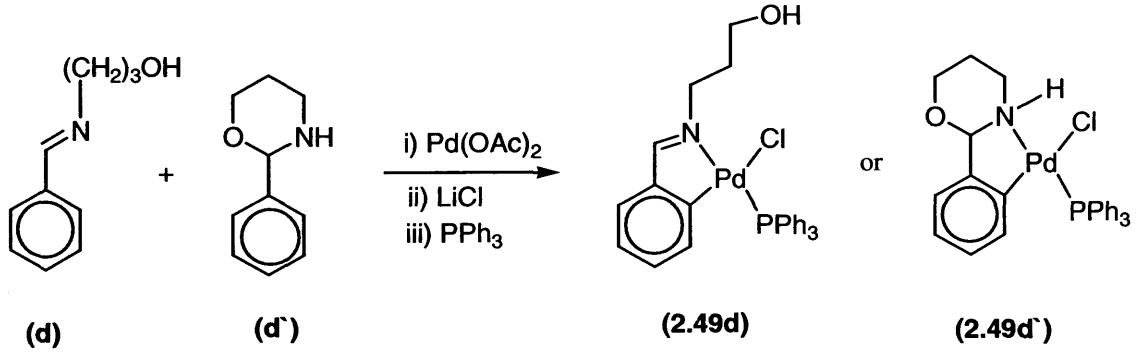

(Scheme 2.28)

The ^1H NMR spectrum of the product shows a doublet at δ 8.17 due to the imine proton, the coupling indicating a P *trans* to N arrangement. The resonance of (H^6) is at δ 6.40. The OH proton is observed at δ 2.97, as found in **(2.49e)**, suggesting that the OH group is not coordinated to the metal. In the aromatic region, there are resonances for the PPh_3 and the four protons for the cyclometallated ligand, appropriate signals are also observed in the $^{13}C-\{^1H\}$ NMR spectrum. Hence the product is assigned as **(2.49d)**.

The FAB mass spectrum shows ions at *m/z* 530 due to $[M-Cl]^+$. The IR spectrum shows the OH absorption at 3436 cm^{-1}, the same as in **(2.49e)**, suggesting that the OH is not coordinated to

the Pd atom, and the imine stretch appears at 1614 cm^{-1}, *c.f.* 1644 cm^{-1} in the free ligand, suggesting the imine is still coordinated. The isolation of only **(2.49d)** in 81% yield, may suggest that during the reactions of the mixture **(d, d`)** conversion of isomer **(d`)** to isomer **(d)** has occurred.

Thus, we have shown that the alcohol coordination in **(2.47e)** and **(2.47d)** could be removed by reaction with PPh_3. Hence, the reaction of **(2.48h)** with PPh_3 was studied to examine the effect on the phenoxide coordination. Tetramer **(2.48h)** reacts with PPh_3 in a 1:4 molar ratio to form the mononuclear species **(2.50h)** in good yield **(Scheme 2.29)**.

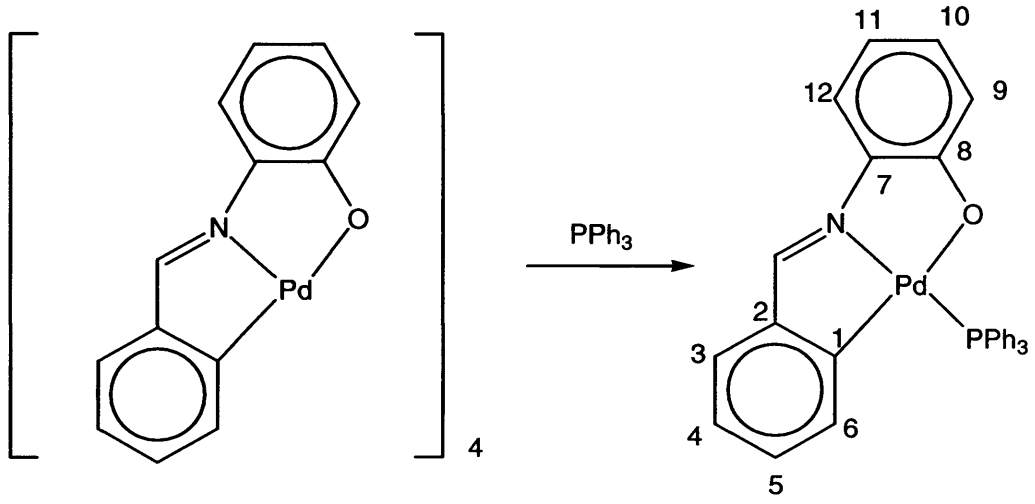

(2.48h) **(2.50h)**

(Scheme 2.29)

The tetrameric structure has been opened due to cleavage of the Pd-O bridge bonds as reported previously for a related complex **(Scheme 2.16)**.[42] The product was characterised by ^1H, $^{13}C\{^1H\}$ and $^{31}P\{^1H\}$ NMR spectroscopy, FAB mass spectrometry, IR spectroscopy, elemental analysis and X-ray diffraction. During the course of this research, this compound was reported by Lopez *et al.*[44]

The $^{31}P\{^1H\}$ spectrum of **(2.50h)** shows a singlet at δ 34.2, confirming the presence of the PPh_3. The ^1H NMR spectrum shows a doublet at δ 7.93 due to the imine proton with coupling to P *trans* to N, and a multiplet at δ 6.02 due to (H^6), 1 ppm upfield from **(2.48h)** suggesting shielding by the PPh_3. The $^{13}C\{^1H\}$ NMR spectrum of **(2.50h)** shows signals corresponding to all the expected carbons. The FAB mass spectrum shows ions at *m/z* 563 due to $[M]^+$. The IR

spectrum of **(2.50h)** shows a band at 1590 cm^{-1} assigned to the imine, which is the same as in the tetramer **(2.48h)**.

The structure of **(2.50h)** was determined by X-ray diffraction and is shown in **Fig. 2.15** with selected bond distances and angles listed in **Table 2.10**. The palladium is in square-planar environment, and the structure confirms the cleavage of the tetramer and coordination of PPh_3 to palladium *trans* to the imine nitrogen.

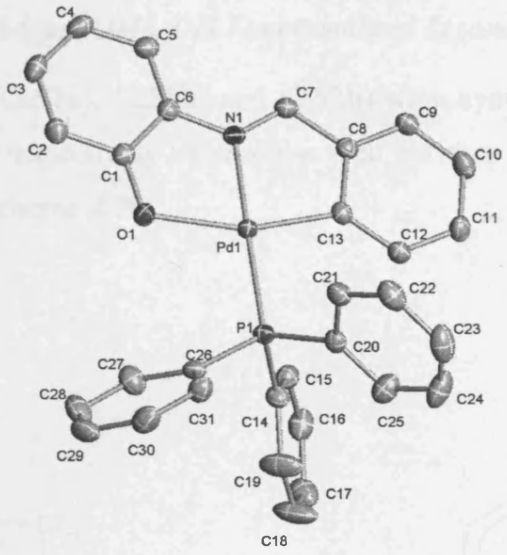

Fig. 2.15 Molecular structure of **2.50h** (All hydrogen atoms have been omitted).

Table 2.10 Selected bond distances [Å] and bond angles [°] for complex **2.50h**

Bond distances\[Å]		**Bond angles\ [°]**	
Pd(1)-C(13)	2.020(2)	N(1)-Pd(1)-P(1)	178.35(6)
Pd(1)-N(1)	2.016(2)	C(13)-Pd(1)-N(1)	81.52(9)
Pd(1)-O(1	2.106 (2)	N(1)-Pd(1)-O(1)	80.68(7)
Pd(1)-P(1)	2.254 (2)	C(13)-Pd(1)-O(1)	162.17(9)
N(1)-C(7)	1.282(3)	O(1)-Pd(1)-P(1)	100.71(5)
O(1)-C(1)	1.322(3)	C(13)-Pd(1)-P(1)	97.11(7)
C(7)-C(8)	1.450(4)		
C(8)-C(13)	1.413(3)		

The Pd-N(1) bond length of [2.016(2) Å] is the same as that [2.012(2) Å] in the related complex $[Pd\{2,3,4\text{-}(MeO)_3C_6HC(H)=N[2\text{-}(O)C_6H_4]\}(PPh_3)]$ **(2.34)**.[42] The Pd-O(1) bond distance [2.106 (2) Å] is similar to the related bond [2.098(2) Å] in **(2.34).** The sum of the angles about the palladium atom is 360°, with N(1)-Pd(1)-C(13) [81.52(9)°] and N(1)-Pd(1)-

O(1) [80.68(7)°] angles significantly less than 90° as a consequence of five-membered ring chelation.

Thus the tridentate C,N,O coordination of **(2.48h)** remains intact after reaction with PPh_3 in contrast with the facile breakage of the Pd-O (alcohol) bond in **(2.47e)** **(Scheme 2.23)** and Pd-O (urea) bond in **(2.38)** **(Scheme 2.18)**[40] on reaction with PPh_3. This is expected since displacement of the anionic phenoxide by neutral PPh_3 would create a zwitterionic species.

2.2.3c Reaction of Cyclopalladated OMe, OH Functionalised Ligands with Pyridine

Mononuclear complexes **(2.51a)**, **(2.51b)** and **(2.52h)** were synthesised in good yield from **(2.43a)**, **(2.43b)** and **(2.48h)** respectively by reaction with pyridine following the same method as for the PPh_3 complexes **(Scheme 2.30)**.

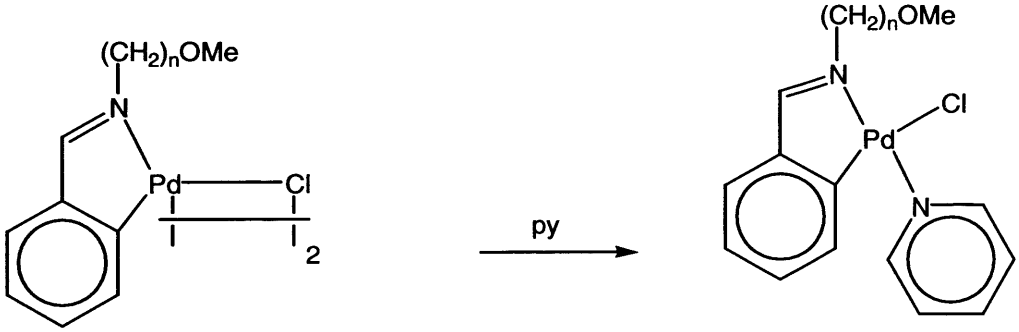

(2.43a, n =2)
(2.43b, n =3)

(2.51a, n = 2)
(2.51b, n = 3)

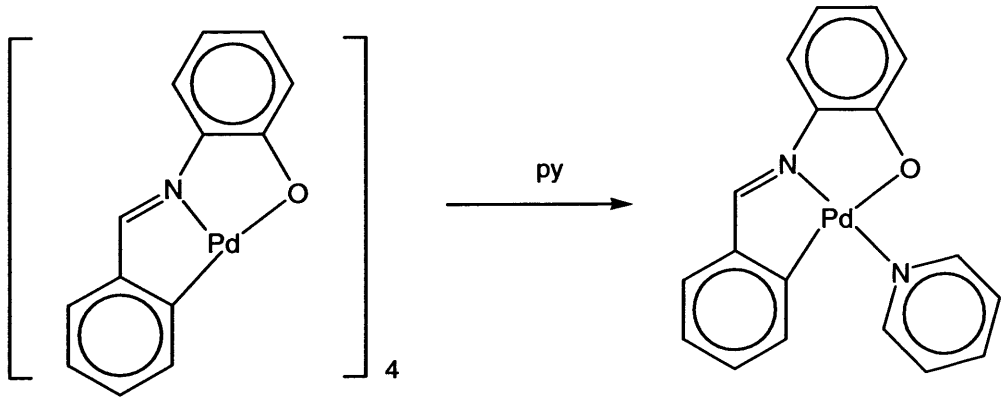

(2.48h)

(2.52h)

(Scheme 2.30)

The ^{1}H NMR spectra of **(2.51a, b)** and **(2.52h)** show singlets at δ 7.90 **(2.51a, b)** and at δ 7.73 **(2.52h)** due to the imine protons. The (H^{6}) doublets appear at δ 6.16 for both **(2.51a, b)**, upfield about 1.2 ppm from **(2.43a, b)** respectively, consistent with a ring current effect of the pyridine. In complex **(2.52h)**, (H^{6}) is observed as a doublet at δ 6.33 only 0.2 ppm upfield from **(2.48h)** because in this case **(2.48h)** already had a ring current from an adjacent imine ligand in the tetramer as discussed earlier. In the aromatic region (in each case), there are four multiplets each integrating to 1H assigned to the cyclometallated phenyl group. The pyridine protons were observed as multiplets in a 2:1:2 ratio at *ca* δ 7.44 (H_m), δ 7.88 (H_p) and δ 8.90 (H_o) for all three complexes.

The ^{13}C-{^{1}H} NMR spectra of **(2.51a, b)** and **(2.52h)** show the expected signals. The imine carbons are observed at δ 177.17, 176.05 and 171.89, and the metallated carbon (C^{1}) at δ 158.15, 158.11 and 152.53 for **(2.51a, b)** and **(2.52h)** respectively. The pyridine carbons were observed as three singlets at *ca.* δ 125, 132 (C_o,C_m) and 154 (C_p). The FAB mass spectra show ions at *m/z* 347 **(2.51a)** and 361 **(2.51b)**, due to $[M-Cl]^{+}$, and 380 **(2.52h)** due to $[M]^{+}$. The IR spectra of **(2.52a, b)** and **(2.52h)** show the imine stretches at 1616, 1614 and 1605 cm^{-1} respectively, confirming that the imine is coordinated to the metal. Microanalysis results are in agreement with the products. Crystallisation of **(2.51a)** from CH_2Cl_2/hexane gave X-ray quality crystals. The structure is shown in **Fig. 2.16** with selected distances and angles in **Table 2.11**.

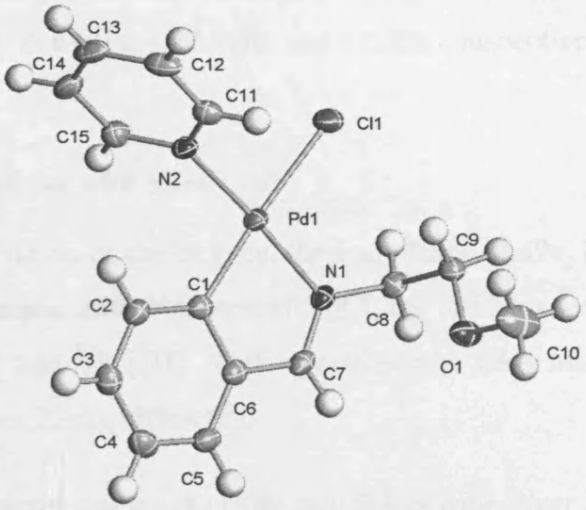

Fig. 2.16 Molecular structure of **2.51a**

Table 2.11 Selected bond distances [Å] and bond angles [°] for complex **2.51a**

Bond distances\[Å]		Bond angles\ [°]	
Pd(1)-C(1)	1.992(2)	C(1)-Pd(1)-N(1)	80.85(8)
Pd(1)-N(1)	2.025(2)	C(1)-Pd(1)-N(2)	94.29(8)
Pd(1)-N(2)	2.042(2)	N(1)-Pd(1)-Cl(1)	95.15(5)
Pd(1)-Cl(1)	2.387(1)	N(2)-Pd(1)-Cl(1)	89.68(5)
N(1)-C(7)	1.277(3)	N(1)-Pd(1)-N(2)	174.51(7)
C(6)-C(1)	1.409(3)	C(1)-Pd(1)-Cl(1)	175.95(6)

The complex adopts the expected square-planar geometry with pyridine *trans* to the imine. The sum of the angles around the palladium atom is 359.97°, with N(1)-Pd(1)-C(1) [80.85(8)°] angles less than 90° as a consequence of five-membered ring chelation. The Pd(1)-C(1) bond distance [1.992(2) Å] is similar to that [1.979(4) Å] in the cyclometallated complex (**2.43a**).

In conclusion, the cyclometallated dimers containing OMe substituents (**2.43a, b, f**) all react easily with PPh_3, and (**2.34a, b**) with pyridine, by cleavage of the chloride-bridges to give (**2.49a, b, f**) and (**2.51a, b**) respectively with the incoming ligand (PPh_3 or py) *trans* to N. A similar result was found for the C_2H_4OH functionalised complex, *ie.* conversion of (**2.43c**) to (**2.49c**). For the C_3H_6OH functionalised imines (**d**) and (**e**), tridentate C,N,O coordination is found for the chloride complexes (**2.47d, e**). These react with PPh_3 with loss of alcohol coordination and isomerisation to provide (**2.49d, e**) with the same P *trans* to N geometry found for other complexes (**2.49**). The tetrameric phenoxide complex (**2.48h**) reacts with PPh_3 or pyridine to give mononuclear complexes (**2.50h**) and (**2.52h**) respectively which retain the tridentate C,N,O coordination.

2.2.4 Reaction of PPh_3 Complexes with Silver Salts

In order to promote coordination of the oxygen, the complexes (**2.49a, b, d, e**) were treated with silver salts to remove chloride. After removal of AgCl, the products were recrystallised and characterised by ^1H, ^{13}C-{^1H} and ^{31}P-{^1H} NMR spectroscopy, FAB mass spectrometry and microanalysis, and in some cases X-ray diffraction.

2.2.4a Reaction of PPh_3 Complexes containing OMe substituent with Silver Salts

Treatment of (**2.49a**) with AgOTf in acetone at room temperature led to the precipitation of AgCl, the possible palladium-containing products are shown in **Scheme 2.31**.

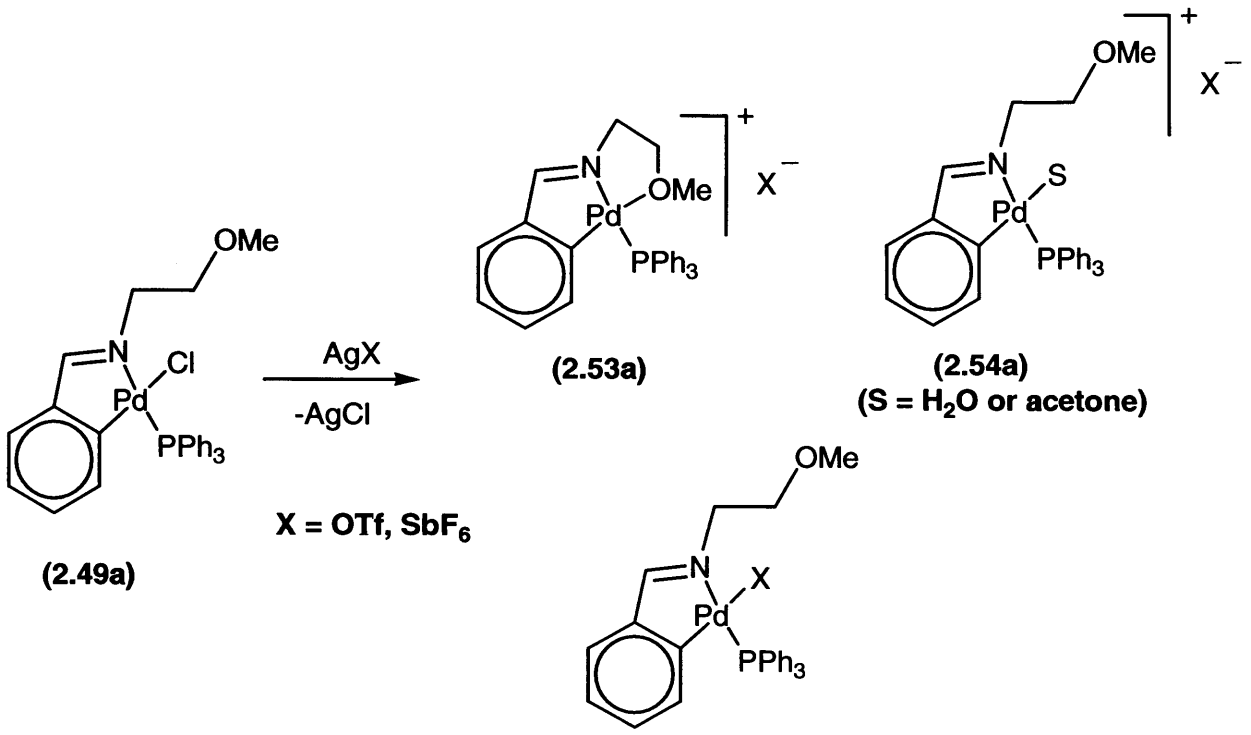

(Scheme 2.31)

The ^{31}P-{^{1}H} spectrum of the product shows a sharp singlet at δ 39.9, suggesting the formation of only one phosphorus-containing product or rapid interconversion of complexes on the NMR timescale. The ^{1}H NMR spectrum showed a doublet due to the imine proton at δ 8.17, the coupling confirming that the PPh_3 is still *trans* to the imine. This is also supported by the signal for (H^6) which is observed at δ 6.35 *ie.* still shielded by the PPh_3. A singlet at δ 3.34 and multiplets at δ 3.78 and 4.02 are assigned to the OMe, CH_2-O and N-CH_2 protons respectively, very slightly upfield *ca.* 0.04 ppm, in each case, from the starting complex; these changes are not large enough to confirm coordination of the OMe. A broad peak integrating to less than two protons is observed at δ 3.35 assigned to water. The ^{13}C-{^{1}H} NMR spectrum of the product shows the imine carbon at δ 176.39 and the OMe at δ 59.50, again very similar shifts to the starting complex δ 177.25 and 59.05 respectively. The metallated carbon (C^1) is observed at δ 150.13, 8.2 ppm upfield from the starting complex. This is consistent with changing the nature of ligand *trans* to (C^1), however it does not distinguish between products **(2.53a)** **(2.54a)** or **(2.55a)**. The FAB mass spectrum of the product showed ions at *m/z* 530 due to $[PdLPPh_3]^+$, as expected for **(2.53a)**, however, **(2.54a)** or **(2.55a)** may show the same ions, by loss of solvent or OTf respectively which may be facile. The IR spectrum shows the imine stretch at 1638 cm^{-1}. Microanalysis of the product suggests the presence of water *ie* **(2.54a)**. However, non-coordinated water of crystallisation may be possible, especially for a salt (*e.g.* see **(2.53b)** later).

To investigate possible fluxional processes, a low temperature ^1H NMR spectrum was obtained. At 253 K the signals of the OMe, CH_2-O, N-CH_2 and H^6 protons were unchanged compared to the spectrum at room temperature, however, the signal due to water had resolved into two broad singlets at δ 4.2 assigned as free water, and a small peak at δ 5.3 assigned to coordinated water (free: coordinated 5:1; note, that the signal due to free water can vary substantially with temperature particularly if hydrogen bonding is possible). Thus, at 253 K there are two species present, the minor one (12%) is **(2.54a)** with H_2O as the solvent. However, the cyclometallated ligand only gives rise to one set of signals even at 253 K. This suggests that the two species are interconverting and the average chemical shifts are seen. Given that exchange of free and coordinated water ($\Delta\delta$ = 1.1 ppm) is slow at 253 K this implies that the ligand signals (exchanging fast) for the two species only have a small chemical shift difference ($\Delta\delta \leq 0.1$ ppm). This suggests the signals are due to species **(2.54a, S = H_2O)** and **(2.54a, S = acetone)** or **(2.55a, X = OTf)**. Complex **(2.53a)** with the CH_2CH_2OMe tether coordinated is expected to show larger changes in chemical shift. Since H_2O is a better ligand than acetone and free water is present, it seems unlikely that the major species is due to acetone coordinated. Therefore we presume that **(2.55a, X = OTf)** is the major species and **(2.54a, S = H_2O)** the minor one. At room temperature exchange of these species is fast and/or the equilibrium lies even further in favour of OTf coordinated **(Scheme 2.32)**.

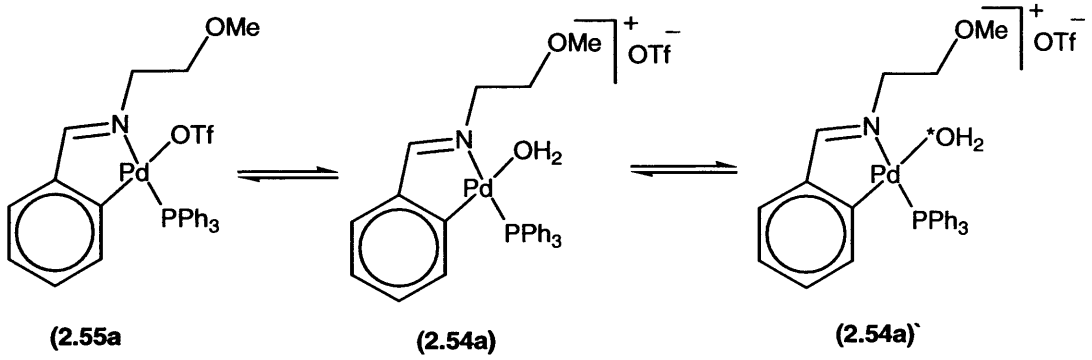

(2.55a **(2.54a)** **(2.54a)`**

(Scheme 2.32)

As mentioned above it was hard to fully characterise the products from the reaction of **(2.49a)** with AgOTf. Hence the reaction was tried using $AgSbF_6$ in place of AgOTf. Since SbF_6 is much less coordinating than OTf, complex **(2.55a, X = SbF_6)** should be less likely to form. In addition, it was felt that the OH_2 ligand found in **(2.54b**, see **Fig 2.18)** may have come from acetone, so CH_2Cl_2 was used as a solvent as it is easier to dry and is less coordinating than acetone.

The $^{31}P-\{^1H\}$ NMR spectrum of the product from **(2.49a)** and $AgSbF_6$ shows a singlet at δ 40.10, *c.f.* 39.9 for the OTf product. The ^1H NMR spectrum shows resonances corresponding to all the expected protons and is similar to the species formed from AgOTf except for the C_2H_4OMe signals. The OMe signal is observed at δ 3.19, 0.2 ppm upfield from **(2.49a)** and 0.15 ppm upfield of the OTf product, possibly indicating shielding of the OMe by PPh_3, which would be close if the OMe coordinates. A similar upfield shift has been observed for coordination of an NMe_2 tether in **(2.16)** **(Scheme 2.9)**.[26] Two multiples due to the OCH_2 and NCH_2 protons are observed at δ 3.84 and 3.94. Whilst the absolute change in chemical shift for each of those signals is small, the separation of the signals has been reduced from almost 0.25 to only 0.1 ppm. This is consistent with a significant change in orientation of the C_2H_4OMe chain as expected for coordination of the OMe. As found in the reaction with AgOTf, water is observed in the ^1H NMR spectrum as a singlet at δ 2.66, however, the signal integrates to less than two protons and the chemical shift suggests the water is not coordinated. The $^{13}C-\{^1H\}$ NMR spectrum is similar to that for the OTf complex, the metallated carbon is at δ 151 7 ppm upfield from **(2.49a)** (*c.f.* δ 150.13 in the OTf complex). At 253 K, the ^1H NMR signals for the OMe and $-CH_2CH_2-$ protons became broader with a small downfield shift of 0.1 ppm for the OMe resonance. In addition, the peak due to water shifted downfield to δ 3.65. These slight changes may be just temperature effects, a more detailed and lower temperature study would be necessary to fully investigate fluxionality of this complex.

In conclusion, at room temperature the major species is **(2.53a, X = SbF_6)** with OMe-coordinated. Microanalysis is also in agreement with this formulation with no water present. At 253 K there are some slight changes, however, only one water signal is observed at δ 3.65, near to what was observed for free water at this temperature in the OTf case (see above). Therefore, with the non-coordinating anion SbF_6 coordination of the OMe group occurs whereas anion coordination is preferred in the case of OTf.

To investigate the effect of the solvent on coordination of the OMe, 1 equivalent of NCMe was added to the NMR sample of **(2.53a, X = SbF_6)** **(Scheme 2.33)**. After addition of NCMe, the CH_2O and NCH_2 signals shift upfield and their separation increases to 0.17 ppm, in contrast, the OMe protons shift downfield 0.21 ppm, all of which are consistent with displacement of OMe by MeCN and the OMe no longer being affected by the ring current of the PPh_3. This is further evidence that the OMe was coordinated before addition of NCMe. The NCMe protons are observed at δ 1.88, 0.12 ppm upfield from free NCMe due to a ring current effect. Therefore, NCMe is a better ligand than ether and displaces the OMe to form **(2.54a, S = NCMe)**.

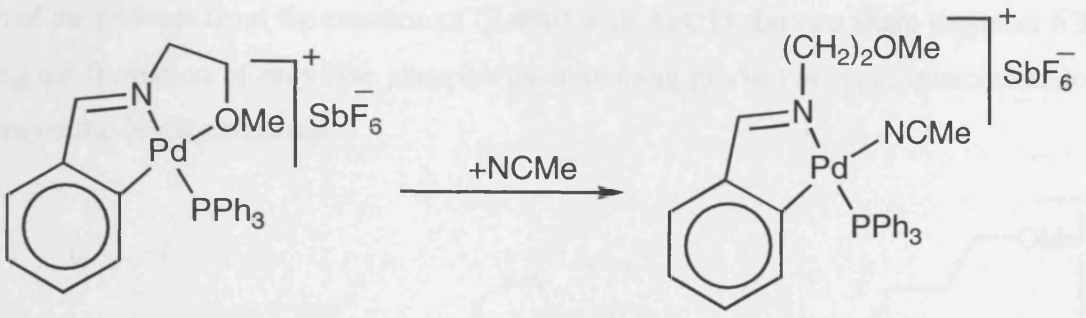

(2.53a, X = SbF_6) **(2.54a, Solvent = NCMe)**

(Scheme 2.33)

Crystallisation of **(2.54a, S = NCMe)** from CH_2Cl_2/hexane gave X-ray quality crystals. The structure is shown in **Fig. 2.17** with selected distances and angles in **Table 2.12**. Complex **(2.54a, S = NCMe)** in **Fig. 2.17** adopts the expected square-planar geometry with PPh_3 *trans* to the imine, and confirms that NCMe occupies the vacant site created by the abstraction of OMe.

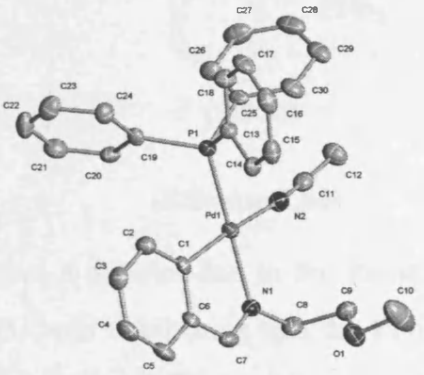

Fig. 2.17 Molecular structure of the cation **(2.54a, S = NCMe)**

Table 2.12 Selected bond distances [Å] and bond angles [°] for complex **(2.54a, S = NCMe)**

Bond distances/[Å]		Bond angles/ [°]	
Pd(1)-C(1)	2.011(5)	N(2)-Pd(1)-P(1)	91.63(13)
Pd(1)-N(1)	2.095(4)	N(1)-Pd(1)-N(2)	92.87(17)
Pd(1)-P(1)	2.271(3)	C(1)-Pd(1)-N(1)	81.31(19)
Pd(1)-N(2)	2.087(4)	C(1)-Pd(1)-P(1)	94.28(15)
C(6)-C(7)	1.434 (7)	C(1)-Pd(1)-N(2)	173.92(18)
N(1)-C(7)	1.271(6)		
O(1)-C(10)	1.396(7)		

To investigate the effect of the length of the tether on coordination of the OMe, complex **(2.49b)** was also reacted with AgOTf and $AgSbF_6$ as shown in **Scheme 2.34** The ^{31}P-{^1H}

spectrum of the product from the reaction of **(2.49b)** with AgOTf shows a sharp singlet at δ 39.8, suggesting the formation of only one phosphorus-containing product or rapid interconversion of complexes on the NMR timescale.

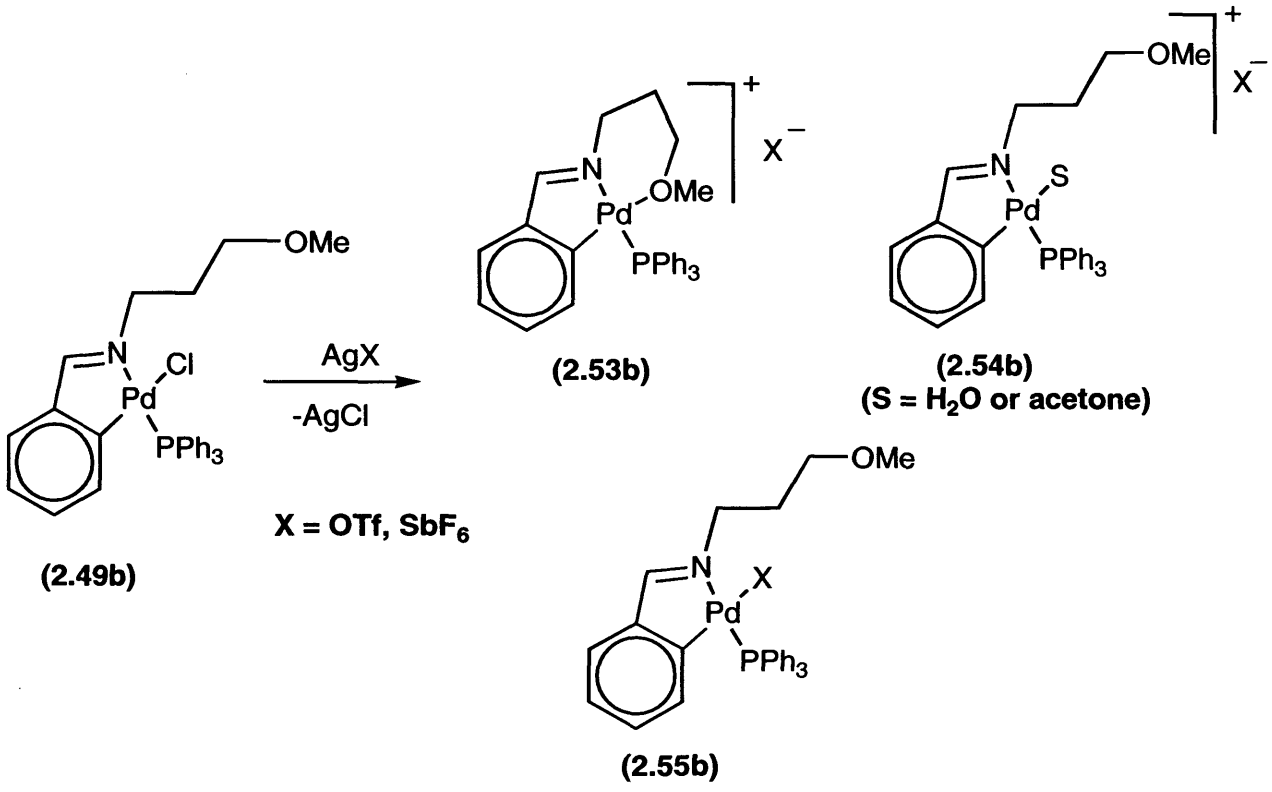

(Scheme 2.34)

The ^{1}H NMR spectrum shows a doublet due to the imine proton at δ 8.20, with the (H^6) proton being observed at δ 6.33, both confirming that the PPh_3 is still *trans* to the imine. The singlet due to the OMe group is observed at δ 3.14, 0.2 ppm upfield from the starting complex (δ 3.38), suggesting that the OMe is shielded by PPh_3, and is coordinated. The spectrum contains two small singlets at δ 3.25 and 2.2 assigned to traces of water and acetone respectively. The ^{13}C-{^{1}H} NMR spectrum of the product shows the imine carbon at δ 175.50, and the OMe carbon at δ 60.45, both resonances are similar shifts to the neutral PPh_3 complex (175.91 and 58.67 respectively). The FAB mass spectrum of the product shows ions at *m/z* 544 due to $[PdLPPh_3]^+$. The IR spectrum of the product shows the imine stretch at 1631 cm^{-1}. Hence, the OTf product seems to be **(2.53b)** but we cannot exclude the possibility of fast exchange with **(2.55b)** and/or **(2.54b, S = H_2O)**. Fortunately a few crystals were obtained that were suitable for X-ray diffraction. Surprisingly, the crystals turned out to contain a mixture of **(2.53b)** and **(2.54b, S = H_2O)** (see later for discussion of the structures). To try and avoid the complication of coordination of the anion the same reaction was attempted using $AgSbF_6$.

After reaction of **(2.49b)** with $AgSbF_6$, the ^{31}P-{^1H} NMR spectrum shows a singlet at δ 39.79. The ^1H NMR spectrum shows the imine and (H^6) protons at δ 8.23 and 6.29, indicating that the imine is still *trans* to the PPh_3. The OMe signal is observed at δ 2.95, 0.38 ppm upfield from **(2.49b)** and 0.2 ppm upfield from the OTf product; this large shift strongly suggesting that the OMe group is shielded by PPh_3 and hence is coordinated. Water is observed as a singlet at δ 1.82, which integrates to less than two protons, suggesting the water is not coordinated. Thus, at room temperature the major species is **(2.53b, X = SbF_6)** with OMe-coordinated. Microanalysis is also in agreement with this formulation with no water present. To investigate possible fluxional processes a low temperature ^1H NMR spectrum was obtained. At 253 K the signal for water resolved into two broad singlets at δ 2.75 (free water) and δ 5.3 (coordinated water) the coordinated water only corresponds to *ca* 25 % of the complex. The signals of the OMe, CH_2-O, N-CH_2 and H^6 protons became broader but do not resolve into separate signals. Thus, at 253 K there are two species present, which are interconverting and the average chemical shifts are seen. The major species (*ca* 75%) is still OMe coordinated **(2.53b, X = SbF_6)**, the minor species (*ca* 25%) has water coordinated **(2.54, S = H_2O)**. The signals due to the cyclometallated ligand are still broad because they are only averaging over a limited chemical shift range (*ca* 0.2 ppm) and only 25% is present in the minor form at 253 K.

The effect of the solvent on coordination of the OMe was also investigated, 1 equivalent of NCMe was added to the NMR sample of **(2.53b, X = SbF_6)**. After addition of NCMe, the OMe protons shift downfield 0.35 ppm, as found for **(2.53a, X = SbF_6)**, consistent with displacement of OMe by NCMe and the OMe no longer being affected by the ring current of the PPh_3. This provides further evidence that the OMe was coordinated before addition of NCMe. In addition, we can now conclude that the shift of the OMe from the OTf reaction (δ 3.14) is intermediate between that δ 2.95 of **(2.53b, X= SbF_6)** containing coordinated OMe, and that δ 3.30 in **(2.54b, S = NCMe)** when the OMe is displaced by NCMe. Thus, the OTf complex shows an average shift and the coordinated OMe of **(2.53b, X = OTf)** must be in fast exchange with coordinated water **(2.54, S = H_2O)** and/or coordinated OTf **(2.55b, X = OTf)**.

As mentioned before, the X-ray structure of the product from the reaction of **(2.49b)** with AgOTf has been determined. Surprisingly, two different products are present in same crystal. In molecule **(A)**, the methoxy group is coordinated to palladium giving a tridentate C,N,O coordination, *i.e.* structure **(2.53b, X = OTf)**. In molecule **(B)**, the cyclometallated ligand is only bidentate and a water molecule is bound in place of the OMe *trans* to the cyclometallated carbon *i.e.* structure **(2.54b, S = H_2O)**.

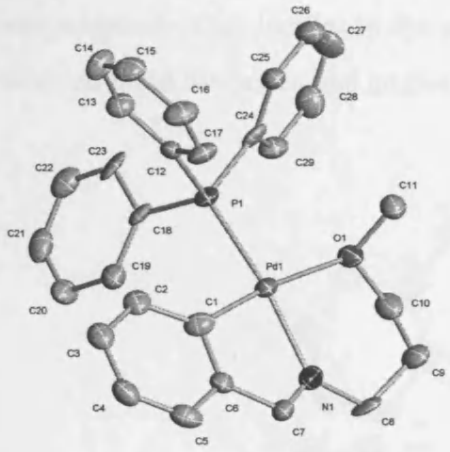

Fig. 2.18 Molecular structure of the cation **(2.53b, X = OTf) (A)**

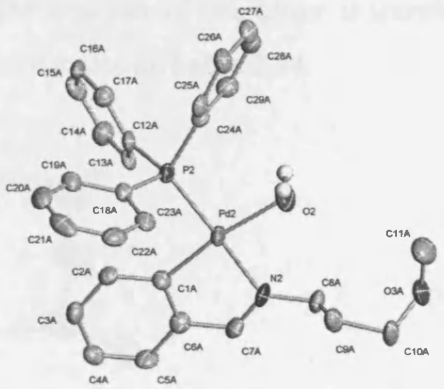

Fig. 2.19 Molecular structure of the cation **(2.54b, S = H_2O) (B)**

Table 2.13 Selected bond distances [Å] and bond angles [°] for complexes **(2.53b, X = OTf)** and **(2.54b, S = OH_2)**

Bond distances/ [Å]	**2.53b (A) (X = OTf)**	**Bond distances/ [Å]**	**2.54b (B)(X = OTf)**
Pd(1)-C(1)	1.997(8)	Pd(2)-C(1A)	1.990(7)
Pd(1)-N(1)	2.096(6)	Pd(2)-N(2)	2.088(7)
Pd(1)-P(1)	2.265(2)	Pd(2)-P(2)	2.259(2)
Pd(1)-O(1)	2.147(5)	Pd(2)-O(2)	2.134(5)
O(1)-C(11)	1.453(8)	O(3A)-C(11A)	1.411(10)
C(1)-C(6)	1.398(10)	C(1A)-C(6A)	1.403(10)
N(1)-C(7)	1.285(10)	N(2)-C(7A)	1.285(9)
Bond angles/ [°]		**Bond angles/** [°]	
C(1)-Pd(1)-N(1)	81.5(3)	C(1A)-Pd(2)-N(2)	81.5(3)
C(1)-Pd(1)-O(1)	170.2(3)	C(1A)-Pd(2)-O(2)	171.9(3)
N(1)-Pd(1)-O(1)	90.6(2)	N(2)-Pd(2)-O(2)	90.5(2)
C(1)-Pd(1)-P(1)	96.1(2)	C(1A)-Pd(2)-P(2)	95.4(2)
O(1)-Pd(1)-P(1)	92.47(15)	O(2)-Pd(2)-P(2)	92.60(17)
N(1)-Pd(1)-P(1)	171.87(18)	N(2)-Pd(2)-P(2)	176.01(19)

The palladium atoms in both complexes are located in a slightly distorted square-planar geometry. The Pd-C, Pd-N, Pd-P and Pd-O bond lengths are all statistically the same in both complexes. The Pd-OH_2 bond distance in **(2.54b, S = H_2O)** [2.134(5) Å] is the same as the Pd-OMe bond length [2.147(5) Å] in **(2.53b, X=OTf)**. The N-Pd-O bond angles are the same in both molecules, suggesting that for motion of the six-membered ring in **(2.53, X = OTf)** does not introduce any additional ring strain.

The structure of (**2.53b, X = SbF_6**) has also been determined by X-ray crystallography and there are two independent molecules in the unit cell. The structure of one cation is shown in **Fig. 2.20** with selected bond distances and angles for both molecules in **Table 2.14**.

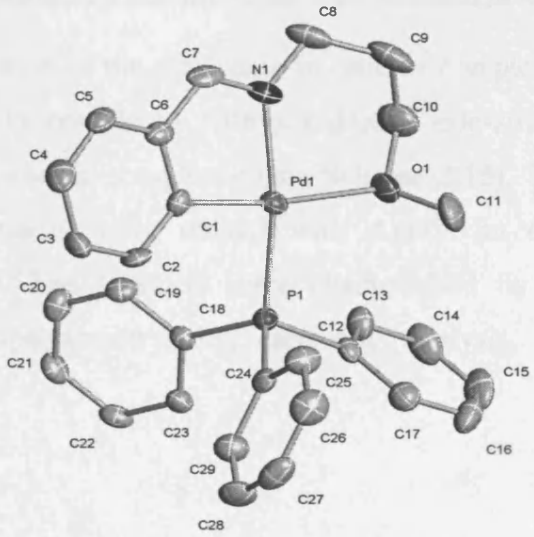

Fig. 2.20 Molecular structure of the cation (**2.53b, X = SbF_6**)

Table 2.14 Selected bond distances [Å] and bond angles [°] for complexes (**2.53b**)

Bond distances/ [Å]	**2.53b, X = SbF_6**	**2.53b, X = SbF_6**
Pd(1)-C(1)	2.014(5)	1.991(5)
Pd(1)-N(1)	2.097(4)	2.063(4)
Pd(1)-P(1)	2.257(2)	2.256(2)
Pd(1)-O(1)	2.187(3)	2.177(3)
C(6)-C(7)	1.452(7)	1.446 (7)
N(1)-C(7)	1.277(6)	1.264(6)
O(1)-C(11)	1.433(6)	1.432(7)
Bond angles/ [°]		
C(1)-Pd(1)-N(1)	82.25(18)	81.62(18)
C(1)-Pd(1)-O(1)	169.28(16)	166.95(16)
N(1)-Pd(1)-O(1)	90.03(15)	87.42(14)
C(1)-Pd(1)-P(1)	94.17(14)	94.60(15)
O(1)-Pd(1)-P(1)	94.55 (10)	97.38(10)
N(1)-Pd(1)-P(1)	170.69(12)	169.66(12)

The cations adopt the expected square planer geometry with PPh_3 trans to the imine and confirms the coordination of OMe and the C,N,O-tridentate nature of the cyclometallated imine. As expected, an average of the Pd(1)-C(1) and Pd(1)-N(1) bond distances of (**2.53b, X = SbF_6**) [2.003 and 2.080 Å respectively] are statistically the same as those [1.997(8) and 2.096(6) Å

respectively] in **(2.53b, X = OTf)**, though the Pd-O bond [2.187(3) or 2.177(3) Å] is slightly longer than the corresponding bond [2.147(5) Å] in **(2.53b, X = OTf)**.

2.2.4a Reaction of PPh_3 Complexes Containing an OH-substituent with AgOTf

The influence of coordination of the side-chain in cationic complexes was also examined for alcohol-substituted ligands. In complexes with a C_2H_4OH side-arm, **(2.31)** showed that the alcohol does coordinate in cationic complexes (see **Scheme 2.15**). The complexes **(2.49d, e)**, containing a C_3H_6OH side-arm, were treated with AgOTf in dichloromethane at room temperature **(Scheme 2.35)**. The products were characterised by ^1H and ^{13}C-{^1H} NMR spectroscopy, FAB mass spectrometry, IR, elemental analysis, and in one case X-ray crystallography.

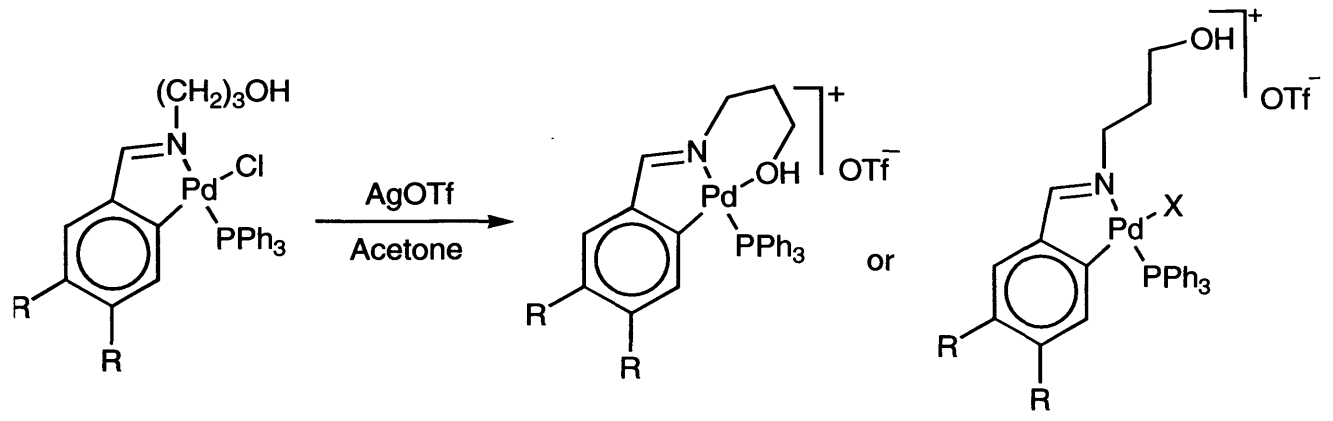

(2.49d, R = H)
(2.49e, R = OMe)

(2.53d, e)

(2.54d, e, X = H_2O, n = 1)
(2.55d, e, X = OTf, n = 0)

(Scheme 2.35)

The ^{31}P-{^1H} NMR spectra of the products from **(2.49d, e)** each show a single resonance at δ 39.90 and 39.85 respectively, suggesting the formation of only one phosphorus-containing product or rapid interconversion on the NMR timescale. The ^1H NMR spectra show the imine proton at δ 8.09 and δ 8.07 as doublets, and the proton (H^6) at δ 6.40 and δ 5.86 respectively, confirming that the PPh_3 is still *trans* to the imine. The hydroxy proton is observed at δ 5.72 and 5.75, a downfield shift of *ca.* 2.75 ppm from the starting complexes **(2.49d)** and **(2.49e)** respectively, consistent with coordination of the OH group to palladium to form **(2.53d, e)**. Similar chemical shifts δ 4.5 and 5.75 for coordinated OH protons are observed for the neutral complex **(2.47e)** and cationic complex **(2.31)**[3] respectively. In both complexes, a singlet is observed at *ca.* δ 1.5 assigned to free water integrating to less than two protons. Thus, in these cases water does not displace OH from coordination.

The ^{13}C-{^{1}H} NMR spectra of **(2.53d)** and **(2.53e)** show no significant changes compared with the starting neutral complexes, hence do not help to confirm the coordination of OH. The FAB mass spectra of **(2.53d)** and **(2.53e)** show ions with maxima at *m/z* 530 and 590 respectively, due to $[PdLPPh_3]^+$and the microanalyses are consistent with the expected products. Hence, the complexes are formulated as **(2.53d)** and **(2.53e)**. This conclusion has been confirmed by X-ray diffraction for **(2.53e)**. The X-ray structure is shown in **Fig. 2.22** with selected distances and angles in **Table 2.15**. The structure confirms that OH coordination has occurred on formation of a cationic complex.

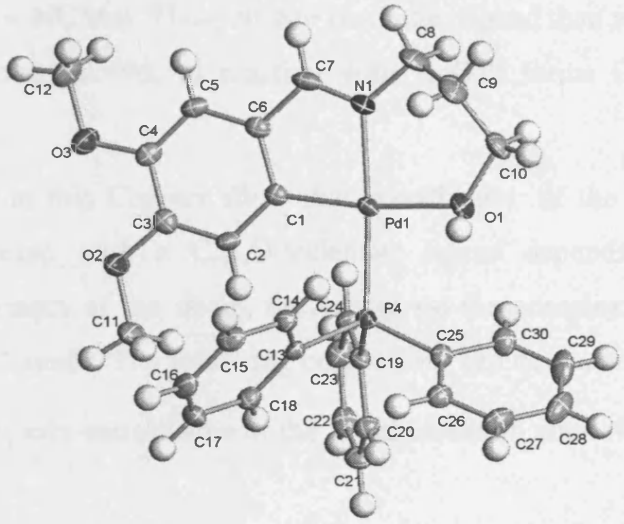

Fig. 2.22 Molecular structure of the cation **2.53e**

Table 2.15 Selected bond distances [Å] and bond angles [°] for complex **2.53e**

Bond distances/ [Å]		**Bond angles/ [°]**	
Pd(1)-C(1)	1.992(4)	C(1)-Pd(1)-N(1)	81.32(16)
Pd(1)-N(1)	2.056(4)	C(1)-Pd(1)-O(1)	171.38(15)
Pd(1)-O(1)	2.138(3)	N(1)-Pd(1)-O(1)	91.24(13)
Pd(1)-P(1)	2.259(2)	N(1)-Pd(1)-P(4)	176.11(11)
N(1)-C(7)	1.269(6)	O(1)-Pd(1)-P(4)	92.40(9)
C(6)-C(7)	1.440(6)	C(1)-Pd(1)-P(4)	91.24(13)

The palladium has square-planar geometry. The Pd(1)-C(1) [1.992(4) Å] and Pd(1)-N(1) [2.056(4) Å] bond distances are similar to those found in the tridentate OMe complex **(2.53b, X = SbF_6)** [1.991(5) and 2.063(4) Å respectively]. The Pd-O(1) bond distance [2.138(3) Å] is

shorter than that [2.216(8) Å] in the related complex **(2.31)**, and shorter than that [2.187(3) Å] in the OMe complex **(2.53b, X = SbF_6)**.

In conclusion, coordination of the pendant arm in cationic complexes depends on the length of the chain, the nature of the O-donor (ether or alcohol) and on the anion used. In the case of ether complexes, **(2.49a, b)** reaction with $AgSbF_6$ leads to C,N,O-tridentate cationic complexes **(2.53a, b, X = SbF_6)**. However, with AgOTf, coordination of OTf is favoured with the C_2H_4OMe complex (and some H_2O coordination at low temperature), with the C_3H_6OMe complex OMe coordination is in fast exchange with either H_2O and/or OTf. Addition of NCMe to **(2.53a, b, X = SbF_6)**; causes displacement of the OMe chelate arm giving C,N-bidentate complexes **(2.53a, b, S = NCMe)**. Thus, NCMe is a better ligand than an ether for these cations. In the alcohol complexes, **(2.49d, e)** reaction with AgOTf forms C,N,O-tridentate cationic complexes.

Overall, the results in this Chapter show that coordination of the pendant oxygen to give cyclometallated complexes with a C,N,O-tridentate ligand depends on the nature of the functional group, the length of the chain, the charge on the complex and the counterion and presence of other weak ligands. The following conclusions can be drawn.

1) A pendant ether only coordinates to the metal centre in cationic complexes, not neutral ones.

2) Coordination of a pendant alcohol can occur in a neutral complex if the ligand has a $(CH_2)_3$ spacer but can occur for either a $(CH_2)_2$ or $(CH_2)_3$ spacer in cationic complexes. This is consistent with an alcohol being a better ligand than an ether. Also, there is less strain in a bicyclic system containing fused five and six-membered rings than in a bicyclic system containing both fused five-membered ring.

3) A phenol substituent deprotonates spontaneously in the reaction with $[Pd(OAc)_2]_3$ giving a tridentate, dianionic C,N,O ligand. This is consistent with the much higher acidity of phenol compared to an alcohol.

4) Anion dependency, is favoured over OMe with a C_2H_4 spacer but with a C_3H_6 spacer OMe coordination is at least competitive. SbF_6 is much less coordinating than OTf .

2.3 Experimental

All reactions were carried out at room temperature in air. The preparation of cationic complexes with silver salts was performed under nitrogen with exclusion of light. ^{1}H, ^{13}C-{^{1}H} and ^{31}P-{^{1}H} NMR spectra were obtained using a Bruker ARX250 or 300 MHz spectrometers, with $CDCl_3$ as solvent, unless otherwise stated. Chemical shifts were recorded in ppm (on δ scale for ^{1}H NMR, with tetramethylsilane as internal reference) and coupling constants are reported in Hz. FAB mass spectra were obtained on a Kratos concept mass spectrometer using NOBA as matrix. The electrospray (ES) mass spectra were recorded using a micromass Quattra LC mass spectrometer with dichloromethane or methanol as the matrix [Masslynx software. open-access autosampler injection]. The infrared spectra were recorded with Universal ATR sampling accessories on a Perkin Elmer Spectrum One FTIR instrument. Microanalyses were performed by the Elemental Analysis Service (University of North London). All starting materials were obtained from Aldrich, with the exception of $[PdCl_2(PhCN)_2]$ which was prepared according to literature method[56] and $[Pd(OAc)_2]_3$ which was used on loan from Johnson Matthey.

Preparation of Imines

Preparation of C_6H_5-C(H)=N$CH_2CH_2OCH_3$ (a)

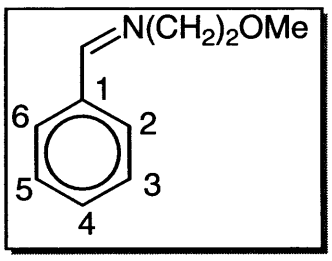

To a solution of benzaldehyde (4.24 g, 39.94 mmol) in CH_2Cl_2 (15 ml), methoxy ethylamine (3 g, 39.94 mmol) and $MgSO_4$ were added. The resulting mixture was stirred at room temperature for 2h, and then filtered. The resulting solution was evaporated to dryness to give a yellow liquid. (5.80 g, 89%). ^{1}H NMR: δ 3.26 (s, 3H, OCH_3), 3.60 (m, 2H, CH_2O), 3.68 (m, 2H, NCH_2), 7.25 (m, 3H, Ar-H), 7.64 (m, 2H, Ar-H), 8.19 (s, 1H, HC=N); ^{13}C NMR: δ 59.37 (OCH_3), 61.65 (CH_2O), 72.68 (NCH_2), 128.69, 129.01, 131.11 (Ar-C^2, C^3, C^4, C^5, C^6), 136.67 (C^1), 163.04 (HC=N). MS (FAB) *m/z*: 164 $[MH]^+$. IR: υ(C=N) 1647 cm^{-1}.

Preparation of C_6H_5-C(H)=N$CH_2CH_2CH_2OCH_3$ (b)

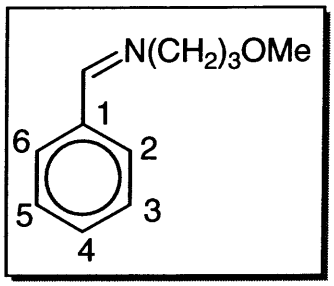

To a solution of benzaldehyde (2.38 g, 22.43 mmol) in CH_2Cl_2 (15 ml), methoxy propylamine (2 g, 22.43 mmol) and $MgSO_4$ were added. The resulting mixture was stirred at room temperature for 2h, and then filtered. The resulting solution was evaporated to dryness to give a yellow liquid. (3.60 g, 91%). ^{1}H NMR: δ 1.98 (q, 2H, *J* 7, -CH_2-), 3.34 (s, 3H, OCH_3), 3.47 (t, 2H, *J* 6.5, CH_2O), 3.69 (dt, 2H, *J* 7, 1, NCH_2), 7.42 (m, 2H, Ar-H), 7.72

(m, 2H, Ar-H), 8.30 (s, 1H, HC=N); ^{13}C NMR: δ 30.92 (-CH_2-), 58.31 (CH_2O), 58.77 (OCH_3), 70.52 (NCH_2), 128.21, 128.77, 130.74 (Ar-C^2, C^3, C^4, C^5, C^6), 136.39 (C^1), 161.62 (HC=N). MS (FAB) *m/z*: 178 $[MH]^+$. IR: υ(C=N) 1647 cm^{-1}.

Preparation of C_6H_5-C(H)-NCH_2CH_2OH (c)

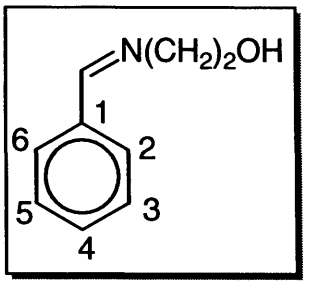

To a solution of benzaldehyde (3.48 g, 32.79 mmol) in CH_2Cl_2 (20 ml), aminoethanol (2 g, 32.79 mmol) and $MgSO_4$ were added. The resulting mixture was stirred at room temperature for 3h, and then filtered. The resulting solution was evaporated to dryness to give an orange liquid. (4.80 g, 98%). ^1H NMR: δ 3.66 (t, 2H, *J* 5, CH_2O), 3.86 (t, 2H, *J* 5, NCH_2), 3.92 (br, 1H, OH), 7.38 (m, 3H, Ar-H), 7.66 (m, 2H, Ar-H), 8.19 (s, 1H, HC=N); ^{13}C NMR: δ 62.23 (CH_2O), 63.85 (NCH_2), 128.64, 128.76, 134.85 (Ar-C^2, C^3, C^4, C^5, C^6), 136.10 (C^1), 163.74 (HC=N). MS (FAB) *m/z*: 149 $[M]^+$. IR: υ(C=N) 1644 cm^{-1}. υ(O-H) 3339 cm^{-1}.

Preparation of C_6H_5-C(H)-$NCH_2CH_2CH_2OH$ (d,d`)

To a solution of benzaldehyde (4.24 g, 39.94 mmol) in CH_2Cl_2 (15 ml), aminopropanol (3 g, 39.94 mmol) and $MgSO_4$ were added. The resulting mixture was stirred at room temperature for 3h, and then filtered. The resulting solution was evaporated to dryness to give a white precipitate. The product was a 2:1 mixture of isomers as determined by ^1H and ^{13}C NMR spectroscopy (see Fig. 2.1). (5.8 g, 89%). ^1H NMR: δ (major isomer) 1.85 (q, 2H, *J* 6, -CH_2-), 3.70 (dt, 2H, *J* 6, 1, CH_2O), 3.75 (t, 2H, *J* 6, NCH_2), 7.34 (m, 3H, Ar-H), 7.75 (m, 2H, Ar-H), 8.20 (s, 1H, HC=N); (minor isomer): heterocyclic ring:(-$CHOCH_2CH_2CH_2NH$-): [1.30 (m, 1H) 3.20 (m, 2H,), 3.85 (dt, 1H, *J* 12, 2.5), 4.30 (m, 1H,), 5.10 (s, 1H,)], 7.25 (m, 3H, Ar-H), 7.48 (m, 2H, Ar-H); ^{13}C NMR: δ (major isomer) 33.48 (-CH_2-), 60.03 (CH_2O), 62.46 (NCH_2), 128.70, 129.28, 131.48 (Ar-C^2, C^3, C^4, C^5, C^6), 136.34 (C^1), 162.02 (HC=N); (minor) 27.23 (-CH_2-), 44.66 (CH_2O), 68.04 (NCH_2), 89.0 (HC-N), 126.41, 128.88 (Ar-C^2, C^3, C^5, C^6), 141.26 (C^1). MS (FAB) *m/z*: 164 $[MH]^+$. IR: υ(C=N) 1644 cm^{-1}. υ(O-H) 3282 cm^{-1}.

Preparation of C_6H_3-3,4-$(CH_3O)_2$-C(H)=$NCH_2CH_2CH_2OH$ (e,e`)

To a solution of 3,4-dimethoxybenzaldehyde (6.64 g, 39.94 mmol) in CH_2Cl_2 (25 ml), amino- propanol (3 g, 39.94 mmol) was added. The mixture was stirred at room temperature overnight, then filtered. The filtrate was evaporated to dryness to give a yellow oil, however, within a few minutes the oil had changed to a white precipitate. The precipitate was a 6:1 mixture of isomers as determined by ^1H and ^{13}C NMR spectroscopy (see Fig. 2.1). (8.55 g, 96%). Anal. calc. for $C_{12}H_{17}O_3N$: C, 64.55; H, 7.67; N, 6.27%. Found: C, 64.48; H, 7.87; N,

6.30%. ^{1}H NMR: δ (major isomer) 1.9 (q, 2H, J 6, -CH_2-), 3.75 (dt, 2H, J 6.5, 1, CH_2O), 3.85 (m, 2H, NCH_2), 3.90 (s, 3H, OCH_3), 3.92 (s, 3H, OCH_3), 6.86 (d, 1H, J 9, H^5), 7.14 (dd, 1H, J 8, 2, H^6), 7.34 (d, 1H, J 2, H^2), 8.16 (s, 1H, HC=N); (minor isomer): heterocyclic ring:-$CHOCH_2CH_2CH_2NH$-): [1.45 (m, 1H), 3.25 (m, 4H), 3.95 (m, 6H, 2 × OMe), 4.27 (m, 1H), 5.12 (s, 1H)], 7.05 (m, 3H, Ar-H); ^{13}C NMR: δ (major) 33.82 (-CH_2-), 56.22, 56.27 (2 × OCH_3), 59.87 (CH_2O), 62.44 (NCH_2), 109.1, 110.88, 123.00 (C^2, C^5, C^6), 129 (C^1), 149.7, 151.85 (C^3, C^4), 161.2 (HC=N); (minor) 27.40 (-CH_2-), 44.84 (CH_2O), 56.27 (OCH_3), 68.32 (NCH_2), 89.00 (HC-N), 109.1, 110.81, 118.39 (C^2, C^5, C^6), 127.20, 133.87 (C^3, C^4), 149.07 (C^1). MS (FAB) *m/z*: 224 $[MH]^+$. IR: υ(C=N) 1648 cm^{-1}. υ(O-H) 3260 cm^{-1}.

Preparation of C_6H_3-C(H)=$NC_6H_4OCH_3$ (f)

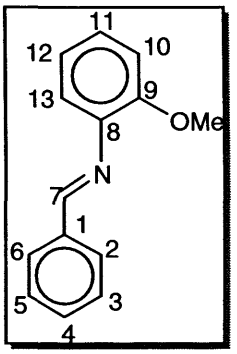

To *o*-anisidine (3.81 g, 30.91 mmol), benzaldehyde (3.28 g, 30.91 mmol) in EtOH (5 ml) (very slowly dropwise at room temperature) was added. The reaction was stirred for 2h. ^{1}H NMR showed a mixture of starting material and product, excess benzaldehyde was added. The reaction was left for 2h, then evaporated to dryness to give a brown oil. (5.95 g, 91%). ^{1}H NMR: δ 3.85 (s, 3H, OCH_3), 6.97 (m, 3H, Ar-H), 7.20 (m, 1H, Ar-H), 7.47 (m, 3H, Ar-H), 7.90 (m, 2H, Ar-H), 8.47 (s, HC=N); ^{13}C NMR: δ 55.6 (OCH_3), 110.59, 111.68, 115.23, 118.69, 120.42, 121.25, 126.86, 128.87, 129.12 (Ar-CH), 136.3 (C^1), 142.07, 152.46 (C^7,C^8), 161 (HC=N). MS(FAB) *m/z*: 212 $[MH]^+$. IR: υ(C=N) 1628 cm^{-1}.

Preparation of C_6H_3-C(H)=NC_6H_4OPh (g)

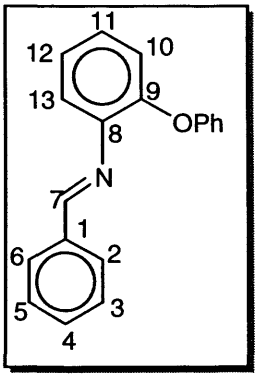

To amine (4.36 g, 23.57 mmol), benzaldehyde (2.2 g, 23.58 mmol) in EtOH (5 ml) (very slowly dropwise at room temperature) was added. The reaction was stirred for 2h. then evaporated to dryness to give a brown solid. (5.20 g, 81%). ^{1}H NMR: δ 6.92-7.80 (m, 14H, Ar-H), 8.48 (s, HC=N). MS(FAB) *m/z*: 274 $[MH]^+$. IR: υ(C=N) 1629 cm^{-1}.

Preparation of C_6H_3-C(H)=NC_6H_4OH (h)

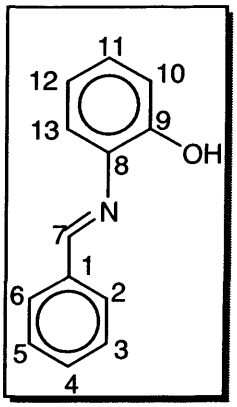

To H_2N-(C_6H_4-2-OH) ((1.03 g, 9.43 mmol), benzaldehyde (1.00 g, 9.43 mmol) in EtOH (5 ml) (very slowly dropwise at room temperature) was added. The resulting mixture was stirred at room temperature for 2h, and then filtered. The resulting solution was evaporated to dryness to give a brown solid. (1.52 g 81.7%). ^{1}H NMR: δ 6.91 (dt, 1H J 8, 1, H^{11}), 7.02 (dd, 1H, J 8, 1, H^{10}), 7.20 (dt, 1H, J 8, 1.5, H^{12}), 7.31 (dd, 1H, J 8, 1.5, H^{13}), 7.50 (m, 1H,

OH), 7.62 (m, 1H, H^4), 7.92 (m, 2H, $H^{3,5}$), 8.12 (m, 2H, $H^{2,6}$), 8.70 (s, 1H, N=CH). ^{13}C NMR: δ 115.22, 116.08, 120.33, 128.70, 129.03, 129.09, 130.42, 131.92, 133.99 (Ar-CH), 135.67 (C^8), 136.03(C^9), 152.49 (C^1), 157.38 (HC=N). MS (FAB) *m/z*: 198 $[MH]^+$. IR: υ(C=N) 1625 cm^{-1}. υ(O-H) 3370 cm^{-1}.

Preparation of Cyclopalladated Complexes:

a) Cyclopalladation of OMe Functionalised Ligand

Acetate dimer complexes

Preparation of $[Pd(\mu\text{-}OAc)\{C_6H_4\text{-}2\text{-}C(H)=NCH_2CH_2OCH_3\text{-}\kappa\text{-}C_1,N\}]_2$ (2.42a)

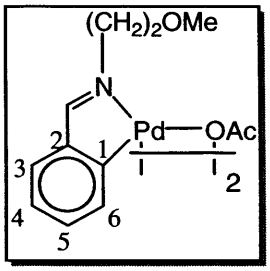

To a suspension of $Pd(OAc)_2$ (0.2 g, 0.92 mmol) in MeOH (35 ml), imine (**a**) (0.15 g, 0.92 mmol) was added. The mixture was stirred at room temperature for 2h, and then filtered over celite to remove (Pd°). The filtrate was evaporated to dryness and the yellow oil was dissolved in dichloromethane. Addition of hexane gave (**2.42a**) as a yellow solid. (0.25 g, 84%). Anal. calc. for $C_{24}H_{30}O_6N_2Pd_2$: C, 43.99; H, 4.61; N, 4.27%. Found: C, 44.08; H, 4.60; N, 4.26%. ^1H NMR: δ 2.13 (s, 3H, OAc), 2.75 (m, 1H, C*H*HO) 3.26 (s, 3H, OCH_3), 3.40 (m, 2H, NC*H*H-CH*H*-O), 3.65 (m, 1H, N-CH*H*), 7.00 (m, 4H, Ar-H), 7.29 (s, 1H, HC=N); ^{13}C NMR: δ 24.67, 181.36 (OAc), 58.79 (CH_2O), 59.09 (OCH_3), 70.04 (NCH_2), 124.16, 126.78, 129.26, 132.07 (Ar-C^3, C^4, C^5, C^6), 146.17 (C^2), 155.51 (C^1), 173.82 (HC=N). MS (FAB) *m/z*: 655 $[M\text{-}H]^+$, 597 $[Pd_2L_2(OAc)]^+$, 268 $[PdL]^+$. IR: υ(C=N) 1610 cm^{-1}. υ(COO) 1565 and 1413 cm^{-1}

Preparation of $[Pd(\mu\text{-}OAc)\{C_6H_4\text{-}2\text{-}C(H)=NCH_2CH_2CH_2OCH_3\text{-}\kappa\text{-}C_1,N\}]_2$ (2.42b)

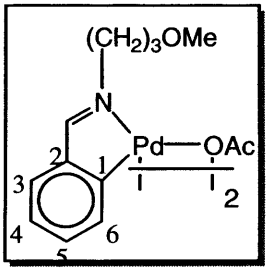

To a suspension of $Pd(OAc)_2$ (0.2 g, 0.89 mmol) in MeOH (35 ml), the imine (**b**) (0.16 g, 0.89 mmol) was added. The mixture was stirred at room temperature for 2h, and then filtered over celite to remove (Pd°). The filtrate was evaporated to dryness and the yellow oil was dissolved in dichloromethane. Addition of hexane gave (**2.42b**) as a yellow solid. (0.24 g, 87%). Anal. calc. for $C_{26}H_{38}O_6N_2Pd_2$: C, 45.69; H, 5.01; N, 4.1%. Found: C, 45.74; H, 5.00; N, 4.02%. ^1H NMR: δ 1.91 (m, 2H, (-CH_2-), 2.13 (s, 3H, OAc), 2.75 (m, 1H, CH*H*-O), 3.24 (s, 3H, OCH_3), 3.25 (m, 3H, C*H*H-O, N-CH_2), 7.00 (m, 4H, Ar-H), 7.19 (s, 1H, HC=N); ^{13}C NMR: δ 24.64, 181.23 (OAc), 28.96 (-CH_2-), 56.14 (CH_2O). 58.63 (OCH_3), 69.13 (NCH_2), 124.09, 126.41, 129.10, 132.14 (Ar = C^3, C^4, C^5, C^6), 145.92 (C^2), 155.43 (C^1), 172.54 (HC=N). MS (FAB) m/s: 684 [M[$^+$, 625 $[M\text{-}OAc]^+$. IR: υ(C=N) 1610 cm^{-1}. υ(COO) 1570 and 1410 cm^{-1}

Chloride dimer complexes

Preparation of [Pd(μ-Cl){C_6H_4-2-C(H)=N$CH_2CH_2OCH_3$-κ-C_1,N}]$_2$ (2.43a)

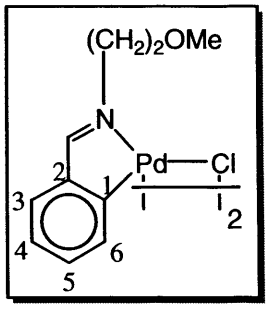

To a suspension of $Pd(OAc)_2$ (0.21g, 0.92 mmol) in MeOH (30 ml), the imine **(a)** (0.15 g, 0.92 mmol) was added. The mixture was stirred at room temperature for 2h, and then filtered over celite to remove (Pd°). The resulting orange solution was treated with LiCl (0.15 g, 3.5 mmol) to give **(2.43a)** as a green precipitate. The solid was filtered, washed with hexane and dried. (0.181 g, 76%); Anal. calc. for $C_{20}H_{24}O_2N_2Pd_2$: C, 40. 30; H, 2.03; N, 4.70%. Found: C, 40.25; H, 2.09; N, 4.64%. ^{1}H NMR: δ 3.37 (s, 3H, OCH_3), 3.76 (s, 4H, N-CH_2-CH_2-O), 7.05(m, 2H, H^4, H^5), 7.22 (m, 1H, H^3), 7.37 (m, 1H, H^6), 7.83 (s, 1H, HC=N); ^{13}C NMR: δ 59.3 (OCH_3), 59.3 (CH_2O), 70.23 (NCH_2), 125.0, 127.69, 130.22, 133.42 (Ar-C^3, C^4, C^5, C^6), 146.33 (C^2), 154.68 (C^1), 176.21 (HC=N). MS (FAB) *m/z*: 608 $[M]^+$, 573 $[M-Cl]^+$. IR: υ(C=N) 1613 cm^{-1}.

Preparation of [Pd(μ-Cl){C_6H_4-2-C(H)=N$CH_2CH_2CH_2OCH_3$-κ-C_1,N}]$_2$ (2.43b)

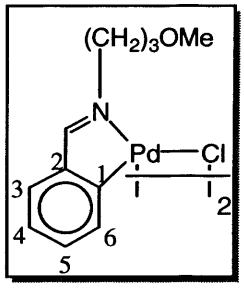

To a suspension of $Pd(OAc)_2$ (0.2 g, 0.89 mmol) in MeOH (35 ml), the imine **(b)** (0.16 g, 0.89 mmol) was added. The mixture was stirred at room temperature for 2h, and then filtered over celite to remove (Pd°). The resulting orange solution was treated with LiCl (0.15 g, 3.5 mmol) to give **(2.43b)** as a green precipitate. The solid was filtered, washed with hexane and air dried. (0.27 g, 95%). Anal. calc. for $C_{22}H_{28}O_2N_2Pd_2$: C, 41.53; H, 4.44; N, 4.40%. Found: C, 41.53; H, 4.52; N, 4.45%. ^{1}H NMR: δ 2.12 (q, 2H, *J* 6, -CH_2-), 3.32 (s, 3H, OCH_3), 3.44 (t, 2H, *J* 6, CH_2O), 3.70 (t, 2H, *J* 6.5, NCH_2), 7.04 (m, 2H, H^4, H^5), 7.20 (m, 1H, H^3), 7.38(m, 1H, H^6), 7.81 (s, 1H, HC=N). ^{13}C NMR: δ 29.71(-CH_2-), 57.02(CH_2O), 58.77(OCH_3), 69.08 (NCH_2), 124.95, 127.46, 130.25, 133.46 (Ar-C^3, C^4, C^5, C^6), 146.09 (C^2), 154.44 (C^1), 174.97(HC=N). MS (FAB) *m/z*: 636 $[M]^+$, 601 $[M-Cl]^+$. IR: υ(C=N) 1611 cm^{-1}.

Preparation of [Pd(μ-Cl){C_6H_4-1-C(H)=N[(2-OCH_3)-C_6H_4]-κ-C_2,N}]$_2$ (2.43f)

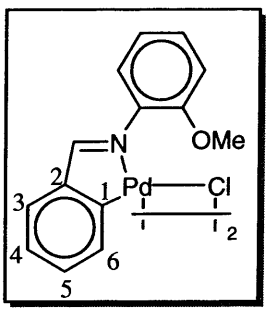

To a suspension of $Pd(OAc)_2$ (0.2 g, 0.89 mmol) in MeOH (40 ml), the imine **(f)** (0.15 g, 0.89 mmol) was added. The mixture was stirred at room temperature for 2h, and then filtered over celite to remove (Pd°). The resulting orange solution was treated with LiCl (0.15 g, 3.5 mmol) to give **(2.43f)** as a brown precipitate. The brown solid was filtered, washed with

hexane and dried under vacuum. (0.25 g, 80%); ^{1}H NMR: δ 3.85 (s, 3H, OCH_3), 6.98 (m, 4H, Ar-H), 7.21 (m, 4H, Ar-H), 7.9 (s, 1H, HC=N). MS (FAB) *m/z*: 669 $[M\text{-}Cl]^+$. IR: υ(C=N) 1602 cm^{-1}.

Preparation of [Pd(μ-Cl){C_6H_4-2-C(H)=N[(2-OC_6H_5)-C_6H_4]-κ-C_1,N}]$_2$ (2.43g)

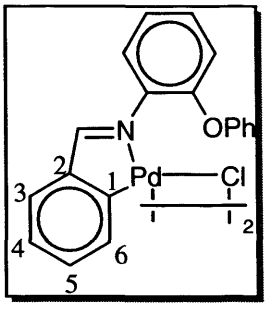

To a suspension of $Pd(OAc)_2$ (0.2 g, 0.89 mmol) in MeOH (40 ml), the imine **(g)** (0.0.24 g, 0.89 mmol) was added. The mixture was stirred at room temperature for 5h, and then filtered over celite to remove (Pd°). The resulting orange solution was treated with LiCl (0.15 g, 3.5 mmol) to give **(2.43g)** as a green precipitate. The green solid was filtered, washed with hexane and dried under vacuum. (0.25 g, 68%); Anal. calc. for $C_{38}H_{28}O_2N_2Cl_2Pd_2$(1 equiv. CH_2Cl_2): C, 51.31; H, 3.29; N, 3.07%. Found: C, 51.37; H, 2.71; N, 3.97%. ^{1}H NMR: δ 6.90-7.45 (m, 13H, Ar-H), 8.00 (s, 1H, HC=N). ^{13}C NMR: δ 119.40, 123.38, 123.84, 124.89, 126.51, 128.64, 128.84, 130.05, 131.06, 133.80 (Ar-CH), 146.38 (C^2), 149.28 (C^9), 155.36 (^iC, OPh), 156.65 (C^1), 177.53 (C=N). MS (FAB) *m/z*: 827 $[M]^+$, 792 $[M\text{-}Cl]^+$. IR: υ(C=N) 1598 cm^{-1}.

Preparation of [Pd(μ-Cl){C_6H_4-1-C(H)=N$CH_2CH_2OCH_3$-κ-C_2,N}]$_2$ (2.45)

To a suspension of $PdCl_2(PhCN)_2$ (0.15g, 0.39 mmol) in MeOH (30 ml), the imine **(a)** (0.13 g, 0.78 mmol) was added. The mixture was stirred at room temperature for 24h, and then filtered over celite to remove (Pd°). The resulting orange solution was treated with LiCl (0.15 g, 3.5 mmol) to give **(2.45)** as a green precipitate. The solid was filtered, washed with hexane and dried. (0.12 g, 61%); Anal. calc. for $C_{20}H_{24}O_2N_2Pd_2$(1 equiv. acetone): C, 49.17; H, 5.74; N, 4.99%. Found: C, 49.84; H, 5.28; N, 5.19%. ^{1}H NMR: δ (major) 3.38 (s, 3H, OCH_3), 4.15 (m, 4H, N-CH_2-CH_2-O), 7.65(m, 3H, H^3, H^4, H^5), 8.00 (s, 1H, C=N), 9.00 (m, 2H, H^2, H^6); (minor) 3.45 (s, 3H, OCH_3), 3.50 (m, 2H, CH_2O), 4.05 (m, 2H, NCH_2), 7.42 (m, 2H, H^3, H^5), 7.60 (m, 1H, H^4), 8.00 (s, 1H, C=N), 8.65 (m, 2H, H^2, H^6), ^{13}C NMR: δ 59.28 (OCH_3), 65.23 (CH_2O), 69.75 (NCH_2), 128.95 (C^3, C^5), 131.06 (C^2, C^6), 133.17 (C^4), 172.28 (HC=N). ^{13}C NMR: δ 59.62 (OCH_3), 65.56 (CH_2O), 70.08 (N-CH_2), 129.28 (C^3, C^5), 131.59 (C^2, C^6), 133.53 (C^4), 172.62 (HC=N). MS (FAB) *m/z*: 469 $[M\text{-}Cl]^+$. IR: υ(C=N) 1637 cm^{-1}.

b) Cyclopalladation of OH Functionalised Ligands

Preparation of [Pd(μ-Cl){C_6H_4-2-C(H)=NCH_2CH_2OH-κ-C_1,N}]$_2$ (2.43c)

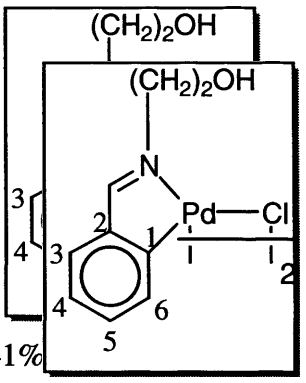

To a suspension of $Pd(OAc)_2$ (0.2 g, 0.89 mmol) in MeOH (35 ml), the imine (**c**) (0.132 g, 0.89 mmol) was added. The mixture was stirred for 2h, and then filtered over celite to remove (Pd°). The filtrate was treated with LiCl (0.15 g, 3.5 mmol) to give (**2.43c**) as a white precipitate. The solid was filtered, washed with hexane and dried under vacuum. (0.165 g, 65%). Anal. calc. for $C_{18}H_{20}O_2N_2$ Cl_2Pd_2(1 equiv.H_2O): C, 36.18; H, 3.69; N, 4.69%. Found: C, 35.86; H, 3.12; N, 4.41% DMSO, RT) 3.52 (br, 4H, -CH_2-CH_2-), 4.55 (m, 1H, OH), 6.90 (br, 2H, H^4, H^5), 7.20 (br, 1H, H^3), 7.75 (br, 1H, H^6), 7.90 (s, 1H, HC=N). MS (FAB) *m/z*: 545 $[2M-Cl]^+$, 254 $[M-Cl]^+$. IR: υ(C=N) 1613 cm^{-1}.

Reaction of imine (d,d`) with $Pd(OAc)_2$

To a suspension of $Pd(OAc)_2$ (0.2 g, 0.89 mmol) in MeOH (35 ml), the imine (**d,d`**) (0.15 g, 0.89 mmol) was added. The mixture was stirred at room temperature for 2h, and then filtered over celite to remove (Pd°). The filtrate was concentrated to a small volume, hexane was added and the solution was left overnight to precipitate. Green crystals were formed (0.06 g, 22%), then filtered, however, the crystals were insoluble in most solvents so the crystal was identified by X-ray diffraction to be (**2.42d'**). The filtrate was separated by chromatography (CH_2Cl_2/MeOH, 10:0.5) giving a yellow solid. The solid was also insoluble. Anal. calc. for $C_{24}H_{30}O_6N_2Pd_2$: C, 43.99; H, 4.61; N, 4.27%. Found: C, 43.93; H, 4.56; N, 4.39%. MS (FAB) *m/z*: 596 $[Pd_2L_2OAc]^+$, 535 $[Pd_2L_2]^+$, 268 $[PdL]^+$. IR: υ(C=N) 1605 cm^{-1}. υ(COO) 1563 and 1413 cm^{-1}. υ(OH) 3396 cm^{-1}.

Reaction of imine (d,d`) with $Pd(OAc)_2$ followed by LiCl

To a suspension of $Pd(OAc)_2$ (0.2 g, 0.89 mmol) in MeOH (35 ml), imine (**d**) (0.15 g, 0.89 mmol) was added. The mixture was stirred at room temperature for 2h, and then filtered over celite to remove (Pd°). The filtrate was treated with LiCl (0.15 g, 3.5 mmol) to give a green precipitate. The precipitate was filtered and washed with hexane. A further amount was obtained by concentration of the filtrate and precipitation with hexane. Anal. calc. for $C_{10}H_{12}OClNPd$: C, 39.50; H, 3.98; N, 4.61%. Found: C, 39.56; H, 3.81; N, 4.52%. MS (FAB) *m/z*: 268 $[PdL]^+$, no sign for dimer (**1.2d'**). IR: υ(C=N) 1585 cm^{-1}. υ(COO) 1555 cm^{-1}. υ(OH) 3118 cm^{-1}.

Reaction of imine (e,e`) with $Pd(OAc)_2$ followed by LiCl

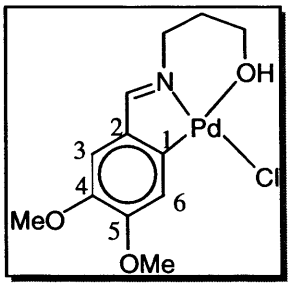

To a suspension of $Pd(OAc)_2$ (0.2 g, 0.89 mmol) in MeOH (35 ml), the imine **(e)** (0.39 g, 1.78 mmol) was added. The mixture was stirred at room temperature for 2h, and then filtered over celite to remove (Pd°). The resulting solution was rotary evaporated to dryness. The resulting solid was dissolved in a small amount of dichloromethane. Addition of hexane gave a green precipitate. The solid was filtered, washed with hexane and dried under vacuum. The green precipitate was washed over silica (CH_2Cl_2/acetone, 9:1), and the filtrate concentrated to small volume and treated with hexane to give more precipitate. The solid was washed with hexane giving **(2.47e)** as a pure isomer by ^1H NMR spectrometry (0.2 g, 62%): Anal. calc. for $C_{24}H_{32}O_6N_2Cl_2Pd_2$: C, 39.58; H, 4.43; N, 3.85%. Found: C, 39.48; H, 4.40; N, 3.92%. ^1H NMR: δ 2.04 (q, 2H, *J* 5, $-CH_2-$), 3.62 (t, 2H, *J* 5, NCH_2), 3.81 (s, 3H, OCH_3), 3.90 (t, 2H, *J* 5, CH_2O), 3.93 (s, 3H, OCH_3), 4.53 (br, 1H, OH), 6.76 (s, 1H, H^3), 7.18 (s, 1H, H^6), 7.72 (s, 1H, HC=N); ^{13}C NMR: δ 31.67 ($-CH_2-$), 56.31 (2 overlaped OMe), 61.93 (overlapped N-CH_2-CH_2), 110.31 (C^3), 117.26 (C^6), 137.05, 147.21 (2xC-OMe), 146.62 (C^2), 149.57 (C^1), 172.75 (N=CH). MS (FAB) *m/z*: 728 $[Pd_2L_2Cl_2]^+$, 693 $[Pd_2L_2Cl]^+$, 365 $[PdLCl]^+$. IR: υ(C=N) 1633 cm^{-1}.

Preparation of $[Pd\{C_6H_4\text{-}2\text{-}C(H)=N[2\text{-}(O)\text{-}C_6H_4]\}]_4$ (2.48h)

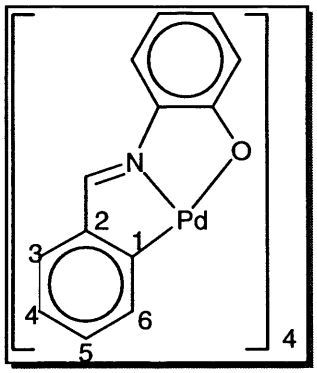

To a suspension of $Pd(OAc)_2$ (0.2 g, 0.89 mmol) in MeOH (40 ml), the imine **(g)** (0.35 g, 1.78 mmol) was added, giving a red solution within a few minutes. The mixture was stirred at room temperature for 2h, then filtered to give a red precipitate. The filtrate was concentrated to a small volume and treated with hexane to give more precipitate. The solid was washed with hexane giving **(2.48h)** as a pure compound. (0.242 g, 91%); Anal. calc. for $[C_{13}H_9ONPd]_4$: C, 51.76; H, 3.01; N, 4.64%. Found: C, 51.89; H, 2.89; N, 4.59%. ^1H NMR: δ 6.41 (m, 2H, Ar-H), 6.52 (m, 1H, Ar-H), 6.55 (dt, 1H, *J* 7.5, 1.5, H^6), 6.82 (t, 1H, *J* 6.5, H^5), 6.96 (m, 1H, Ar-H), 6.98 (dt, 1H, *J* 8, 1, H^4), 7.12 (s, 1H, N=C), 7.50 (d, 1H, *J* 7.5, H^3); ^{13}C NMR: δ 115.64, 116.79, 123.11, 124.18, 126.67, 119.72, 130.51, 132.66 (Ar-C); 157.6 (^8C). MS (FAB) *m/z*: 1207 $[M]^+$, 602 $[M]^+$. IR: υ(C=N) 1591 cm^{-1}.

Preparation of PPh_3 Complexes:

Preparation of [PdCl{C_6H_4-2-C(H)=N$CH_2CH_2OCH_3$-κ-C_1,N}(PPh_3)] (2.49a)

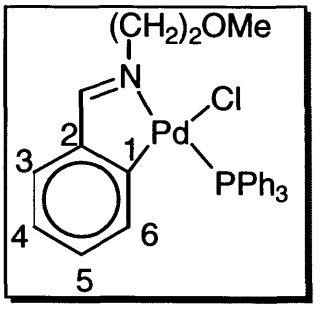

To a solution of $[PdL_aCl]_2$ **(2.43a)** (0.07 g, 0.113 mmol) in CH_2Cl_2 (10 ml), PPh_3 (0.07 g, 0.26 mmol) was added. This solution was stirred at room temperature for 5h, then the reaction was monitored by ^{31}P NMR and no free PPh_3 was observed. The solvent was removed under reduced pressure affording green crystals. (0.055 g, 81%); Anal. calc. For $C_{28}H_{27}ONClPdP$: C, 59.38; H, 4.81; N, 2.47%. Found: C, 59.45; H, 4.72; N, 2.54%. ^1H NMR: δ 3.38 (s, 3H, OCH_3), 3.81 (m, 2H, CH_2O), 4.10 (m, 2H, NCH_2), 6.39 (t, 1H, *J* 6, H^6), 6.53 (dt, 1H, *J* 6.5, 1, H^5), 6.90 (dt, 1H, *J* 6.5, 1, H^4), 7.29 (dd, 1H, *J* 7.5, 1.5, H^3), 7.39 (m, 9H, (H_m, H_p)PPh_3), 7.75 (m, 6H, (H_o) PPh_3), 8.13 (d, 1H, *J* 8, HC=N); ^{13}C NMR: δ 58.61 (CH_2O), 59.05 (OCH_3), 71.35 (NCH_2), 124.19, 129.98, 130.92, 138.36 (Ar-C^3, C^4, C^5, C^6), 128.25 (d, *J* 11.2, (C_m) PPh_3), 130.90 ((C_p)PPh_3), 131.70 ((C_i)PPh_3), 135.68 (d, *J* 11.5, (C_o) PPh_3), 148.48 (C^2), 158.31 (C^1), 177.25 (HC=N). ^{31}P-{^1H} NMR: 39.50. MS (FAB) *m/z*: 530 $[M-Cl]^+$. IR: υ(C=N) 1626 cm^{-1}.

Preparation of [PdCl{C_6H_4-2-C(H)=N$CH_2CH_2CH_2OCH_3$-κ-C_2,N}(PPh_3)] (2.49b)

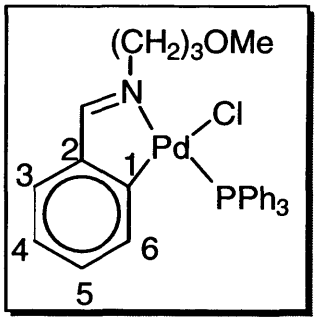

To a solution of $[PdL_bCl]_2$ **(2.43b)** (0.07 g, 0.11 mmol) in CH_2Cl_2 (10 ml), PPh_3 (0.06 g, 0.22 mmol) was added. The solution was stirred at room temperature for 4h, then the reaction was monitored by ^{31}P NMR and no free PPh_3 was observed. The solvent was removed under reduced pressure affording **(2.49b)** as a green solid. Some amount of the solid was dissolved in dichloromethane (1 ml) and treated with hexane (1 ml) to give crystals. (0.155 g, 82%). Anal. calc. for $C_{29}H_{29}ONPClPd$: C, 60.01; H, 5.04; N, 2.41%. Found: C, 59.92; H, 5.13; N, 2.34%. ^1H NMR: δ 2.17 (q, 2H, *J* 6.5, -CH_2-), 3.33 (s, 3H, OCH_3), 3.47 (t, 2H, *J* 6, CH_2O), 4.02 (m, 2H, NCH_2), 6.39 (t, 1H, *J* 6, H^6), 6.53 (dt, 1H, *J* 6.5, 1, H^5), 6.90 (dt, 1H, *J* 6.5, 1, H^4), 7.29 (dd, 1H, *J* 7.5, 1.5, H^3), 7.38 (m, 9H, (H_m,H_p) PPh_3), 7.73 (m, 6H, (H_o) PPh_3), 8.12 (d, 1H, *J* 8, N=CH); ^{13}C NMR: δ 30.77 (-CH_2-), 56.40 (CH_2O), 58.67 (OCH_3), 69.91 (NCH_2), 124.19, 127.89, 129.88, 138.45 (Ar-C^3, C^4, C^5, C^6), 128.22 (d, *J* 11, (C_m) PPh_3), 130.89 ((C_p) PPh_3), 131.69 ((C_i) PPh_3), 135.65 (d, *J* 11.5, (C_o) PPh_3), 148.35 (C^2), 158.21 (C^1), 175.91 (HC=N); ^{31}P-{^1H} NMR: 42.49. MS (FAB) *m/z*: 579 $[M]^+$, 544 $[M-Cl]^+$. IR: υ(C=N) 1626 cm^{-1}.

Preparation of [PdCl{C_6H_4-2-C(H)=NCH_2CH_2OH-$_K$-C_1,N}(PPh_3)] (2.49c)

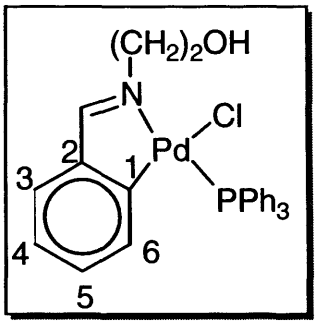

To a solution of $[PdL_cCl]_2$ (**2.43c**) (0.07 g, 0.12 mmol) in CH_2Cl_2 (25 ml), PPh_3 (0.064 g, 0.24 mmol) was added. The reaction was stirred at room temperature for 4h, the solvent was then removed under reduced pressure affording a white solid. The solid was dissolved in dichloromethane and treated with hexane giving (**2.49c**). (0.069 g, 51.8%). Anal. calc. for $C_{27}H_{25}ONPClPd$: C, 58.71; H, 4.56; N, 2.54%. Found: C, 58.56; H, 4.36; N, 2.37%. ^{1}H NMR: δ 2.59 (s, 1H, OH), 4.04 (s, 2H, CH_2O), 4.13 (s, 2H, NCH_2), 6.41 (t, 1H, *J* 6.5, H^6), 6.56 (t, 1H, *J* 7, H^5), 6.93 (t, 1H, *J* 7.5, H^4), 7.30 (d, 1H, *J* 7.5, H^3), 7.38 (m, 9H, (H_m, H_p) PPh_3), 7.75 (m, 6H, (H_o) PPh_3), 8.18 (d, 1H, *J* 7.5, HC=N); ^{13}C NMR: δ 60.84 (CH_2O), 62.63 (NCH_2), 124.30, 130.15, 138.37 (Ar-C^3, C^4, C^5, C^6), 128.29 (d, *J* 11, (C_m) PPh_3), 130.92 ((C_p) PPh_3), 131.74 ((C_i) PPh_3), 135.55 (d, *J* 12, (C_o) PPh_3), 148.12 (C^2), 158.01 (C^1), 177.1 (HC=N); ^{31}P-{^{1}H} NMR: 41.14. MS (FAB) *m/z*: 551 $[M]^+$, 516 $[M\text{-}Cl]^+$. IR: υ(C=N) 1624 cm^{-1}. υ(OH) 3430 cm^{-1}.

Preparation of [PdCl{C_6H_4-2-C(H)=N[2-(OCH_3)-C_6H_4]-$_K$-C_1,N}(PPh_3)] (2.49f)

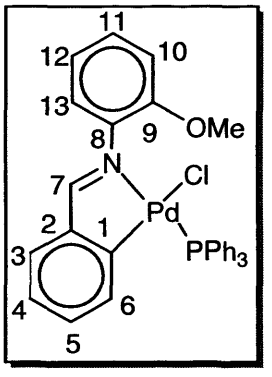

To a solution of $[PdL_fCl]_2$ (**2.43f**) (0.07 g, 0.1 mmol) in CH_2Cl_2 (10 ml), PPh_3 (0.05 g, 0.199 mmol) was added. The reaction was stirred at room temperature for 5h, then the reaction was monitored by ^{31}P NMR and no free PPh_3 was observed. The solvent was removed under reduced pressure affording (**2.49f**) as a green solid. (0.11 g, 90%); Anal. calc. for $C_{32}H_{27}ONPClPd$(1 equiv. CH_2Cl_2): C, 56.68; H, 4.18; N, 2.00%. Found: C, 56.21; H, 3.41; N, 1.81%. ^{1}H NMR: δ 3.87 (s, 3H, OCH_3), 6.47 (t, 1H, *J* 6.55, H^6), 6.61 (t, 1H, *J* 6, H^5), 6.94 (m, 3H, Ar-H), 7.19 (dt, 1H, *J* 8, 1, H^4), 7.28 (dd, 1H, J 8, 1.5, H^3), 7.37 (m, 10H, Ar-H, (H_m,H_p) PPh_3), 7.77 (m, 6H, (H_o) PPh_3), 8.25 (d, 1H, *J* 7.5, HC=N); ^{13}C NMR: δ 56.28 (OCH_3), 111.87, 120.01, 125.60, 127.87, (Ar-C^{10}, C^{11}, C^{12}, C^{13}), 124.22, 129.30, 131.70 (Ar-C^3, C^4, C^5,), 138.63 (C^6, *J* 11), 128.19 (d, *J* 11, (C_m) PPh_3), 130.84 ((C_p) PPh_3), 131.02 (C^8), 131.70 ((C_i) PPh_3), 135.78 (d, *J* 12, (C_o) PPh_3), 148.53 (C^2), 152.04 (C^9), 159.61 (C^1), 178.08 (HC=N); ^{31}P-{^{1}H} NMR: 42.9. MS (FAB) *m/z*: 613 $[M]^+$, 578 $[M\text{-}Cl]^+$. IR: υ(C=N) 1613 cm^{-1}.

Preparation of [PdCl{C_6H_4-2-C(H)=N$CH_2CH_2CH_2OH$-$_K$-C_1-N}(PPh_3)] (2.49d)

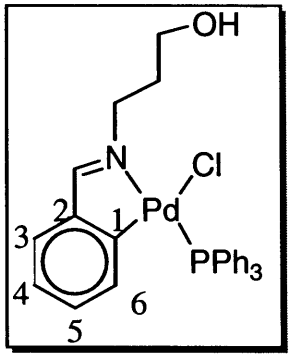

To a solution of isomers **(1.47d)** and **(2.43d')** (0.07 g, 0.11 mmol) in CH_2Cl_2 (25 ml), PPh_3 (0.06 g, 0.23 mmol) was added. The reaction was stirred at room temperature for 4h, then the solvent removed under reduced pressure to dryness to give a green precipitate. The precipitate was washed with hexane and dried under vacuum. (0.105 g, 81%); Anal. calc. for $C_{30}H_{31}ONPClPd$: C, 60.62; H, 5.26; N, 2.36%. Found: C, 60.52; H, 4.99; N, 2.29%. ^{1}H NMR: δ 2.07 (q, 2H, J 6.5, -CH_2-), 2.97 (m, 1H, OH), 3.83 (m, 2H, CH_2O), 4.11 (m, 2H, NCH_2), 6.40 (m, 1H, H^6), 6.54 (dt, 1H, J 7, 1, H^5), 6.92 (dt, 1H, J 7, 1, H^4), 7.29 (dd, 1H, J 7.5, 1, H^3), 7.40 (m, 9H, (H_m,H_p) PPh_3), 7.73 (m, 6H, (H_o) PPh_3), 8.17 (d, 1H, J 8, HC=N); ^{13}C NMR: δ 36.92 (-CH_2-), 55.57(CH_2O), 60.05 (NCH_2), 125.52, 129.79, 131.23, 139.53 (Ar-C^3, C^4, C^5, C^6), 129.45 (d, J 11, (C_m) PPh_3), 132.16 ((C_p) PPh_3), 132.59 ((C_i) PPh_3), 136.72 (d, J 12, (C_o) PPh_3), 149.41 (C^2), 158.85 (C^1), 177.74 (HC=N); ^{31}P-{^{1}H} NMR: 42.67. MS (FAB) *m/z*: 530 $[M-Cl]^+$. IR: υ(C=N) 1614 cm^{-1}. υ(O-H) 3436 cm^{-1}.

Preparation of [PdCl{C_6H_4-4,5-(OCH_3)$_2$-2-C(H)=N$CH_2CH_2CH_2OH$-$_K$-C_1-N}(PPh_3)] (2.49e)

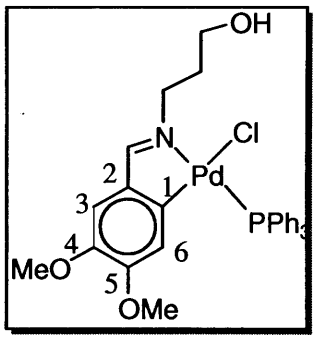

To a solution of isomer **(2.47e)** (0.07 g, 0.1 mmol) in CH_2Cl_2 (25 ml), PPh_3 (0.05 g, 0.19 mmol) was added. The reaction was stirred at room temperature for 4h, then the solvent removed under reduced pressure to dryness to give a green precipitate. The solid was washed with hexane. A small amount of the product was dissolved in dichloromethane and treated with hexane to give **(2.49e)** as a green crystals one of which was suitable for X-ray diffraction. (0.09 g, 75%). Anal. calc. for $C_{30}H_{31}O_3NPClPd$: C, 57.52; H, 4.99; N, 2.24%. Found: C, 57.61; H, 5.03; N, 2.29%. ^{1}H NMR: δ 2.05 (q, 2H, J 6.5, -CH_2-), 2.84 (s, 3H, OMe), 2.99 (br, 1H, OH), 3.77 (s, 3H, OMe), 3.81 (m, 2H, CH_2O), 4.04 (m, 2H, NCH_2), 5.95 (d, 1H, J 6, H^6), 6.86 (s, 1H, H^3), 7.40 (m, 9H, (H_m,H_p) PPh_3), 7.75 (m, 6-H, (H_o) PPh_3), 8.06 (d, 1H, J 8, HC=N); ^{13}C NMR: δ 35.75 (-CH_2-), 53.75 (CH_2O), 55.05, 55.81 (2 × OCH_3), 58.71 (NCH_2), 110.46 (C^3), 121.51 (d, J 11.5, C^6), 128.16 (d, J 11, (C_m) PPh_3), 130.93 ((C_p) PPh_3), 131.18 ((C_i) PPh^3), 135.37 (d, J 12, (C_o) PPh_3), 139.62, 145.58 (^{4}C,^{5}C), 148.81 (C^2), 151.08 (C^1), 175.45 (HC=N); ^{31}P-{^{1}H} NMR: 43.14. MS (FAB) *m/z*: 627 $[M]^+$, 590 $[M-Cl]^+$. IR: υ(C=N) 1620 cm^{-1}. υ(O-H) 3436 cm^{-1}.

Preparation of [PdCl{C_6H_4-C(H)=N[2-(O)C_6H_4]-$_K$-C_2,N,O}(PPh_3)] (2.50h)

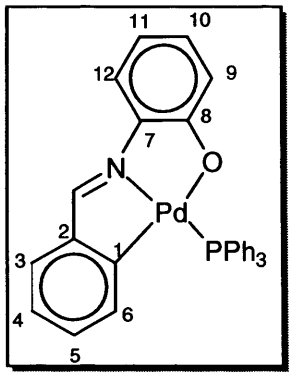

To a solution of [PdL_g] (**2.48h**) (0.07 g, 0.06 mmol) in CH_2Cl_2 (17 ml), PPh_3 (0.06 g, 0.23 mmol) was added, giving a deep pink solution within a few seconds. This solution was stirred at room temperature for 2h. Treatment with hexane gave (**2.50h**) as a deep red solid. The product was recrystallised from dichloromethane/hexane to give red crystals which were suitable for X-ray diffraction. (0.12 g, 92%); Anal. calc. for $C_{31}H_{24}OPNPd$(1/2 equiv. H_2O): C, 65.45; H, 4.37; N, 2.45%. Found: C, 64.96; H, 3.88; N, 2.47%. ^{1}H NMR: δ 6.02 (m, 1H, H^6), 6.35 (t, 1H, *J* 7, Ar-H), 6.44 (t, 1H, *J* 7.5, H^5), 6.51 (d, 1H, *J* 8.5, Ar-H), 6.81 (t, 1H, *J* 7.3, Ar-H), 6.93 (t, 1H, *J* 7.5, H^4), 7.11 (m, 2H, Ar-H), 7.42 (m, 9H, (H_m,H_p) PPh_3), 7.68 (m, 6H, (H_o) PPh_3), 7.93 (d, 1H, *J* 10, HC=N); ^{13}C NMR: δ 113.76, 115.78, 121.94, 124.44, 127.86, 128.44, 131.75, 137.71 (Ar-C^3, C^4, C^5, C^6, C^9, C^{10}, C^{11}, C^{12}), 129.94 (C^7), 128.49 (d, *J* 11, (C_m) PPh_3), 130.37 ((C_i) PPh_3), 130.90 ((C_p) PPh_3), 135.02 (d, *J* 12.5, (C_o) PPh_3), 154.99 (C^1), 156.72 (HC=N); ^{31}P-{^{1}H} NMR: 34.2. MS (FAB) *m/z*: 563 $[M]^+$. IR: υ(C=N) 1590 cm^{-1}.

Preparation of Pyridine Complexes:

Preparation of [PdCl{C_6H_4-2-C(H)=N$CH_2CH_2OCH_3$-$_K$-C_1,N}(py)] (2.51a)

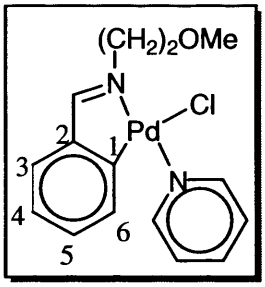

To a solution of [$PdL_aCl]_2$ (**2.43a**) (0.07 g, 0.12 mmol) in CH_2Cl_2 (10 ml), pyridine (0.02 g, 0.24 mmol) was added. The reaction was stirred at room temperature overnight then evaporated to a small volume. Treatment with hexane gave (**2.51a**) as a green solid. The product was recrystallised from dichloromethane/hexane to give green crystals which were suitable for X-ray diffraction. (0.062 g, 71%). Anal. calc. for $C_{15}H_{17}ON_2ClPd$: C, 47.02; H, 4.47; N, 7.31%. Found: C, 46.97; H, 4.50; N, 7.31%. ^{1}H NMR: δ 3.38 (s, 3H, OCH_3), 3.87 (m, 2H, CH_2O), 3.89 (m, 2H, NCH_2), 6.16 (d, 1H, *J* 7.5, H^6), 6.93 (dt, 1H, *J* 7.5, 1.5, H^5), 7.05 (dt, 1H, *J* 7.5, 1.5, H^4), 7.29 (dd, 1H, *J* 7.5. 1, H^3), 7.44 (m, 2H, (H_m) py), 7.86 (m, 1H, (H_p) py), 7.91 (s, 1H, N=CH), 8.90 [d, 2H, *J* 5, (H_o) py]; ^{13}C NMR: δ 59.07 (OCH_3), 60.03 (CH_2O), 70.76 (NCH_2), 124.72, 127.68, 130.5, 138.23 (Ar-C^3, C^4, C^5, C^6), 125.65, 132.04, 153.36 [C_m, C_p, C_o (py)], 147.04 (C^2), 158.15 (C^1), 177.17 (HC=N). MS (FAB) *m/z*: 382 $[M]^+$, 347 $[M-Cl]^+$, 268 $[M-pyCl]^+$. IR: υ(C=N) 1616 cm^{-1}.

Preparation of [PdCl{C_6H_4-2-C(H)=N$CH_2CH_2CH_2OCH_3$-κ-C_1,N}(py)] (2.51b)

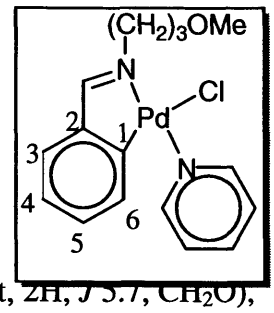

To a solution of $[PdL_bCl]_2$ **(2.43b)** (0.07 g, 0.11 mmol) in CH_2Cl_2 (10 ml), pyridine (0.02 g, 0.22 mmol) was added. The reaction was stirred at room temperature for 5h, and then evaporated to small volume. Treatment with hexane gave **(2.51b)** as a yellow solid. (0.075 g, 86%). Anal. calc. for $C_{16}H_{19}ON_2ClPd$: C, 48.38; H, 4.82; N, 7.05%. Found: C, 48.45; H, 4.75; N, 7.11%. ^{1}H NMR: δ 2.24 (q, 2H, J 6.2 Hz, -CH_2-), 3.33 (s, 3H, OCH_3), 3.48 (t, 2H, J 5.7, CH_2O), 3.90 (t, 2H, J 6.7, NCH_2), 6.16 (d, 1H, J 7.3, H^6), 6.94 (dt, 1H, J 7.5, 1.5, H^5), 7.05 (dt, 1H, J 7.5, 1, H^4), 7.28 (m, 1H, H^3), 7.44 (m, 2H, H_m (py)), 7.86 (m, 1H, (H_p) py), 7.90 (s, 1H, N=CH), 8.89 (d, 2H, J 5, (H_o) py); ^{13}C NMR: δ 30.27 (-CH_2-), 57.39 (CH_2O), 58.66 (OCH_3), 69.36 (NCH_2), 124.75, 127.41, 130.47, 138.23 (Ar-C^3, C^4, C^5, C^6), 125.65, 132.10, 153.37 [C_m,C_p,C_o (py)], 146.92 (C^2), 158.11 (C^1), 176.05 (HC=N). MS (FAB) *m/z*: 396 $[M]^+$, 361 $[M\text{-}Cl]^+$, 282 $[M\text{-}pyCl]^+$. IR: υ(C=N) 1614 cm^{-1}.

Preparation of [PdCl{C_6H_4-2-C(H)=N[-2-(O)-C_6H_4-κ-C_1,N}(py)] (2.52h)

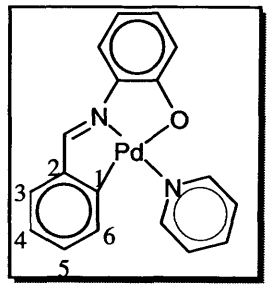

To a solution of $[PdL_g]$ **(2.48h)** (0.07 g, 0.06 mmol) in CH_2Cl_2 (15 ml), pyridine (0.02 g, 0.23 mmol) was added, giving a deep pink solution within a few seconds. This solution was stirred at room temperature for 3h, and then evaporated to small volume. Treatment with hexane gave **(2.52h)** as a deep red solid. (0.075 g, 85%); Anal. calc. for $C_{18}H_{14}ON_2Pd$(1 equiv. H_2O): C, 54.27; H, 4.02; N, 7.04%. Found: C, 54.43; H, 3.17; N, 6.66%. ^{1}H NMR: δ 6.33 (d, 1H, J 7, H^6), 6.70 (m, 7H, Ar-H), 7.44 (m, 2H,(H_m) py), 7.73 (s, 1H, HC=N), 7.85 (m, 1H, (H_p) py), 8.85 (dd, 2H, J 5, 1.5, (H_o) py]; ^{13}C NMR: δ 114.24, 115.92, 121.69, 124.85, 127.77, 129.88, 132.08, 138.40 (Ar-C^3, C^4, C^5, C^6, C^9, C^{10}, C^{11}, C^{12}), 125.81, 132.20, 152.57 (C_m,C_p,C_o (py)), 135.74 (C^8), 153.53 (C^1), 157.61 (HC=N), 171.89 (C^9). MS (FAB) *m/z*: 380 $[M]^+$. IR: υ(C=N) 1605 cm^{-1}.

Preparation of Palladium Cationic Complexes:

Preparation of [Pd{C_6H_4-2-C(H)=N$CH_2CH_2OCH_3$-κ-C_1,N,O}(PPh_3)][OTf] (2.53a) or (2.54a) or (2.55a)

To a suspension of $[PdL_aClPPh_3]$ **(2.49a)** (0.07 g, 0.12 mmol) in acetone (15 ml), AgOTf (0.03 g, 0.12 mmol) was added. The mixture was stirred under N_2 with exclusion of light for 2h. This suspension was filtered over celite to remove AgCl. The resulting solution was evaporated to dryness affording an oil product. Treatment with Et_2O gave a brown solid. (0.07 g, 80%); Anal. calc. for $C_{29}H_{27}O_4NPSF_3Pd$: C, 51.25; H, 3.97; N, 2.06%. Found: C, 52.06; H, 4.46; N,

1.99%. ^{1}H NMR: δ 3.34 (s, 3H, OMe), 3.78 (t, 2H, *J* 4.5, CH_2O), 4.02 (q, 2H, *J* 4.5, NCH_2), 6.35 (m, 1H, H^6), 6.56 (dt, 1H, *J* 7.5, 1, H^5), 6.96 (t, 1H, *J* 7.5, H^4), 7.30 (dd, 1H, *J* 7.5, 2, H^3), 7.47 (m, 9H, (H_m,H_p) PPh_3), 7.71 ([m, 6H, (H_o) PPh_3), 8.17 (d, 1H, *J* 7.5, HC=N); ^{13}C NMR: δ 58.28 (CH_2O), 59.50 (OCH_3), 72.19 (NCH_2), 125.47, 129.51 (^{4}C,^{5}C), 130.59 (d, *J* 5.5, C^3), 138.34 (d, *J* 12, C^6), 128.50 ((C_i) PPh_3), 129.08 (d, *J* 12, (H_m) PPh_3), 131.77 (d, *J* 2.5, (C_p) PPh_3), 135.27 (d, *J* 12, (C_o) PPh_3), 148.04 (C^2), 150.13 (C^1), 176.39 (HC=N); ^{31}P-{^{1}H} NMR: 39.94. MS (FAB) *m/z*: 530 $[M\text{-}OTf]^+$. IR: υ(C=N) 1638 cm^{-1}.

Preparation of [Pd{C_6H_4-2-C(H)=N$CH_2CH_2CH_2OCH_3$-κ-C_1,N,O}(PPh_3)][OTf] (2.53b) or (2.54b) or (2.55b)

To a suspension of [PdL_bClPPh_3] **(2.49b)** (0.07 g, 0.12 mmol) in acetone (15 ml), AgOTf (0.03 g, 0.12 mmol) was added. The suspension was stirred under N_2 with exclusion of light for 2h. This solution was filtered over celite to remove AgCl. The filtrate was evaporated to dryness affording a brown oil. Treatment with Et_2O gave a pale white solid. (0.75 g, 85%); ^{1}H NMR: δ 2.11 (q, 2H, *J* 6, -CH_2-), 3.14 (s, 3H, OCH_3), 3.75 (t, 2H, CH_2O), 3.91 (q, 2H, *J* 5.5, -CH_2), 6.33(m, 1H, H^6), 6.56 (dt, 1H, *J* 7.5, 1, H^5), 6.98 (t, 1H, *J* 7.5, H^4), 7.34 (dd, 1H, *J* 7.5, 1.5, H^3), 7.48 (m, 9H, (H_m,H_p) PPh_3), 7.70 (m, 6H, (H_o) PPh_3), 8.20 (d, 1H, *J* 8, HC=N); ^{13}C NMR: δ 29.23 (-CH_2-), 55.89 (CH_2O), 60.45 (OMe), 71.47 (NCH_2), 125.72, 129.56 (C^4, C^5), 130.70 (d, *J* 5.5, C^3), 138.32 (d, *J* 12, C^6), 128.24 (C_i), 129.20 (d, *J* 11, C_m (PPh_3)), 131.98 (d, *J* 2.5, C_p (PPh_3)), 135.15 [d, *J* 12.5, C_o (PPh_3)], 147.67 (C^2), 149.57 (C^1), 175.50 (HC=N); ^{31}P-{^{1}H) NMR: 39.85. MS (FAB) *m/z*: 544 $[M\text{-}OTf]^+$. IR: υ(C=N) 1631 cm^{-1}.

Preparation of [Pd{C_6H_4-2-C(H)=N$CH_2CH_2OCH_3$-κ-C_1,N,O}(PPh_3)](SbF_6) (2.53a)

To a suspension of [PdL_aClPPh_3] **(2.49a)** (0.12 g, 0.21 mmol) in dry CH_2Cl_2 (15 ml), $AgSbF_6$ (0.073 g, 0.21 mmol) was added. The mixture was stirred under N_2 with exclusion of light for 2h. This suspension was filtered over celite to remove AgCl. The resulting solution was evaporated to dryness affording an oily product.

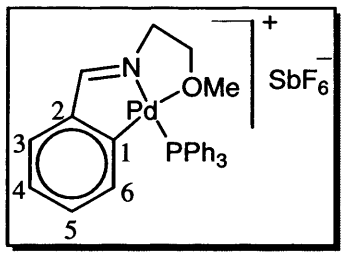

Treatment with Et_2O gave **(2.53a)** as a pale white solid. (0.151 g, 91%); Anal. calc. for $C_{28}H_{27}ONPSbF_6Pd$: C, 43.87; H, 3.55; N, 1.83%. Found: C, 43.69; H, 3.39; N, 1.83%. ^{1}H NMR: δ 3.19 (s, 3H, OMe), 3.84 (m, 2H, CH_2O), 3.94 (m, 2H, NCH_2), 6.32 (dd, 1H, *J* 7.5, 4.5, H^6), 6.59 (dt, 1H, *J* 7.5, 1.5, H^5), 6.99 (t, 1H, *J* 7.5, H^4), 7.37 (dd, 1H, *J* 7.5, 1.5, H^3), 7.50 (m, 9H, (H_m,H_p) PPh_3), 7.70 (m, 6H, (H_o) PPh_3), 8.22 (s, 1H, HC=N); ^{13}C NMR: δ 57.42 (CH_2O), 60.04 (OCH_3), 73.85 (NCH_2), 125.91, 130.16 (C^3,C^4, C^5), 138.34 (d, *J* 12, C^6), 128.18 ((C_i) PPh_3), 129.36 (d, *J* 12, (H_m) PPh_3), 132.18(d, *J* 2.5, (C_p) PPh_3), 135.10 (d, *J* 12, (C_o) PPh_3), 148.79 (C^2),

151.00 (C^1), 177.04 (HC=N); ^{31}P-{^1H} NMR: 39.94. MS (FAB) *m/z*: 530 $[M\text{-}SbF_6]^+$. IR: υ(C=N) 1626 cm^{-1}.

Preparation of [Pd{C_6H_4-2-C(H)=N$CH_2CH_2CH_2OCH_3$-$_K$-C_1,N,O}(PPh_3)](SbF_6) (2.53b)

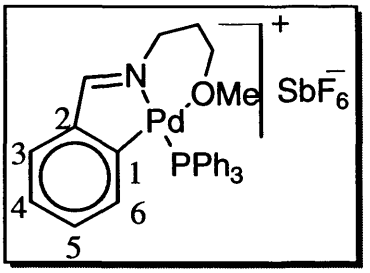

To a suspension of [PdL_bClPPh_3] (**2.49b**) (0.085 g, 0.15 mmol) in acetone (15 ml), $AgSbF_6$ (0.051 g, 0.15 mmol) was added. The suspension was stirred under N_2 with exclusion of light for 2h. This solution was filtered over celite to remove AgCl. The filtrate was evaporated to dryness affording (**2.53b**) as a brown oil. Treatment with Et_2O gave a pale white solid. (0.098 g, 83.8%); Anal. calc. for $C_{29}H_{29}ONPSbF_6Pd$: C, 44.62; H, 3.74; N, 1.79%. Found: C, 44.55; H, 3.63; N, 1.84%.^1H NMR: δ 2.15 (q, 2H, *J* 5.5, -CH_2-), 2.95 (s, 3H, OCH_3), 3.62 (t, 2H, *J* 5.5, CH_2O), 3.92 (q, 2H, *J* 5, NCH_2), 6.29 (dd, 1H, *J* 7.5, 6, H^6), 6.58 (t, 1H, *J* 7.5, H^5), 7.01 (t, 1H, *J* 7.5, H^4), 7.37 (dd, 1H, *J* 7.5, 1.5, H^3), 7.55 (m, 9H, (H_m,H_p) PPh_3), 7.68 (m, 6H, (H_o) PPh_3), 8.23 (d, 1H, *J* 8, HC=N); ^{13}C NMR: δ 28.36 (-CH_2-), 56.24 (CH_2O), 62.43 (OMe), 73.71 (NCH_2), 126.12, 130.07, 130.799 (C^3,C^4, C^5), 138.32 (d, *J* 10, C^6), 128.15 ((C_i) PPh_3), 129.43 (d, *J* 11, C_m (PPh_3), 132.28 (C_p (PPh_3)], 135.12 (d, *J* 13, C_o (PPh_3), 147.60 (C^2), 175.62 (HC=N); ^{31}P-{^1H} NMR: 39.85. MS (FAB) *m/z*: 544 $[M\text{-}SbF_3]^+$. IR: υ(C=N) 1633 cm^{-1}.

Preparation of [Pd{C_6H_4-2-C(H)=N$CH_2CH_2CH_2OH$-$_K$-C_1,N,O}(PPh_3)][OTf] (2.53d)

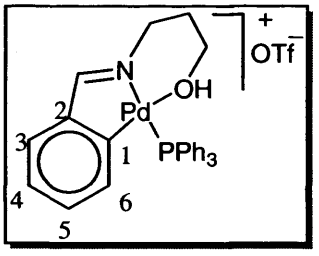

To a suspension of [PdL_aClPPh_3] (**2.49d**) (0.04 g, 0.06 mmol) in acetone (15 ml), AgOTf (0.02 g, 0.06 mmol) was added. The mixture was stirred under N_2 with exclusion of light for 2h. This suspension was filtered over celite to remove AgCl. The resulting solution was evaporated to dryness affording a oil product. Treatment with Et_2O gave (**2.53d**) as a beige precipitate. (0.036 g, 82%); Anal. calc. for $C_{29}H_{27}O_4NPSF_3Pd$: C, 51.22; H, 4.00; N, 2.06%. Found: C, 51.06; H, 3.96; N, 1.98%. ^1H NMR: δ 1.97 (q, 2H, *J* 5.5, -CH_2-), 3.69 (q, 2H, *J* 4.5, CH_2O), 3.80 (q, 2H, *J* 4.5, NCH_2), 5.72 (t, 1H, *J* 4.5, OH), 6.29 (dd, 1H, *J* 7.5, 5.5, H^6), 6.51 (dt, 1H, *J* 7.5, 1.5, H^5), 6.88 (dt, 1H, *J* 7.5, 1, H^4), 7.23 (dd, 1H, *J* 7.5, 1.5, H^3), 7.35 (m, 9H, (H_m,H_p) PPh_3), 7.60 (m, 6H, (H_o) PPh_3), 8.09 (d, 1H, *J* 8, HC=N); ^{13}C NMR: δ 30.72 (-CH_2-), 56.30 (CH_2O), 63.52 (NCH_2), 125.39, 129.27 (^4C,^5C), 130.91 (d, *J* 5.5, C^3), 138.53 (d, *J* 11, C^6), 127.82 ((C_i) PPh_3), 128.90 (d, *J* 11, (C_m) PPh_3), 131.74 (d, *J* 2.5, (C_p) PPh_3), 135.35 (d, *J* 12, (C_o) (PPh_3), 147.15 (C^2), 150.32 (C^1), 174.45 (HC=N); ^{31}P-{^1H} NMR: 39.81. MS (FAB) *m/z*: 530 $[M\text{-}OTf]^+$. IR: υ(C=N) 1637 cm^{-1}.

Preparation of [Pd{C_6H_4-4,5-$(OCH_3)_2$-2-C(H)=N$CH_2CH_2CH_2OH$-$_K$-C_1,N,O}(PPh_3)][OTf] (2.53e)

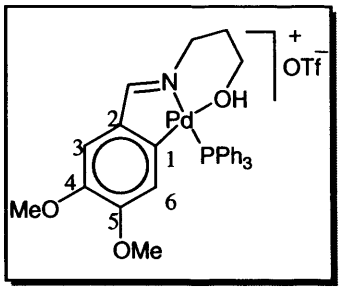

To a suspension of [PdL_eClPPh_3] (**2.49e**) (0.07 g, 0.11 mmol) in acetone (15 ml), AgOTf (0.03 g, 0.11 mmol) was added. The suspension was stirred under N_2 with exclusion of light for 2h, and then filtered over celite to remove AgCl. The filtrate was evaporated to dryness giving an oil product. Treatment with Et_2O gave a beige solid. (0.072 g, 86%); Anal. calc. for $C_{31}H_{31}O_6NPSF_3Pd$(1/2 equiv. CH_2Cl_2): C, 48.40; H, 4.05; N, 1.75%. Found: C, 48.76; H, 3.88; N, 1.64%. ^{1}H NMR: δ 2.00 (q, 2H, J 4.5, -CH_2-), 2.86 (s, 3H, OCH_3), 3.69 (m, 2H, CH_2O), 3.79 (s, 3H, OCH_3), 3.96 (m, 2H, NCH_2), 5.75 (br, 1H, OH), 5.86 (d, 1H, J 5.5, H^6), 6.91 (s, 1H, H^3), 7.49 (m, 9H, (H_m,H_p) PPh_3), 7.66 (m, 6H, (H_o) PPh_3), 8.07 (d, 1H, J 8, HC=N); ^{13}C NMR: δ 30.83 (-CH_2-), 55.43, 56.15 (2 × OCH_3), 55.98 (CH_2O), 63.68 (NCH_2), 111.79 (C^3), 121.62 (d, J 12, C^6), 127.84 ((C_i) PPh_3), 128.51, 138.68 (C^4, C^5), 129.00 (d, J 11, C_m (PPh_3), 131.88 (d, (C_p) PPh_3), 135.35 (d, J 12.6, (C_o) PPh_3), 146.51 (C^1), 173.75 (HC=N); ^{31}P-{^{1}H) NMR: 39.86. MS (FAB) *m/z*: 590 $[M\text{-}OTf]^+$. IR: υ(C=N) 1637 cm^{-1}.

Bibliography

1 A. Fernandez, D. Vazquez-Garcia, J. J. Fernandez, M. Lopez-Torres, A. Suarez, S. Castro-Juiz, J. M. Ortigueira, and J. M. Vila, *New J. Chem.*, 2002, **26**, 105.

2 J. M. Vila, M. Gayoso, M. T. Pereira, M. L. Torres, J. J. Fernandez, A. Fernandez, and J. M. Ortigueira, *J. Organomet. Chem.*, 1997, **532**, 171.

3 C. Cativiela, L. R. Falvello, J. Carlos Gines, R. Navarro, and E. P. Urriolabeitia, *New J. Chem.*, 2001, **25**, 344.

4 P. Braunstein and F. Naud, *Angew. Chem., Int. Ed.*, 2001, **40**, 680.

5 A. Bader and E. Lindner, *Coord. Chem. Rev.*, 1991, **108**, 27.

6 C. S. Slone, D. A. Weinberger, and C. Mirkin, A., *Prog. Inorg. Chem.*, 1999, **48**, 233.

7 H. Werner, A. Stark, M. Schulz, and J. Wolf, *Organometallics*, 1992, **11**.

8 J. R. Fulton, A. W. Holland, D. J. Fox, and R. G. Bergman, *Acc. Chem. Res.*, 2002, **35**, 44.

9 S. E. Kegley, C. J. Schaverien, J. H. Freudenberger, and R. G. Bergman, *J. Am. Chem. Soc.*, 1987, **109**, 6563.

10 J. F. Hartwig, R. A. Andersen, and R. G. Bergman, *Organometallics*, 1991, **10**, 1875.

11 I. Omae, *Chem. Rev.*, 1979, **79**, 287.

12 P. L. Holland, R. A. Andersen, R. G. Bergman, J. Huang, and S. P. Nolan, *J. Am. Chem. Soc.*, 1997, **199**, 12800.

13 J. Errington, W. S. McDonald, and B. L. Shaw, *J. Chem. Soc. Dalton Trans.*, 1980, 2312.

14 W. T. S. Huck, F. C. J. van Veggel, B. L. Kropman, D. M. A. Blank, E. G. Keim, M. M. A. Smithers, and D. M. Reinhoudt, *J. Am. Chem. Soc.*, 1995, **117**, 8293.

15 M. Ohff, A. Ohff, M. E. van Boom, and D. Milstein, *J. Am. Chem. Soc.*, 1997, **119**, 11697.

16 L. Kuil, H. Luitjes, D. M. Grove, J. W. Zwikker, J. G. Linden, A. M. Roelofsen, L. W. Jenneskens, W. Drenth, and G. Koten, *Organometallics*, 1994, **13**, 468.

17 P. Steenwinkel, R. A. Gossage, T. Maunula, D. M. Grove, and G. van Koten, *Chem. Eur. J.*, 1998, **4**, 763.

[18] D. E. Bergbreiter, P. L. Osburn, and Y.-S. Liu, *J. Am. Chem. Soc.*, 1999, **121**, 9531.

[19] R. B. Bedford, *Chem. Commun.*, 2003, 1787.

[20] G. R. Newkome, W. E. Puckett, V. K. Gupta, and G. E. Kiefer, *Chem. Rev.*, 1986, **86**, 451.

[21] Y. Motoyama, Y. Mikami, and H. Kawakami, *Organometallics*, 1999, **18**, 3584.

[22] S. Perez, C. Lopez, A. Caubet, X. Solans, and M. Font-Bardia, *New J. Chem.*, 2003, **27**, 975.

[23] M. Crespo, M. Font-Bardia, and X. Solans, *Organometallics*, 2004, **23**, 1708.

[24] M. Crespo, *Polyhedron*, 1996, **15**, 1981.

[25] J. M. Vila, M. T. Pereira, J. M. Ortigueira, D. Lata, M. Lopez Torres, J. J. Fernandez, A. Fernandez, and H. Adams, *J. Organomet. Chem.*, 1998, **566**, 93.

[26] A. Fernandez, P. Uria, J. J. Fernandez, M. Lopez-Torres, A. Suarez, D. Vazquez-Garcia, M. T. Pereira, and J. M. Vila, *J. Organomet. Chem.*, 2001, **620**, 8.

[27] A. Fernandez, D. Vazquez-Garcia, J. J. Fernandez, M. Lopez-Torres, A. Suarez, R. Mosteiro, and J. M. Vila, *J. Organomet. Chem.*, 2002, **654**, 162.

[28] A. Fernandez, D. Vazquez-Garcia, J. J. Fernandez, M. Lopez-Torres, A. Suarez, S. Castro-Juiz, and J. M. Vila, *Eur. J. Inorg. Chem.*, 2002, 2389.

[29] S. Chattopadhyay, C. Sinha, P. Basu, and A. Chakravorty, *J. Organomet. Chem.*, 1991, **414**, 421.

[30] A. Amoedo, M. Grana, J. Martinez, T. Pereira, M. Lopez-Torres, A. Fernandez, J. J. Fernandez, and J. M. Vila, *Eur. J. Inorg. Chem.*, 2002, 613.

[31] X. Riera, A. Caubet, C. Lopez, V. Moreno, E. Freisinger, M. Willermann, and B. Lippert, *J. Organomet. Chem.*, 2001, **629**, 97.

[32] X. Riera, A. Caubet, C. Lopez, V. Moreno, X. Solans, and M. Font-Bardia, *Organometallics*, 2000, **19**, 1384.

[33] S. Perez, C. Lopez, A. Caubet, R. Bosque, X. Solans, M. F. Bardia, A. Roig, and E. Molins, *Organometallics*, 2004, **23**, 224.

[34] C. Lopez, S. Perez, X. Solans, and M. Font-Bardia, *J. Organomet. Chem.*, 2002, **650**, 258.

[35] D. Vazquez-Garcia, A. Fernandez, J. J. Fernandez, M. Lopez-Torres, A. Suarez, J. M. Ortigueira, J. M. Vila, and H. Adams, *J. Organomet. Chem.*, 2000, **595**, 199.

[36] J. M. Vila, M. T. Pereira, J. M. Ortigueira, M. Grana, D. Lata, A. Suarez, J. J. Fernandez, A. Fernandez, M. Lopez-Torrer, and H. Adams, *J. Chem. Soc. Dalton Trans.*, 1999, 4193.

[37] F. Basuli, P. Chattopadhyay, and C. Sinha, *Polyhedron*, 1996, **15**, 2439.

[38] A. Caubet, C. Lopez, X. Solans, and M. Font-Bardia, *J. Organomet. Chem.*, 2003, **669**, 164.

[39] T. Kawamoto, I. Nagasawa, and H. Kuma, *Inorg. Chem.*, 1996, **35**, 2427.

[40] A. Fernandez, M. Lopez-Torres, A. Suarez, J. M. Ortigueira, T. Pereira, J. J. Fernandez, J. M. Vila, and H. Adams, *J. Organomet. Chem.*, 2000, **598**, 1.

[41] S. Das and S. Pal, *J. Organomet. Chem.*, 2004, **689**, 352.

[42] A. Fernandez, D. Vazquez-Garcia, J. J. Fernandez, M. Lopez-Torres, A. Suarez, S. Castro-Juiz, and J. M. Vila, *New J. Chem.*, 2002, **26**, 398.

[43] A. Fernandez, E. Pereira, J. J. Fernandez, M. Lopez-Torres, A. Suarez, R. Mosteiro, and J. M. Vila, *Polyhedron*, 2002, **21**, 39.

[44] C. Lopez, A. Caubet, S. Perez, X. Solans, and M. Font-Bardia, *J. Organomet. Chem.*, 2003, **681**, 82.

[45] E. Steiner and F. A. L. L`Eplattenier, *Helv. Chim. Acta.*, 1978, **61**, 2264.

[46] J. M. Vila, M. T. Pereira, J. M. Ortigueira, M. Lopez-Torrer, D. Castineiras, J. J. Fernandez, and A. Fernandez, *J. Organomet. Chem.*, 1998, **56**, 21.

[47] M. Nonoyama, *J. Inorg. Nucl. Chem.*, 1980, **42**, 297.

[48] J. Albert, A. Gonzalez, J. Granell, R. Moragas, C. Puerta, and P. Valerga, *Organometallics*, 1997, **16**, 3775.

[49] P. Ghosh, A. Pramanik, N. Bag, Lahiri, K., and A. Chakravorty, *J. Organomet. Chem.*, 1993, **454**, 237.

[50] M. Crespo, M. Font-Bardia, S. Perez, and X. Solans, *J. Organomet. Chem.*, 2002, **642**, 171.

[51] A. D. Ryabov, L. Kuzmina, V. A. Polyakov, G. M. Kazankov, E. S. Ryabova, M. Pfeffer, and R. van Eldik, *J. Chem. Soc., Dalton Trans.*, 1995, 999.

[52] G. Balavoine and J. C. Clinet, *J. Organomet. Chem.*, 1990, **390**, C84.

[53] T. Izumi, H. Watabe, and A. Kasahara, *Bull. Chem. Soc. Jpn.*, 1981, **54**, 1711.

[54] C.-L. Chen, Y.-H. Liu, S.-M. Peng, and S.-T. Liu, *J. Organomet. Chem.*, 2004, **689**, 1806.

[55] A. J. Davenport, D. L. Davies, J. Fawcett, and D. R. Russell, *J. Chem. Soc. Dalton Trans.*, 2002, 3260.

[56] J. R. Doyle, P. E. Slade, and H. B. Janassen, *Inorg. Synth.*, 1960, **6**, 218.

Chapter Three:

Synthesis of Half-sandwich Cyclometallated Complexes

Chapter Three – Synthesis of half-sandwich cyclometallated complexes

3.1 Introduction

3.1.1 Arene Ru, Cp Rh and Cp*Ir half-sandwich cyclometallated complexes*

A half–sandwich compound is a complex containing a π-bonded ligand, usually an arene or a cyclopentadienyl ring, occupying three facial coordination sites of the metal centre. There are then one to four sites available for coordination of other ligands. The main focus of this chapter will be the synthesis and reactivity of arene ruthenium and Cp*M (M = Rh, Ir) complexes containing a bidentate chelating C,N ligand (**Fig. 3.1**).

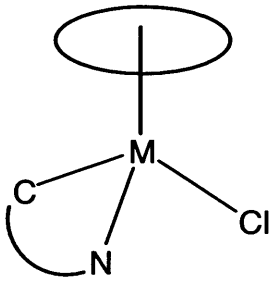

(Fig. 3.1)

The usual precursors to these mononuclear half-sandwich complexes are the dimers $[RuCl_2(arene)]_2$,[1] $[IrCl_2Cp^*]_2$[2] and $[RhCl_2Cp^*]_2$[2] which are air stable and are readily synthesized from commercially available $RuCl_3 \cdot xH_2O$, $IrCl_3 \cdot xH_2O$ and $RhCl_3 \cdot xH_2O$ respectively (**Scheme 3.1**).

$$RuCl_3.xH_2O + \alpha\text{-phellandrene} \xrightarrow[EtOH]{\text{reflux}} [RuCl_2(p\text{-cymene})]_2 \quad \textbf{(3.1)}$$

$$MCl_3.xH_2O + Cp^*H \xrightarrow[MeOH]{\text{reflux}} [MCl_2Cp^*]_2$$

(3.2, M = Ir)
(3.3, M = Rh)

(Scheme 3.1)

The dimers **(3.1)**, **(3.2)** and **(3.3)** undergo many analogous reactions.[3-5] Thus treatment with monodentate ligands L (L = PPh_3, py) gives half-sandwich complexes $[RuCl_2(L)(p\text{-cymene})]$[5] and $[MCl_2(L)Cp^*]$[3, 6] (M = Ir, Rh). A wide variety of half-sandwich complexes with bidentate ligands are known, *e.g.* neutral ligands (N,N),[7] **(3.4)**, (P,P)[4] **(3.5)**, (P,N)[8] **(3.6)** or anionic ligands *e.g.* (N,O)[9] **(3.7)**, (P,O)[10] **(3.8)**, (O,O)[11] **(3.9)** **(Fig 3.2)**. However, few articles focus on half-sandwich complexes containing a C, X (X = N, O, P) bidentate group with C,P being the most common.[12-16]

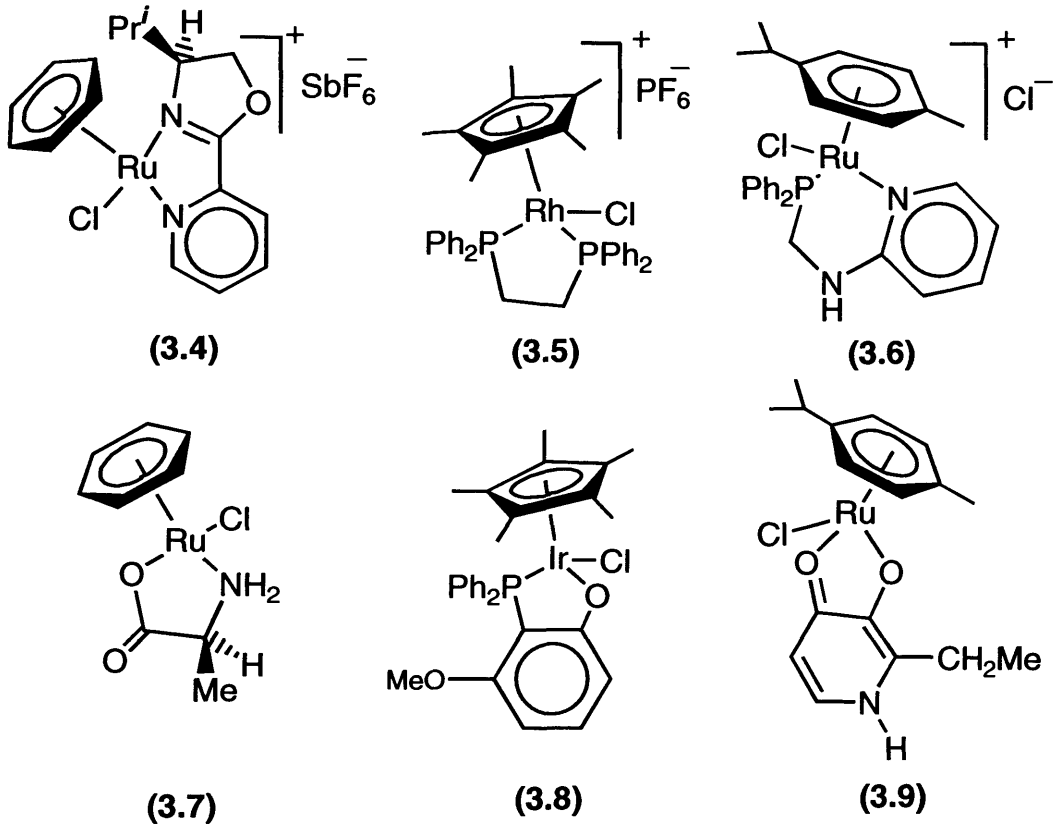

(3.4) **(3.5)** **(3.6)**

(3.7) **(3.8)** **(3.9)**

(Fig. 3.2)

3.1.2 Arene Ru half-sandwich cyclometallated complexes of N-donor ligands

Arene ruthenium cyclometallated complexes show interesting reactivity particularly in C-C bond forming reactions with alkenes and alkynes (see **Ch. 4**). Recently ruthenium aryl complexes have been shown to be intermediates in a catalytic Heck type coupling.[17] In addition, $[RuCl(dmba)(C_6H_6)]$ (dmbaH = N,N-dimethylbenzylamine) has been used as an intermediate in the synthesis of ruthenium complexes for bioelectrochemical applications (see **Ch. 1**).[18] The first arene ruthenium cyclometallated complex **(3.10)** was prepared by Pfeffer *et al.*[19] **(Scheme 3.2)**.

Notably, attempts to prepare similar complexes by transmetallation of $[RuCl_2(arene)]_2$ with organolithium reagents were not successful.[19]

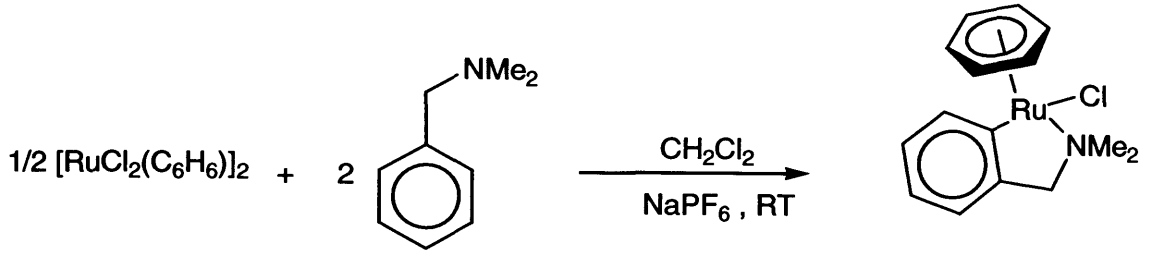

(3.10)

(Scheme 3.2)

This C-H activation method gives **(3.10)** in low yield (38%). Pfeffer *et al.* showed that transmetallation with mercury reagents gave better yields **(Scheme 3.3)**.[20]

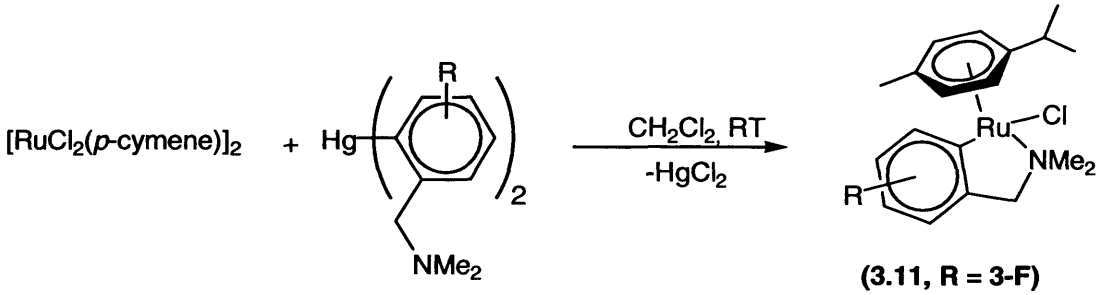

(3.11, R = 3-F)
(3.12, R = 3-Me)
(3.13, R = 2,3-OCH_2O)
(3.14, R = 2,4-$(MeO)_2$)

(Scheme 3.3)

Complexes **(3.11-3.13)** were formed in very high yield (>95%), suggesting there is little influence of the electronic nature of the phenyl substituents on the transmetallation process. However, increased steric bulk on the phenyl ring impedes formation of the complexes as evidenced by the reduced yield, (42%), of **(3.14)**. Another, more recent, example of an arene ruthenium cyclometallated complex synthesised from a mercury reagent is **(3.15)**.[21]

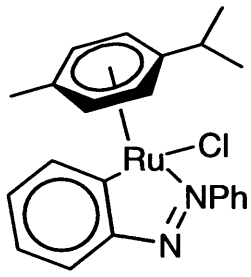

(3.15)

In order to avoid the use of toxic mercury reagents, Pfeffer *et al.*[22] tried to improve the C-H activation method for affecting the cycloruthenation of N-containing ligands. Reaction of $[RuCl_2(C_6H_6)]_2$ with N,N-dimethylbenzylamine, NaOH as base and KPF_6 in NCMe (heated at 45 °C for 3h) led to formation of the corresponding cyclometallated complex **(3.17)** in good yield. Pfeffer and co-workers proposed the pathway shown in **(Scheme 3.4)**.

Pfeffer suggested that the much improved yields of cycloruthenated compounds obtained by this method as compared to the results in **(3.10)** may be explained by ready formation of cationic intermediate **(3.16)**; cationic species may facilitate an electrophilic C-H activation step.

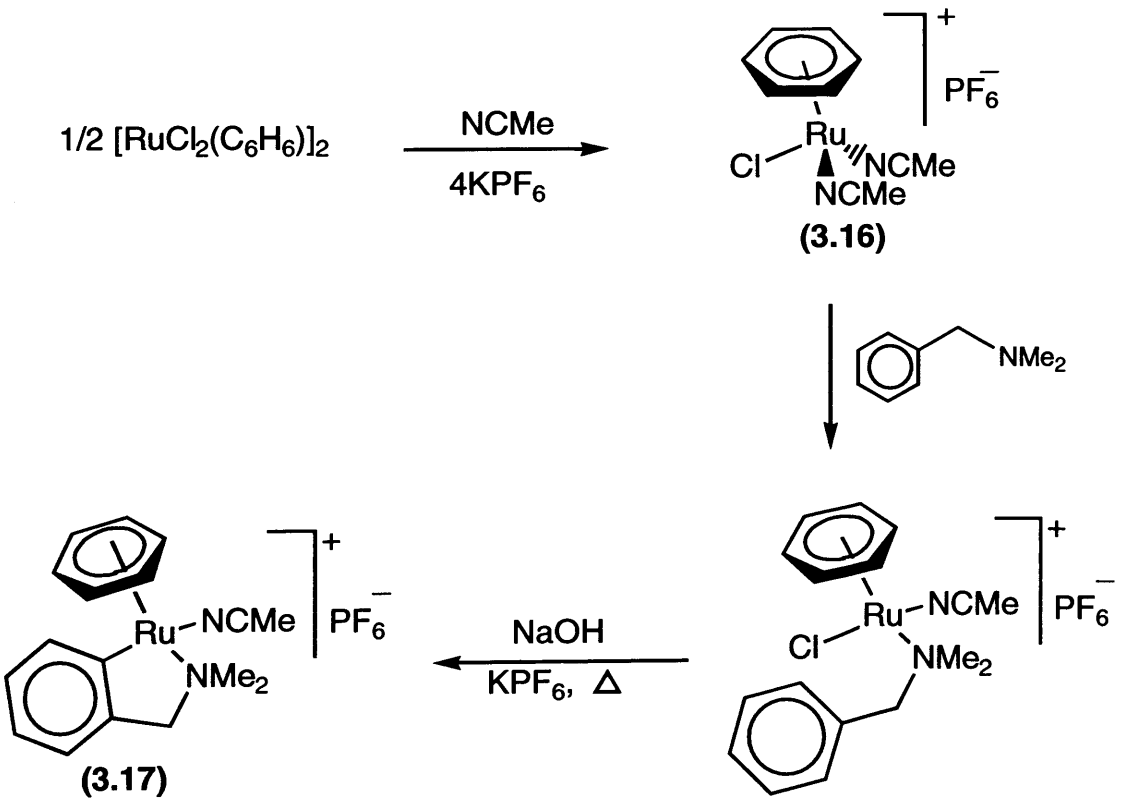

(Scheme 3.4)

The enhanced cyclometallation with cations has also been also demonstrated by Boncella.[23] Thus $[RuCl_2(PMe_3)(C_6H_6)]$ reacts with benzylideneaniline and $AgBF_4$ to give the cationic orthometallated imine complex **(3.18)** **(Scheme 3.5)**. Similarly, a cycloruthenated benzodiazepine **(3.19)** was reported in 2002,[24] in this case $NaBPh_4$ was used to abstract chloride and NEt_3 was used as a base **(Scheme 3.6)**.

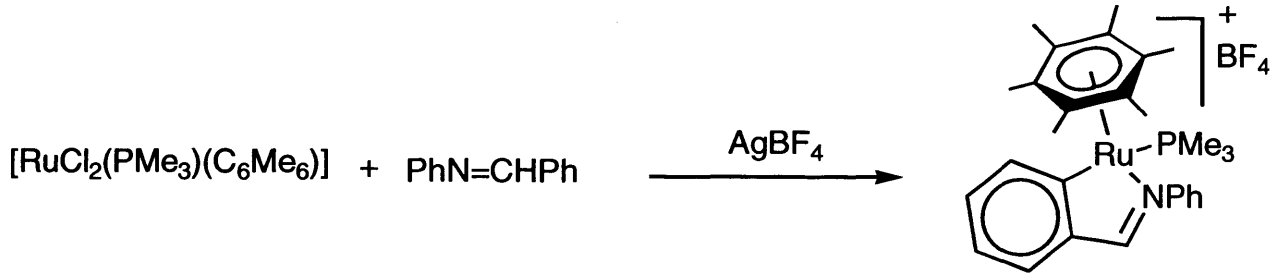

(Scheme 3.5) **(3.18)**

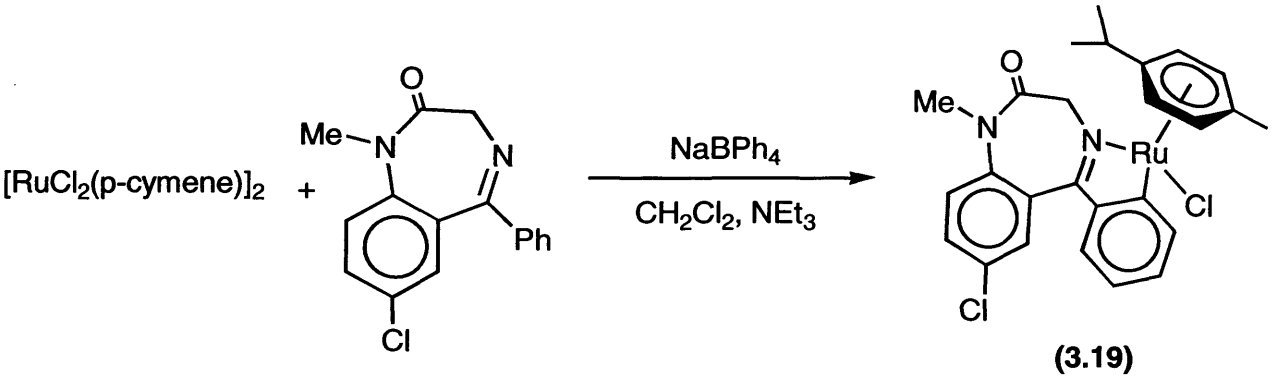

(3.19)

(Scheme 3.6)

*3.1.3 Cp*M (M= Ir, Rh) half-sandwich cyclometallated complexes of N-donor ligands*

Half-sandwich Cp*M (M = Rh, Ir) complexes undergo intermolecular C-H bond activation reactions with a wide range of organic molecules[25, 26] (as discussed in **Section 1.4.1**). However cyclometallation of nitrogen donor ligands with Cp* M (M = Rh, Ir) complexes is rare, though cyclometallation of phosphorus containing ligands has been identified in C-H activation studies with Cp*M (M = Rh, Ir), Thus, C-H activation with loss of H_2 or alkane or benzene can give rise to cyclometallated complexes e.g. **(3.20),**[16] **(3.21)**[13] and **(3.22)**[15] containing C,P-bidentate ligands **(Scheme 3.7)**.

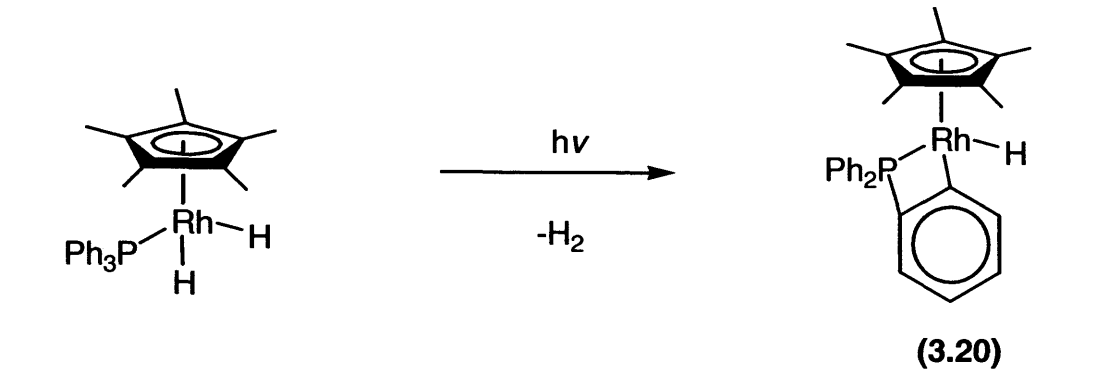

(3.20)

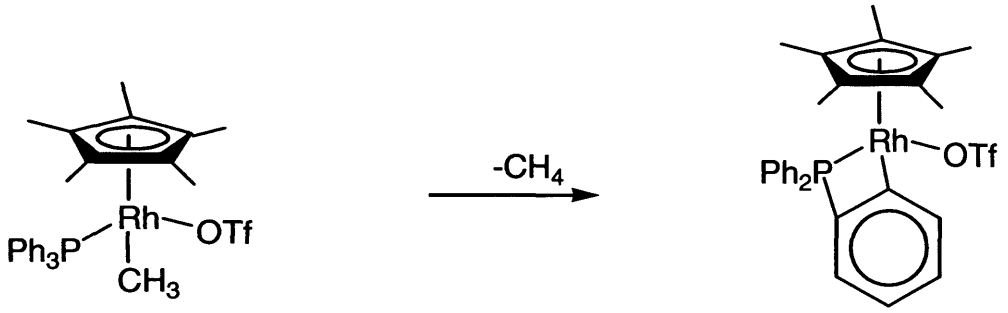

(3.21)

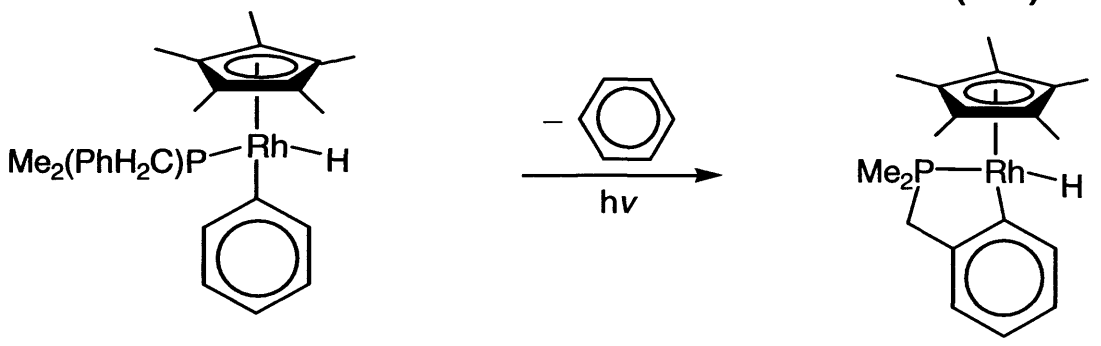

(3.22)

(Scheme 3.7)

Another cyclometallated complex **(3.23)** containing a C,O-bidentate ligand can be prepared by transmetallation **(Scheme 3.8)**.[27]

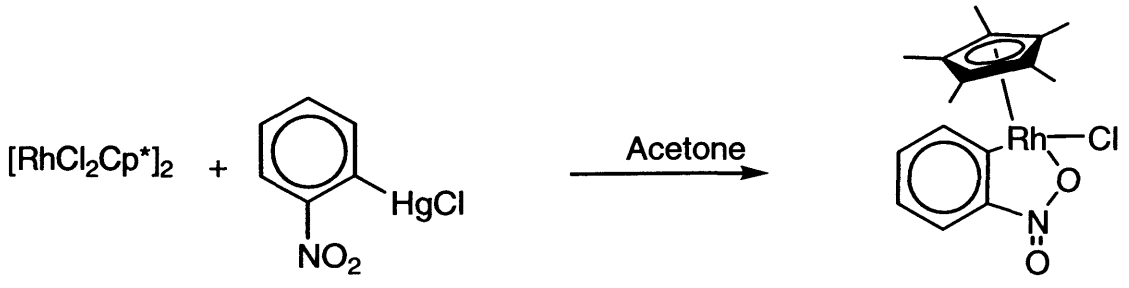

(3.23)

(Scheme 3.8)

Prior to our work, complexes of Cp*M (M = Rh, Ir) with cyclometallated nitrogen donor ligands have been reported by only two groups. Tilset *et al.*[28] prepared **(3.24)** *via* C-H activation **(Scheme 3.9)**. Surprisingly C-H activation of a methyl group occurred in preference to coordination of the second imine. Treatment of **(3.24)** with triethylamine served to remove HCl, and neutral compound **(3.25)** was isolated.

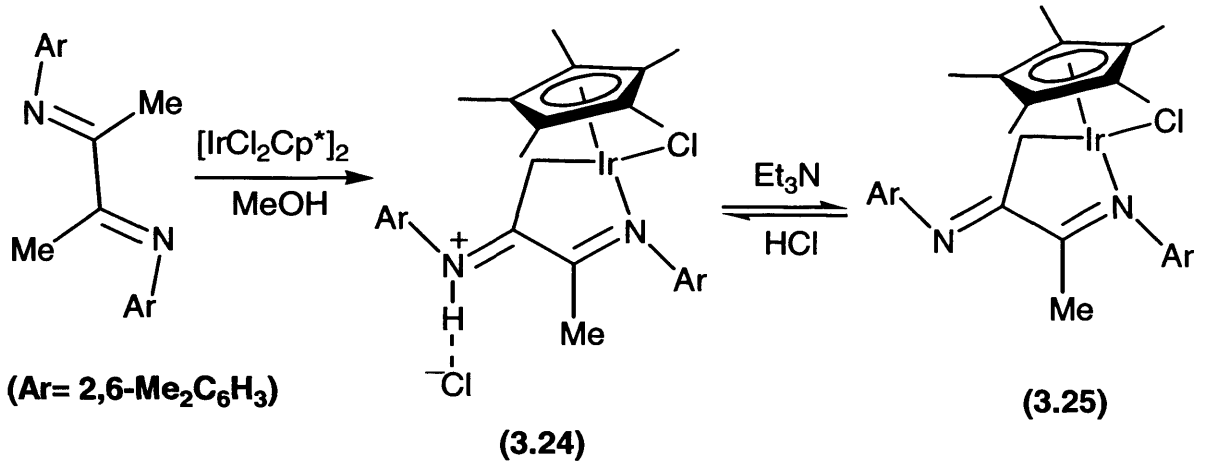

(Ar= 2,6-$Me_2C_6H_3$) **(3.24)** **(3.25)**

(Scheme 3.9)

Beck *et al.*[29] reported that reaction of oxazolone **(3.26, R = Me)** with $[IrCl_2Cp^*]_2$ in the presence of NaOAc formed half-sandwich complex **(3.27)** as a mixture of diasteromers **(Scheme 3.10)**. When **(3.26, R = H)** was used, an unusual dimeric complex **(3.28)** with a bridging cyclometallated ligand could be obtained.

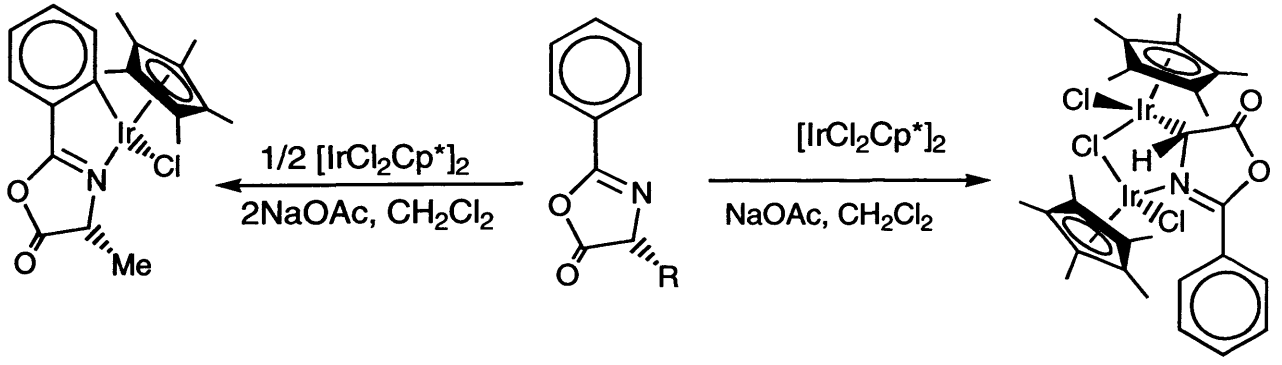

(3.27) **(3.26, R = H, Me)** **(3.28)**

(Scheme 3.10)

Attempts to form similar cyclometallated complexes *e.g* **(3.29)** via a lithium reagent were unsuccessful **(Scheme 3.11)** as found previously with arene ruthenium (see above).

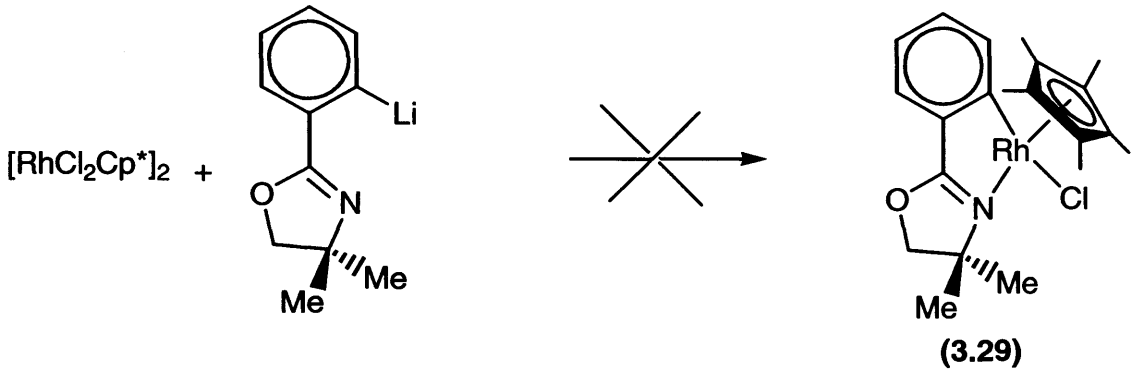

(3.29)

(Scheme 3.11)

This chapter describes our attempts to establish the scope of acetate-assisted C-H activation for the synthesis of arene ruthenium and Cp*M (M = Rh, Ir) half-sandwich cyclometallated complexes containing nitrogen donor ligands. The mechanism of this process has also been investigated and will be discussed.

3.2 Results and Discussion

3.2.1 Preparation of ligands

We have selected imines, amines, oxazolines, pyrroles and a pyridine (L_1-L_{11}, **Fig. 3.3**) to test the scope of cyclometallation by arene ruthenium and Cp*M (M = Ir, Rh) precursors in the presence of NaOAc. Ligands (L_4, L_8, L_9, L_{10}) were prepared in a similar manner to (L_1) and (L_2) as described in **Ch. 2**. Imine (L_7) was synthesised by treatment of pyrrole carboxyaldehyde and 3,5-dimethylaniline in refluxing EtOH for 18h. Ligand (L_6) was prepared according to the method of Denmark[30], whilst ligands (L_3, L_5, L_{11}) were obtained from Aldrich.

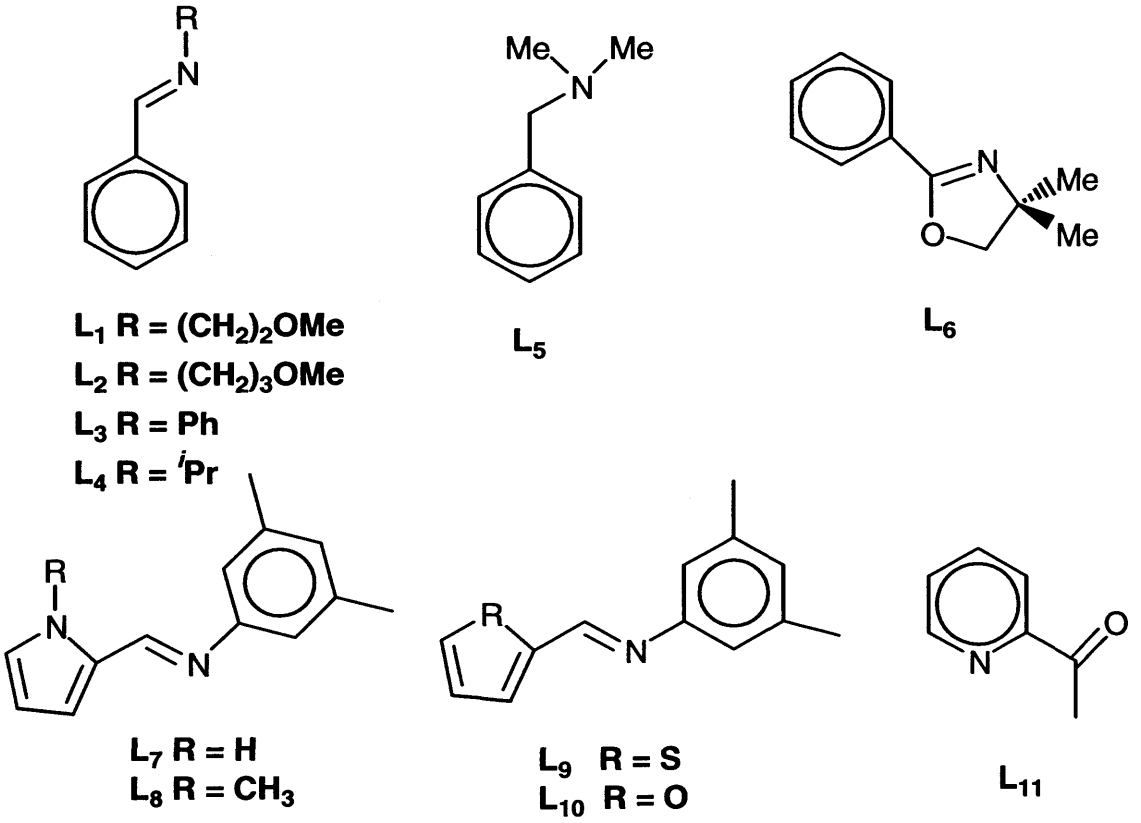

(Fig. 3.3)

The ^{1}H NMR spectra of ligands (L_4, L_7, L_9, L_{10}) showed they were pure, however, (L_8) showed a mixture of starting material and product. Therefore, in reactions with (L_8), excess 2-methyl pyrrole carboxyaldehyde was added to ensure the maximum amount of imine and minimum amount of unreacted amine; excess aldehyde does not effect the cyclometallation (see later).

3.2.2 Preparation of half-sandwich cyclometallated complexes

As mentioned in **Ch. 2**, cyclopalladation occurs more easily starting with $[Pd(OAc)_2]_3$ rather than with $PdCl_2$. In some cases addition of acetate to a palladium chloride complex can induce cyclometallation of a ligand.[31] As mentioned above, Beck reported acetate-assisted cyclometallation of an oxazolone by $[IrCl_2Cp^*]_2$.[29] Our results on the use of NaOAc to promote cyclometallation of nitrogen donor ligands in arene ruthenium and Cp*M (M= Ir, Rh) complexes are described below. All new compounds were characterised by ^1H and ^{13}C-$\{^1H\}$ NMR spectroscopy, FAB mass spectrometry, IR, elemental analysis and in some cases X-ray crystallography.

3.2.2a Imines

The results of the reactions of imines (L_1-L_3) with arene ruthenium and Cp*M (M = Ir, Rh) dimers in the presence of NaOAc at room temperature are shown in **Scheme 3.12.**

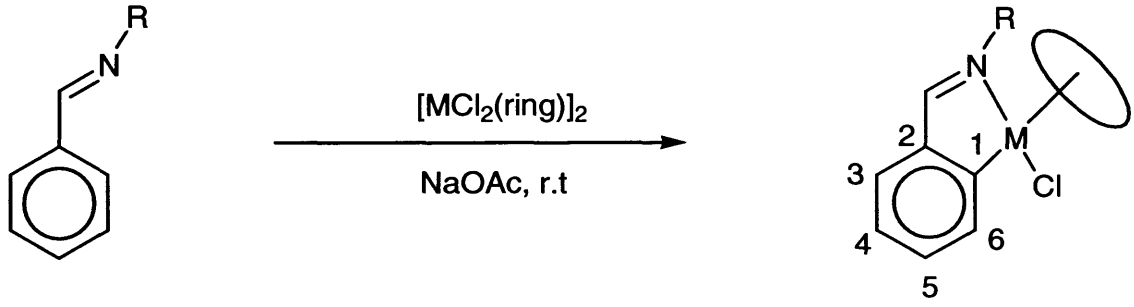

L	R	Cp*Ir	Cp*Rh	*p*-Cymene Ru
L_1	$(CH_2)_2OMe$	(3.30a) √	(3.30b) √	(3.30c) √
L_2	$(CH_2)_3OMe$	(3.31a) √	(3.31b) √	(3.31c) √
L_3	Ph	(3.32a) √	(3.32b) √	(3.32c) X

(√ = ligand cyclometalates, X = ligand does not cyclometalate)

(Scheme 3.12)

Reactions of (L_1) and (L_2) with $[IrCl_2Cp^*]_2$ in CH_2Cl_2 in the presence of NaOAc led to formation of **(3.30a, 3.31a)** in good yield. The ^1H NMR spectra show a 1:1 ratio of the Cp* and the imine ligand with singlets at δ 1.72 and *ca.* 3.35 due to Cp* and OMe respectively and the imine proton being observed at δ 8.37 or δ 8.31 for **(3.30a)** or **(3.31a)** respectively. In both complexes, the NCH_2 protons are inequivalent, two overlapped multiplets being observed at δ 4.19 **(3.30a)**, and at δ 4.13 **(3.31a)**, respectively. This inequivalence is consistent with the chiral centre at the metal, and demonstrates that epimerisation at the metal is slow on the NMR timescale (see later for discussion of epimerisation). Both complexes show the expected signals

for an orthometallated phenyl group; both have two doublets of triplets at *ca* δ 6.97 (H^4) and at *ca.* δ 7.15 (H^5) and two doublets at δ 7.52 (H^3) and at δ 7.76 (H^6). In the ^{13}C-{^1H} NMR spectra, the metallated carbons are observed at δ 168.73 or δ 168.59, for **(3.30a)** and **(3.31a)** respectively, approximately 33 ppm downfield from the corresponding signals in the free ligands.

The FAB mass spectra of **(3.30a, 3.31a)** showed ions at *m/z* 525 and 539 due to $[M]^+$ and fragment ions at *m/z* 490 $[M\text{-}Cl]^+$ and 504 $[M\text{-}Cl]^+$ for **(3.30a, 3.31a)** respectively. The IR spectra of **(3.30a, 3.31a)** show the imine stretch at *ca* 1595 cm^{-1} about 50 cm^{-1} less than the free ligand as expected for coordination of the imine. The microanalysis is consistent with the expected products, and the X-ray structure of **(3.30a)** (see later) confirms the expected cyclometallated product.

The influence of the nature of the imine substituent on the course of the cyclometallation was also probed by using benzylideneaniline **(L_3)**. In this case reaction with $[IrCl_2Cp^*]_2$ in the presence of NaOAc led to formation of a mixture of products. The ^1H NMR spectrum of the mixture suggested the presence of the cyclometallated imine complex **(3.32a)** contaminated with another Cp*Ir complex containing a non-metallated phenyl, which was subsequently identified as the aniline complex **(3.33)**. Thus, during the course of the reaction some of the initial imine had hydrolysed and the resulting amine complexed to the $[IrCl_2Cp^*]_2$ to form **(3.33)**. Complex **(3.33)** could be isolated by passing the mixture through a short column of silica and eluting with CH_2Cl_2/NCMe (10/1). The ^1H NMR spectrum of **(3.33)** shows a singlet at δ 1.55 and a broad singlet at δ 5.55 due to the Cp* and NH_2 respectively. In the aromatic region, three multiplets integrating to 5H are assigned to the non-metallated phenyl. The FAB mass spectrum showed a molecular ion at *m/z* 491.

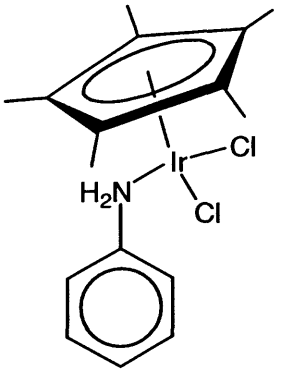

(3.33)

If the imine is hydrolysing to form benzaldehyde and aniline then addition of excess benzaldehyde may reverse this reaction and prevent the formation of significant amounts of

aniline and hence **(3.33)**. Thus, the reaction was repeated in the presence of benzaldehyde. This led to formation of solely **(3.32a)** which could be isolated in 84 % yield.

The ^{1}H NMR spectrum of **(3.32a)** shows singlets at δ 1.47 and 8.31 due to the Cp* and imine proton respectively. In the aromatic region, multiplets integrating to 9H are assigned to the N-phenyl substituent and the orthometallated phenyl group. The ^{13}C-{^{1}H} NMR spectrum shows the expected carbons for **(3.32a)**. The FAB mass spectrum showed the molecular ion at *m/z* 543 and a fragment ion at *m/z* 508 $[M\text{-}Cl]^{+}$. The υ(N=C) absorption is observed at 1582 cm^{-1} *i.e.* lower energy than the free ligand (1626 cm^{-1}) as expected for coordination of the imine. The structures of cyclometallated imine complexes **(3.30a, 3.32a)** have been determined by X-ray crystallography and are shown in **Figs. 3.4** and **3.5** respectively with selected bond distances and angles in **Table 3.1**.

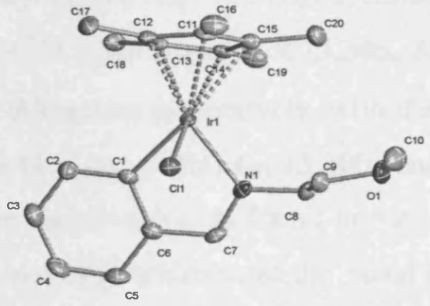

Fig. 3.4 Molecular structure of **(3.30a)**

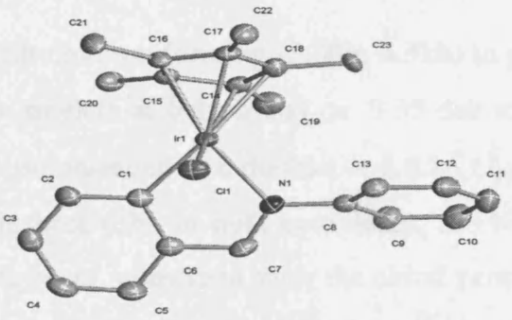

Fig. 3.5 Molecular structure of **(3.32a)**

Table 3.1 Selected bond distances [Å] and bond angles [°] for **(3.30a)** and **(3.32a)**

Bond distances/[Å]	**(3.30a)**	**(3.32a)**	**Bond distances/[Å]**	**(3.30a)**	**(3.32a)**
Ir(1)-C(1)	2.036(3)	2.040(4)	Ir-C(Cp*)	2.148(3)	2.137(4)
Ir(1)-N(1)	2.078(3)	2.105(4)	Ir-C(Cp*)	2.155(4)	2.157(4)
Ir(1)-Cl(1)	2.397(1)	2.402(1)	Ir-C(Cp*)	2.159(4)	2.162(4)
N(1)-C(7)	1.290(5)	1.293(5)	Ir-C(Cp*)	2.252(3)	2.246(5)
			Ir-C(Cp*)	2.279(4)	2.255(4)
Bond angles/ [°]			**Bond angles/** [°]		
C(1)-Ir(1)-N(1)	77.84(13)	77.33(18)	N(1)-Ir(1)-Cl(1)	86.09(8)	89.55(11)
C(1)-Ir(1)-Cl(1)	85.53(11)	88.49(15)			

The structures of **(3.30a, 3.32a)** each depict a typical three legged piano stool structure with a pseudo-octahedral geometry about the metal, with only the N(1)-Ir-C(1) chelate angles, [77.84(13) and 77.33(18)° respectively] being significantly less than the 90° expected for an octahedron. The Ir-N(1) bond distance [2.078(3) Å] in **(3.30a)** is shorter than that [2.105(4) Å] in

(3.32a) but is the same as that, [2.073(3) Å], in the related Cp*Ir cyclometallated diazabutadiene complex **(3.24, Scheme 3.9)**. The Ir-C(1) bond distances [2.036(3) and 2.040(4) Å] are the same in both complexes and are shorter than that, [2.165(3) Å] in **(3.24)**, consistent with a bond to an sp^2 rather than an sp^3 carbon. Both complexes **(3.30a, 3.32a)** show significant variations in the Ir-C bond lengths to the π-bound ring; there are three short Ir-C bonds [2.137(4)-2.162(4) Å], and two longer ones [2.214(13)-2.278(2) Å], which are approximately *trans* to the metallated carbon. In **(3.32a)** the phenyl substituent on nitrogen is rotated out of the plane of the cyclometallated fragment (dihedral angle C(7)-N(1)-C(8)-C(9) = 128.6^0) and is approximately parallel to the Cp*; presumably this is to minimize unfavourable steric interactions with the Cp*.

Having found that imines derived from benzaldehyde cyclometallated easily with $[IrCl_2Cp^*]_2$, the reactions of these ligands with $[RhCl_2Cp^*]_2$ were examined. In these cases, hydrolysis of the ligands seemed to be more of a problem, so excess benzaldehyde was used in some cases (see experimental for details).

The alkyl imines **(L_1)** and **(L_2)** cyclometallated with rhodium forming **(3.30b, 3.31b)** in good yields. The ^1H NMR spectra of **(3.30b, 3.31b)** show singlets at δ 1.66 and *ca.* 3.35 due to the Cp* and OMe group respectively, with the imine proton observed as a doublet at δ 8.16 (J_{RhH}, 4 Hz) and 8.11 (J_{RhH}, 4 Hz) for **(3.30b)** and **(3.31b)** respectively. In both complexes, the NCH_2 protons are inequivalent, as found in the iridium complexes, consistent with the chiral centre at the metal and epimerisation at the metal being slow on the NMR timescale. In each case, the cyclometallation was obvious from the observation of only four protons in the phenyl region and only four carbons with protons attached in the phenyl region of the ^{13}C-{^1H} NMR spectra. The metallated carbon is observed as a doublet (J_{RhC}, 33 Hz) at δ 184.03 and 183.93 for **(3.30b, 3.31b)** respectively with the imine carbon at δ 173.97 and 172.97 respectively. The FAB mass spectra of **(3.30b, 3.31b)** show ions at *m/z* 435 and 449 corresponding to $[M]^+$ and fragment ions at *m/z* 400 and 414 due to $[M\text{-}Cl]^+$. The IR spectra of **(3.30b, 3.31b)** show υ(N=C) at *ca.* 1605 cm^{-1}, about 40 cm^{-1} less than the free ligand as expected for coordination of the imine.

As found for $[IrCl_2Cp^*]_2$, reaction of benzylideneaniline **(L_3)** with $[RhCl_2Cp^*]_2$ and NaOAc in the presence of excess benzaldehyde led to isolation of the cyclometallated product **(3.32b)**. The ^1H NMR spectrum of **(3.32b)** shows multiplets integrating to nine protons in the aromatic region, four due to the cyclometallated ring and five protons assigned to the phenyl substituent. A singlet is observed at δ 1.43 due to Cp* and a doublet at δ 8.18 (J_{RhH}, 4 Hz) assigned to the imine, the coupling to rhodium confirming the coordination of imine. In the ^{13}C-{^1H} NMR spectrum the metallated carbon is observed at δ 185.55 as a doublet (J_{RhC}, 33 Hz).

Crystals of **(3.30b)**, and **(3.32b)** suitable for X-ray determination were obtained from dichloromethane/hexane. The structures are shown in **Figs. (3.6 and 3.7)**, and selected bond distances and angles are listed in **Table 3.2**.

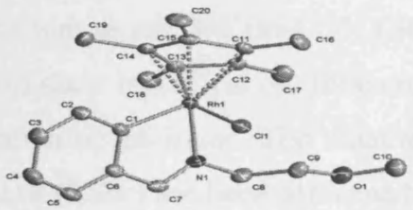

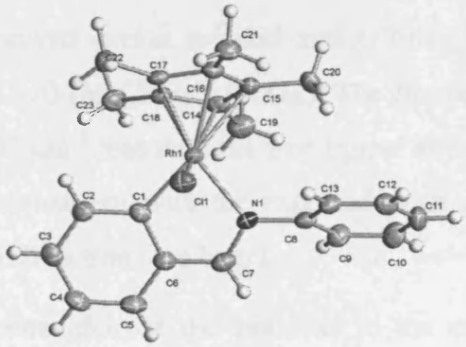

Fig. 3.6 Molecular structure of **(3.30b)** **Fig. 3.7** Molecular structure of **(3.32b)**

Table 3.2 Selected bond distances [Å] and bond angles [°] for **(3.30b and 3.32b)**

Bond distances/[Å]	**(3.30b)**	**(3.32b)**	**Bond distances/[Å]**	**(3.30b)**	**(3.32b)**
Rh(1)-C(1)	2.027(2)	2.032(3)	Rh-C(Cp*)	2.147(2)	2.123(3)
Rh(1)-N(1)	2.089(2)	2.115(3)	Rh-C(Cp*)	2.153(2)	2.149(3)
Rh(1)-Cl(1)	2.3982(6)	2.399(2)	Rh-C(Cp*)	2.166(2)	2.150(3)
N(1)-C(7)	1.283(3)	1.281(4)	Rh-C(Cp*)	2.250(2)	2.250(3)
			Rh-C(Cp*)	2.278(2)	2.250(3)
Bond angles/ [°]			**Bond angles/** [°]		
C(1)- Rh(1)-N(1)	78.73(7)	78.33(12)	N(1)-Rh(1)-Cl(1)	88.41(4)	92.06(8)
C(1)- Rh(1)-Cl(1)	86.03(5)	89.64(10)			

The complexes adopt the expected pseudo-octahedral structure. The bond lengths are similar in both complexes and with the corresponding iridium complexes. In **(3.32b)**, the phenyl substituent on nitrogen is approximately parallel to the Cp* as found in the corresponding iridium complex **(3.32a)**. The Cp* ligands show similar distortions to those in **(3.30a, 3.32a)**, thus, nitrogen and chloride atoms are *trans* to the three short Rh-C bonds [2.123(3)- 2.150(3) Å] whereas the two longer Rh-C bonds [2.250(2)-2.278(2) Å] are *trans* to the metallated carbon.

Similar reactions were investigated with $[RuCl_2(p\text{-cymene})]_2$. Thus, **($L_1$)** and **($L_2$)** cyclometallated easily with $[RuCl_2(p\text{-cymene})]_2$ to form **(3.30c)** and **(3.31c)** respectively. The ^1H NMR spectra of **(3.30c, 3.31c)** both show four multiplets due to the aromatic protons of the *p*-cymene. Thus, the mirror plane present in $[RuCl_2(p\text{-cymene})]_2$ has been lost as expected for formation of chiral at metal complexes. The NCH_2 protons are also inequivalent; consistent with

the chiral metal centre and that the rate of epimerisation is slow on the NMR timescale. In the ^{13}C-{^1H} NMR spectra, the metallated carbon is observed at *ca.* δ 188, approximately 53 ppm downfield from the corresponding signals in the free ligands. In both cases the imine carbon is also downfield *ca.* 13 ppm from the free ligand, at δ 173.69 and 172.77 for **(3.30c)** and **(3.31c)** respectively, confirming the coordination of the imine to the metal.

The FAB mass spectra of **(3.30c)** and **(3.31c)** showed ions at *m/z* 433 and 447 due to $[M]^+$ and fragment ions at *m/z* 398 $[M\text{-}Cl]^+$ **(3.30c),** and at 410 $[M\text{-}Cl\text{-}H_2]^+$ **(3.31c)**. The IR spectra of **(3.30c, 3.31c)** show υ(N=C) at *ca.* 1600 cm^{-1}, about 47 cm^{-1} less than the free ligand as expected for coordination of the imine. The microanalysis is consistent with the expected products, and the structure of **(3.30c)** has been confirmed by X-ray diffraction (see later).

Reaction of **(L_3)** with $[RuCl_2(p\text{-cymene})]_2$ and benzaldehyde did not lead to the expected cyclometallated product **(3.32c)** or to the aniline complex $[RuCl_2(NH_2Ph)(p\text{-cymene})]$ by imine hydrolysis. The ^1H NMR spectrum showed signals due to unreacted benzylideneaniline and the presence of acetate and *p*-cymene in 1:1 ratio which was identified as $[RuCl(O_2CMe)(p\text{-cymene})]$ **(3.34)** (see below). The reaction was repeated in the absence of benzylideneaniline and give **(3.34)** in good yield. The reaction of $[RuCl_2(C_6H_6)]_2$ with a large excess of NaOAc has been reported previously to give $[RuCl(O_2CMe)(C_6H_6)]$.[32]

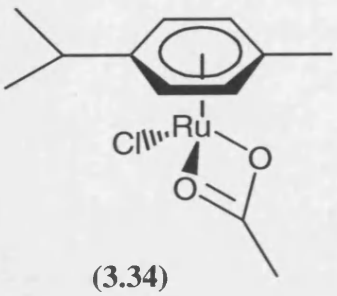

(3.34)

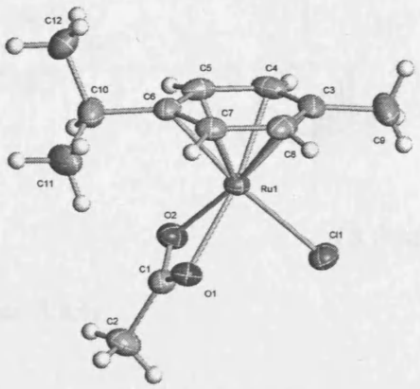

(Fig 3.8)

The mass spectrum shows a peak at *m/z* 292 corresponding to $[RuCl(O_2CMe)(p\text{-cymene})]$; however there are additional peaks at *m/z* 601 due to a dimer $[Ru_2Cl_2(OAc)(p\text{-cymene})_2]$. Crystallisation of the product from CH_2Cl_2/hexane gave X-ray quality crystals. The X-ray structure **(Fig. 3.8)**, shows it to be $[RuCl(O_2CMe)(p\text{-cymene})]$ with a bidentate acetate as proposed previously;[32] selected bond lengths and angles are listed in **Table 3.3**.

Table 3.3 Selected bond distances [Å] and bond angles [°] for complex **(3.34)**

Bond distances/[Å]			
Ru-O(2)	2.151(2)	O(1)-C(1)	1.266(3)
Ru-O(1)	2.166(2)	O(2)-C(1)	1.266(3)
Ru-Cl(1)	2.389(1)		
Bond angles [°]			
O(1)-Ru-Cl(1)	84.92(5)	O(2)-Ru-O(1)	60.31(7)
O(2)-Ru-C(1)l	85.75(5)		

From the results described so far imines (L_1) and (L_2), with an electron-donating substituent, cyclometallate more easily than the aryl substituted imine (L_3). To try and understand the substituent effects in more detail ^{i}Pr-substituted imine (L_4) was used. This has a more bulky substituent but has no OMe group which could potentially coordinate. Since the ruthenium system seems to be more sensitive to substituent effects, imine (L_4) was reacted with $[RuCl_2(p\text{-cymene})]_2$ using the same method as for **(3.30c)**. The cyclometallation occurred and **(3.35c)** was formed in good yield (**Scheme 3.13**). The product was characterised by ^{1}H and ^{13}C-{^{1}H} NMR spectroscopy, FAB mass spectrometry, IR and elemental analysis.

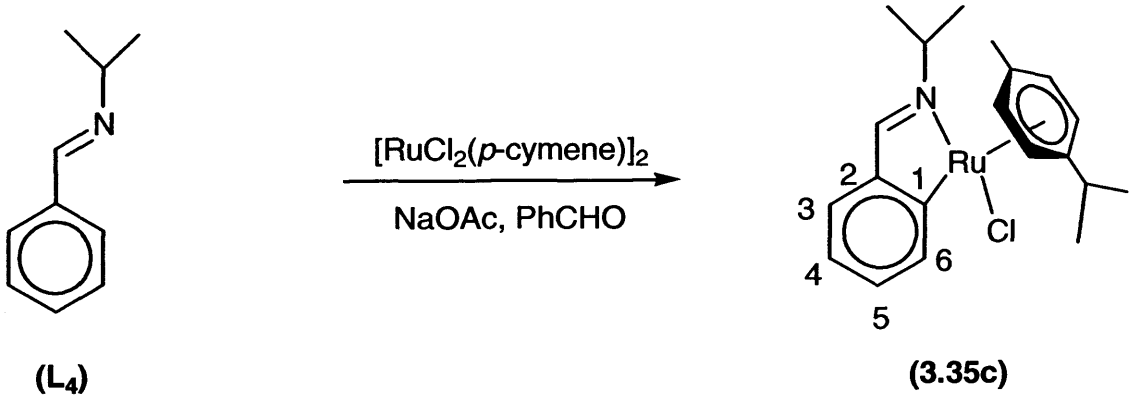

(L_4) **(3.35c)**

(Scheme 3.13)

The ^{1}H NMR spectrum of **(3.35c)** shows the imine proton at δ 8.08, 0.22 ppm less than that in free ligand, confirming the coordination of the imine to the metal. The two isopropyl groups, each give rise to two doublets at δ 0.77 and 1.06 (*p*-cymene) and δ 1.53 and 1.57 (N^{i}Pr), all four aromatic protons of the *p*-cymene are also inequivalent. These data are consistent with the metal centre being chiral and epimerisation being slow on the NMR timescale. Cyclometallation is confirmed by the observation of four multiplets in the aromatic region. The ^{13}C-{^{1}H} NMR spectrum shows the expected signals with the metallated and imine carbons being observed at δ

186.55 and 168.10 respectively. FAB mass spectrometry shows a molecular ion at *m/z* 417 $[M]^+$ and fragment ion at *m/z* 382 $[M\text{-}Cl]^+$. The IR spectrum shows υ(C=N) at 1601 cm^{-1}, 28 cm^{-1} less than the free ligand as expected for coordination of the imine. Crystals of **(3.30c)** and **(3.35c)** were suitable for X-ray diffraction; the structures are shown in **Fig. 3.9** and **Fig. 3.10**, with selected distances and angles in **Table 3.4**.

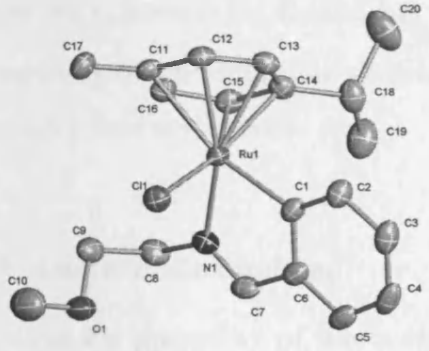

Fig. 3.9 Molecular structure of **(3.30c)**

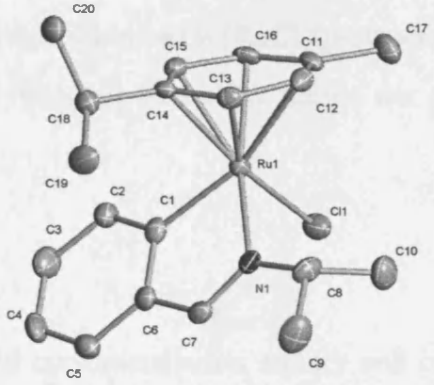

Fig. 3.10 Molecular structure of **(3.35c)**

Table 3.4 Selected bond distances [Å] and bond angles [°] for **(3.30c** and **3.35c)**

Bond distances [Å]	**(3.30c)**[a]	**(3.35c)**
Ru(1)-C(1)	2.043 (2)	2.035(4)
Ru(1)-N(1)	2.080 (2)	2.090(3)
Ru(1)-Cl(1)	2.418(1)	2.406(1)
C(1)-C(6)	1.418(3)	1.403(5)
N(1)-C(7)	1.284(3)	1.289(4)
Ru-C(*p*-cymene)	2.171(2)	2.165(4)
Ru-C(*p*-cymene)	2.177(2)	2.169(4)
Ru-C(*p*-cymene)	2.186(2)	2.170(4)
Ru-C(*p*-cymene)	2.200(2)	2.211(4)
Ru-C(*p*-cymene)	2.284(2)	2.306(4)
Ru-C(*p*-cymene)	2.288(2)	2.309(4)
Bond angles/ [°]		
C(1)-Ru(1)-N(1)	77.85(7)	78.15(14)
C(1)-Ru(1)-Cl(1)	85.37(5)	85.85(10)
N(1)-Ru(1)-Cl(1)	87.84(5)	88.39(8)

[a] Average values for two independent molecules

The coordination geometry of the metal centres in **(3.30c)** and **(3.35c)** are essentially octahedral with the η^6-*p*-cymene ring carbons occupying one face of the octahedron, the remaining sites being occupied by a chloride and the cyclometallated imine. Complex **(3.30c)** shows two independent molecules in the unit cell, the only major difference between these being the orientation of the $(CH_2)_2OMe$ chain and a lengthening of the Ru-Cl bond in one molecule. The

Ru-C(1) bond lengths, Ru-N bond lengths and chelate bite angles are the same in **(3.30c)** and **(3.35c)** and similar to those in **(3.30a, b)** and **(3.32a, b)**. In both **(3.30c)** and **(3.35c)** the *p*-cymene coordination shows an η^4, η^2distortion with four short bonds [2.165(4)-2.211(4) Å], and two longer bonds [2.284(2)-2.309(4) Å], approximately *trans* to the metallated carbon, as found in (*p*-cymene)Ru complex **(3.15)**.[21]

In conclusion all the imines **(L_1-L_3)** cyclometallated with $[IrCl_2Cp^*]_2$ and $[RhCl_2Cp^*]_2$, but only the alkyl imines **(L_1, L_2 and L_4)** were cyclometallated with $[RuCl_2(p\text{-cymene})]_2$. Therefore, the reactivity of the dimers is shown to be [Ir~Rh>Ru], and alkyl imines are cyclometallated more easily than aryl imines.

3.2.2b Amines and oxazolines

To test the generality of this acetate-assisted cyclometallation amines and oxazolines were investigated. Reaction of $[IrCl_2Cp^*]_2$ with N,N-dimethylbenzylamine **(L_5)** in CH_2Cl_2 at room temperature in the presence of NaOAc led to formation of complex **(3.36a)** in good yield **(Scheme 3.14)**.

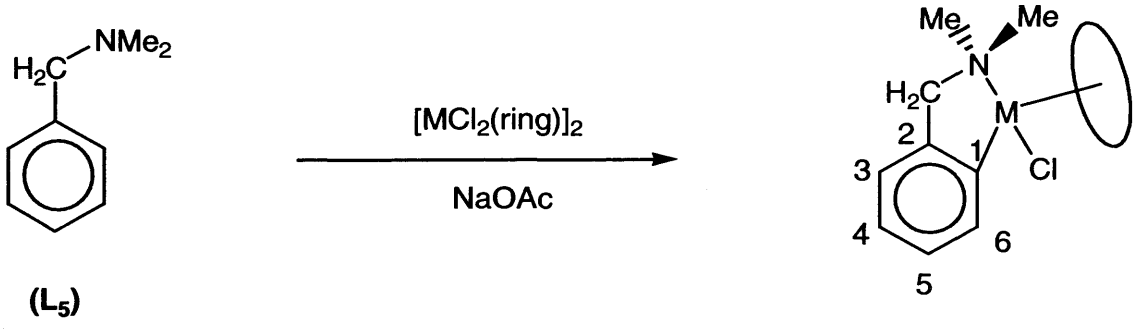

(L_5) **(3.36)**

√ = ligand cyclometalates,
X = ligand does not cyclometalate

a	**Cp*Ir**	**√**
b	**Cp*Rh**	**X**
c	**(p-cymene)Ru**	**X**

(Scheme 3.14)

The ^1H NMR spectrum of **(3.36a)** shows that coordination and cyclometallation of **(L_5)** has occurred. Thus, the NMe_2 group resonances are observed as two singlets at δ 2.90 and 3.03, *ca.* 0.7 ppm downfield from **(L_5)** as expected for coordination of the amine. The benzyl protons are also inequivalent giving two mutually coupled doublets at δ 3.26 and 4.38. The phenyl group shows four inequivalent protons as expected for the orthometallated product. The ^{13}C-{^1H} NMR spectrum shows only four arene CH groups and two signals for the NMe_2 group. The

inequivalence of the CH_2 protons and the methyls of the NMe_2 is consistent with the chiral centre at the metal. Moreover, it demonstrates that epimerisation at the metal and decoordination of the nitrogen is slow on the NMR timescale. The FAB mass spectrum showed a molecular ion at *m/z* 497. The structure of **(3.36a)** has been determined by X-ray crystallography and is shown in **Fig. 3.11** with selected bond distances and angles listed in **Table 3.5**.

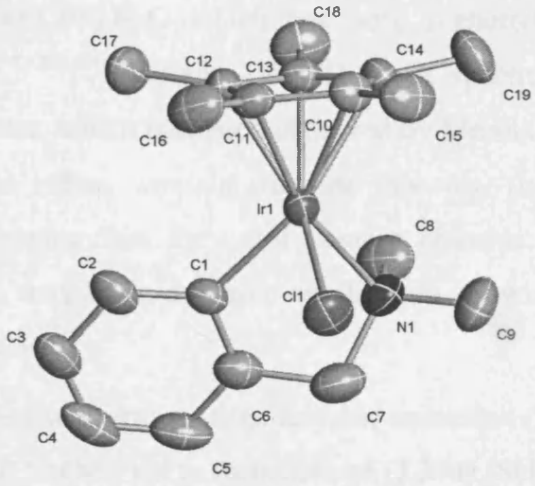

Fig. 3.11 Molecular structure of **(3.36a)**

Table 3.5 Selected bond distances [Å] and bond angles [°] for **(3.36a)**

Bond distances [Å]		**Bond angles [°]**	
Ir(1)-C(1)	2.044(5)	C(1)-Ir(1)-Cl(1)	85.86(14)
Ir(1)-N(1)	2.186(4)	C(1)-Ir(1)-N(1)	78.48(18)
Ir(1)-Cl(1)	2.404(2)	N(1)-Ir(1)-Cl(1)	86.69(12)
N(1)-C(7)	1.472(7)		

The structure of **(3.36a)** depicts a typical three-legged piano stool structure, which has pseudo-octahedral geometry about the metal. The Ir-C(1) bond distance [2.044(5) Å] is similar to that [2.036(3) Å] in **(3.30a)**, but the Ir-N(1) bond distance [2.186(4) Å] is longer than that [2.078(3) Å] in **(3.30a)** as expected for an sp^3 N atom compared with an sp^2 one. The Cp* ligand shows a similar distortion to the imine complexes **(3.30a, b)** and **(3.32a, b)**, thus, the nitrogen and chlorides are *trans* to the three short Ir-C bonds [2.140(4)- 2.159(4) Å] whereas the two longer Ir-C bonds [2.241(4)- 2.259(5) Å] are *trans* to the metallated carbon.

The corresponding reactions were also attempted with $[RhCl_2Cp^*]_2$ and $[RuCl_2(p\text{-cymene})]_2$, but in neither case was the corresponding product **(3.36b)** or **(3.36c)** obtained. After work up and washing the solids with hexane, no signals due to **(L_5)** were observed in the ^1H NMR spectra in either case. However, in both cases the starting dimers had reacted implying that they had

reacted with NaOAc. In case of $[RuCl_2(p\text{-cymene})]_2$, the product was **(3.34)** as discussed earlier. The reaction of $[RhCl_2Cp^*]_2$ with NaOAc leads to a solid which showed broad signals in the ^1H NMR spectrum which can be assigned to Cp* protons and to acetate protons. However, the chemical shifts of the signals are not consistent between all samples, neither is their relative integration. The integration is often not a simple ratio equivalent to one or two acetates per Cp*. In one case we were able to isolate crystals suitable for X-ray diffraction which were determined to be $[Rh(OH_2)(\eta^1\text{-}O_2CMe)_2Cp^*].H_2O$ which has been prepared previously by reaction of $[RhCl_2Cp^*]_2$ with AgOAc.[4, 33, 34] However, the ^1H NMR spectrum of this batch of crystals showed no evidence for water, which had been observed by Merola *et al.*[33] In addition, the mass spectra of these samples often contain dimeric species (*m/z* 605) corresponding to $[Rh_2(O_2CMe)Cl_2Cp^*_2]^+$ showing that they still contain chloride. Thus, the solid may be a mixture, which in solution, may be in dynamic equilibrium allowing exchange of chloride and acetate through dimeric species.

Having had more success with imines than amines, oxazoline **(L_6)** was examined. Reaction of **(L_6)** with $[IrCl_2Cp^*]_2$ and NaOAc led to formation of **(3.37a)** **(Scheme 3.15)**.

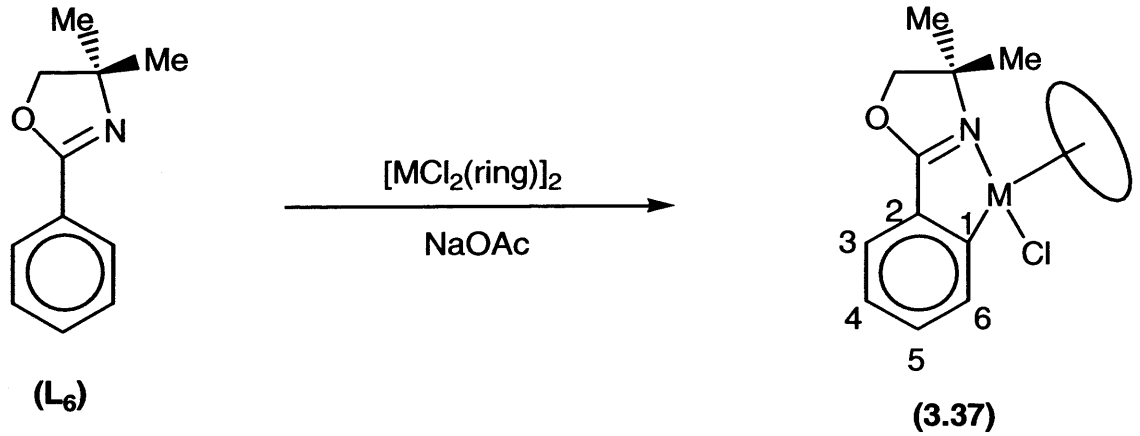

(L_6) **(3.37)**

√ = ligand cyclometalates,

X = ligand does not cyclometalate

a	**Cp*Ir**	**√**
b	**Cp*Rh**	**X**
c	**(p-cymene)Ru**	**X**

(Scheme 3.15)

The ^1H NMR spectrum of **(3.37a)** showed two mutually coupled doublets at δ 4.43 and 4.55 and two singlets at δ 1.50 and 1.53 due to OCH_2 protons and the CMe_2 group respectively. The inequivalence of the methyls and of the OCH_2 protons is consistent with the chiral centre at the metal. Four proton resonances in the aromatic region were observed as expected for cyclometallation. In the $^{13}C\text{-}\{^1H\}$ NMR spectrum, the metallated carbon is observed at δ 178.17, and the two methyls at δ 26.54 and 28.87. The FAB mass spectrum showed a molecular ion at

m/z 537 and a fragment ion at *m/z* 502 $[M\text{-}Cl]^+$. The IR spectrum shows υ(N=C) at 1623 cm^{-1} about 30 cm^{-1} less than the free ligand as expected for coordination of the oxazoline.

Similar reactions of **(L_6)** with $[RhCl_2Cp^*]_2$ and $[RuCl_2(p\text{-cymene})]_2$ at room temperature failed to give cyclometallated products **(3.37b)** or **(3.37c)**. As for N,N-dimethylbenzylamine the rhodium reaction gave a mixture of Cp*Rh products and **(3.34)** could be isolated from the ruthenium reaction.

3.2.3 Mechanistic study

The detailed mechanism and role(s) of acetate in these reactions is not yet clear, however, some key intermediates are presented in **Scheme 3.16** and are discussed further below.

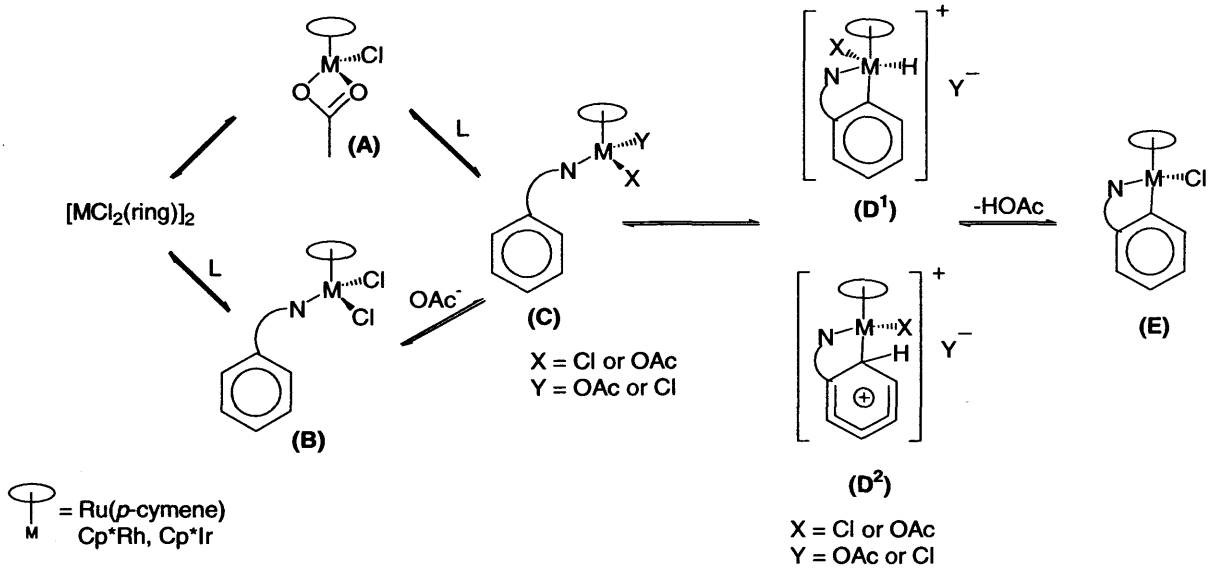

(Scheme 3.16)

Our attempts to isolate a complex of type **(B)** **(Scheme 3.16)** by direct reaction of the dimers with these ligands have so far failed. In the case of **(L_5)** and **(L_6)**, there is no reaction with $[IrClCp^*]_2$ or in the case of imine **(L_3)** hydrolysis occurs to give the primary amine complexes *e.g.* $[IrCl_2(NH_2Ph)Cp^*]$ **(3.33)** (see earlier). In an attempt to suppress hydrolysis, **(L_1)** was reacted with $[IrCl_2Cp^*]_2$ in the absence of NaOAc, with 10 equivalents of benzaldehyde. However, this still led to hydrolysis of the imine and formation of $[IrCl_2\{H_2N(CH_2)_2OMe\}Cp^*]$ **(3.38)**. The ^1H NMR spectrum shows a 1:1 ratio of the Cp* and the amine ligand with singlets at δ 1.70 and 3.37 due to Cp* and OMe respectively. No signals were observed in the aromatic region confirming the hydrolysis of the imine ligand. A broad singlet integrating to two protons assigned to the NH_2 group is also evidence for the hydrolysis. The structure of **(3.38)** has been

determined by X-ray crystallography **(Fig 3.12)** and selected bond distances and angles are listed in **Table 3.6**.

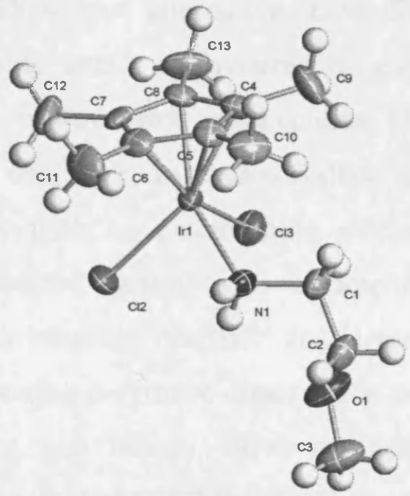

Fig. 3.12 Molecular structure of **(3.38)**

Table 3.6 Selected bond distances [Å] and bond angles [°] for **(3.38)**

Bond distances/[Å]			
Ir-N(1)	2.130(5)	N(1)-C(1)(2)	1.266(3)
Ir-Cl(2)	2.408(2)	Ir-Cl(3)	2.428(2)
Bond angles/[°]			
Cl(2)-Ir-N(1)	81.26(19)	Cl(3)-Ir-N(1)	83.26(15)
Cl(2)-Ir-Cl(3)	89.91(6)		

The role of acetate as a base has also been explored. Thus, there is no reaction between **(L_5)** and $[IrCl_2Cp^*]_2$ using NEt_3 or 1,4-diazabicyclo[2,2,2]octane as base in place of NaOAc. This suggests that acetate may help facilitate break up of the dimer and exchange of a chloride ligand. This is further evidenced by the fact that all the dimers react with acetate. In the case of ruthenium we isolated **(3.34)**, a species of type **(A)** **(Scheme 3.16)**. Complex **(3.34)** reacts with **(L_1)** to form the cyclometallated product **(3.30c)** in the absence of added acetate, though in not such high yield. Another special feature of acetate may be its ability to act as an intramolecular base as has been proposed in palladium cyclometallation reactions[35] and discussed in **Section 1.4.2**. Intramolecular hydrogen bonding observed in $[Rh(OH_2)(\eta^1\text{-}O_2CMe)_2Cp^*]\cdot H_2O$[33] shows this may also be possible for these half-sandwich cyclometallation reactions.

In order for C–H activation to occur a vacant site is needed, therefore loss of an anion from **(C)** is likely to be necessary as found in a related Cp*Ir system[36] (as described in **Scheme 1.5**). The two most likely mechanisms for the C–H activation step are; oxidative addition of the aryl C–H bond to give M^V (M = Ir, Rh) or Ru^{IV} cations followed by reductive elimination of HX (*i.e. via* **D^1**), or electrophilic attack of the metal on the arene (*i.e. via* a Wheland intermediate **D^2**) followed by loss of a proton. These two alternatives have different requirements for electron density at the metal. Electrophilic attack is favoured by electron poor metal centers whilst oxidative addition is favoured by electron-rich metal centres. The failure of **(L_5)**, a good σ-donor ligand but with no π-acceptor character, to cyclometallate with $[RhCl_2Cp^*]_2$ and $[RuCl_2(p\text{-cymene})]_2$ would be consistent with an electrophilic mechanism. In agreement with that, cyclometallation of **(L_5)** is possible starting with a more electrophilic, cationic ruthenium complex, though with a stronger base *viz.* NaOH;[22] and is more efficient with $[RuCl_2(C_6H_6)]_2$ rather than the more electron donating *p*-cymene dimer.[19] The use of a more electrophilic starting material is investigated further, see below. However, Bergman *et al.* have shown that intermolecular C–H activation with [IrMe(OTf)(L)Cp*] {L = PMe_3 **(1.8)** or $P(OMe)_3$ **(1.9)** **(Scheme 1.5)**} proceeds *via* dissociation of triflate which is favoured by electron donating ligands, *i.e.* the rate with PMe_3 is faster than with $P(OMe)_3$.[36] Similar increased rates of C–H activation with more electron donating substituents have been observed for platinum diimine complexes.[37] This is in agreement with our observations that the alkyl-substituted imines **(L_1)** and **(L_2)** cyclometallate more easily than the aryl-substituted one **(L_3)**, and with the reduced reactivity of the oxazoline **(L_6)** containing the electron withdrawing oxygen atom. Thus, electron donating ligands may help in promoting loss of an anion and creating a vacant coordination site, however too much donation may then be detrimental in reducing the electrophilicity of the metal if the C–H activation step is electrophilic in nature. Preliminary DFT calculations suggest that an electrophilic mechanism *via* an agostic C-H bond is energetically favoured over oxidative addition in the cyclometallation of **(L_5)** by $[IrCl_2Cp^*]_2$.[38]

3.2.4 Attempts to cycloruthenate (L_3, L_6) using a cationic precursor

As mentioned previously Pfeffer showed that cyclometallation by arene ruthenium complexes proceeded better with cationic precursors **(Scheme 3.4)**.[22] Hence cyclometallation of **(L_3)** and **(L_6)** which fails starting with the neutral dimer $[RuCl_2(p\text{-cymene})]_2$ was attempted using a cationic precursor. Stirring $[RuCl_2(p\text{-cymene})]_2$ in NCMe in the presence of KPF_6 is known to produce $[RuCl(NCMe)_2(p\text{-cymene})][PF_6]$.[39] A suspension of $[RuCl_2(p\text{-cymene})]_2$, benzylideneaniline **($L_3$)** or oxazoline **($L_6$)** (2 equivalent), NaOAc (2 equivalent) and KPF_6 (4

equivalent) was heated for 3-24 h at 45 ^{0}C in NCMe (**Scheme 3.17**). The reactions were monitored by ES mass spectrometry; the peaks at *m/z* 181 and 175 $[M]^+$ due to (L_3) and (L_6) decline in intensity while peaks at *m/z* 416 and 410 $[(p\text{-cymene})Ru(L\text{-}H)]^+$, L_3 and L_6 respectively, increase. After 24 hours (**3.39c**) or 3 hours (**3.40c**) only peaks for the product were observed.

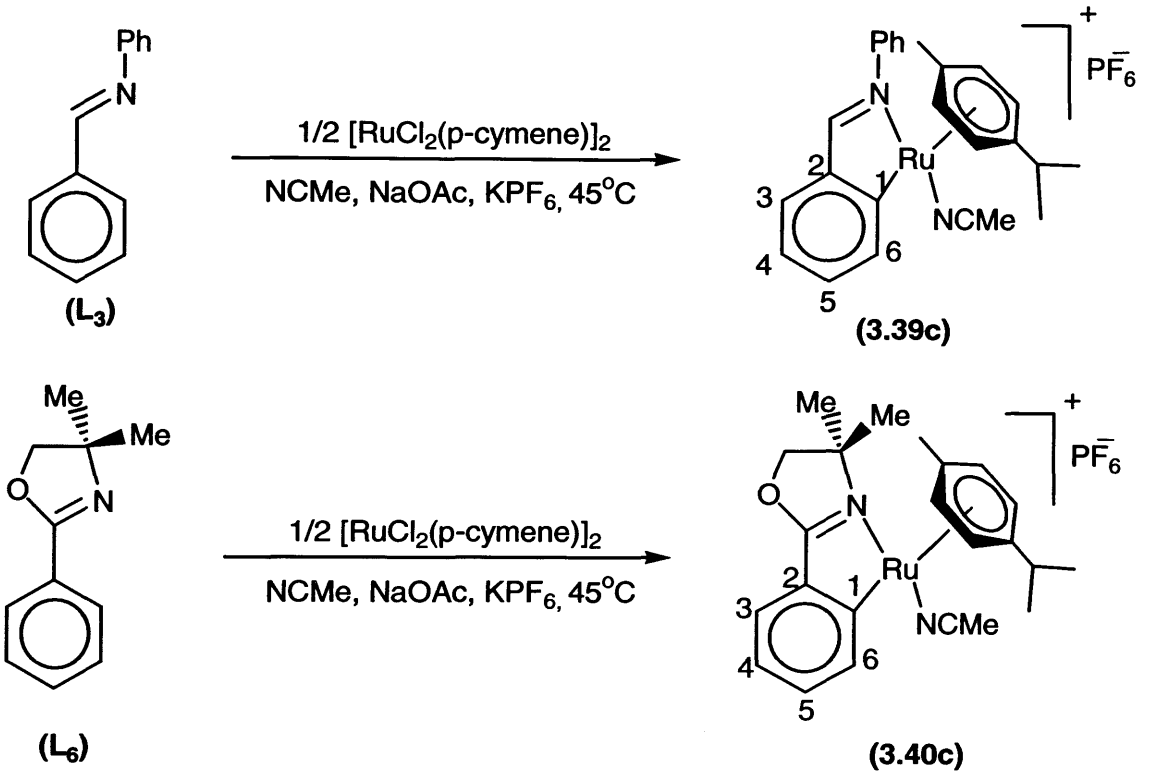

(Scheme 3.17)

In each case, the cyclometallated product (**3.39c**) and (**3.40c**) were isolated as air-stable cationic complexes in good yield, and were identified by ^{1}H and ^{13}C-{^{1}H} NMR spectroscopy, FAB mass spectrometry, IR spectroscopy and microanalysis. The ^{1}H NMR spectra of (**3.39c**) and (**3.40c**) are consistent with the proposed structures *i.e.* they show, four multiplets in the low field region integrating to 4H as expected for the cyclometallated phenyl, and an extra five protons assigned to the phenyl substituent in (**3.39c**). Both complexes show sharp singlets due to coordinated NCMe at δ 2.30 (**3.39c**) and 2.21 (**3.40c**), 0.30 and 0.2 ppm respectively downfield compared to free NCMe. In both complexes, four multiplets each integrating to 1H are assigned to the *p*-cymene, the inequivalence consistent with the chiral metal centre. The CMe_2 protons in (**3.40c**) give rise to two singlets at δ 1.47 and 1.57. The inequivalence of the methyls and of the *p*-cymene protons is consistent with the rate of epimerisation being slow on the NMR timescale.

The ^{13}C-{^{1}H} NMR spectra of **(3.39c)** and **(3.40c)** show only four CH signals for metallated phenyl and the metallated carbon is observed at δ 182.34 **(3.39c)** and δ 175.92 **(3.40c)**.

The FAB mass spectra of **(3.39c)** and **(3.40c)** showed ions at *m/z* 457 and 410 due to $[M]^+$ and fragment ions at *m/z* 416 and 451 $[M\text{-}Cl]^+$ for **(3.39c, 3.40c)** respectively. The IR spectra of **(3.39c)** and **(3.40c)** show the imine absorption at 1581 cm^{-1} and 1622 cm^{-1}, shifted to lower energy by about 50 cm^{-1} and 30 cm^{-1} respectively compared with the free ligands.

A similar reaction of $[RhCl_2Cp^*]_2$ and **(L_6)** with NaOAc and KPF_6 in NCMe at 45° C failed to give cyclometallated cationic product **(3.40b)**. The ^{1}H NMR spectrum showed signals due to unreacted **(L_6)** and signals due to Cp* and acetate. The FAB mass spectrum showed a peak at *m/z* 605 corresponding to $[Rh_2(O_2CMe)Cl_2Cp^*_2]^+$. Washing with hexane removed **(L_6)** and the metal-containing species were recrystallised from CH_2Cl_2/Hexane. The ^{1}H NMR spectrum shows two singlets at δ 1.55 (30H) and 2.10 (3H) assigned to Cp* and OAc respectively, the complex was identified as for $[Rh_2(O_2CMe)Cl_2Cp^*_2][PF_6]$ and confirmed by X-ray crystallography. The failure of this reaction may reflect the different reactivity of $[RhCl_2Cp^*]_2$ with NCMe compared with $[RuCl_2(p\text{-cymene})]_2$ rather than a failure of the C-H activation step.

3.2.5 Activation of other sp^2 C-H bonds (heterocycles)

Activation of the sp^2 C-H bonds of heterocycles is known,[40, 41] and some examples of cyclometallated complexes containing such ligands have been mentioned in **Ch. 1**. To test acetate-assisted cyclometallation of heterocycles, and to study the influence of the nature of heterocyclic ligands on the course of the cyclometallation, imines **(L_7-L_{10})** derived from heterocyclic aldehydes have been investigated. Pyrrole imine **(L_7)** was reacted with $[MCl_2Cp^*]_2$ (M = Rh, Ir) and $[RuCl_2(p\text{-cymene})]_2$ **(Scheme 3.18)** in an attempt to activate a C-H bond of the pyrrole and give C,N-bidentate complexes **(3.42)**. However, N,N-coordination by deprotonation of the N-H of the pyrrole may also be possible to give **(3.41)**. Arene ruthenium and Cp*M (M= Ir, Rh) complexes with anionic pyrrolyl imine chelates are known,[42, 43] in these cases deprotonation of the pyrrole is usually carried out using a strong base NaH or NaOMe before coordination. The products were obtained in high yield and were characterised by ^{1}H, and ^{13}C-{^{1}H} NMR spectroscopy, FAB mass spectrometry, IR spectroscopy and microanalysis.

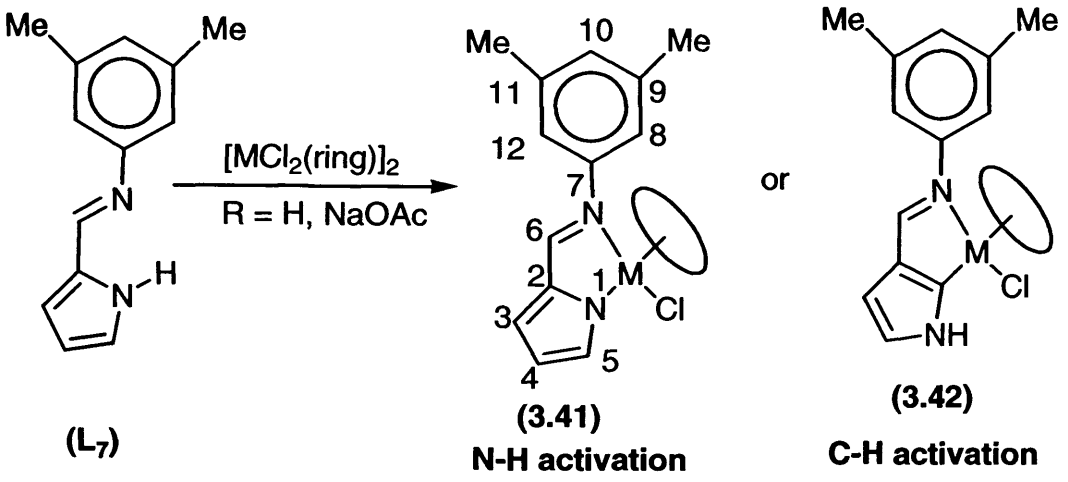

(L7)

(3.41)
N-H activation

(3.42)
C-H activation

(ring)M	N-H activation	C-H activation
Cp*Ir	(3.41a) √	(3.42a) x
Cp*Rh	(3.41b) √	(3.42b) x
p-Cymene Ru	(3.41c) √	(3.42c) x

(√ = ligand cyclometalate) **(Scheme 3.18)**

The ^{1}H NMR data of the iridium product shows a 1:1 ratio of the Cp* and the pyrrole ligand. The imine proton is observed at δ 7.74, 0.5 ppm upfield from the free ligand, confirming the coordination of the imine. Three multiplets each integrating to 1H, at δ 6.38, 6.78 and 7.17 are assigned to the pyrrole ring protons (identified by ^{1}H-^{1}H noesy) as expected for the N,N chelating product **(3.41a)** (the C,N product **(3.42a)** would only show two doublets). The ^{13}C-{^{1}H} NMR spectrum shows three corresponding carbons with protons attached at δ 113.72, 118.02 and 135.35 (identified by ^{1}H-^{13}C Cosy). The imine carbon and (C^{2}) are observed at δ 157.97 and 142.25 respectively, 8 ppm and 10 ppm downfield from the corresponding signals in the free ligand, confirming coordination of the ligand. The FAB mass spectrum showed an ion at *m/z* 560 $[M]^{+}$ and fragment ion at *m/z* 525 $[M\text{-}Cl]^{+}$. The υ(C=N) is observed at 1595 cm^{-1}, 27 cm^{-1} less than the free ligand as expected for coordination of the imine. The absence of a υ(N-H) band is consistent with the deprotonation of the N-H and coordination of the pyrrole nitrogen to the metal.

The ^{1}H NMR spectra of **(3.41b)** and **(3.41c)** show similar features to **(3.41a)**, with three multiplets assigned to the pyrrole ring protons as expected for the N,N chelating product. The imine proton is observed at δ 7.66 **(3.41b)** and 7.58 **(3.41c)**, *ca.* 0.6 ppm upfield from the free ligand, confirming the coordination of the imine. The four aromatic protons of the *p*-cymene in **(3.41c)** are inequivalent, consistent with the chiral metal centre.

The ^{13}C-{^{1}H} NMR spectra of **(3.41b, c)** show the imine carbon at *ca.* δ 157 and (C^2) at *ca* δ 140, both carbons downfield from the free ligand as for **(3.41a)**. The FAB mass spectra of **(3.41b)** and **(3.41c)** showed molecular ions at *m/z* 470 and 468 and fragment ions at *m/z* 435 and 433 due to $[M\text{-}Cl]^+$. The IR spectra of **(3.41b)** and **(3.41c)** show the imine absorption at 1595 cm^{-1} and 1607 cm^{-1}, shifted to lower energy by about 27 cm^{-1} and 15 cm^{-1} respectively compared with the free ligand, confirming the coordination of the imine.

Careful recrystallisation of **(3.41a)** and **(3.41c)** from dichloromethane/ether gave crystals suitable for X-ray diffraction. The X-ray structures are shown in **Figs. 3.13** and **3.14** with selected distances and angles in **Table 3.7**. The structures, confirm the N,N coordination of the ligand.

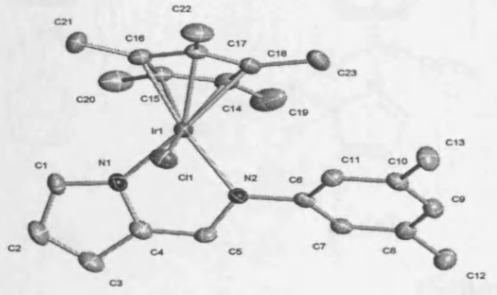

Fig. 3.13 Molecular structure of **(3.41a)**

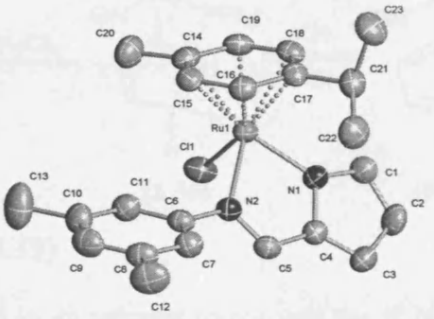

Fig. 3.14 Molecular structure of **(3.41c)**

Table 3.7 Selected bond distances [Å] and bond angles [°] for **(3.41a)** and **(3.41c)**

Bond distances/[Å]	**(3.41a)**	**(3.41c)**
M(1)-N(1)	2.069(3)	2.035(2)
M(1)-N(2)	2.123(3)	2.094(2)
M(1)-Cl(1)	2.395 (1)	2.401(1)
N(1)-C(4)	1.378(5)	1.375(3)
N(2)-C(5)	1.298(4)	1.297(4)
Bond angles/[°]		
N(2)-M(1)-Cl(1)	86.24(9)	86.11(7)
N(1)-M(1)-Cl(1)	85.92(9)	86.53(7)
N(1)-M(1)-N(2)	76.39(12)	77.05(9)

The M-N (pyrrole) bond distances [2.069(3) Å in **(3.41a)** and 2.035(2) Å in **(3.41c)**] are slightly shorter than the M-N (imine) bond distances [2.123(3) Å and 2.094(2) Å respectively], consistent with the formally anionic nature of the N(pyrrole).[42, 43] In both complexes, the xylyl substituent is rotated out of the plane of the pyrrole and is approximately parallel to the Cp* or *p*-

cymene ring respectively, as found in (**3.32a** and **3.32b**); presumably this is to minimize unfavourable steric interactions with the Cp* and *p*-cymene rings.

It is not clear whether formation of the N,N complexes (**3.41**) rather than C,N complexes (**3.42**) is due to a kinetic and/or thermodynamic preference. A preference for N-H activation over C-H activation has previously been observed for pyrrole-pyridine ligands.[42-44] However, Gladysz *et al.*[45] showed that treatment of N-pyrrole complex (**3.43**) with TfOH led to protonation at C_2 to give (**3.44**) which isomerised to form C-bonded cationic complex (**3.45**). This could be treated with KH to form the neutral C-bonded complex (**3.46**) (**Scheme 3.19**).

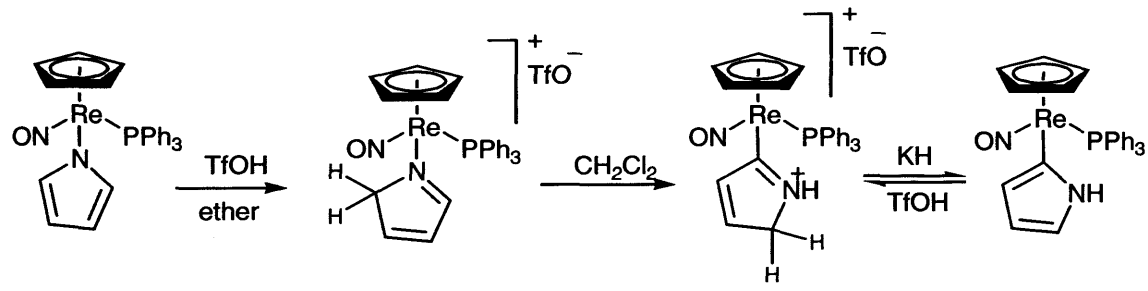

(3.43) (3.44) (3.45) (3.46)

(Scheme 3.19)

Thus (**3.41c**) was reacted with trifloroacetic acid in an attempt to convert the N,N isomer to a C,N complex (**3.42**). The reaction was monitored by ^{1}H NMR spectroscopy. The spectrum showed a new (*p*-cymene) Ru species with one doublet at δ 1.30 assigned to ^{i}Pr of *p*-cymene and two mutually coupled doublets at δ 5.40 and 5.6 (CH, cymene ring) confirming the complex was a mirror plane consistent with the formation of [RuCl(η^2-CO_2CF_3)(*p*-cymene)] similar to (**3.34**). The spectrum also shows signals due to the pyrrole imine ligand, the imine proton being observed at δ 8.20. Thus, it appears that protonation of (**L7**) and dissociation from the metal may have occurred. To identify the organic product, (**L7**) was reacted with CF_3CO_2H. The ^{1}H NMR spectrum showed the same signals as the reaction of (**3.41c**) with the acid. The signals are similar to those of (**L7**) with an additional broad peak at δ 10.20 due to protonation of the imine nitrogen. The imine proton and carbon are observed at δ 8.20 and at δ 144.75 respectively (*c.f.* δ 8.24 and 149.95 in (**L7**) and δ 7.58 and 156.56 in (**3.41c**)). The ^{13}C{^{1}H} NMR spectrum shows a quartet at δ 161.50 (J_{CF}, 38.5 Hz) due to the O_2CCF_3 anion. The υ(C=N) is observed at 1668 cm^{-1} (*c.f.* 1622 cm^{-1} in (**L7**)). Crystallisation of the product from CH_2Cl_2/hexane gave a crystal suitable for X-ray diffraction. The structure is shown in (**Fig. 3.15**) with selected distances and angles in **Table 3.8**. The structure shows that (**L7**) has been protonated at the imine nitrogen and the

O_2CCF_3 anion is hydrogen bonded to both N-H protons of the cation. The imine hydrogen bond distance [1.920 Å] is longer than that pyrrole hydrogen bond [2.036(3) Å] in **(3.30a)**, but the Ir-N(1) bond distance [2.186(4) Å] is longer than that [1.798 Å] as expected for typical sp^2 N atom compared with delocalized sp^2 one. The O(1)-H(1)-N(1) bond angle [160.48°] is slightly smaller than that in O(1)-H(2)-N(2) [173.11°].

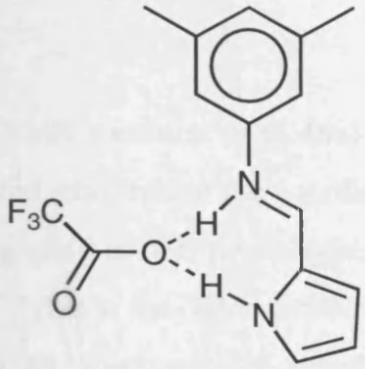

(3.47)

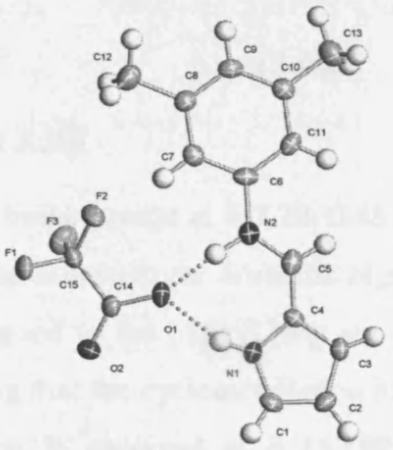

Fig. 3.15 Molecular structure of **(3.47)**

Table 3.8 Selected bond distances [Å] and bond angles [°] for complex **(3.47)**

Bond distances /[Å]			
N(2)-C(5)	1.293(3)	NH(2)-O(1)	1.798
N(1)-C(4)	1.376(2)	C(4)-C(5)	1.398(3)
N(1)-C(1)	1.339(3)	O(1)-C(14)	1.254(2)
C(1)-C(2)	1.379(3)	O(2)-C(14)	1.219(2)
C(2)-C(3)	1.376(3)	C(6)-N(2)	1.436(3)
NH(1)-O(1)	1.920	C(3)-C(4)	1.391(3)
Bond angles/ [°]			
N(1)-C(4)-C(3)	107.0(2)	N(2)-C(5)-C(4)	125.5(2)
C(3)-C(4)-C(5)	125.2(2)	C(5)-N(2)-C(6)	125.9(2)
O(1)-H(1)-N(1)	160.48	O(1)-H(2)-N(2)	173.11

The N(pyrrole)-C(4) and the N(imine)-C(5) bond distances [1.376(2) Å and 1.293(3) Å respectively] are similar to those in **(3.41a)** [1.378(5) and 1.298(4) Å respectively].

Since N-H activation occurred in preference to C-H activation for **(L_7)**, the corresponding N-methylated ligand **(L_8)** was tried. In this case only C-H activation is possible. Reaction of **(L_8)** with $[IrCl_2Cp^*]_2$ and NaOAc for 4 hours gave the expected product **(3.48a)** in good yield **(Scheme 3.20)**.

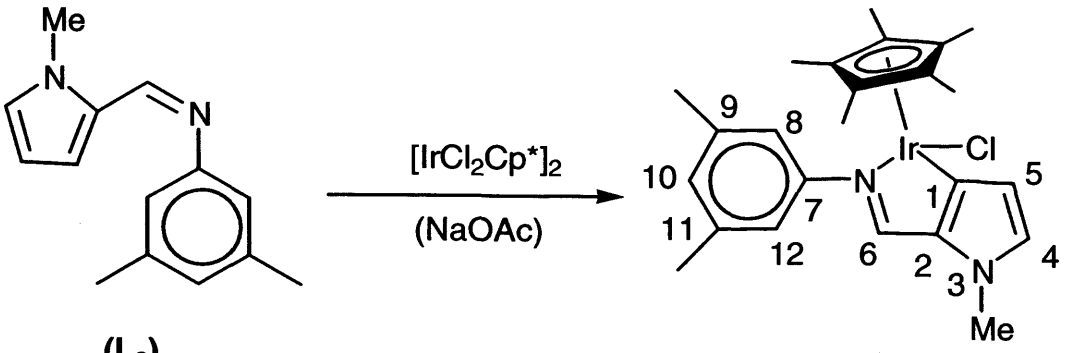

(L_8) **(3.48a)**

(Scheme 3.20)

The ^{1}H NMR spectrum of **(3.48a)** shows the imine proton at δ 7.79, 0.48 ppm upfield from the free ligand, confirming the coordination of the imine. In the aromatic region, there are four signals integrating to 5H, two singlets (3H) assigned to the phenyl ring and two doublets at δ 6.41 and 6.78 due to the N-Me pyrrole, confirming that the cyclometallation has occurred. In the ^{13}C-{^{1}H} NMR spectrum, the metallated carbon is observed at δ 157.09. The FAB mass spectrum showed a molecular ion at *m/z* 574 and a fragment ion at *m/z* 539 $[M\text{-}Cl]^+$. The υ(C=N) is observed at 1610 cm^{-1}, 55 cm^{-1} less than the free ligand as expected for coordination of the imine.

Having found that N-Me pyrrole cyclometallated easily with $[IrCl_2Cp^*]_2$ in the presence of NaOAc, cyclometallation of other five-membered ring heterocycles, thiophene **(L_9)** and furan **(L_{10})**, was investigated **(Scheme 3.21)**. The reaction of **(L_9)** with $[IrCl_2Cp^*]_2$ was monitored by mass spectrometry which showed that it required 30 h to reach completion compared with only 4 hours for formation of the N-Me pyrrole complex **(3.48a)**.

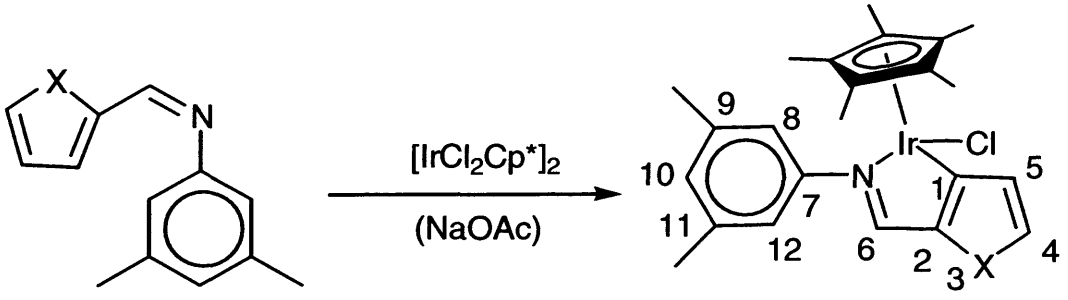

(L_9, X = S)
(L_{10}, X = O)

(3.49a, X = S)
(3.50a, X = O)

(Scheme 3.21)

The ^{1}H NMR spectrum of **(3.49a)** showed the imine proton at δ 8.14, 0.39 ppm upfield compared with the free ligand, consistent with the coordination of the imine. Only two multiplets due to the thiophene ring are observed at δ 7.34 and 7.62, confirming cyclometallation of the

heterocycle, as found in **(3.48a)**. The FAB mass spectrum showed a molecular ion at *m/z* 577 and a fragment ion at *m/z* 542 $[M\text{-}Cl]^+$. The IR spectrum showed the υ(C=N) at 1601 cm^{-1} *i.e.* about 15 cm^{-1} less than the free ligand as expected for coordination of the imine.

Reaction of **(L_{10})** with $[IrCl_2Cp^*]_2$ was monitored by ES mass spectrometry and after 24 hours all the ligand had reacted. Several iridium-containing species were observed, including ions at m/z 567 $[Cp^*Ir(L_{10})NCMe]$ suggesting cyclometallation had occurred. The ^1H NMR spectrum of the crude product also showed more than two Ir species and several complex signals in aromatic region. Unfortunately it was not possible to isolate any pure products even after chromatography through silica.

The structures of **(3.48a)** and **(3.49a)** have been determined by X-ray crystallography and selected bond distances and angles are listed in **Table 3.9**. The structures **(Figs. 3.16** and **3.17)** confirm cyclometallation of the heterocycle in each case.

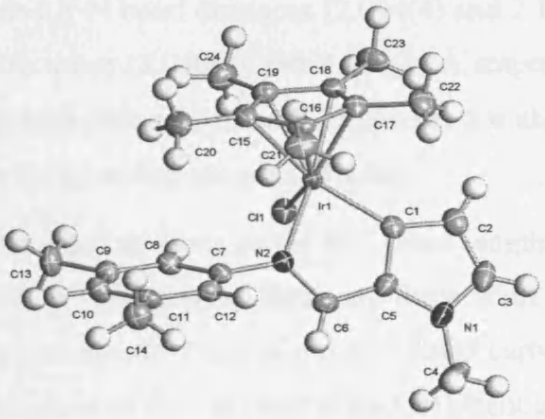

Fig. 3.16 Molecular structure of **(3.48a)**

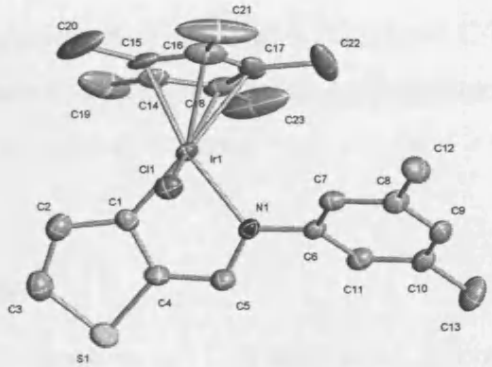

Fig. 3.17 Molecular structure of **(3.49a)**

Table 3.9 Selected bond distances [Å] and bond angles [°] for **(3.48a)** and **(3.49a)**

Bond distances/[Å]	(3.48a)	(3.49a)
Ir(1)-C(1)	2.019(5)	2.024(4)
Ir(1)-N	2.094(4)	2.113(4)
M(1)-Cl(1)	2.394(2)	2.393(2)
N-C(6)	1.304(7)	1.425(5)
Ir-C(η-Cp*)	2.133(4)	2.135(5)
Ir-C(η-Cp*)	2.136(5)	2.147(5)
Ir-C(η-Cp*)	2.139(5)	2.154(5)
Ir-C(η-Cp*)	2.234(5)	2.224(6)
Ir-C(η-Cp*)	2.244(5)	2.251(6)
C(1)-Ir(1)-N(1)	77.68(18)	77.64(16)
C(1)-Ir(1)-Cl(1)	88.07(13)	89.07(13)
N-Ir(1)-Cl(1)	87.80(10)	87.81(11)

The complexes adopt a typical three legged piano stool structure. The Ir-C(1) bond distances [2.019(5) and 2.024(4) Å] and Ir-N bond distances [2.094(4) and 2.113(4) Å] are similar in both complexes and are similar to those [2.040(4) and 2.105(4) Å respectively] in the related imine complex **(3.32a)**. The Ir-N bond distances in both complexes are also similar to the Ir-N(imine) distance [2.123(3) Å] in the N,N-bonded complex **(3.41a)**.

Both complexes show similar variations in the Ir-C bond lengths to the π-bound ring as for the other cyclometallated MCp* complexes. There are three short Ir-C bonds and two longer ones, the longer ones are approximately *trans* to the metallated carbon. The xylyl substituent on nitrogen is rotated out of the plane of the cyclometallated fragment and is approximately parallel to the Cp*; presumably due to unfavourable steric interactions with the Cp* as found for **(3.41a)**.

In conclusion, activation of an heterocyclic sp^2 C-H bond did not occur in pyrrole ligand ($\mathbf{L_7}$) due to the competition from deprotonation of the N-H. However, with the N-methylated ligand, activation of a C-H bond occurred. Activation of a thiophene C-H is also possible though the reaction with furan was not successful. Hence the ease of cyclometallation of heterocyclic rings with $[IrCl_2Cp^*]_2$ is pyrrole > thiophene >> furan.

3.2.6 (sp^3) C-H bond activation

Cyclometallation is not restricted to sp^2 C-H activation, activation of an sp^3 C-H bond of a methyl of a diimine to form **(3.24)**[28] and an sp^3 C-H bond of phenyl oxazolone to form **(3.28)**[29] have already been demonstrated with $[IrCl_2Cp^*]_2$. Ligand ($\mathbf{L_{11}}$) contains rather acidic sp^3 C-H

bonds and a nitrogen donor atom. Thus we have investigated reaction of (L_{11}) with $[MCl_2Cp^*]_2$ (M = Ir, Rh) and $[RuCl_2(p\text{-cymene})]_2$ in the presence of NaOAc (**Scheme 3.22**).

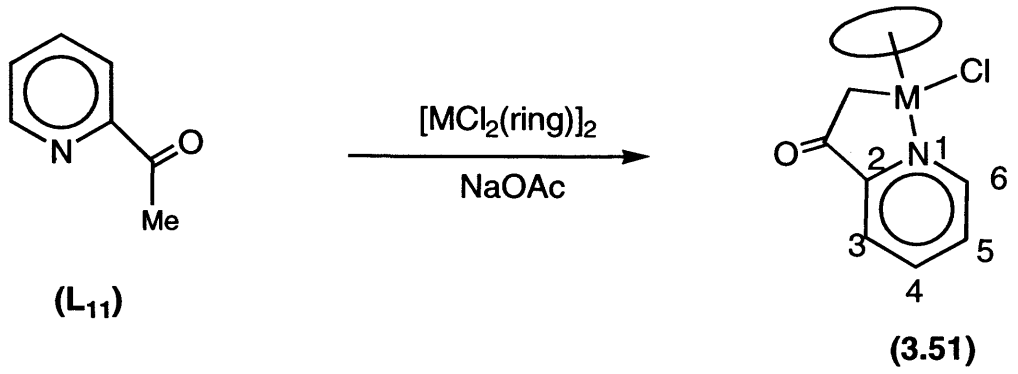

(L_{11}) **(3.51)**

√ = ligand cyclometalates,

X = ligand does not cyclometalate

a	**Cp*Ir**	√
b	**Cp*Rh**	√
c	**(p-cymene)Ru**	√

(Scheme 3.22)

Reaction of (L_{11}) with $[IrCl_2Cp^*]_2$ was monitored by ES mass spectrometry and after 4 hours all the ligand had reacted. Several iridium-containing species were observed, including ions at m/z 569 $[Cp^*Ir(L_{11})_2\text{-H}]$ and 448 $[Cp^*Ir(L_{11})\text{-H}]$ suggesting cyclometallation had occurred. The ^{1}H NMR spectrum of the crude product also showed more than two Ir species and several signals for pyridine protons. Unfortunately it was not possible to isolate any pure products even after chromatography through silica.

The reaction with $[RhCl_2Cp^*]_2$ gave **(3.51b)** in good yield. The ^{1}H NMR spectrum of **(3.51b)** shows a signal at δ 1.57 due to Cp*, four multiplets in the aromatic region, each integrating to 1H due to the pyridine ring. However, there is no methyl signal instead two mutually coupled doublets of doublets are observed at δ 2.84 (J = 7, 1 Hz) and 3.84 (J = 7, 1 Hz) (the additional coupling is to Rh) assigned to a metal bound CH_2. These resonances confirm the expected sp^3 C-H activation and their inequivalence shows that epimerisation at the metal is slow on the NMR timescale. In the ^{13}C-{^{1}H} NMR spectrum, the CH_2 carbon is observed at δ 45.33 as a doublet (J_{RhC} 22 Hz). The FAB mass spectrum of **(3.51b)** showed an ion at *m/z* 393 due to $[M]^+$ and a fragment ion at *m/z* 358 due to $[M\text{-Cl}]^+$.

Crystals of **(3.51b)** suitable for X-ray determination were obtained from dichloromethane/hexane. The structure confirms the activation of an sp^3 C-H bond of a methyl group and is shown in **Fig. (3.18)**, with selected bond distances and angles listed in **Table 3.10**.

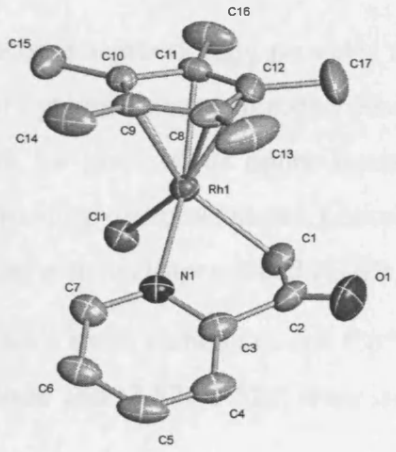

Fig. 3.18 Molecular structure of **(3.51b)**

Table 3.10 Selected bond distances [Å] and bond angles [°] for **(3.51b)**

Bond distances /[Å]			
Rh(1)-C(1)	2.138(3)	Rh-C(Cp*)	2.157(3)
Rh(1)-N(1)	2.113(2)	Rh-C(Cp*)	2.160(3)
Rh(1)-Cl(1)	2.4289(9)	Rh-C(Cp*)	2.222(3)
C(1)-C(2)	1.453(5)	Rh-C(Cp*)	2.231(3)
Rh-C(Cp*)	2.141(3)		
Bond angles /[°]			
C(1)-Rh(1)-N(1)	77.84(11)	N(1)-Rh(1)-Cl(1)	89.70(7)
C(1)-Rh(1)-Cl(1)	89.18(11)		

Complex **(3.51b)** has a pseudo-octahedral geometry about the metal. The Rh-C(1) bond length [2.138(3) Å] is similar to the Ir-CH_2 bond length [2.165(3) Å] in **(3.24)**, and is longer than the Rh-C(phenyl) bonds in **(3.30b)** and **(3.32b)** [2.027(2) and 2.032(3) Å respectively] consistent with a bond to an sp^3 carbon rather than an sp^2 one. The Rh-N bond length [2.113(2) Å] is similar to the Rh-N(imine) bonds in **(3.30b)** and **(3.32b)**, [2.089(2) and 2.115(3) Å respectively]. As found for Cp* complexes, **(3.51b)** shows an η-Cp* coordination with three short Rh-C bonds [2.141(3)- 2.160(3) Å] and two longer ones [2.222(3)-2.231(3) Å].

Reaction of **(L_{11})** with $[RuCl_2(p\text{-cymene})]_2$ led to several ruthenium-containing species in the ES mass spectrum including *m/z* 495 which could possibly be assigned as [(*p*-cymene)Ru(L_{11})$_2$OH]. The ^{1}H NMR spectrum showed the presence of free *p*-cymene as well as some signals in the aromatic region due to a pyridine. However as for the iridium reaction no pure products could be isolated.

3.2.7 Half-sandwich cyclometallated phosphite complexes

Having shown that the acetate-assisted methodology provides a facile, high yield route to a range of half-sandwich complexes of cyclometallated nitrogen donor ligands it was of interest to see if the same method would work for phosphorus donor ligands. As mentioned in **Section 3.1.3**, half-sandwich complexes containing cyclometallated phosphines are known.[13, 15, 16, 46-50] Examples of half-sandwich complexes with cyclometallated $P(OPh)_3$ are also known [51, 52]

Triphenylphosphite was reacted with arene ruthenium and Cp*M (M= Ir, Rh) dimers in the absence of NaOAc at room temperature and **(3.52a-3.52c)** were isolated in good yield **(Scheme 3.23)**.

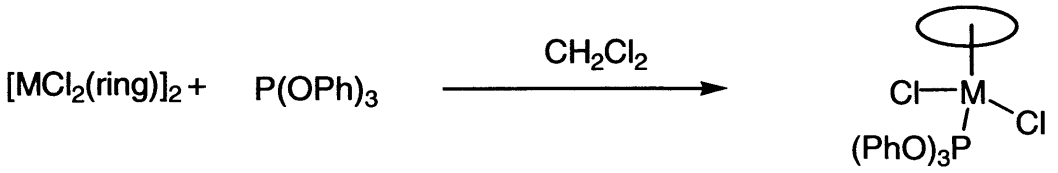

Cp*Ir	Cp*Rh	*p*-Cymene Ru
(3.52a)	**(3.52b)**	**(3.52c)**

(Scheme 3.23)

The $^{31}P-\{^1H\}$ NMR spectra showed a singlet at δ 65.35 **(3.52a)** and at 104.57 **(3.52c)**, or a doublet at δ 103.56 (J_{RhP} = 240 Hz) **(3.52b)**, upfield from the free ligand (δ 127.82), suggesting the coordination of the phosphite ligand to the metal. The ^1H NMR spectra of **(3.52a, b)** show a doublet due to Cp* at δ 1.52 and 1.60 respectively, each coupling to phosphorus. The spectrum of **(3.52c)** shows a doublet at δ 1.10 and septet at δ 2.68 due to the isopropyl (*p*-cymene), and two doublets (2H each) for the four aromatic protons of the *p*-cymene, consistent with a mirror plane at the metal. In all the complexes, multiplets integrating to 15 protons are observed in the aromatic region assigned to the $(OPh)_3$ group, confirming that the phosphite ligand is bound to the metal. The complexes **(3.52a-c)** were then treated with NaOAc in CH_2Cl_2 **(Scheme 3.24)**. Complex **(3.52a)** cyclometallated easily to provide **(3.53a)**.

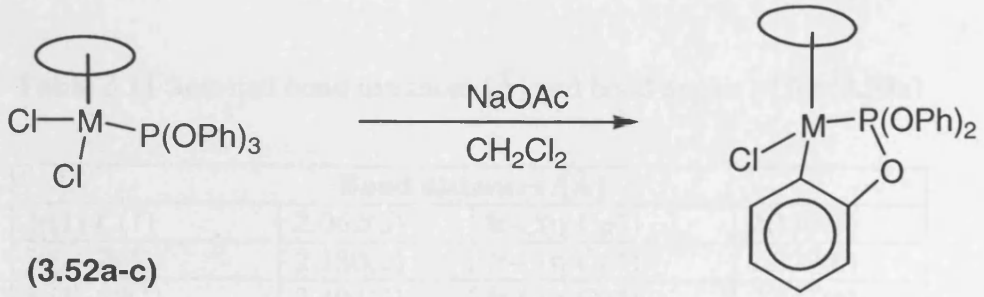

(3.52a-c)

√ = ligand cyclometalates,

X = ligand does not cyclometalate

3.53a	**Cp*Ir**	**√**
3.53b	**Cp*Rh**	**X**
3.53c	**(p-cymene)Ru**	**X**

(Scheme 3.24)

The ^{31}P-{^{1}H} NMR spectrum of **(3.53a)** shows a singlet at δ 109.63, 44 ppm downfield compared to the starting material as expected for formation of a five-membered ring.[51, 53] The ^{1}H NMR spectrum shows a doublet at δ 1.78 (J_{PH} = 3 Hz) due to the Cp* and there are multiplets integrating to 14 protons in the aromatic region as expected for the orthometallated product. The FAB mass spectrum shows a molecular ion at *m/z* 672 and a fragment ion at *m/z* 637 due to [M-Cl]$^{+}$.

The structure of **(3.53a)** has been determined by X-ray crystallography **(Fig. 3.19)** and selected bond distances and angles are listed in **Table 3.11**.

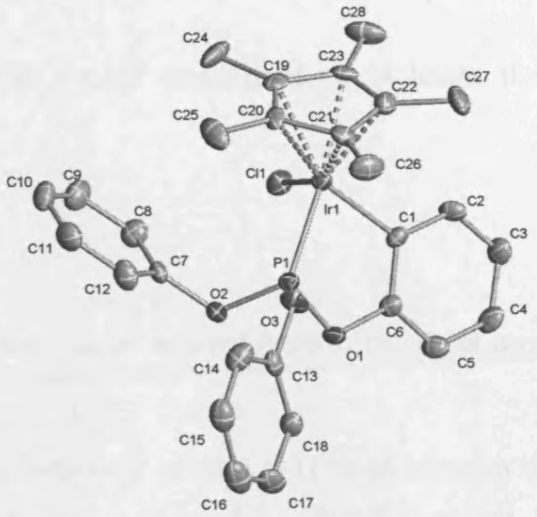

Fig. 3.19 Molecular structure of **(3.53a)**

Table 3.11 Selected bond distances [Å] and bond angles [°] for **(3.53a)**

Bond distances /[Å]			
Ir(1)-C(1)	2.062(6)	Ir-C(η-Cp*)	2.170(7)
Ir(1)-P(1)	2.180(2)	Ir-C(η-Cp*)	2.229(6)
Ir(1)-Cl(1)	2.404(2)	Ir-C(η-Cp*)	2.241(6)
P(1)-O(1)	1.604(4)	Ir-C(η-Cp*)	2.245(6)
P(1)-O(2)	1.610(4)	Ir-C(η-Cp*)	2.251(6)
Bond angles /[°]			
C(1)-Ir(1)-Cl(1)	82.26(17)	P(1)-Ir(1)-Cl(1)	94.76(6)
C(1)-Ir(1)-P(1)	79.08(17)		

The structure adopts a typical three legged piano stool structure with pseudo-octahedral geometry about the metal. Only the P(1)-Ir-C(1) chelate angle, [79.08(17) Å], is significantly less than the 90° expected for an octahedron, this is similar to that P-Rh-C chelate angle [80.9(2)°] found in [RhCl(Cp*){*o*-$Ph_2PN(H)C_6H_3C(O)Ph$-P,C}].[53]

Reaction of **(3.52b)** with NaOAc was monitored by ES mass spectrometry and after 24 hours all the ligand had reacted. Several rhodium-containing species were observed, including ions at m/z 588 [Cp*Rh$(POPh)_3$+NCMe-H] and 547 [Cp*Rh$(POPh)_3$-H] suggesting cyclometallation had occurred. The ^{31}P {^1H} and ^1H NMR spectrum of the crude product also showed more than two Cp*Rh species, and several signals for starting material protons (in the ^1H NMR spectrum). Unfortunately it was not possible to isolate any pure products even after chromatography through silica.

Reaction of **(3.52c)** with NaOAc was stirred for 24 hours, the ^1H NMR spectrum showed only unreacted **(3.52c)**.

Conclusion

The main conclusions that can be inferred from this study of acetate-assisted cyclometallation are as follows:

1) Acetate-assisted activation of an aryl C-H bond nitrogen donor ligands occurs at room temperature with [$RuCl_2$(*p*-cymene)]$_2$ and [MCl_2Cp^*]$_2$ (M = Ir, Rh) and provides a mild, high yield route to half-sandwich cyclometallated complexes.

2) The ease of cyclometallation depends on the nature of the donor, and decreases in the order alkyl imines > aryl imines > oxazolines ~ amine.

3) The ease of cyclometallation depends on the metal component, and decreases in the order Cp*Ir > Cp*Rh > (arene)Ru. However, an alternative procedure using NCMe as solvent provides a route to additional (arene) Ru complexes but not Cp*Rh ones.

4) Acetate plays several roles in the process: (i) It activates the dimers to react with nitrogen donor ligands. (ii) It acts as a base (probably intramolecularly). (iii) By coordinating in a bidentate fashion it may stabilise reactive intermediates.

5) Acetate assisted cyclometallation method can also be used for activation of N-H bonds, sp^2 C-H bonds of heterocycles and sp^3 C-H bonds.

3.3 Experimental

The spectroscopic techniques/instruments used were as described in Chapter Two. ^{1}H, ^{13}C and ^{31}P NMR spectra were obtained using a Bruker ARX250 or 300 MHz spectrometers, with $CDCl_3$ as solvent, unless otherwise stated.

Preparation of Imines

Preparation of C_6H_5-C(H)=N^{i}Pr (L_4)

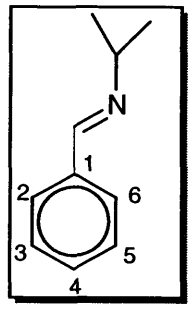

To a solution of benzaldehyde (6.23 g, 58.70 mmol) in CH_2Cl_2 (25 ml), isopropyl amine (3.47 g, 58.70 mmol) and formic acid (one drop) were added. The resulting mixture was stirred at room temperature for 2h. The resulting solution was evaporated to dryness to give a yellow liquid: (7.80 g, 90%). ^{1}H NMR: δ 1.28 (d, 6H, *J* 7, CH*MeMe*`), 3.55 (sept, 1H, *J* 7, C*H*MeMe), 7.40 (m, 3H, Ar-H), 7.73 (m, 2H, Ar-H), 8.30 (s, 1H, HC=N); $\delta_C$ 24.16 (CH*MeMe*`), 61.66 (*CH*MeMe`), 128.04, 128.50, 130.34 ($C^2$, $C^3$, $C^4$, $C^5$, $C^6$), 136.49 ($C^1$), 158.26 (N=CH). MS (FAB) *m/z*: 148 $[MH]^+$. $\upsilon$(C=N) 1629 $cm^{-1}$. CHMe*Me*`

Preparation of C_4H_3NH-2-C(H)=N(3,5-$Me_2C_6H_3$) (L_7)

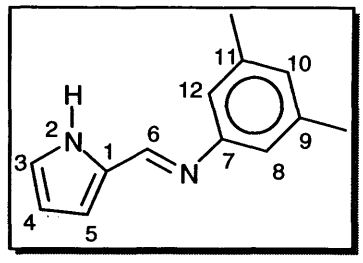

To a solution of pyrrole 2-carboxaldehyde (3.00 g, 31.6 mmol) in EtOH (50 ml), 3,5-dimethyl aniline (3.82 g, 31.60 mmol) and *p*-TSA (one drop) were added. The resulting mixture was refluxing for 18h, and then filtered. The resulting solution was evaporated to dryness to give a reddish brown precipitate, which was washed with hexane: (5.20 g, 83%). Calc. For $C_{14}H_{16}N_2$: C, 79.21, H, 7.60, N, 13.20. Found: C, 79.12, H, 7.28, N, 13.40%. ^{1}H NMR: δ 2.21 (s, 6H, 2xMe), 6.24 (dd, 1H, *J* 3.5, 2.5, H^4), 6.65 (dd, 1H, *J* 3.5, 1.5, H^3), 6.77 (br, 1H, H^5), 6.83 (s, 2H, H^8, H^{12}), 6.84 (s, 1H, H^{10}), 8.24 (s, 1H, HC=N); δ_C 21.51 (2xMe), 110.47 (C^4), 116.77 (C^3), 118.93 (C^8, C^{12}), 123.51 (C^5), 127.39 (C^{10}), 131.00 (C^1), 139.03 (C^9, C^{11}), 149.95 (C^6), 152.04 (C^7). MS (FAB) *m/z*: 199 $[MH]^+$. IR: υ(C=N) 1622 cm^{-1}. υ(N-H) 3227 cm^{-1}.

Preparation of C_4H_3NMe-2-C(H)=N(3,5-$Me_2C_6H_3$) (L_8)

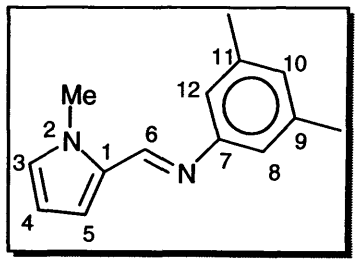

To a solution of N-methyl pyrrole, 2-carboxaldehyde (1.02 g, 9.31 mmol) in CH_2Cl_2 (10 ml), 3,5-dimethylaniline (1.13 g, 9.31 mmol) and formic acid (one drop) were added. The resulting mixture was stirred at room temperature for 2h, and then filtered. The resulting solution was evaporated to dryness to give a reddish brown liquid: (1.75 g, 88%). ^{1}H NMR: δ 2.31 (s, 6H, 2xMe), 4.00 (s, 3H, CH_3), 6.18 (dd, 1H, *J* 3.5, 2, H^4), 6.63 (dd, 1H, *J*

3.5, 1, H^3), 6.74 (m, 1H, H^5), 6.76 (s, 2H, H^8, H^{12}), 6.80 (s, 1H, H^{10}), 8.27 (s, 1H, HC=N). υ(C=N) 1665 cm^{-1}.

Preparation of C_4H_3S-2-C(H)=N(3,5-$Me_2C_6H_3$) (L_9)

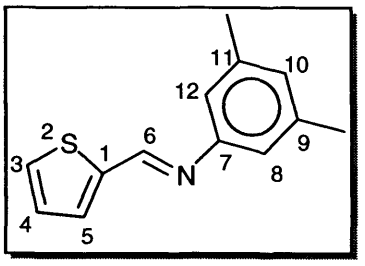

To a solution of thiophene 2-carboxaldehyde (0.90 g, 8.04 mmol) in CH_2Cl_2 (10 ml), 3,5-dimethyl aniline (0.97 g, 8.04 mmol) and formic acid (one drop) were added. The resulting mixture was stirred at room temperature for 3h, and then filtered. The resulting solution was evaporated to dryness to give a yellow liquid: (1.52 g, 88%). ^{1}H NMR: δ 2.30 (s, 6H, 2xMe), 6.80 (m, 3H, H^8, overlapping with singlet for H^{10}, H^{12}), 7.10 (m, 1H, H^4), 7.40 (m, 2H, H^3, H^5), 8.50 (s, 1H, HC=N). δ_C 21.25 (2xMe), 113.04, 118.75, 127.64, 130.04, 131.90 (C^3, C^4, C^5, C^8, C^{10}, C^{12}), 138.28 (C^9, C^{11}), 142.98 (C^1), 151.34 (C^7), 152.51 (C^6). IR: υ(C=N) 1615 cm^{-1}.

Preparation of $C_4H_3OCH_2$-2-C(H)=N(3,5-$Me_2C_6H_3$) (L_{10})

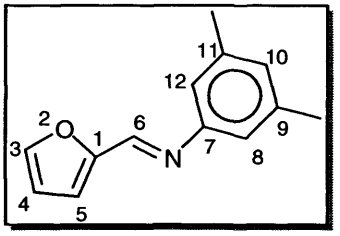

To a solution of 2-furaldehyde (0.39 g, 4.02 mmol) in CH_2Cl_2 (10 ml), and 3,5-dimethyl aniline (0.49 g, 4.02 mmol) were added. The resulting mixture was stirred at room temperature for 3h, and then filtered. The resulting solution was evaporated to dryness to give a red liquid: (0.70 g, 87%). ^{1}H NMR: δ 2.20 (s, 6H, 2xMe), 6.51 (m, 1H, H^4), 6.80 m, 3H, H^5, overlapping with singlet for H^8, H^{12}), 6.90 (m, 1H, H^3), 7.51 (s, 1H, H^{10}), 8.22 (s, 1H, HC=N).

General procedure for cyclometallation reactions

Sodium acetate and the appropriate dimer [MCl_2Cp^*]$_2$ (M = Rh, Ir) or [$RuCl_2$(*p*-cymene)]$_2$ were added to a solution of the ligand in dichloromethane (15–25 ml). The mixture was stirred for several hours, then filtered through Celite. The filtrate was evaporated to dryness and then washed with hexane to remove excess ligand. The cyclometallated products were usually pure at this stage but the compounds could be recrystallised from CH_2Cl_2/hexane. Details of individual reactions are shown below.

[IrCl{C_6H_4-2-C(H)-N(CH_2)$_2$$OCH_3$-$\kappa C,N$}Cp*] (3.30a)

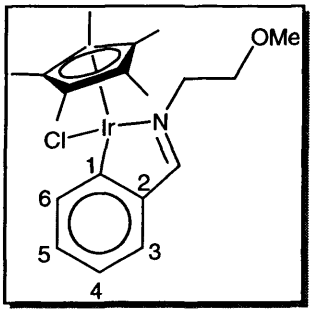

This was prepared from NaOAc (70 mg, 0.85 mmol), [$IrCl_2Cp^*$]$_2$ (200 mg, 0.25 mmol), and imine (L_1) (80 mg, 0.50 mmol); after stirring for 5 h, **(3.30a)** was isolated as an orange solid (255 mg, 96%). Calc. for $C_{20}H_{27}ClIrNO$: C, 45.75, H, 5.18, N, 2.67. Found: C, 45.65, H, 5.18, N, 2.62%. ^{1}H NMR: δ 1.72 (s, 15H, Cp*), 3.37 (s, 3H, OMe), 3.85 (m, 2H, CH_2O), 4.19 (m, 2H, NCH_2), 6.97 (dt, 1H, *J* 7.5, 1, H^4), 7.15 (dt, 1H, *J* 7.5, 1.5, H^5), 7.52 (dd,

1H, *J* 7.5, 1, H^3), 7.76 (d, 1H, *J* 7.5, H^6), 8.37 (s, 1H, HC=N). ^{13}C NMR: δ 9.25 (C_5Me_5), 59.00 (OMe), 61.89 (CH_2O), 70.34 (NCH_2), 88.88 (C_5Me_5), 121.97, 128.52, 131.71, 134.71 (C^3, C^4, C^5, C^6), 146.42 (C^2), 168.73 (C^1Ir), 176.31 (HC=N). MS (FAB): *m/z* 525 $[M]^+$, 490 $[M-Cl]^+$. IR: ν(C=N) 1596 cm^{-1}.

[RhCl{C_6H_4-2-C(H)=N(CH_2)$_2$OMe-$_K$*C,N*}Cp*] (3.30b)

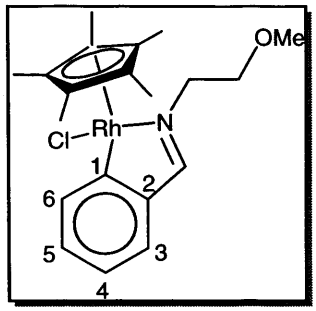

This was prepared from NaOAc (33 mg, 0.40 mmol), $[RhCl_2Cp^*]_2$ (100 mg, 0.16 mmol), imine (**L_1**) (53 mg, 0.32 mmol) and benzaldehyde (33 mg, 0.31 mmol); after stirring for 5 h, **(3.30b)** was isolated as a red solid (125 mg, 89%). Calc. for $C_{20}H_{27}ClNORh$: C, 55.12, H, 6.24, N, 3.21. Found: C, 54.92, H, 6.39, N, 3.15%. ^1H NMR: δ 1.66 (s, 15H, Cp*), 3.38 (s, 3H, OMe), 3.87 (m, 2H, CH_2O), 4.01 (m, 1H, NC*H*H`), 4.20 (m, 1H, NCH*H*`), 7.00 (dt, 1H, *J* 7.5, 1, H^4), 7.21 (dt, 1H, *J* 7.5, 1.5, H^5), 7.42 (dd, 1H, *J* 7.5, 1.5, H^3), 7.77 (d, 1H, *J* 7.5, H^6), 8.16 (d, 1H, J_{RhH} 4, HC=N). ^{13}C NMR: δ 9.49 (C_5Me_5), 59.11 (OMe), 60.75 (CH_2O), 70.62 (NCH_2), 96.03 (d, J_{RhC} 6, C_5Me_5), 122.67, 128.46, 130.95, 136.01 (C^3, C^4, C^5, C^6), 145.49 (C^2), 173.97 (HC= N), 184.03 (d, J_{RhC} 33, C^1Rh). MS (FAB): *m/z* 435 $[M]^+$, 400 $[M-Cl]^+$. IR: ν(C=N) 1606 cm^{-1}.

[RuCl{C_6H_4-2-C(H)=N(CH_2)$_2$OCH$_3$-$_K$*C,N*}(*p*-cymene)] (3.30c)

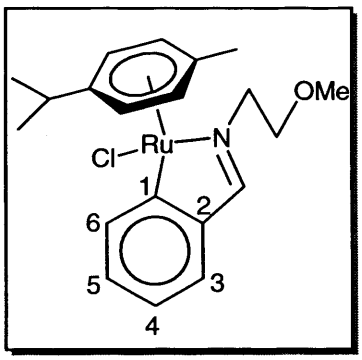

This was prepared from NaOAc (67 mg, 0.82 mmol), $[RuCl_2$(*p*-cymene)$]_2$ (200 mg, 0.33 mmol), and imine (**L_1**) (107 mg, 0.66 mmol) and benzaldehyde (35 mg, 0.33 mmol); after stirring for 5 h, **(3.30c)** was isolated as a brown solid (230 mg, 82%). Calc. For $C_{20}H_{26}ClNORu$: C, 55.48, H, 6.05, N, 3.24. Found: C, 55.54, H, 6.05, N, 3.29%. ^1H NMR: δ 0.83 (d, 3H, *J* 7, CH*Me*Me`), 1.06 (d, 3H, *J* 7, CHMe*Me*`), 2.07 (s, 3H, Cy-*Me*), 2.49 (sept, 1H, *J* 7, C*H*MeMe`), 3.39 (s, 3H, OMe), 3.98 (m, 2H, CH_2O), 4.26 (m, 2H, NCH_2), 4.82 (d, 1H, *J* 6, Cy), 4.99 (d, 1H, *J* 6, Cy), 5.58 (d, 1H, *J* 6, Cy), 5.62 (d, 1H, *J* 6, Cy), 6.95 (t, 1H, *J* 7, H^4), 7.12 (dt, 1H, *J* 7.5, 1.5, H^5), 7.41 (dd, 1H, *J* 7.5, 1, H^3), 8.05 (s, 1H, HC=N), 8.12 (d, 1H, *J* 7.5, H^6). ^{13}C NMR: δ 18.96 (MeC_6H_4), 21.42, 23.21, (2 × Me(^{i}Pr)), 31.04 (CH(^{i}Pr)), 58.97 (OMe), 65.30 (CH_2O), 70.69 (NCH_2), 80.17, 80.89, 90.07, 91.24 (CH (C_6H_4Cy)), 101.89, 102.62 (C (C_6H_4 Cy)), 122.33, 128.90, 129.71, 139.07 (C^3, C^4, C^5, C^6), 145.38 (C^2), 173.69 (HC=N), 188.48 (C^1Ru). MS (FAB): *m/z* (%) 433 $[M]^+$, 398 $[M-Cl]^+$. IR: ν(C=N) 1601 cm^{-1}.

[IrCl{C_6H_4-2-C(H)=N(CH_2)$_3$OCH_3-$_K$*C,N*}Cp*] (3.31a)

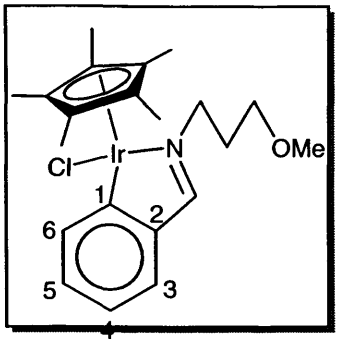

This was prepared from NaOAc (70 mg, 0.85 mmol), [$IrCl_2Cp^*]_2$ (200 mg, 0.25 mmol), and imine (**L_2**) (90 mg, 0.50 mmol); after stirring for 5 h, (**3.31a**) was isolated as an orange precipitate (260 mg, 96%). Calc. for $C_{21}H_{29}ClIrNO$: C, 46.78, H, 5.42, N, 2.60. Found: C, 46.80, H, 5.46, N, 2.68%. ^{1}H NMR: δ 1.72 (s, 15H, Cp*), 2.17 (m, 2H, CH_2), 3.33 (s, 3H, OMe), 3.43 (m, 2H, CH_2O), 4.13 (m, 2H, NCH_2), 6.98 (dt, 1H, *J* 7.5, 1, H^4), 7.16 (dt, 1H, *J* 7.5 1.5, H^5), 7.52 (dd, 1H, *J* 7.5, 1, H^3), 7.76 (d, 1H, *J* 7.5, H^6), 8.31 (s, 1H, HC=N). ^{13}C NMR: δ 9.20 (C_5Me_5), 29.02 (CH_2), 58.75 (OMe), 59.81 (CH_2O), 69.75 (NCH_2), 88.87 (C_5Me_5), 121.96, 128.16, 131.61, 134.73 (C^3, C^4, C^5, C^6), 146.27 (C^2), 168.59 (C^1Ir), 175.55 (HC=N); MS (FAB): *m/z* 539 $[M]^+$, 504 $[M\text{-}Cl]^+$. IR: ν(C=N) 1593 cm^{-1}.

[RhCl{C_6H_4-2-C(H)=N(CH_2)$_3$OCH_3-$_K$*C,N*}Cp*] (3.31b)

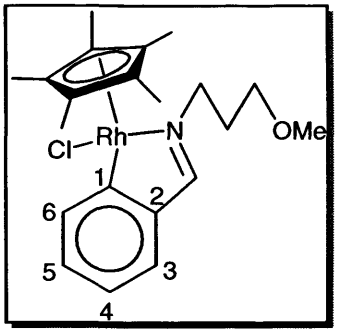

This was prepared from NaOAc (66 mg, 0.81 mmol), [$RhCl_2Cp^*]_2$ (200 mg, 0.32 mmol), and imine (**L_2**) (115 mg, 0.65 mmol); after stirring for 5h, (**3.31b**) was isolated as a red solid (275 mg, 95%). Calc. for $C_{21}H_{29}ClNORh$: C, 56.07, H, 6.50, N, 3.11. Found: C, 55.98, H, 6.44, N, 3.15%. ^{1}H NMR: δ 1.66 (s, 15H, Cp*), 2.21 (m, 2H, CH_2), 3.32 (s, 3H, OMe), 3.44 (m, 2H, CH_2O), 3.93 (m, 1H, NC*H*H`), 4.12 (m, 1H, NCH*H*`), 7.01 (dt, 1H, *J* 7.5, 1, H^4), 7.22 (dt, 1H, *J* 7.5, 1.5, H^5), 7.41 (dd, 1H, *J* 7.5, 1.5, H^3), 7.77 (d, 1H, *J* 7, H^6), 8.11 (d, 1H, J_{RhH} 4, HC=N). ^{13}C NMR: δ 9.41 (C_5Me_5), 29.32 (CH_2), 58.64 (CH_2O), 58.75 (OMe), 69.72 (NCH_2), 95.98 (d, J_{RhC} 6, C_5Me_5), 122.62, 128.08, 130.81, 136.01 (C^3, C^4, C^5, C^6), 145.32 (C^2), 172.97 (HC= N), 183.93 (d, J_{RhC} 33, C^1Rh). MS (FAB): *m/z* 449 $[M]^+$, 414 $[M\text{-}Cl]^+$, 412 $[M\text{-}Cl\text{-}H_2]^+$. IR: ν(C= N) 1604 cm^{-1}.

[RuCl{C_6H_4-2-C(H)=N(CH_2)$_3$OCH_3-$_K$*C,N*}(*p*-cymene)] (3.31c)

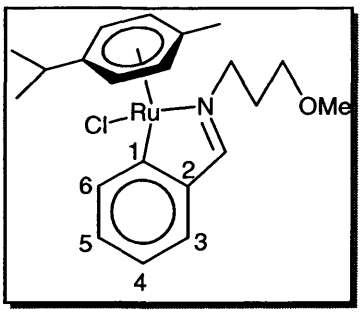

This was prepared from NaOAc (35 mg, 0.43 mmol), [$RuCl_2$(*p*-cymene)]$_2$ (100 mg, 0.16 mmol), and imine (**L_2**) (58 mg, 0.33 mmol) and benzaldehyde (18 mg, 0.17 mmol); after stirring for 5 h, (**3.31c**) was isolated as a red solid (123 mg, 84%). Calc. For $C_{21}H_{28}ClNORu$: C, 56.43, H, 6.31, N, 3.13. Found: C, 56.61, H, 6.22, N, 3.13%. ^{1}H NMR: δ 0.80 (d, 3H, *J* 7, CH*Me*Me`), 1.06 (d, 3H, *J* 7, CHMe*Me*`), 2.10 (s, 3H, Cy–Me), 2.37 (m, 2H, CH_2), 2.49 (sept, 1H, *J* 7, C*H*MeMe`), 3.36 (s, 3H, OMe), 3.47 (m, 2H, CH_2O), 4.17 (m, 2H, NCH_2), 4.82 (d, 1H, *J* 6.5, Cy), 4.95 (d, 1H, *J* 6, Cy), 5.64 (d, 2H, *J* 6.5, Cy), 6.96 (dt, 1H, *J* 7.5, 1, H^4), 7.13 (dt, 1H, *J* 7.5, 1.5, H^5), 7.41 (dd, 1H, *J* 7.5, 1, H^3), 8.01 (s, 1H, HC=N), 8.12 (d, 1H, *J* 7.5, H^6). ^{13}C NMR: δ 18.98 (*Me*C_6H_4), 21.23, 23.49 (*MeMe*

(^{i}Pr)), 29.53 (CH_2), 31.04(CH (^{i}Pr)), 58.83 (OMe), 62.97 (CH_2O), 69.82 (NCH_2), 79.58, 81.26, 89.79, 91.71 (CH (C_6H_4 Cy)), 101.21, 103.31 (C(C_6H_4 Cy)), 122.34, 128.61, 129.68, 139.07 (C^3, C^4, C^5, C^6), 145.19 (C^2), 172.77 (HC=N), 188.31 (C^1Ru). MS (FAB): *m/z* 447 $[M]^+$, 410 $[M\text{-}Cl\text{-}H_2]^+$. IR: ν(C=N) 1602 cm^{-1}.

[IrCl{C_6H_4-2-C(H)=NPh-$_K$*C,N*}Cp*] (3.32a)

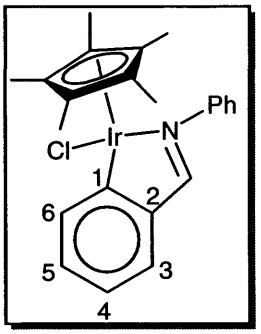

This was prepared from NaOAc (13 mg, 0.16 mmol), $[IrCl_2Cp^*]_2$ (50 mg, 0.06 mmol), imine (**L_3**) (23 mg, 0.13 mmol) and benzaldehyde (7 mg, 0.07 mmol); after stirring for 5 h, (**3.32a**) was isolated as a red precipitate (57 mg, 84%). Calc. For $C_{23}H_{25}ClIrN$: C, 50.86, H, 4.64, N, 2.58. Found: C, 50.78, H, 4.68, N, 2.59%. ^{1}H NMR: δ 1.47 (s, 15H, Cp*), 7.02 (dt, 1H, *J* 7.5, 1, H^4), 7.20 (dt, 1H, *J* 7.5, 1.5, H^5), 7.30 (m, 1H, Ph), 7.40 (t, 2H, *J* 7.5, Ph), 7.57 (m, 2H, Ph), 7.62 (dd, 1H, *J* 7.5, 1, H^3), 7.85 (d, 1H, *J* 7.5, H^6), 8.31 (s, 1H, HC=N). ^{13}C NMR: δ 8.90 (C_5Me_5), 89.39 (C_5Me_5), 122.14, 122.67, 127.43, 129.16, 129.75, 132.62, 135.29 (C^3, C^4, C^5, C^6 and Ph), 147.15 (C^2), 152.00 (Ph), 170.68 (C^1Ir), 175.58 (HC=N). MS (FAB): *m/z* 543 $[M]^+$, 508 $[M\text{-}Cl]^+$. IR: ν(C=N) 1582 cm^{-1}.

[RhCl{C_6H_4-2-C(H)=NPh-$_K$*C,N*}Cp*] (3.32b)

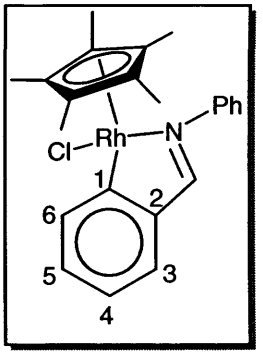

This was prepared from NaOAc (66 mg, 0.80 mmol), $[RhCl_2Cp^*]_2$ (200 mg, 0.32 mmol), imine (**L_3**) (120 mg, 0.65 mmol) and benzaldehyde (35 mg, 0.33 mmol); after stirring for 5 h, (**3.32b**) was isolated as a red precipitate (178 mg, 71%). Calc. For $C_{23}H_{25}ClNRh$: C, 60.87, H, 5.55, N, 3.09. Found: C, 60.63, H, 5.85, N, 3.00%. ^{1}H NMR: δ 1.43 (s, 15H, Cp*), 7.06 (t, 1H, *J* 7.5, H^4), 7.27 (t, 1H, *J* 7.5, H^5), 7.30 (t, 1H, *J* 7.5, Ph), 7.42 (t, 2H, *J* 7.5, Ph), 7.54 (dd, 1H, *J* 7.5, 1, H^3), 7.62 (d, 2H, *J* 8, Ph), 7.85 (d, 1H, *J* 8, H^6), 8.18 (d, 1H, J_{RhH} 4, HC=N). ^{13}C NMR: δ 9.10 (C_5Me_5), 96.42 (d, J_{RhC} 6.5, C_5Me_5), 122.32, 122.89, 127.42, 129.28, 129.58, 131.64, 136.58 (C^3, C^4, C^5, C^6 and Ph), 146.32 (C^2), 151.24 (Ph), 172.50 (HC=N), 185.55 (d, J_{RhC} 33, C^1Rh). MS (FAB): *m/z* 453 $[M]^+$, 418 $[M\text{-}Cl]^+$. IR: ν(C=N) 1598 cm^{-1}.

Reaction of *N,N*-dimethylbenzylamine with $[RhCl_2Cp^*]_2$

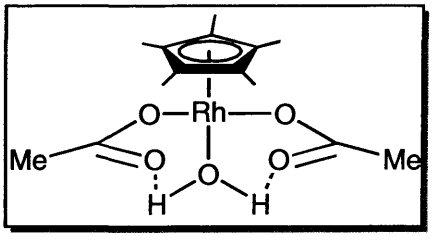

A mixture of *N,N*-dimethylbenzylamine (**L_5**) (87 mg, 0.65 mmol), NaOAc (55 mg, 0.67 mmol), and $[RhCl_2Cp^*]_2$ (200 mg, 0.32 mmol), was stirred in dichloromethane for 20 h. The mixture was filtered through Celite and evaporated to dryness. The ^{1}H NMR spectrum showed a broad resonance at *ca.* δ 1.7 due to Cp* and another signal at *ca.* δ 1.95. The mass spectrum showed ions at *m/z* 237 [RhCp*], 297 [Rh(OAc)Cp*], 545

$[Rh_2Cl_2Cp^*_2\text{-}H]$, 581 $[Rh_2Cl_3Cp^*_2]$, and 605 $[Rh_2Cl_2(OAc)Cp^*_2]$. Crystals were grown by diffusion of hexane into a dichloromethane solution. The X-ray structure showed the crystals to be $[Rh(OH_2)(\eta^1\text{-}O_2CMe)_2Cp^*]\cdot H_2O$.

Reaction of *N,N*-dimethylbenzylamine with $[RuCl_2(p\text{-cymene})]_2$

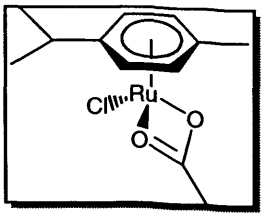

A mixture of *N,N*-dimethylbenzylamine (88 mg, 0.66 mmol), NaOAc (67 mg, 0.82 mmol), and $[RuCl_2(p\text{-cymene})]_2$ (200 mg, 0.33 mmol), was stirred in dichloromethane for 20 h. The mixture was filtered through Celite and evaporated to dryness. The ^{1}H NMR spectrum showed the presence of $[RuCl(\eta^2\text{-}O_2CMe)\text{-}(p\text{-cymene})]$ **(3.34)** by comparison with literature data.[32] This was further characterised by X-ray diffraction.

$[RuCl\{C_6H_4\text{-}2\text{-}C(H)=N^iPr\text{-}_\kappa C,N\}(p\text{-cymene})]$ (3.35c)

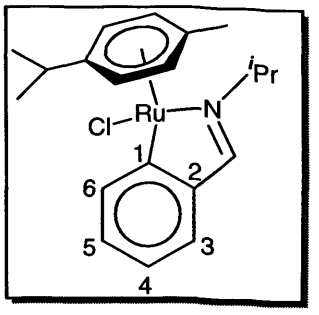

This was prepared from NaOAc (50 mg, 0.61 mmol), $[RuCl_2\text{-}(p\text{-cymene})]_2$ (150 mg, 0.25 mmol), and imine **(L_4)** (72 mg, 0.49 mmol) and benzaldehyde (26 mg, 0.25 mmol); after stirring overnight, **(3.35c)** was isolated as a green solid (120 mg, 59%). Calc. For $C_{20}H_{26}ClNRu$(1/3 equiv. CH_2Cl_2): C, 54.92, H, 5.99, N, 3.15. Found: C, 55.42, H, 5.69, N, 3.17%. ^{1}H NMR: δ 0.77 (d, 3H, *J* 7, Cy(CH*Me*Me`)), 1.06 (d, 3H, *J* 7, Cy(CHMe*Me*`)), 1.53 (d, 3H, J 6.5, N^{i}Pr*Me*), 1.57 (d, 3H, *J* 7, N^{i}Pr*Me*`), 2.11 (s, 3H, Cy-*Me*), 2.48 (sept, 1H, *J* 7, Cy*CH*MeMe), 4.48 (sept, 1H, *J* 7, N^{i}PrCH), 4.75 (d, 1H, *J* 6, Cy), 4.95 (d, 1H, *J* 6, Cy), 5.63 (d, 2H overlapping, *J* 6, Cy), 5.94 (d, 1H, *J* 6, Cy), 6.94 (t, 1H, *J* 7, H^4), 7.11 (t, 1H, *J* 7.5, H^5), 7.38 (d, 1H, *J* 7.5, H^3), 8.08 (s, 1H, HC= N), 8.10 (d, 1H, *J* 7.5, H^6). ^{13}C NMR: δ 18.02 (Cy-*Me*C_6H_4), 20.20 (Cy-CH*Me*Me`) 22.22 (N$^i$Pr*Me*), 22.56 (Cy-CHMe*Me*`), 23.39 (N^{i}Pr*Me*`), 30.08 (Cy*CH*MeMe`), 63.74 (N^{i}Pr*CH*), 78.31, 79.41, 89.32, 91.06 (CH (C_6H_4Cy)), 103.18, 103.06 (C (C_6H_4 Cy)), 121.25, 127.66, 128.13, 128.54, (C^3, C^4, C^5, C^6), 144.72 (C^2), 168.10 (HC=N), 186.55 (C^1Ru). MS (FAB): *m/z* (%) 417 $[M]^+$, 382 $[M\text{-}Cl]^+$. IR: ν(C= N) 1601 cm^{-1}.

$[IrCl\{C_6H_4\text{-}2\text{-}CH_2NMe_2\text{-}_\kappa C,N\}Cp^*]$ (3.36a)

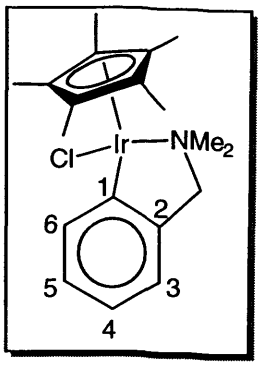

This was prepared from NaOAc (50 mg, 0.61 mmol), $[IrCl_2Cp^*]_2$ (200 mg, 0.25 mmol), and *N,N*-dimethylbenzylamine **(L_5)** (85 mg, 0.63 mmol); after stirring for 20 h, **(3.36a)** was isolated as an orange precipitate (177 mg, 71%). Calc. for $C_{19}H_{27}ClIrN$: C, 45.91, H, 5.47, N, 2.82. Found: C, 45.87, H, 5.56, N, 2.79%. ^{1}H NMR: δ 1.63 (s, 15H, Cp*), 2.90 (s, 3H, NMe), 3.03 (s, 3H, NMe`), 3.26 (d, 1H, *J* 13, NCH), 4.38 (d, 1H, *J* 13, NCH`), 6.86 (dt, 1H, *J* 7, 1, H^4), 6.98 (t, 1H, *J* 7, H^5), 7.05 (d, 1H, *J* 7, H^3), 7.61 (d, 1H, *J* 7, H^6). ^{13}C NMR: δ 9.47

(C_5Me_5), 51.81, 57.47 (2 × NMe), 73.72 (NCH_2), 87.61 (C_5Me_5), 121.56, 122.38, 126.47, 134.65 (C^3, C^4, C^5, C^6), 148.30 (C^2), 151.38 (C^1Ir). MS (FAB): *m/z* 497 $[M]^+$, 460 $[M\text{-}Cl\text{-}H_2]^+$.

[IrCl{C_6H_4-2-Me_2oxaz)-$\kappa C,N$}Cp*] (3.37a)

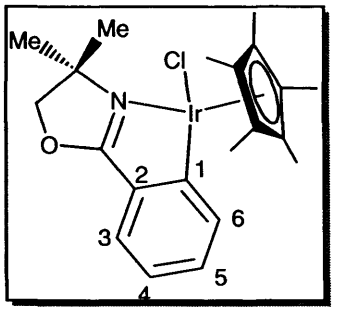

This was prepared from NaOAc (16 mg, 0.20 mmol), $[IrCl_2Cp^*]_2$ (63 mg, 0.08 mmol), and oxazoline (**L_6**) (28 mg, 0.16 mmol); after stirring for 5 h, **(3.37a)** was isolated as an orange precipitate (62 mg, 74%). Calc. for $C_{21}H_{27}ClIrNO$: C, 46.96, H, 5.07, N, 2.61. Found: C, 46.72, H, 4.89, N, 2.54%. ^1H NMR: δ 1.50 (s, 3H, Me), 1.53 (s, 3H, Me), 1.79 (s, 15H, Cp*), 4.43 (d, 1H, *J* 8, OC*H*H'), 4.55 (d, 1H, *J* 8, OCH*H*'), 6.99 (dt, 1H, *J* 7.5, 1, H^4), 7.24 (dt, 1H, *J* 7.5, 1.5, H^5), 7.42 (dd, 1H, *J* 7.5, 1, H^3), 7.75 (d, 1H, *J* 7.5, H^6). ^{13}C NMR: δ 10.14 (C_5Me_5), 26.54 (Me), 28.87 (Me), 67.51 (CMe_2), 82.95 (OCH_2), 88.05 (C_5Me_5), 121.89, 126.51, 132.35, 135.37 (C^3, C^4, C^5, C^6), 162.81 (NCO), 178.17 (C^1Ir). MS (FAB): *m/z*. 537 $[M]^+$, 502 $[M\text{-}Cl]^+$. IR: ν(C=N) 1623 cm^{-1}.

[$IrCl_2${$NH_2(CH_2)_2OCH_3$}Cp*] (3.38)

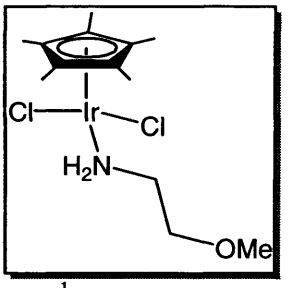

A mixture of (**L_1**) (21 mg, 0.13 mmol), benzaldehyde (136 mg, 1.28 mmol) and $[IrCl_2Cp^*]_2$ (50 mg, 0.063 mmol), was stirred in dichloromethane for 4 h. The mixture was evaporated to dryness and washed with hexane to give an orange precipitate (52 mg, 87%). Calc. for $C_{13}H_{24}Cl_2IrNO$: C, 32.98, H, 5.11, N, 2.96. Found: C, 32.86, H, 5.47, N, 2.84%. ^1H NMR: δ 1.70 (s, 15H, Cp*), 3.13 (m, 2H, CH_2O), 3.37 (s, 3H, OMe), 3.42 (m, 2H, NCH_2), 3.80 (br, 2H, NH_2). ^{13}C NMR: δ 9.28 (C_5Me_5), 46.70 (CH_2O), 59.14 (OMe), 72.79 (NCH_2), 84.98 (C_5Me_5).

General procedure for cyclometallation reactions in NCMe solvent

Sodium acetate, KPF_6 and $[MCl_2Cp^*]_2$ (M = Ir, Rh) or $[RuCl_2(p\text{-cymene})]_2$ were added to a solution of the ligand in acetonitrile (10 ml). The mixture was heated for several hours, then filtered through Celite. The filtrate was evaporated to dryness and then washed with hexane to remove excess ligand to give the cyclometallated products. The compounds could be recrystallised from dichloromethane/hexane.

[Ru(NCMe){C_6H_4-2-C(H)=NPh-$\kappa C,N$}(p-cymene)][PF_6] (3.39c)

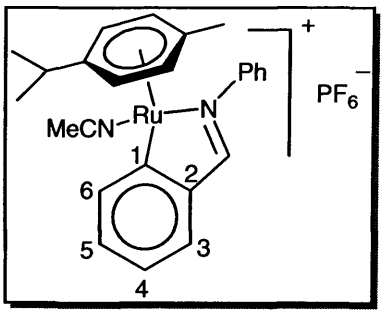

This was prepared from NaOAc (34 mg, 0.41 mmol), $[RuCl_2(p\text{-cymene})]_2$ (100 mg, 0.16 mmol), imine (**L_3**) (59 mg, 0.33 mmol), benzaldehyde (17 mg, 0.16 mmol) and KPF_6 (120 mg, 0.65 mmol); after heating overnight, **(3.39c)** was isolated as a green solid (132

mg, 68%). Calc. For $C_{25}H_{27}N_2RuPF_6$ (1 equiv. NCMe): C, 45.35, H, 4.21, N, 4.07. Found: C, 44.86, H, 3.99, N, 4.63%. ^{1}H NMR: δ 0.97 (d, 3H, *J* 7, CH*Me*Me`), 0.98 (d, 3H, *J* 7, CHMe*Me*`), 2.03 (s, 3H, Cy-Me), 2.30 (s, 3H, NCMe), 2.36 (sept, 1H, *J* 7, CyC*H*MeMe), 5.25 (d, 1H, *J* 6, Cy), 5.33 (d, 1H, *J* 6, Cy), 5.61 (d, 2H, *J* 6, Cy), 5.77 (d, 1H, *J* 6, Cy), 7.16 (t, 1H, *J* 7.5, H^4), 7.27 (dt, 1H, *J* 7.5, 1.5, H^5), 7.28 (m, 1H, Ph), 7.42 (m, 1H, Ph), 7.60 (m, 4H, H^3, Ph), 8.13 (d, 1H, *J* 7.5, H^6), 8.24 (s, 1H, HC=N). ^{13}C NMR: δ 3.93 (NCMe), 18.76 (Cy-*Me*C_6H_4), 22.34, 22.51 (Cy-CH*MeMe*`), 31.08 (CyC*H*MeMe), 87.61, 89.54, 91.61, 92.49 (CH (C_6H_4Cy)), 102.71, 104.47 (C (C_6H_4 Cy)), 124.92 (NCMe), 122.26, 124.25, 128.82, 130.02, 130.83, 131.67, 139.61 (C^3, C^4, C^5, C^6, Ph), 146.60 (C^2), 153.35 (^{i}CPh), 174.36 (HC=N), 182.34 (C^1Ru). MS (FAB): *m/z* (%) 457 $[M]^+$, 416 $[M\text{-NCMe}]^+$. IR: ν(C= N) 1627 cm^{-1}.

[Ru(NCMe){C_6H_4-2-Me_2oxaz)-$_k$*C,N*}(p-cymene)] [PF_6] (3.40c)

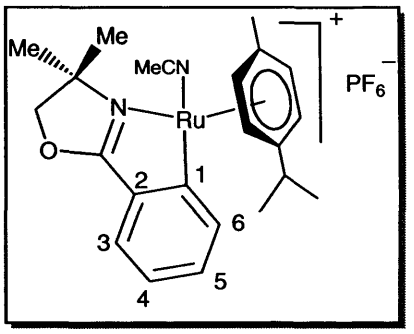

This was prepared from NaOAc (34 mg, 0.41 mmol), $[RuCl_2(p\text{-cymene})]_2$ (100 mg, 0.16 mmol), imine (**L_6**) (57 mg, 0.33 mmol) and KPF_6 (120 mg, 0.65 mmol); after heating for 3h, **(3.40c)** was isolated as a green solid (180 mg, 92%). Calc. For $C_{23}H_{29}N_2ORuPF_6$: C, 46.39, H, 4.91, N, 4.70. Found: C, 46.23, H, 4.80, N, 4.62%. ^{1}H NMR: δ 0.84 (d, 3H, *J* 7, CH*Me*Me`), 1.09 (d, 3H, *J* 7, CHMe*Me*`), 1.47 (s, 3H, oxaz-Me), 1.57 (s, 3H, oxaz-Me), 2.14 (s, 3H, Cy-Me), 2.21 (s, 3H, NCMe), 2.48 (sept, 1H, *J* 7, CyC*H*MeMe), 4.50 (s, 2H, NCH_2), 5.21 (d, 1H, *J* 6, Cy), 5.26 (d, 1H, *J* 6, Cy), 5.92 (d, 2H, *J* 6, Cy), 6.07 (d, 1H, *J* 6, Cy), 7.08 (dt, 1H, *J* 7.5, 1, H^4), 7.29 (dt, 1H, *J* 7.5, 1.5 H^5), 7.40 (dd, 1H, J 7.5, 1, H^3), 8.03 (d, 1H, *J* 7.5, H^6). ^{13}C NMR: δ 3.54 (NCMe), 18.97 (Cy-*Me*C_6H_4), 21.35, 23.54 (Cy-CH*MeMe*`), 27.65, 28.04 (oxaz-MeMe`) 31.28 (CyCHMeMe), 67.28 (^{i}*C*Me_2), 81.55, 82.24, 91.35, 91.37, (CH (C_6H_4Cy)), 81.95 (CH_2), 104.64, 105.92 (C (C_6H_4 Cy)), 124.03 (NCMe), 123.83, 126.99, 131.92, 139.72 (C^3, C^4, C^5, C^6), 173.12 (NCO), 175.92 (C^1Ru). MS (FAB): *m/z* (%) 410 $[M]^+$, 451 $[M\text{-NCMe}]^+$. IR: ν(C=N) 1622 cm^{-1}.

[IrCl{C_4H_3N-2-C(H)=N(3,5-$Me_2C_6H_3$)-$_K$N,N}(η-C_5Me_5)] (3.41a)

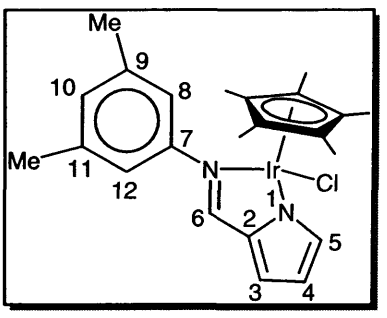

This was prepared from NaOAc (27 mg, 0.33 mmol), $[IrCl_2Cp^*]_2$ (105 mg, 0.13 mmol), and pyrrole imine (**L_7**) (53 mg, 0.26 mmol); after stirring overnight, **(3.41a)** was isolated as a yellow precipitate (120 mg, 81%). Calc. for $C_{23}H_{28}N_2ClIr$: C, 49.32, H, 5.04, N, 5.00. Found: C, 49.22, H, 4.90, N, 4.95%. ^{1}H NMR: δ 1.50 (s, 15H, Cp*), 2.33 (s, 6H, 2x Me), 6.38 (dd, 1H, *J* 3.5, 1.5, H^4), 6.78 (d, 1H, *J* 3.5, H^3), 6.86 (s, 1H, H^{10}), 7.11 (s, 2H, H^8, H^{12}), 7.17 (br s, 1H, H^5), 7.74 (s, 1H, HC=N). ^{13}C NMR:

δ 8.85 (C_5Me_5), 21.45 (2x Me), 86.30 (C_5Me_5), 113.72 (C^4), 118.02 (C^3), 121.45 (C^8, C^{12}), 128.07 (C^{10}), 135.35 (C^5), 138.55 (C^9, C^{11}), 142.25 (C^2), 151.43 (C^7), 157.97 (C^6). MS (FAB): *m/z* 560 $[M]^+$, 525 $[M\text{-}Cl]^+$.

[RhCl{C_4H_3N-2-C(H)=N(3,5-$Me_2C_6H_3$)-$_K$N,N}(η-C_5Me_5)] (3.41b)

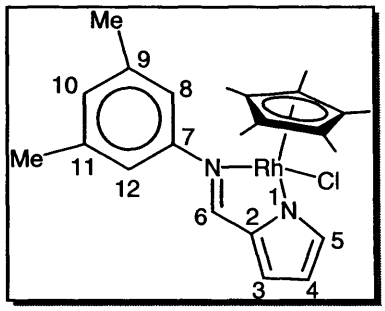

This was prepared from NaOAc (43 mg, 0.53 mmol), $[RhCl_2Cp^*]_2$ (130 mg, 0.21 mmol), and pyrrole imine (L_7) (84 mg, 0.42 mmol); after stirring overnight, **(3.41b)** was isolated as a brown precipitate (180 mg, 91%). Calc. for $C_{23}H_{28}N_2ClRh$: C, 58.67, H, 5.99, N, 5.95. Found: C, 58.45, H, 45.95, N, 5.74%. ^1H NMR: δ 1.49 (s, 15H, Cp*), 2.34 (s, 6H, 2x Me), 6.37 (dd, 1H, *J* 4, 2, H^4), 6.81 (dd, 1H, *J* 4, 1, H^3), 6.86 (s, 1H, H^{10}), 7.16 (s, 2H, H^8, H^{12}), 7.31 (br s, 1H, H^5), 7.66 (d, 1H, J_{RhH} 2.5, HC=N). ^{13}C NMR: δ 8.96 (C_5Me_5), 21.28 (2x Me), 94.18 (d, J_{RhC} 8, C_5Me_5), 113.73 (C^4), 118.08 (C^3), 121.26 (C^8, C^{12}), 127.78 (C^{10}), 136.19 (C^5), 138.56 (C^9, C^{11}), 140.73 (C^2), 151.00 (C^7), 157.65 (C^6). MS (FAB): *m/z* 470 $[M]^+$, 435 $[M\text{-}Cl]^+$. IR: ν(C= N) 1595 cm^{-1}.

[RuCl{C_4H_3N-2-C(H)=N(3,5-$Me_2C_6H_3$)-$_K$N,N}(η-*p*-cymene)] (3.41c)

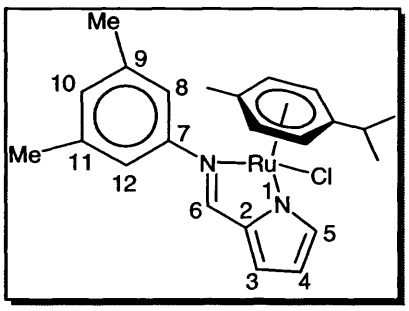

This was prepared from NaOAc (43 mg, 0.53 mmol), $[RuCl_2(p\text{-cymene})]_2$ (130 mg, 0.13 mmol), and pyrrole imine (L_7) (85 mg, 0.44 mmol); after stirring overnight, **(3.41c)** was isolated as a yellow precipitate (175 mg, 88%). Calc. for $C_{23}H_{27}N_2ClRu$: C, 59.03, H, 5.82, N, 5.99. Found: C, 58.79, H, 5.60, N, 5.58%. ^1H NMR: δ 0.95 (d, 3H, *J* 7, CH*Me*Me`), 1.07 (d, 3H, *J* 7, CHMe*Me*`), 2.18 (s, 3H, Cy-*Me*), 2.37 (s, 6H, 2x Me(Ar)), 2.53 (sept, 1H, *J* 7, C*H*MeMe`), 4.92 (d, 1H, *J* 6, Cy), 5.08 (d, 1H, *J* 6, Cy), 5.14 (d, 1H, *J* 6, Cy), 5.42 (d, 1H, *J* 6, Cy), 6.34 (dd, 1H, *J* 4, 1, H^4), 6.77 (d, 1H, *J* 4, H^3), 6.90 (s, 1H, H^{10}), 7.21 (s, 2H, H^8, H^{12}), 7.49 (s, 1H, H^5), 7.58 (s, 1H, HC=N). ^{13}C NMR: δ 18.86 (*Me*C_6H_4), 21.56 (2x*Me*Ph), 22.87 (2xMe (^{i}Pr)), 31.04(CH (^{i}Pr)), 81.77, 81.99, 84.43, 84.97 (CH (C_6H_4 Cy)), 99.79, 101.24 (C(C_6H_4 Cy)), 113.99 (C^4), 118.05 (C^3), 120.78 (C^8, C^{12}), 128.08 (C^{10}), 135.70 (C^5), 139.47 (C^9, C^{11}), 140.92 (C^2), 154.68 (C^7), 156.56 (C^6). MS (FAB): *m/z* 468 $[M]^+$, 433 $[M\text{-}Cl]^+$. IR: ν(C= N) 1607 cm^{-1}.

Reaction of (3.41c) with CF_3CO_2H

To a solution of **(3.41c)** (200 mg, 0. 43 mmol) in CH_2Cl_2 (15 ml), CF_3CO_2H (one drop) was added. The resulting mixture was stirred at room temperature for 18 h, and then filtered. The resulting solution was evaporated to dryness to give a brown precipitate, the solid was then

washed with hexane: The ^{1}H NMR spectrum showed a mixture of organic and complex species, see **section 3.2.5** for discussion.

Reaction of (L_7) with CF_3CO_2H

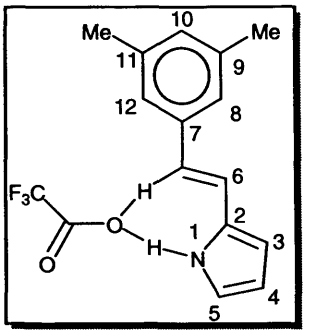

To a solution of (L_3) (100 mg, 0.51 mmol) in CH_2Cl_2 (10 ml), CF_3CO_2H (one drop) was added. The resulting mixture was stirred at room temperature overnight. The resulting solution was evaporated to dryness to give a yellow precipitate (**3.47**), the solid was then washed with hexane: (65 mg, 49%). Calc. For $C_{14}H_{16}N_2$: C, 57.69, H, 4.84, N, 8.97. Found: C, 55.26, H, 4.60, N, 8.45%. ^{1}H NMR: δ 2.36 (s, 6H, 2xMe), 6.05 (d, 1H, J 3.5, H^4), 7.00 (s, 1H, H^{10}), 7.07 (s, 2H, H^8, H^{12}), 7.32 (d, 1H, J 3.5, H^3), 7.70 (s, 1H, H^5), 8.20 (s, 1H, HC=N), 10.20 (br, 1H, C=NH); ^{13}C NMR: δ 21.41 (2xMe), 115.75, 131.05, 138.48 (C^3, C^4, C^5), 117.11 (C^8, C^{12}), 132.72 (C^{10}), 140.70 (C^9, C^{11}), 123.69, 137.3 (C^2, C^7), 144.75 (C^6), 161.50 (q, J_{CF} 38.5, CF_3). IR: υ(C=N) 1668 cm^{-1}.

[IrCl{C_4H_2N-3-CH_3-2-C(H)=N(3,5-$Me_2C_6H_3$)-$_\kappa$C,N}(η-C_5Me_5)] (3.48a)

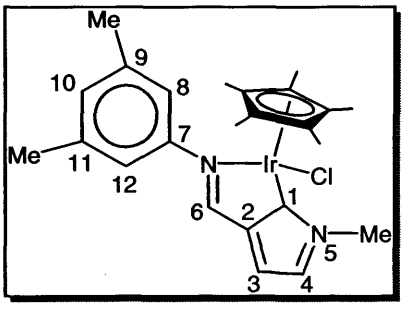

This was prepared from NaOAc (19 mg, 0.23 mmol), $[IrCl_2Cp^*]_2$ (70 mg, 0.09 mmol), and pyrrole imine (L_8) (38 mg, 0.18 mmol); after stirring for 4 hours, (**3.48a**) was isolated as a brown precipitate (88 mg, 88%). Calc. for $C_{24}H_{30}N_2ClIr$(1equiv. CH_2Cl_2): C, 45.60, H, 4.86, N, 4.25. Found: C, 46.56, H, 4.51, N, 3.94%. ^{1}H NMR: δ 1.54 (s, 15H, Cp*), 2.33 (s, 6H, 2x Me), 3.78 (s, 3H, NMe), 6.41 (d, 1H, J 2, H^5), 6.78 (d, 1H, J 2, H^4), 6.82 (s, 1H, H^{10}), 7.14 (s, 2H, H^8, H^{12}), 7.79 (s, 1H, HC=N). ^{13}C NMR: δ 9.21 (C_5Me_5), 21.49 (2x Me), 34.87 (NMe) 86.25 (C_5Me_5), 112.85 (C^3), 120.56 (C^8, C^{12}), 127.36 (C^{10}), 131.51 (C^4), 138.33 (C^9, C^{11}), 145.105 (C^2), 152.54 (C^7), 155.92 (C^6), 157.09 (C^1). MS (FAB): *m/z* 574 $[M]^+$, 539 $[M\text{-}Cl]^+$. ν(C=N) 1610 cm^{-1}.

[IrCl{C_4H_2S-2-C(H)=N(3,5-$Me_2C_6H_3$)-$_\kappa$C,N}(η-C_5Me_5)] (3.49a)

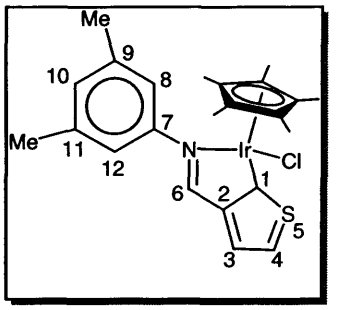

This was prepared from NaOAc (18 mg, 0.22 mmol), $[IrCl_2Cp^*]_2$ (70 mg, 0.09 mmol), and pyrrole imine (L_9) (38 mg, 0.18 mmol); after stirring for 30 hours, (**3.49a**) was isolated as an brown precipitate (90 mg, 88%). Calc. for $C_{23}H_{27}SNClIr$: C, 47.86, H, 4.71, N, 2.43. Found: C, 46.27, H, 4.31, N, 2.11%. ^{1}H NMR: δ 1.53 (s, 15H, Cp*), 2.35 (s, 6H, 2x Me), 6.89 (s, 1H, H^{10}), 7.17 (s, 2H, H^8, H^{12}), 7.34 (d, 1H, J 5, H^5), 7.62 (d, 1H, J 5, H^4), 8.14 (s, 1H, HC=N). MS (FAB): *m/z* 577 $[M]^+$, 542 $[M\text{-}Cl]^+$. IR: ν(C=N) 1601 cm^{-1}.

Reaction of acetyl pyridine with $[IrCl_2Cp^*]_2$

This was prepared from NaOAc (26 mg, 0.32 mmol), $[IrCl_2Cp^*]_2$ (100 mg, 0.13 mmol) and 2-acetyl pyridine ($\mathbf{L_{11}}$) (31 mg, 0.26 mmol); after stirring for 4 h, **the solution** was evaporated to dryness to give a red solid. The solid was then washed with hexane and diethylether. ES^+ and ^1H NMR spectrum showed several species, see **section 3.2.6** for discussion.

$[RhCl\{C_5H_4N\text{-}2\text{-}C(=O)CH_2\text{-}_\kappa C,N\}Cp^*]$ (3.51b)

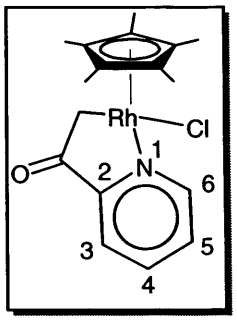

This was prepared from NaOAc (58.7 mg, 0.49 mmol), $[RhCl_2Cp^*]_2$ (150 mg, 0.24 mmol) and 2-acetyl pyridine ($\mathbf{L_{11}}$) (53 mg, 0.44 mmol); after stirring for 20 h, **(3.51b)** was isolated as a red solid. The solid was then washed with hexane and diethylether (150 mg, 78%). Calc. for $C_{17}H_{21}ClNORh$: C, 51.86, H, 5.38, N, 3.56. Found: C, 51.82, H, 5.21, N, 3.46%. ^1H NMR: δ 1.57 (s, 15H, Cp*), 2.84 (dd, 1H, *J* 7, 1, C*H*H`), 3.84 (dd, 1H, *J* 7, 1, C*H*H`), 7.49 (m, 1H, H^5), 7.65 (m, 1H, H^3), 7.89 (dt, 1H, *J* 7.5, 1.5, H^4), 8.65 (m, 1H, H^6). ^{13}C NMR: δ 8.82 (C_5Me_5), 45.33 (d, J_{RhC} 22, CH_2), 94.36 (d, J_{RhC} 7, C_5Me_5), 121.44, 127.44, 138.89, 151.49 (C^3, C^4, C^5, C^6), 159.15 (C^2), 197.64 (C=O). MS (FAB): *m/z* 393 $[M]^+$, 358 $[M\text{-}Cl]^+$.

Reaction of acetyl pyridine with $[RuCl_2(p\text{-cymene})]_2$

This was prepared from NaOAc (50 mg, 0.61 mmol), $[RuCl_2(p\text{-cymene})]_2$ (150 mg, 0.25 mmol) and 2-acetyl pyridine ($\mathbf{L_{11}}$) (59.3 mg, 0.49 mmol); after stirring for 4 h, the solution was evaporated to dryness to give a red solid. The solid was then washed with hexane and diethylether. ES^+ and ^1H NMR spectrum showed several species, see **section 3.2.6** for discussion.

Preparation of $[IrCl_2\{P(OPh)_3\}Cp^*]$ (3.52a)

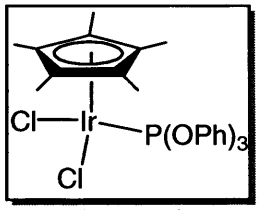

To a solution of $[IrCl_2Cp^*]_2$ (250 mg, 0. 32 mmol) in CH_2Cl_2 (25 ml), $P(OPh)_3$ (196 mg, 0.63 mmol) was added. The resulting mixture was stirred at room temperature for 5h. The resulting solution was evaporated to dryness to give a yellow precipitate **(3.52a)**, the solid then washed with hexane: (362 mg, 80%). ^1H NMR: δ 1.52 (d, 15H, *J* 3, Cp*), 7.11 (m, 3H, H_p (OPh)), 7.28 (m 12H, H_o, H_m (OPh)). ^{13}C NMR 8.92 (C_5Me_5), 95.30 (C_5Me_5), 121.47 (C_m, OPh), 125.05 (C_p, OPh), 129.61 (C_o, OPh), 151.55 (d, *J* 11, ^iC, OPh). $^{31}P\text{-}\{^1H\}$ NMR: 65.35.

Preparation of $[RhCl_2\{P(OPh)_3\}Cp^*]$ (3.52b)

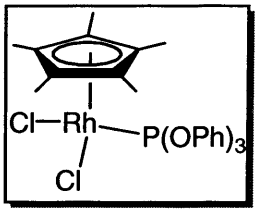

To a solution of $[RhCl_2Cp^*]_2$ (200 mg, 0. 32 mmol) in CH_2Cl_2 (25 ml), $P(OPh)_3$ (200 mg, 0.65 mmol) was added. The resulting mixture was stirred at

room temperature for 6h. The resulting solution was evaporated to dryness to give a brown precipitate (**3.52b**), the solid then washed with hexane: (290 mg, 73%). ^{1}H NMR: δ 1.60 (d, 15H, *J* 3, Cp*), 7.10 (m, 3H, H_p (OPh)), 7.30 (m 12H, H_o, H_m (OPh)). ^{31}P-{^{1}H} NMR: 103.56 (d, J_{RhP} 240 Hz).

Preparation of [$RuCl_2${P(OPh)$_3$}(*p*-cymene)] (3.52c)

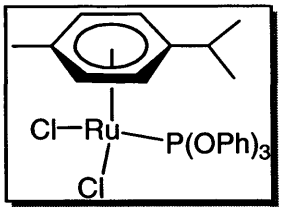

To a solution of [$RuCl_2$(*p*-cymene)]$_2$ (200 mg, 0. 33 mmol) in CH_2Cl_2 (25 ml), P(OPh)$_3$ (196 mg, 0.63 mmol) was added. The resulting mixture was stirring at room temperature overnight. The resulting solution was evaporated to dryness to give a brown precipitate (**3.52c**), the solid then washed with hexane: (300 mg, 74%).^{1}H NMR: δ. 1.10 (d, 6H, *J* 7, CH*MeMe*`), 1.78 (s, 3H, Cy-*Me*), 2.68 (sept, 1H, *J* 7, C*H*MeMe`), 5.03 (d, 2H, *J* 6, Cy), 5.35 (d, 2H, *J* 6, Cy), 7.10 (m, 3H, H_p (OPh)), 7.23 (m 12H, H_o, H_m (OPh)). ^{31}P-{^{1}H} NMR: 104.57.

[IrCl{C_5H_4N-2-C(=O)CH_2-$_K$*C*,*N*}Cp*] (3.53a)

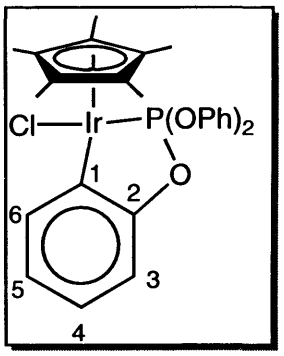

This was prepared from NaOAc (35 mg, 0.43 mmol) and (**3.52a**) (200 mg, 0.28 mmol); after stirring overnight, (**3.53a**) was isolated as an orange solid. The solid was then washed with hexane and diethylether (170 mg, 89%). Calc. for $C_{28}H_{29}ClO_3IrP$: C, 50.03 H, 4.35. Found: C, 50.14, H, 4.30%. ^{1}H NMR: δ 1.78 (s, 15H, Cp*), 6.87-7.43 (m, 14H, Ar-H). ^{31}P-{^{1}H} NMR: 109.63. MS (FAB): *m/z* 672 $[M]^+$, 637 $[M\text{-}Cl]^+$.

Bibliography

1 M. A. Bennett, T. Huang, T. W. Matheson, and A. K. Smith, *Inorg. Synth.*, 1982, **21**, 75.

2 C. White, A. Yates, P. M. Maitlis, and D. M. Heinekey, *Inorg. Synth.*, 1992, **29**, 228.

3 P. M. Maitlis, *Acc. Chem. Res.*, 1978, **11**, 301.

4 J. W. Kang, K. Moseley, and P. M. Maitlis, *J. Am. Chem. Soc.*, 1969, **91**, 5970.

5 M. A. Bennett, M. I. Bruce, and T. W. Matheson, in 'Comprehensive Organometallic Chemistry', ed. F. G. A. Stone and E. Abel, 1982.

6 R. P. Hughes, *Comprehensive Organometallic Chemistry. Pergamon Press*, 1982, **5**, 277.

7 A. J. Davenport, D. L. Davies, J. Fawcett, S. A. Garratt, and D. R. Russell, *J. Chem. Soc. Dalton Trans.*, 2000, 4432.

8 S. E. Durran, M. B. Smith, M. Z. Slawin, and J. W. Steed, *J. Chem. Soc. Dalton Trans.*, 2000, 2771.

9 D. F. Dersnah and M. C. Baird, *J. Organomet. Chem.*, 1977, **127**, C55.

10 Y. Yamamoto, K. Sugawara, and X.-H. Han, *J. Chem. Soc., Dalton Trans.*, 2002, 195.

11 G. Capper, L. C. Carter, D. L. Davies, J. Fawcett, and D. R. Russell, *J. Chem. Soc. Dalton Trans.*, 1996, 1399.

12 W. D. Jones and V. L. Kuykendall, *Inorg. Chem.*, 1991, **30**, 2615.

13 H. F. Luecke and R. G. Bergman, *J. Am. Chem. Soc.*, 1997, **119**, 11538.

14 R. Kramer, K. Polborn, H. Wanjek, I. Zahn, and W. Beck, *Chem. Ber.*, 1990, **123**, 767.

15 W. D. Jones and F. J. Feher, *J. Am. Chem. Soc.*, 1985, **107**, 620.

16 A. H. Janowicz and R. G. Bergman, *J. Am. Chem. Soc.*, 1983, **105**, 3929.

17 V. Ritleng, M. Pfeffer, and C. Sirlin, *Organometallics*, 2003, **22**, 347.

18 A. D. Ryabov, V. S. Sukharev, L. Alexandrova, R. Le Lagadec, and M. Pfeffer, *Inorg. Chem.*, 2001, **40**, 6529.

19 H. C. L. Abbenhuis, M. Pfeffer, J.-P. Sutter, A. de Cian, J. Fischer, H. L. Ji, and J. H. Nelson, *Organometallics*, 1993, **12**, 4464.

20 M. Pfeffer, J.-P. Sutter, and E. P. Urriolabeitia, *Inorg. Chim. Acta*, 1996, **249**, 63.

[21] R. K. Rath, S. G. Valavi, K. Geetha, and A. R. Chakravarty, *J. Organomet. Chem.*, 2000, **596**, 232.

[22] S. Fernandez, M. Pfeffer, V. Ritleng, and C. Sirlin, *Organometallics*, 1999, **18**, 2390.

[23] G. C. Martin and J. M. Boncella, *Organometallics*, 1989, **12**, 2968.

[24] J. Perez, V. Riera, A. Rodriguez, and D. Miguel, *Organometallics*, 2002, **21**, 5437.

[25] M. Pfeffer, J. P. Sutter, M. A. Rotteveel, A. De Cian, and J. Fischer, *Tetrahedron*, 1992, **48**, 2427.

[26] M. Pfeffer, *Pure Appl. Chem.*, 1992, **64**, 335.

[27] J. Vicente and J. A. Abad, *J. Chem. Soc. Dalton Trans.*, 1990, 1459.

[28] B. J. Wik, C. Romming, and M. Tilset, *J. Mol. Catal. A.*, 2002, **189**, 23.

[29] W. Bauer, M. Prem, K. Polborn, K. Sunkel, W. Steglich, and W. Beck, *Eur. J. Inorg. Chem.*, 1998, 485.

[30] S. E. Denmark, N. Nakajima, J. C. Nicaise, A. M. Faucher, and J. P. Edwards, *J. Org. Chem.*, 1995, **60**, 4884.

[31] X. Riera, A. Caubet, C. Lopez, V. Moreno, E. Freisinger, M. Willermann, and B. Lippert, *J. Organomet. Chem.*, 2001, **629**, 97.

[32] D. A. Tocher, R. O. Gould, T. A. Stephenson, M. A. Bennett, J. P. Ennett, T. W. Matheson, L. Sawyer, and V. K. Shah, *J. Chem. Soc. Dalton Trans.*, 1983, 1571.

[33] P. M. Boyer, C. P. Roy, J. M. Bielski, and J. S. Merola, *Inorg. Chim. Acta*, 1996, **245**, 7.

[34] J. W. Kang, K. Moseley, and P. M. Maitlis, *J. Am. Chem. Soc.*, 1969, **91**, 5970.

[35] A. D. Ryabov, *Chem. Rev.*, 1990, **90**, 403.

[36] D. M. Tellers, C. M. Yung, B. A. Arndtsen, D. R. Adamson, and R. G. Bergman, *J. Am. Chem. Soc.*, 2002, **124**, 1400.

[37] H. A. Zhong, J. A. Labinger, and J. E. Bercaw, *J. Am. Chem. Soc.*, 2002, **124**, 1378.

[38] M. Polleth and S. A. Macgregor, in 'unpublished results'.

[39] F. B. McCormick, D. D. Cox, and W. B. Gleason, *Organometallics*, 1993, **12**, 610.

[40] E. C. Constable, *Polyhedron*, 1984, **3**, 1037.

[41] D. W. Evans, G. R. Baker, and G. R. Newkome, *Coord. Chem. Rev.*, 1989, **93**, 155.

[42] H. Brunner, R. Oeschey, and B. Nuber, *Organometallics*, 1996, **15**, 3616.

[43] H. Brunner, T. Kollnberger, T. Burgemeister, and M. Zabel, *Polyhedron*, 2000, **19**, 1519.

[44] H. Brunner, R. Oeschey, and B. Nuber, *Inorg. Chem.*, 1995, **34**, 3349.

[45] T. J. Johnson, L. J. Alvey, M. Brady, C. L. Mayne, A. M. Arif, and J. A. Gladysz, *Chem. Eur. J.*, 1995, **1**, 294.

[46] G. Parshall, *Acc. Chem. Res.*, 1970, **3**, 139.

[47] R. D. Simpson, *Organometallics*, 1997, **16**, 1797.

[48] A. M. Tezeciak and J. J. Ziolkowski, *J. Organomet. Chem.*, 2000, **597**, 69.

[49] R. B. Bedford, S. Castillon, P. A. Chaloner, C. Claver, E. Fernandez, P. B. Hitchcock, and A. Ruiz, *Organometallics*, 1996, **15**, 3990.

[50] M. Laing, M. J. Nolte, E. Singleton, and E. van der Stok, *J. Organomet. Chem.*, 1978, **146**, 77.

[51] S. C. Thompson, C. White, and P. M. Maitlis, *J. Organomet. Chem.*, 1977, **136**, 87.

[52] M. I. Bruce, R. C. F. Gardner, and F. G. A. Stone, *J. Organomet. Chem.*, 1972, **40**, C39.

[53] K. G. Gaw, A. M. Z. Slawin, and M. B. Smith, *Organometallics*, 1999, **18**, 3255.

Chapter Four:

Reactivity Of Half-sandwich Cyclometallated Complexes

Chapter Four – Reactivity of Half-sandwich Cyclometallated Complexes

4.1 Introduction

Reactivity of cyclometallated complexes

The metal-carbon σ bond of cyclometallated complexes is reactive toward various nucleophilic reagents.[1] Most studies have involved insertion reactions of cyclopalladated complexes with carbon monoxide,[2, 3] alkenes[4, 5] and alkynes.[6, 7] Such insertion reactions are usually regiospecific and offer a potentially important methodology in organic synthesis, particularly in the synthesis of heterocyclic compounds. Reactivity of cyclometallated complexes of other metals is much less studied though Ru and Rh complexes are intermediates in catalytic reactions involving alkene insertion **(see Ch. 1)**.[4]

4.1.1 Insertion of alkynes

An example of the insertion of one or two alkynes into the Pd-C bond is shown in **Scheme 4.1**.[8]

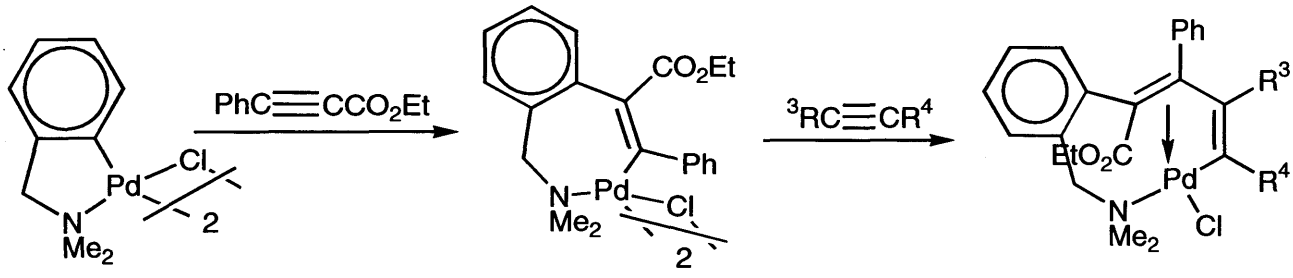

(1.11) **(4.1)** **(4.2)**

(Scheme 4.1)

The product formed **(4.1)** or **(4.2)** depends on the nature of the alkynes used. With electron deficient alkynes *e.g.* PhC≡CCO$_2$Et, monoinsertion products **(4.1)**, which are formed regiospecifically can be isolated. However, with more electron rich alkynes *e.g.* PhC≡CPh only diinsertion product **(4.2)** is observed even if only one equivalent of alkyne per Pd atom is used. Complexes **(4.1)** can insert a second alkyne to form complexes containing two different alkynes **(4.2)**. The second insertion of an unsymmetrical alkyne is not regiospecific and led to mixtures of two isomers.

In some cases organic heterocycles can be formed. Refluxing of the iodide (**4.3**) for 3h led to a significant amount of metallic Pd together with a deep red solution, from which two heterocyclic products (**4.4**) and (**4.5**) could be isolated as shown in **Scheme 4.2**.[9]

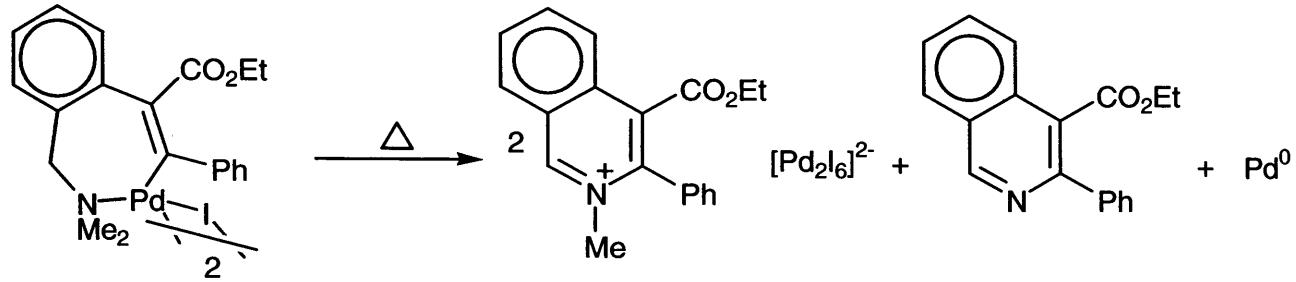

(4.3) **(4.4)** **(4.5)**

(Scheme 4.2)

There are not many examples of insertion of alkynes into cyclometallated Ru-C bonds reported in the literature. In 1997, Pfeffer *et al.*[10] reported an example of insertion of an alkyne into the Ru-C bond of a cycloruthenated complex (**Scheme 4.3**). The iodide-bridged cycloruthenated complex (**4.6**) reacted easily to form (**4.7**), however, no reaction occurred with the corresponding chloride-bridged complex.

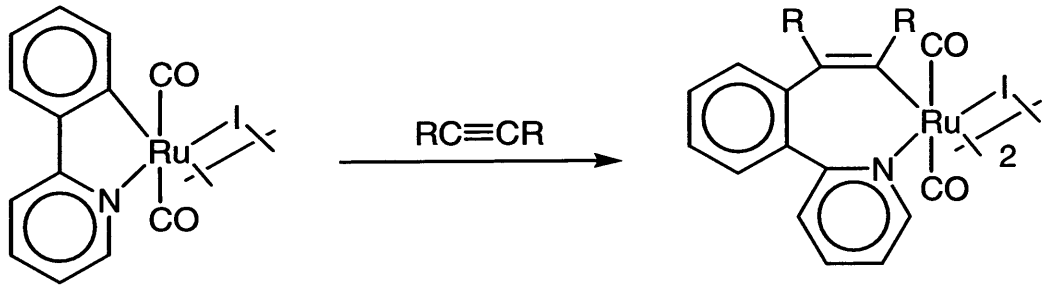

(4.6) **(4.7, R= CO_2Me)**

(Scheme 4.3)

Pfeffer *et al.*[11] also described the first examples of insertion of alkynes into the Ru-C bond of a half-sandwich cycloruthenated complex (**4.8**) as shown in **Scheme 4.4**.

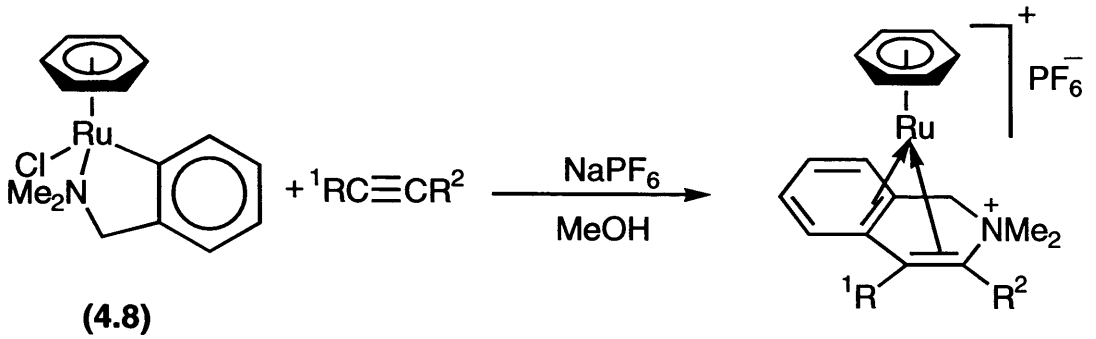

(4.8)

(4.9a, $R^1 = R^2 =$ Ph)
(4.9b, $R^1 = R^2 =$ Et)
(4.9c, $R^1 =$ Me, $R^2 =$ Ph)
(4.9c`, $R^1 =$ Ph, $R^2 =$ Me)
(4.9d, $R^1 = {}^t$Bu, $R^2 =$ Me)

(Scheme 4.4)

Reaction of **(4.8)** with 1 equivalent of alkyne and $NaPF_6$ in MeOH at room temperature afforded the isoquinolinium complexes **(4.9a-d)** in good yield. In the reaction with MeC≡CPh, the substituents have similar steric bulk, consequently, two regioisomer **(4.9c)** and **(4.9c`)** were formed. The more bulky alkyne **(d)** gave a slower reaction and a lower yield but only formed one regioisomer **(4.9d)**, with the larger substituent (^{t}Bu) being found on the carbon atom adjacent to the aryl group. Electron poor alkynes *e.g.* $EtO_2CC{\equiv}CPh$ reacted but the isoquinolinium complexes could not be isolated in pure form. No reactions occurred in the absence of $NaPF_6$, hence, they suggested that loss of chloride must occur to give a more active cationic complex before reaction with the alkyne. Similar observations have been seen for related palladacycle reactions.[9, 12, 13] Pfeffer *et al.* suggested two possible mechanisms for the alkyne insertion with **(4.8)**. Either, insertion into the Ru-C bond or into the Ru-N bond to afford intermediate **(A)** or **(B)** respectively **(Fig. 4.1)**, followed by the reductive elimination and C-N bond formation resulting in **(4.9)**. The postulated intermediates **(A)** or **(B)** could not be isolated suggesting that reductive elimination to form isoquinolinium derivatives occurs very readily. On the basis of formation of **(4.7)**, Pfeffer concluded that insertion occurs into the M-C bond *ie. via* **(A)**.

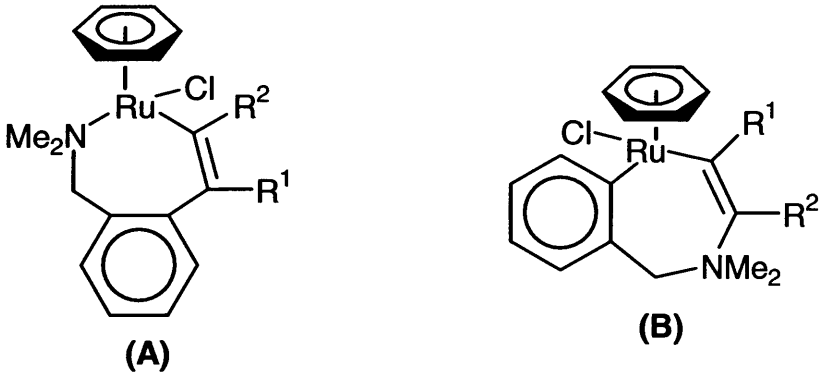

(A) **(B)**

(Fig. 4.1)

The isoquinolinium complexes (**4.9**) are formally Ru(0), however, they are surprisingly stable. Attempts to liberate the heterocyclic unit from the isoquinolinium complexes by reaction with excess Lewis base (e.g. NCMe, pyridine, CO) or heating or uv-irradiation all failed. Liberation of the heterocycle only occurred when complexes (**4.9**) reacted with $CuBr_2$ (**Scheme 4.5**).

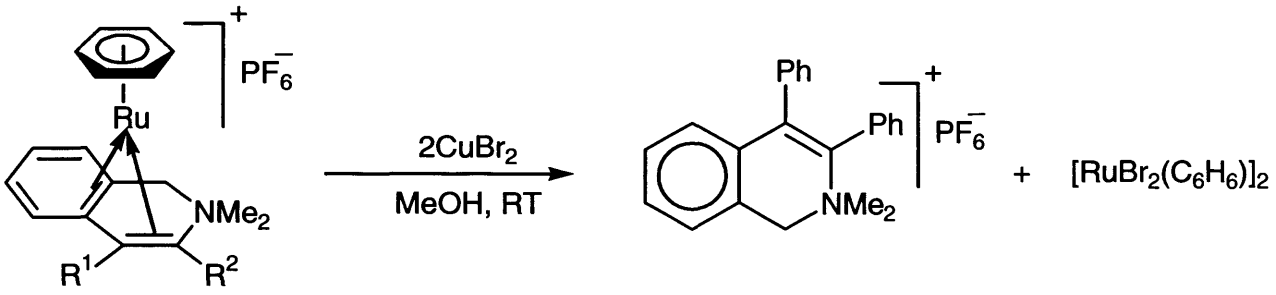

(**4.9a**) (**4.10**)

(**Scheme 4.5**)

4.1.2 *Insertion of alkenes*

The Heck reaction involves insertion of an alkene into a metal-carbon σ-bond followed by β-hydrogen elimination, a few examples were described in **Ch. 1**. Ritleng *et al.*[4] have described a similar process for cycloruthenated complex (**4.8**) which reacts with ethene at low pressure (1.5 atm) to afford the Heck product (**4.12**) (yield 81%) and an organometallic compound (**4.11**) (yield 19%) as shown in **Scheme 4.6**.

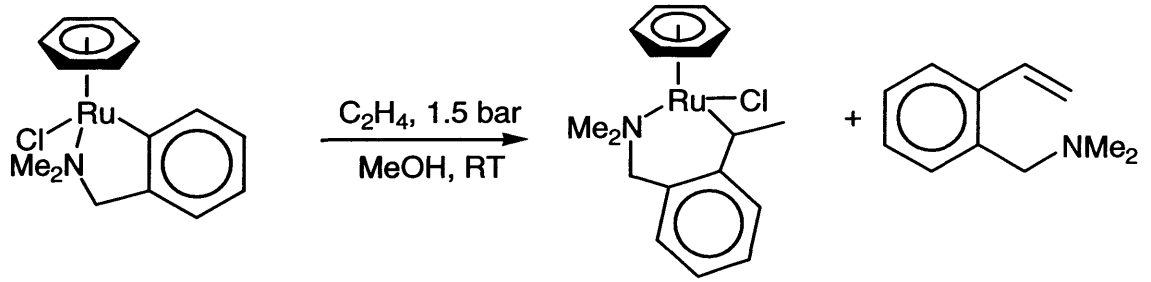

(**4.8**) (**4.11**) (**4.12**)

(**Scheme 4.6**)

The ratio of (**4.11**) to (**4.12**) changed when the chloride ligand of the starting material was removed. Thus, cationic (**4.13**) led to a much higher yield (87%) of the organometallic (**4.14**)

after reaction with ethene (**Scheme 4.7**). Only one diastereomer was observed by ^{1}H NMR in both cases, indicating that these reactions occur with a high level of diastereoselectivity.

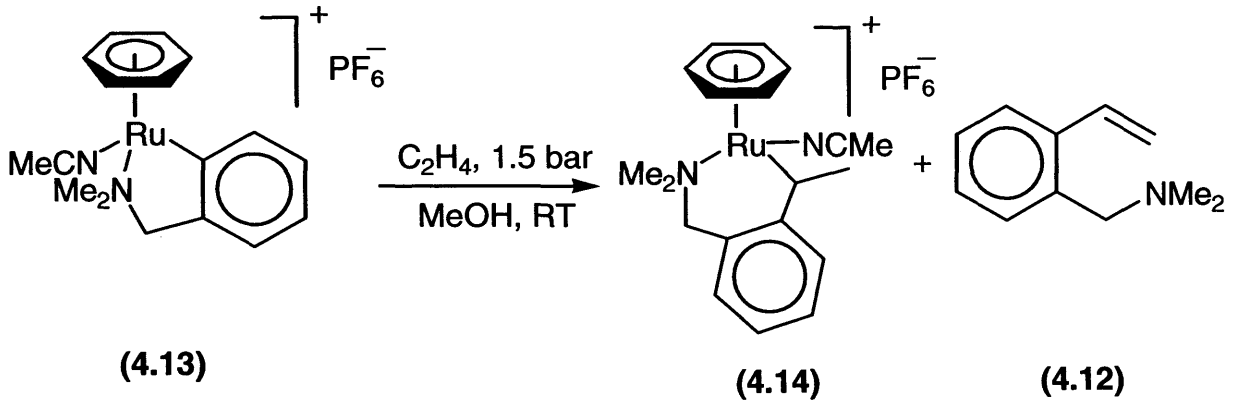

(4.13) **(4.14)** **(4.12)**

(Scheme 4.7)

The formation of (**4.11**) was rationalised according to the reaction path depicted in **Scheme 4.8**. Insertion of ethene into the Ru-C bond in (**4.8**) forms (**4.15**) which undergoes β-H elimination to the alkene hydride complex (**4.16**). This can either decompose to give the alkene (**4.12**) as in the Heck reaction or reinsertion can occur to give (**4.11**) which is an isomer of (**4.15**).

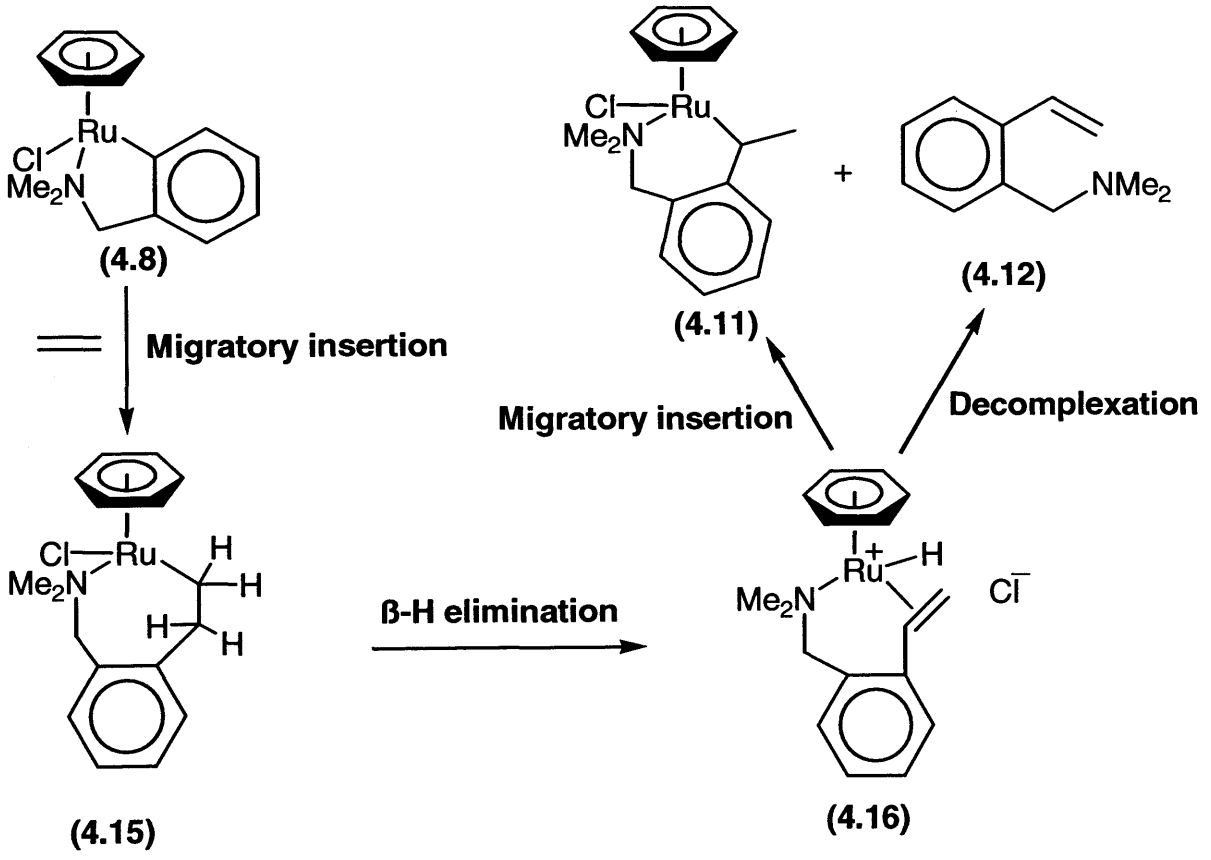

(Scheme 4.8)

4.1.4 Insertion of CO

Insertion of CO into M-C bonds is one of the most thoroughly studied processes in homogeneous catalysis.[14, 15] Cyclopalladated complex **(4.17)** reacts with CO by insertion into the M-C bond to form **(4.18)** in good yield **(Scheme 4.9)**.[16]

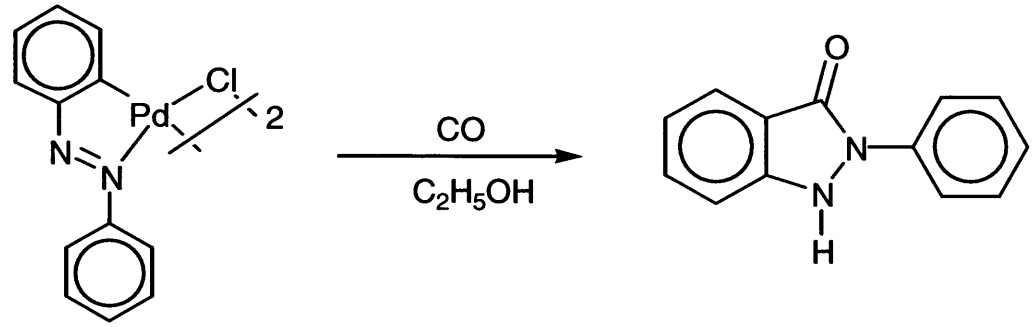

(4.17) **(4.18)**

(Scheme 4.9)

To our knowledge the only reported reaction of a cyclometallated half-sandwich complex with CO is that shown in **Scheme 4.10**. In this case coordination of CO occurs but there is no insertion into the M-C bond.[17]

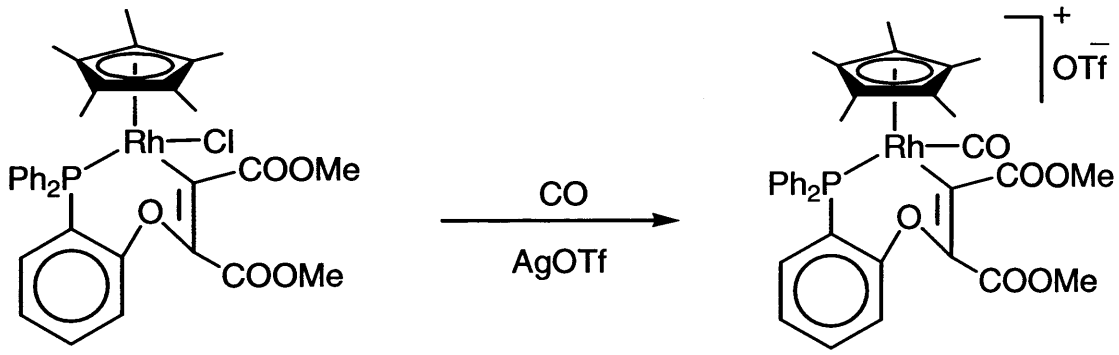

(4.19) **(4.20)**

(Scheme 4.10)

4.2 Results and Discussion

As mentioned in the previous section, there have been very few studies of the reactivity of cyclometallated half-sandwich complexes with unsaturated molecules. We have therefore investigated reactions of such complexes with CO, ethene and alkynes. During our initial studies we found that the chloride complexes reacted slowly if at all and gave low yields (see later). Therefore we set out to make cationic complexes containing a labile NCMe ligand. As mentioned above cationic complexes are much more reactive than the corresponding neutral ones.[11]

4.2.1 Reaction of Half-sandwich Cyclometallated Complexes with Acetonitrile

4.2.1a Imines

The replacement of chloride by acetonitrile was achieved by stirring the complexes **(3.30a, b)**, **(3.31a, c)** and **(3.32a)** overnight in acetonitrile in the presence of KPF_6. Pure complexes **(4.21a, b)**, **(4.22a, c)** and **(4.23a)** were isolated by filtration of the crude reaction mixture through celite, to remove the KCl and excess KPF_6, and were characterised by ^1H and $^{13}C\text{-}\{^1H\}$ NMR spectroscopy, FAB mass spectrometry, IR spectroscopy, elemental analysis and in some cases X-ray crystallography.

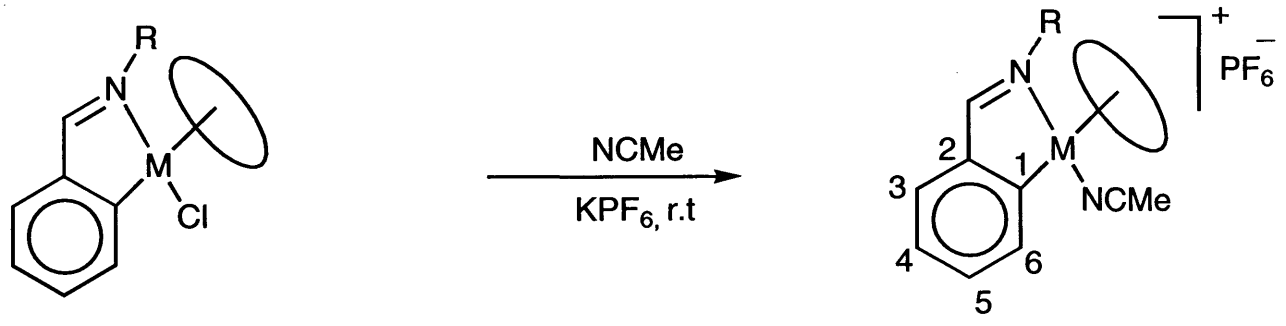

(3.30, R = C_2H_4OMe)
(3.31, R = C_3H_6OMe)
(3.32, R = Ph)

(a = Cp*Ir)
(b = Cp*Rh)

(4.21)
(4.22)
(4.23)

(Scheme 4.11)

The ^1H NMR spectra of **(4.21a)** and **(4.22a)** show a 1:1 ratio of the Cp* and the imine ligand with singlets at *ca.* δ 1.72 and *ca* δ 3.34 due to Cp* and OMe respectively. In both complexes, the imine proton is observed at δ 8.40, a similar shift to those, δ 8.37 and 8.31, found in **(3.30a)** and **(3.31a)** respectively, confirming that the imine is still coordinated to the metal. A singlet integrating to 3 protons, at δ 2.36 and 2.37 for **(4.21a)** and **(4.22a)** respectively, is assigned to NCMe, *ca.* 0.36 ppm downfield compared to free NCMe as expected for coordination of NCMe. The CH_2O protons of **(4.21a)** give rise to two multiplets, at δ 3.66 and 3.84, the inequivalence,

suggesting that epimerisation at the metal is slow on the NMR timescale as found for the chloride **(3.30a)**. The OCH_2 signals of **(4.22a)** are overlapping but epimerisation is still likely to be slow on the NMR timescale. At room temperature, addition of 1 equivalent of NCMe to the NMR sample of **(4.21a)** gave rise to an extra sharp singlet for free NCMe with no significant change in the signal for the coordinated NCMe. This also indicates that NCMe exchange and fluxionality is slow on the NMR timescale.

The ^{13}C-{^1H} NMR spectra of **(4.21a)** and **(4.22a)**, show similar signals to those in the starting chloride complexes, with extra peaks at δ 3.71 and 3.65, **(4.21a)** and **(4.22a)** respectively, assigned to the methyl in NCMe and the quaternary carbon at *ca.* δ 119. The FAB mass spectra of **(4.21a)** and **(4.22a)** showed ions at *m/z* 490 and 502 respectively due to $[M\text{-}NCMe]^+$. The IR spectra of both show the imine stretch at 1606 cm^{-1}, a similar value to those 1596 and 1604 cm^{-1} in **(3.30a)** and **(3.31a)** respectively, suggesting that the imine is still coordinated.

The ^1H NMR spectrum of **(4.23a)** shows coordinated NCMe as a sharp singlet integrating to 3H at δ 2.49, 0.49 ppm downfield from free NCMe suggesting that dissociation is slow on the NMR timescale. The imine proton is observed at δ 8.42, similar to that δ 8.31 in **(3.32a)** confirming the coordination of the imine. The ^{13}C-{^1H} NMR spectrum shows NCMe carbons at δ 3.72 and 120.06 with the metallated carbon being observed at δ 163.67. The presence of NCMe was also confirmed by FAB mass spectrometry, a molecular ion is observed at *m/z* 549 and a fragment ion at *m/z* 508 due to $[M\text{-}NCMe]^+$. The υ(N=C) absorption is observed at 1583 cm^{-1}, the same as in the starting material. Crystallisation from CH_2Cl_2/hexane gave X-ray quality crystals of **(4.23a)**, the structure is discussed later.

The ^1H and ^{13}C-{^1H} NMR spectra of the Cp* Rh complexes **(4.21b)** and **(4.22b)** are very similar to the Cp*Ir ones and show the expected signals. Thus, in both complexes the NCMe protons are observed as a sharp singlet at δ *ca.* 2.22, 0.22 ppm downfield from free NCMe. In both complexes, the NCH_2 protons give rise to two multiplets, at δ 4.01 and 4.16 **(4.21b)** and at δ 3.92 and 4.10 **(4.22b)**; the inequivalence is consistent with epimerisation being slow on the NMR timescale. The imine proton is observed as a doublet at 8.24 (J_{RhH} 4 Hz) for both complexes, confirming that the imine is still coordinated. The ^{13}C-{^1H} NMR spectra show signals for the NCMe at δ 3.5 and δ 123.65 [quaternary carbon not observed in **(4.21b)**]. The FAB mass spectra of **(4.21b)** and **(4.22b)** show ions at *m/z* 400 and 414 respectively corresponding to $[M\text{-}NCMe]^+$. The IR spectra show υ(N=C) at 1614 cm^{-1} for both complexes.

Recrystallisation from dichloromethane/hexane gave X-ray quality crystals of **(4.23a)** and **(4.21b)**. The crystal structures of these complexes are shown in **Fig. 4.2**, with selected bond distances and angles in **Table 4.1**.

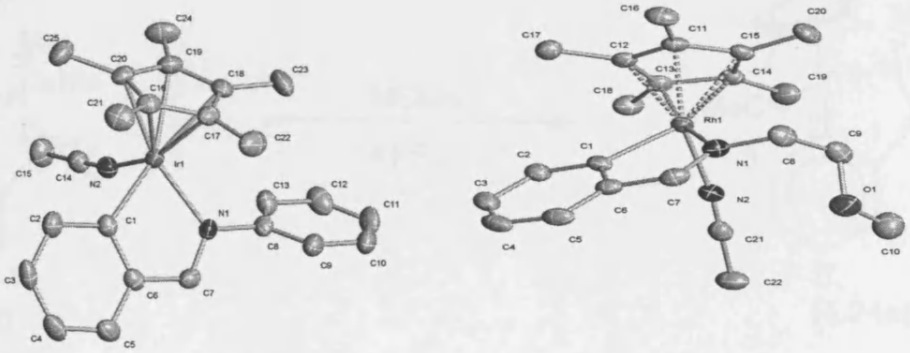

(4.23a) **(4.21b)**

Fig. 4.2 Molecular structures of the cations of **(4.23a)** and **(4.21b)**

Table 4.1 Selected bond distances [Å] and bond angles [°] for **(4.23a)** and **(4.21b)**

Bond distances/[Å]	**(4.23a)**	**(4.21b)**		**(4.23a)**	**(4.21b)**
M(1)-C(1)	2.048(3)	2.032(3)	M-C(Cp*)	2.157(3)	2.146(3)
M(1)-N(1)	2.095(2)	2.090(3)	M-C(Cp*)	2.161(3)	2.172(3)
M(1)-N(2)	2.044(3)	2.069(3)	M-C(Cp*)	2.240(3)	2.243(3)
N(1)-C(7)	1.287(4)	1.277(4)	M-C(Cp*)	2.258(3)	2.273(3)
M-C(Cp*)	2.138(3)	2.141(3)			
bond angles/[°]					
C(1)- M (1)-N(2)	87.57(11)	83.80(11)	N(1)- M(1)-N(2)	92.29(10)	89.74(10)
C(1)- M(1)-N(1)	77.52(11)	78.54(11)	N(2)-C(14)-C(15)	178.2(4)	

The complexes adopt the expected pseudo-octahedral structure with the Cp* ligand occupying three facial coordination sites of the metal and confirms the coordination of NCMe. As found in the other cyclometallated complexes, both complexes show two long [2.240(3) to 2.273(3) Å] and three short [2.138(3) to 2.172(3) Å] M-C bonds to the Cp*, with the longer ones approximately *trans* to the metallated carbon. The M-N(imine) bond lengths [2.095(2) and 2.090(3) Å] in **(4.23a)** and **(4.21b)**, are statistically unchanged from those [2.105(4) and 2.089(2) Å] in the precursors, as is also the case for the M-C(1) bond lengths. The M-N(imine) bond lengths are longer than the M-N(NCMe) [2.044(3) and 2.069(3) Å] consistent with bonds to an sp^2 rather than an sp nitrogen. As found in **(3.32a)**, the phenyl substituent on nitrogen in **(4.23a)** is rotated out of the plane of the cyclometallated fragment (dihedral angle C(7)-N(1)-C(8)-C(9) = 122.8°) and is approximately parallel to the Cp*.

4.2.1b Amines and oxazolines

Having found that the chloride in the imine complexes was replaced easily by NCMe to form cationic species, similar reactions of the amine **(3.36a)** and oxazoline **(3.37a)** were investigated **(Scheme 4.12)**.

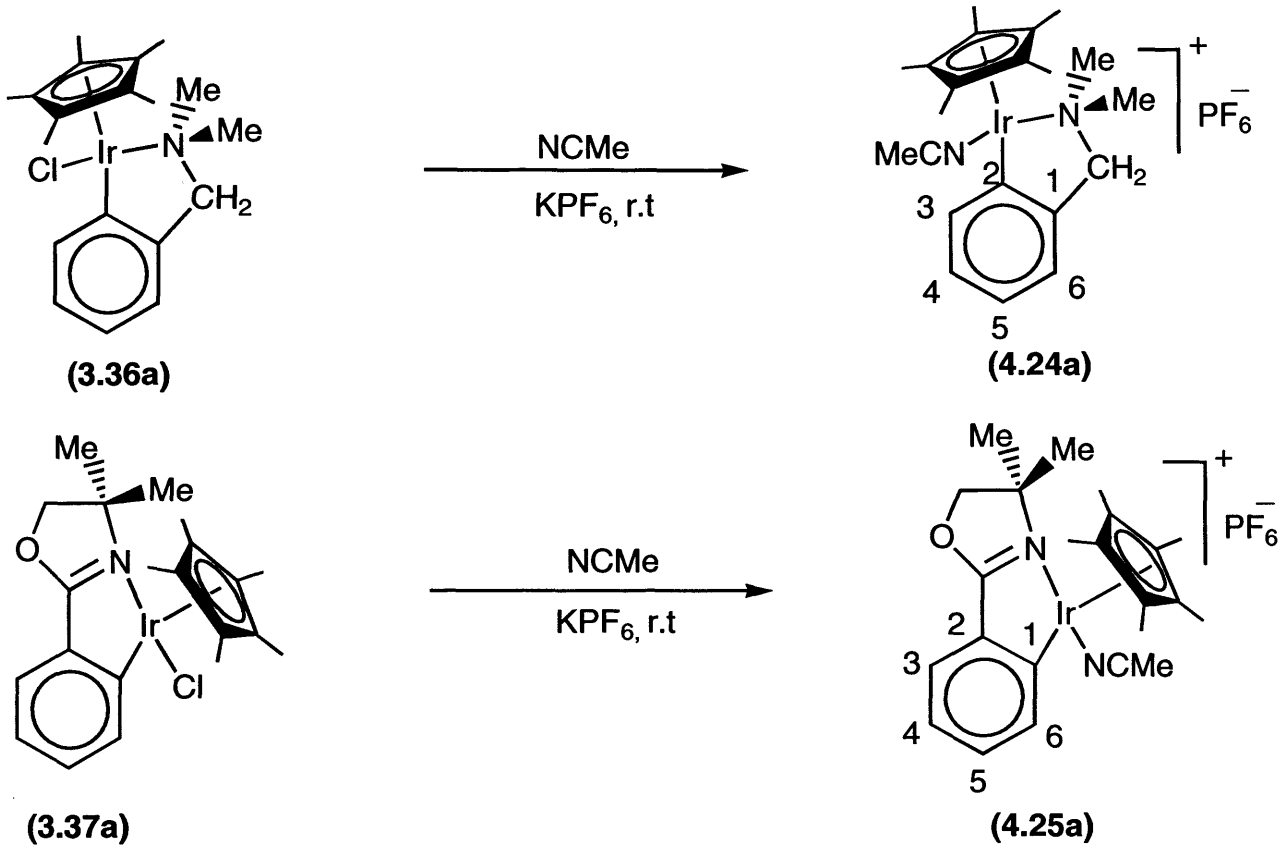

(Scheme 4.12)

The ^{1}H NMR spectrum of **(4.24a)** shows NCMe protons at δ 2.56, 0.56 ppm downfield from free NCMe, confirming the coordination of NCMe. A broad singlet is observed at δ 2.91 due to two methyls in NMe_2 group and a sharp singlet at δ 3.80 for CH_2 group. The ^{13}C-{^{1}H} NMR spectrum also showed the NMe_2 group as a broad signal at δ 53.66. These observations suggest that loss of the NCMe occurs at a rate comparable to the NMR timescale at room temperature and epimerisation **(Scheme 4.13)** is faster than for the comparable chloride complex **(3.37a)** and Ru amine cationic complex **(3.17)**. Cooling this sample to 263 K caused the broad singlet for the NMe_2 protons to resolve into two sharp singlets at δ 2.78 and 3.10, however, the CH_2 does not resolve into two doublets (at δ 3.75 and 3.85) until the temperature is lowered to 233 K, as expected for the smaller chemical shift difference between the CH_2 protons than between the two methyls in the NMe_2 group. The resolved signals at low temperature indicate that interconversion is slow on the NMR timescale. At 263 K, the NCMe singlet, which was observed at δ 2.56 at room temperature resolved into two singlets at δ 2.56 (coordinated NCMe)

and 1.99 (free NCMe) (20:1 ratio), consistent with exchange of free and coordinated NCMe being slow at this temperature. The mechanism of epimerisation involves loss of NCMe and then a "windscreen-wiper" motion of the cyclometallated ligand, via a 16-electron species (**A**) in which the C,N ligand is perpendicular to the Cp* ligand (**Scheme 4.13**). Similar processes have been proposed previously for half-sandwich complexes.[18]

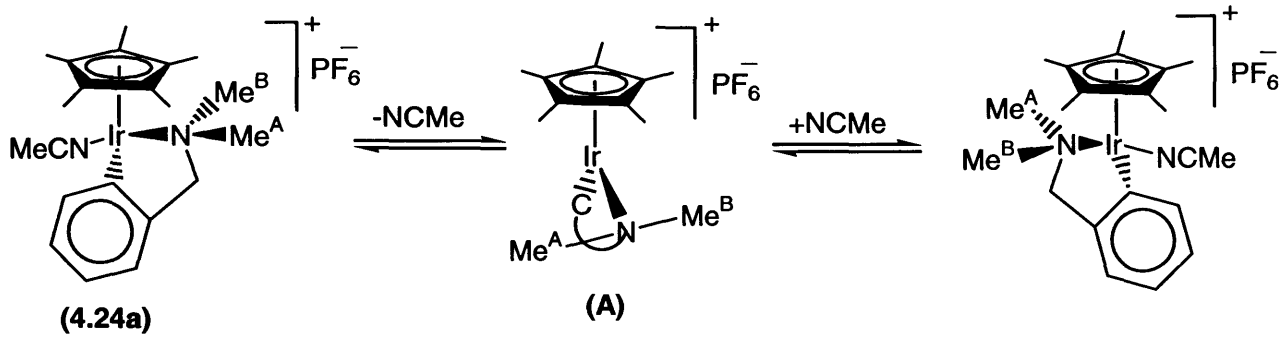

(4.24a) **(A)**

(Scheme 4.13)

(Empimerisation of (4.24a))

The ^{13}C-{^{1}H} NMR spectrum shows the NCMe carbons at δ 3.87 and 120.37 with the metallated carbon being observed at δ 149.54. The FAB mass spectrum shows a fragment ion at *m/z* 460 due to $[M\text{-}NCMe\text{-}H_2]^+$.

The ^{13}C-{^{1}H} NMR spectrum of (**4.25a**) shows NCMe carbons at δ 3.45 and 119.64, and the oxazoline methyl substituents are observed at δ 27.00 and 28.27. However, the oxazoline methyls in ^{1}H NMR spectrum are equivalent, giving a broad singlet at δ 1.47 as are the CH_2 protons, giving rise to a sharp singlet at δ 4.58. The equivalence of the CMe_2 and of the CH_2 protons, suggests that interconversion is fast on the NMR timescale as found for (**4.24a**). The ^{1}H NMR spectrum also showed the presence of coordinated NCMe as a broad singlet at δ 2.42, 0.42 ppm downfield from free NCMe. At 273 K the broad singlet for the CMe_2 protons had resolved into two sharp singlets at δ 1.44 and 1.54, and the broad singlet due to NCMe resolved into two singlets at δ 2.42 (coordinated NCMe) and 2.02 (free NCMe) (10:1 ratio), the latter observation consistent with exchange of free and coordinated NCMe being slow. Further cooling to 233 K led to resolution of the CH_2 signal to two mutually coupled doublets at δ 4.40 and 4.70. The resolved signals at low temperature indicate that epimerisation is slow on the NMR timescale. The fluxionality occurs by a similar mechanism to (**4.24a**) described above (**Scheme 4.13**).

The FAB mass spectrum shows a fragment ion at *m/z* 502 due to $[M\text{-}NCMe]^+$. The υ(N=C) is observed at 1622 cm^{-1}, the same as found in the starting chloride complex. The structure of

(4.25a) has been determined by X-ray crystallography **(Fig. 4.3)** and selected bond distances and angles are listed in **Table 4.2**

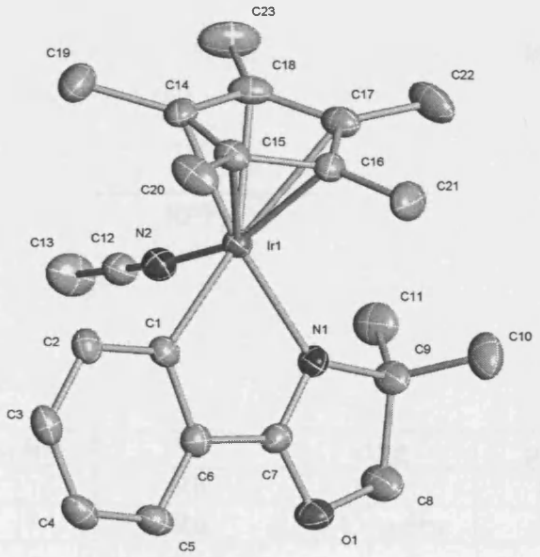

Fig. 4.3 Molecular structure of the cation of **(4.25a)**

Table 4.2 Selected bond distances [Å] and bond angles [°] for **(4.25a)**

Bond distances/[Å]		**Bond angles/ [°]**	
Ir(1)-C(1)	2.068(3)	C(1)-Ir(1)-N(2)	88.62(12)
Ir (1)-N(2)	2.050(3)	C(1)-Ir(1)-N(1)	77.08(12)
Ir (1)-N(1)	2.118(3)	N(1)-Ir(1)-N(2)	82.85(11)
N(1)-C(7)	1.272(4)	N(2)-C(12)-C(13)	179.1(4)

The complex adopts the expected pseudo-octahedral structure and confirms the coordination of NCMe. The chelate bite angle C(1)-Ir(1)-N(1) [77.08(12)°] is similar to that angle in imine complex **(4.23a)** [77.52(11)°]. The Ir-N(1) bond length [2.118(3) Å] and the Ir-C(1) bond length [2.068(3) Å] are slightly longer than those [2.095(2) and 2.048(3) Å respectively] in **(4.23a)**. The M-N(1) bond length is longer than the M-N(2) consistent with a bond to an sp^2 rather than an sp nitrogen.

4.2.1c pyrrole

Having established that the C,N cyclometallated complexes underwent easy substitution of chloride by MeCN, the corresponding reactions of the N,N pyrrolyl imine were investigated. Reaction of **(3.41b)** and **(3.41c)** with KPF_6 in acetonitrile for 24 h **(Scheme 4.15)** gave products

(4.26b) and **(4.26c)** respectively in good yield which were characterised by ^{1}H and ^{13}C-{^{1}H} NMR spectroscopy, FAB mass spectrometry, IR, elemental analysis and X-ray crystallography for **(4.26b)**.

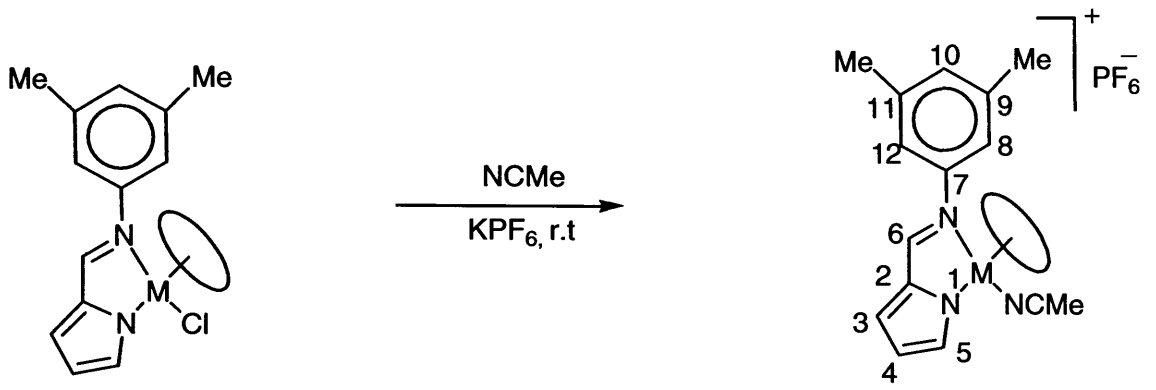

starting chloride	M	ring	products
(3.41b)	Rh	Cp*	(4.26b)
(3.41c)	Ru	p-Cymene	(4.26c)

(Scheme 4.15)

The ^{1}H NMR spectra of **(4.26b)** and **(4.26c)** show a 1:1 ratio of the Cp* or *p*-cymene and the pyrrole ligand with additional singlets (3H) at δ 2.29 and 2.33 respectively due to coordinated NCMe. In **(4.26c)**, the isopropyl group gives rise to two doublets at δ 1.05 and 1.09 and a septet at δ 2.56 with four multiplets for the inequivalent aromatic protons of *p*-cymene ring, consistent with the chiral metal centre and demonstrates that the rate of epimerisation is slow on the NMR timescale. The lack of suitable substituents on **(4.26b)** prevents conclusions about the rate of epimerisation in this case.

The ^{13}C-{^{1}H} NMR spectra of **(4.26b)** and **(4.26c)** are similar to the chloride complexes **(3.41b)** and **(3.41c)** respectively with extra peaks being observed at δ 3.38 and 122.93 for **(4.26b)** and 3.72 and 124.34 **(4.26c)** assigned to coordinated NCMe. The FAB mass spectra of **(4.26b)** and **(4.26c)** show ions with maxima at *m/z* 435 and 433 respectively corresponding to $[M\text{-}NCMe]^{+}$. In both complexes, the imine stretch is observed at *ca.* 1590 cm^{-1}, the same as in the chloride precursors. For **(4.26b)** coordination of NCMe was also confirmed by X-ray diffraction. The structure of the cation is shown in **Fig. 4.4**, with selected bond distances and angles in **Table 4.3**.

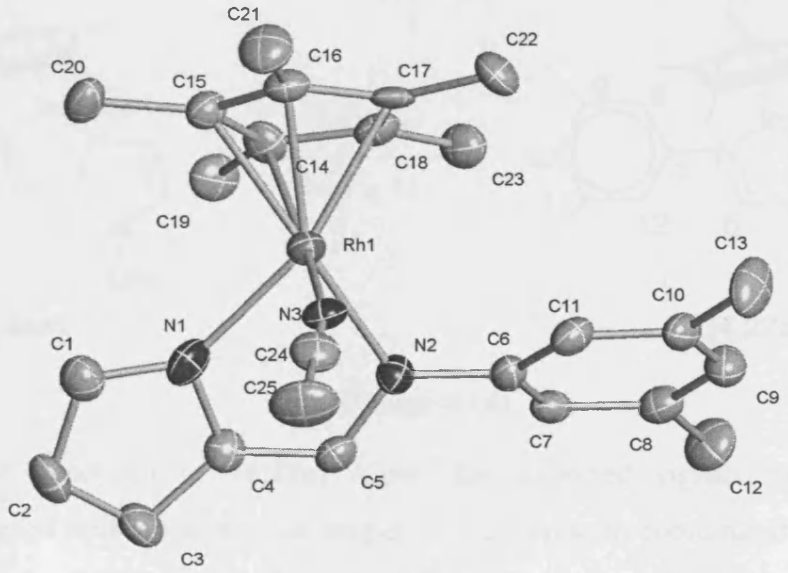

Fig. 4.4 Molecular structure of the cation of **(4.26b)**

Table 4.3 Selected bond distances [Å] and bond angles [°] for **(4.26b)**

Bond distances/[Å]		**Bond angles/ [°]**	
Rh(1)-N(1)	2.081(5)	N(1)-Rh(1)-N(2)	77.01(17)
Rh (1)-N(2)	2.113(4)	N(1)-Rh(1)-N(3)	85.61(17)
Rh (1)-N(3)	2.086(4)	N(2)-Rh(1)-N(3)	89.30(16)
N(1)-C(4)	1.368(7)		

The complex adopts the expected pseudo-octahedral structure, and confirms the coordination of NCMe. The Rh-N(1) bond [2.081(5) Å] and Rh-N(3) bond [2.086(4) Å] are statistically the same length and are shorter than the Rh-N(2) bond [2.113(4) Å]. The Rh-N(1) and Rh-N(2) bond lengths are the same as those in **(3.41a)** [2.069(3) and 2.123(3) Å respectively]. As found in **(3.41a)**, the phenyl substituent on nitrogen is also rotated out of the plane of the cyclometallated fragment and is approximately parallel to the Cp*.

The reactivity of the pyrrole C,N-cyclometallated complex **(3.48a)** with NCMe was also investigated giving **(4.27a)** in good yield **(Scheme 4.16)**.

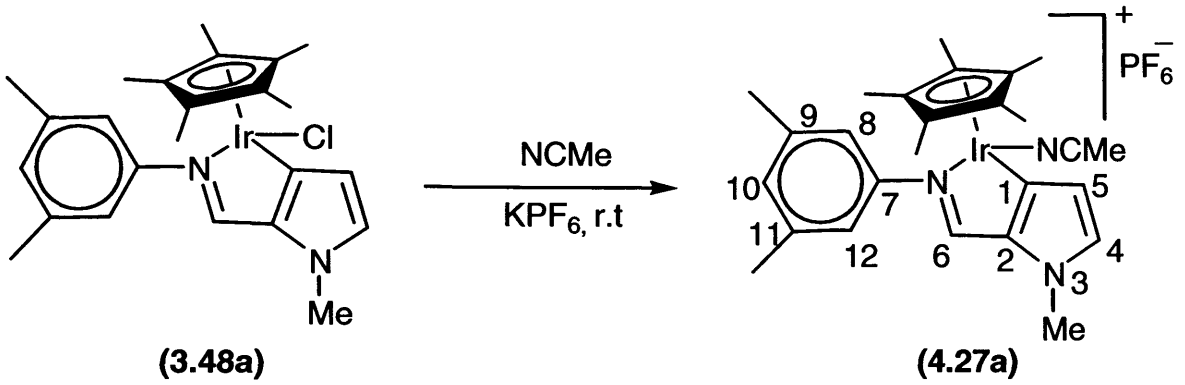

(3.48a) **(4.27a)**

(Scheme 4.16)

The ^{1}H NMR spectrum of **(4.27a)** shows the expected signals for Cp* and the cyclometallated ligand with an additional singlet at δ 2.50 due to coordinated NCMe, 0.5 ppm downfield from the free NCMe. In the ^{13}C-{^{1}H} NMR spectrum, NCMe carbons are observed at δ 3.93 and 119.40, confirming the coordination of NCMe. The FAB mass spectrum of **(4.27a)** shows an ion with at *m/z* 539 corresponding to $[M\text{-}NCMe]^{+}$.

There are two conclusions from the results of formation of cationic acetonitrile complexes described above: **a)** Exchange of chloride by acetonitrile to form cationic cyclometallated complexes occurs easily in good yields with all the C,N and N,N ligands studied. **b)** At room temperature epimerisation of the amine and oxazoline cyclometallated cationic complexes **(4.24a)** and **(4.25a)** is faster than in imines **(4.21-4.23)** and as expected faster than the chlorides. **c)** epimerisation of the Ir amine **(4.24a)** is faster than the corresponding Ru amine **(4.17)**.[19]

4.2.2 Reactions of cationic cyclometallated complexes with CO

Insertion of CO into an M-C bond is well known (and some examples were described in **Section 4.1.4**). Therefore, the reaction of some of the cationic complexes with CO was investigated. Complexes **(4.21a)**, **(4.22a)** and **(4.22b)** each react with CO in $CDCl_3$ at room temperature. As soon as the ^{1}H NMR spectrum is run, all the starting material has disappeared and signals for other Cp*M cyclometallated complexes are seen along with a peak due to free NCMe. The similarity of the spectra to the NCMe complexes suggests the NCMe has been replaced by CO but that insertion into the M-C bond has not occurred. The solution was evaporated to dryness to give pure solids which were characterised by ^{1}H and ^{13}C-{^{1}H} NMR spectroscopy, FAB mass spectrometry, IR, elemental analysis, and X-ray crystallography for **(4.28a)** **(Scheme 4.17)**.

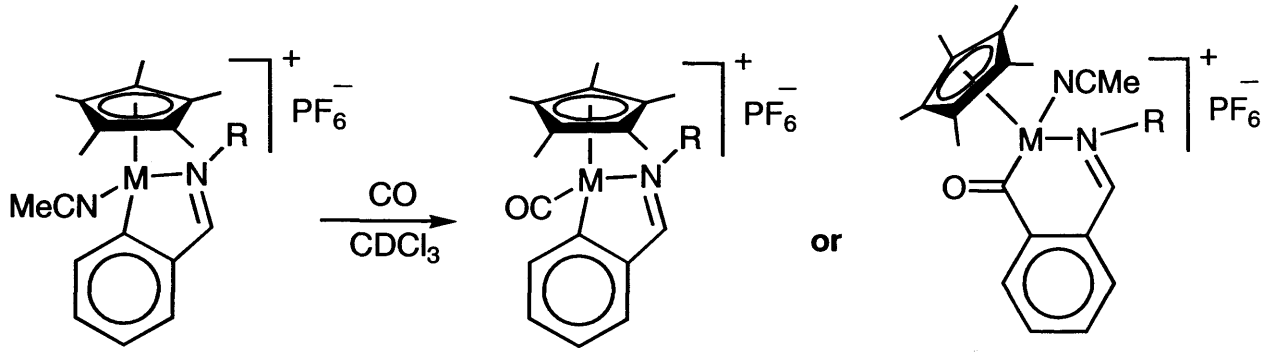

(4.21, R = C_2H_4OMe) **(a = Cp*Ir)** **(4.28a)** **(4.29a)**
(4.22, R = C_3H_6OMe) **(b = Cp*Rh)** **(4.30a)** **(4.31a)**
(4.30b) **(4.31b)**

(Scheme 4.17)

The ^1H NMR spectrum of **(4.28a)** shows no signal assigned to NCMe, suggesting the displacement of NCMe, (if CO insertion occurred NCMe would probably recoordinate to give an 18-electron complex as shown in **(4.29a)**). The IR spectrum showed an intense peak at *ca.* 2033 cm^{-1} assigned to a terminal CO, this is similar to that of 2068 cm^{-1} for related cationic Cp*Rh complex **(4.20)** **(Scheme 4.10)**.[17] If insertion had occurred, υ(CO) would be expected at around 1700 cm^{-1}. The NCH_2 protons give rise to two multiplets at δ 3.90 and 4.17; the inequivalence is consistent with the chiral centre at the metal, and demonstrates that there is no epimerisation at the metal or at least it is slow on the NMR timescale. In the $^{13}C-\{^1H\}$ NMR spectrum, the metallated carbon is observed at δ 151, the presence of CO can be observed at δ 165. The FAB mass spectrum showed ions at *m/z* 518 due to $[M]^+$, confirming the presence of CO, and fragment ions at *m/z* 490 due to $[M-CO]^+$.

The ^1H NMR spectra of **(4.30a)** and **(4.30b)** are very similar in both complexes and showed no signal assigned to NCMe as found in **(4.28a)**. The IR spectra show υ(C≡O) at 2032 and 2060 cm^{-1} for **(4.30a)** and **(4.30b)** respectively, ruling out **(4.31a)** and **(4.31b)** as possible products. The NCH_2 protons give rise to two multiplets at δ 3.85 and 4.08 **(4.30a)**; the inequivalence consistent with the chiral centre at the metal, and demonstrates that no epimerisation at the metal occurred or at least is slow on the NMR timescale. The NCH_2 signals of **(4.30b)** are overlapping but epimerisation is still likely to be slow on the NMR timescale. The $^{13}C-\{^1H\}$ NMR spectra show the metallated carbon as a singlet at δ 151 for **(4.30a)** and as a doublet at δ 169.65 (J_{RhC} 28 Hz) for **(4.30b)**, and the terminal CO as a singlet at δ 164.78 **(4.30a)** and a doublet at δ 185.40 (J_{RhC} 74 Hz) **(4.30b)**.

The FAB mass spectra of **(4.30a)** and **(4.30b)** showed ions at *m/z* 532 and 442 due to $[M]^+$, confirming the presence of CO, and fragment ions at *m/z* 504 and 414 $[M\text{-}CO]^+$ respectively. The structure of **(4.28a)** has been determined by X-ray crystallography and is shown in **Fig. 4.5** with selected bond distances and angles in **Table 4.4**.

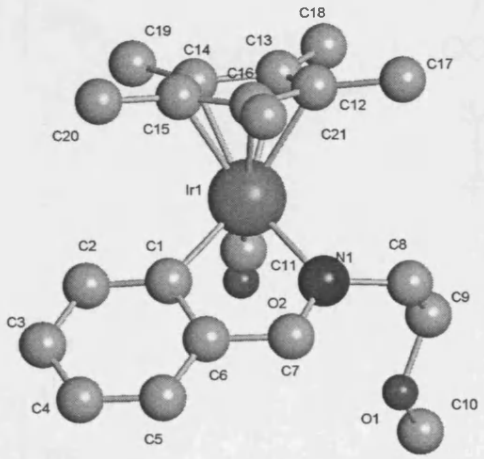

Fig. 4.5 Molecular structure of **(4.28a)**

Table 4.4 Selected bond distances [Å] and bond angles [°] for **(4.28a)**

Bond distances/[Å]			
Ir(1)-C(1)	2.069(4)	Ir-C(Cp*)	2.201(5)
Ir (1)-N(1)	2.081(4)	Ir-C(Cp*)	2.202(5)
Ir (1)-C(11)	1.871(5)	Ir-C(Cp*)	2.223(5)
C(6)-C(7)	1.424(6)	Ir-C(Cp*)	2.261(5)
C(11)-O(2)	1.138(6)	Ir-C(Cp*)	2.265(5)
Bond angles / [°]			
N(1)-Ir(1)-C(11)	93.01(17)	C(1)-Ir(1)-N(1)	77.48(16)
C(1)-Ir(1)-C(11)	89.00(18)	O(2)-C(11)-Ir(1)	179.1(4)

The complex adopts the expected pseudo-octahedral structure, and confirms the coordination of CO to the metal centre. The Ir-C(1) bond length [2.069(4) Å] and the C(1)-Ir(1)-N(1) bond angle [77.48(16)°] are similar to those of the corresponding neutral chloride complex **(3.30a)** [2.078(3) Å and 77.84(13)° respectively], however the Ir-N(1) bond is slightly longer than that [2.081(4) Å versus 2.036(3) Å]. The Ir-C(1) bond length is longer than the Ir-C(11) bond length [1.871(5) Å] consistent with a bond to an sp^2 rather than sp carbon.

Having found that CO did not insert into the M-C bond of the cyclometallated imine complexes at room temperature, the reaction of CO with the cyclometallated amine and

oxazoline complexes were examined. The reaction of **(4.24a)** and **(4.25a)** with CO in $CDCl_3$ led to formation of new Cp*Ir complexes and a peak due to free NCMe as determined by the ^1H NMR spectroscopy, suggesting the formation of the terminal carbonyl complexes **(4.32a)** and **(4.33a)** **(Scheme 4.18)**.

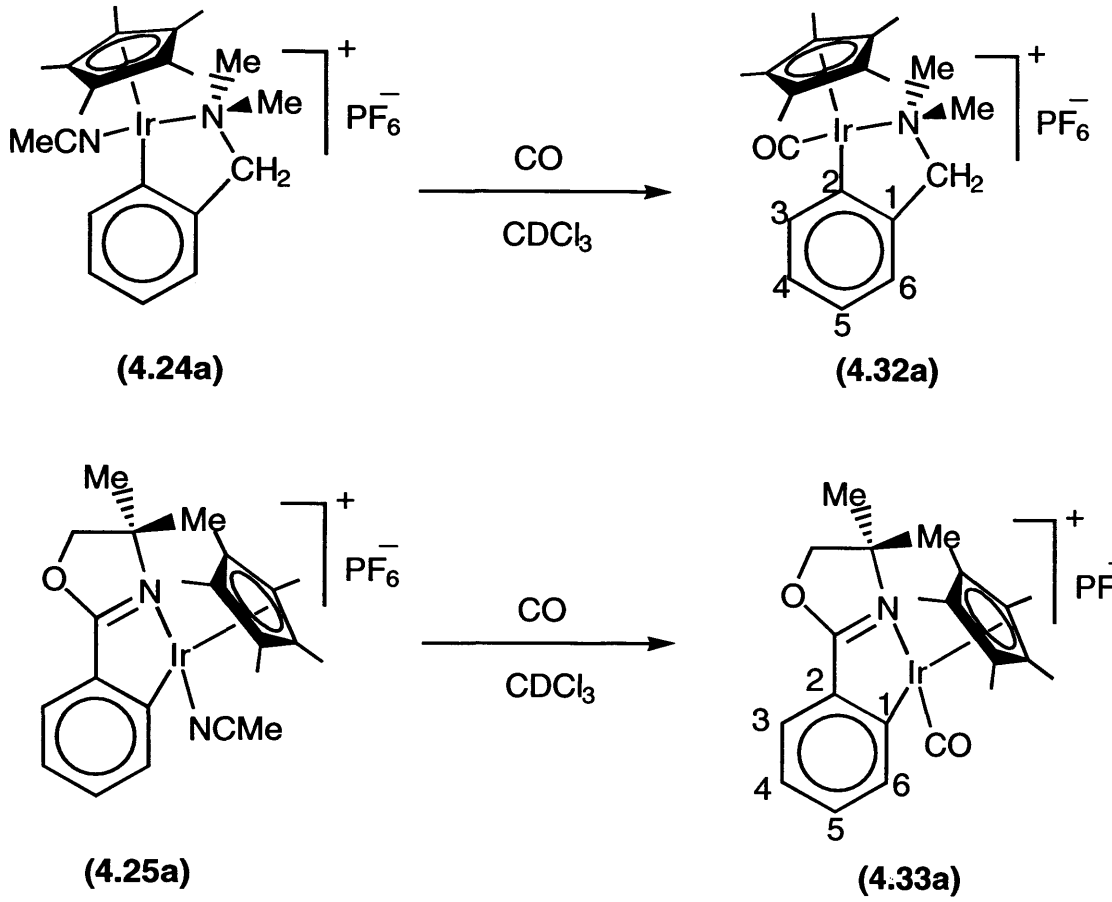

(Scheme 4.18)

The ^1H NMR spectrum of **(4.32a)** shows signals due to the Cp* and the cyclometallated ligand, the NMe_2 group gives two sharp singlets (δ 3.13 and 3.21) and the CH_2 group occurs as two mutually coupled doublets (δ 3.82 and 4.05). Thus **(4.32a)**, unlike **(4.24a)**, is not fluxional on the NMR timescale, loss of CO is presumably more difficult than loss of NCMe from **(4.24a)**. The $^{13}C\text{-}\{^1H\}$ NMR spectrum also shows two singlets for the NMe_2 carbons at δ 57.45 and 61.07, and the CO carbon is observed at δ 170.04, consistent with a terminal carbonyl. The presence of CO is also confirmed by FAB mass spectrometry, a molecular ion being seen at *m/z* 490. The υ(CO) is observed at 2034 cm^{-1} (*c.f.* 2033-2060 cm^{-1} in the **4.28a, 4.30a** and **4.30b**) as expected for a terminal carbonyl.

The ^1H NMR spectrum of **(4.33a)** shows the CMe_2 group as two singlets at δ 1.30 and 1.50, the OCH_2 protons are also inequivalent giving two mutually coupled doublets at δ 4.20 and 4.22.

These observations are consistent with a chiral metal centre and that no epimerisation occurs on the NMR timescale, in contrast to epimerisation in **(4.25a)** which occurs at a rate comparable to the NMR timescale. In the ^{13}C-{^{1}H} NMR spectrum, the methyls of the CMe_2 group are also inequivalent at δ 27.05 and 27.85, and the terminal CO is observed at δ 165.52. The FAB mass spectrum shows a molecular ion at *m/z* 530 and a fragment ion at *m/z* 502 $[M\text{-}CO]^+$. The υ(CO) absorption is observed at 2042 cm^{-1} as expected for a terminal CO.

There are two conclusions from the reactions with CO described above: **a)** At room temperature, CO readily displaces NCMe but it does not insert into the M-C bond. **b)** Dissociation of CO is more difficult than loss of NCMe, therefore, the carbonyl complexes are not fluxional on the NMR timescale if at all.

4.2.3 Reactions of cationic complexes with ethene

As mentioned in **section 4.1.3**, Ritleng[4] described the insertion of ethene at (1.5 atm) into the Ru-C bond of **(4.8)** to afford **(4.11)** and **(4.12)** **(Scheme 4.6)**. Therefore, the reaction of acetonitrile complexes **(4.21a)** and **(4.22a)** with ethene (1 atm) in dichloromethane was investigated. Simple substitution of NCMe by ethene would give **(4.34a)** or **(4.36a)** if insertion occurred, recoordination of NCMe is likely as found previously for **(4.14)**[4] to form **(4.35a)** or **(4.37a)** **(Scheme 4.19)**. The products were characterised by ^{1}H and ^{13}C-{^{1}H} NMR spectroscopy, FAB mass spectrometry, IR, elemental analysis and X-ray crystallography for **(4.34a)**.

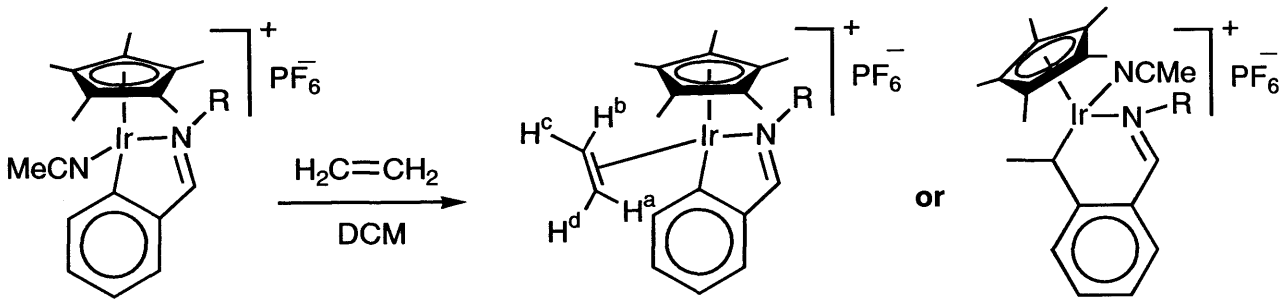

(4.21a) **(4.22a)**

(4.34a, R = $(CH_2)_2OMe$) **(4.36a, R = $(CH_2)_3OMe$)**

(4.35a) **(4.37a)**

(Scheme 4.19)

In both products, NCMe was not observed in ^{1}H NMR spectrum of the product, suggesting the products are **(4.34a)** and **(4.36a)** respectively. The ^{1}H NMR spectra of **(4.34a)** and **(4.36a)** show a 1:1 ratio of the Cp* and the imine ligand with singlets at δ 1.71 and 1.62 due to Cp* and at *ca.* δ 3.30 assigned to OMe. The NCH_2 protons give rise to two overlapping multiplets at δ

4.15 (**4.34a**) and 4.00 (**4.36a**) consistent with the chiral centre at the metal, and demonstrates that epimerisation at the metal is slow on the NMR timescale. In both complexes, two triplets each integrating to 2H, at δ 3.03 and 3.10 (**4.34a**) and at δ 2.90 and 2.98 (**4.36a**), are assigned to coordinated ethene. Complexes (**4.35a**) and (**4.37a**) would be expected to show a 3H doublet and 1H quartet due to CHMe group if insertion had occurred. The observation of two triplets for the ethene demonstrates that the ethene is rotating fast, and therefore, that $\mathbf{H^a}$ and $\mathbf{H^c}$ are equivalent as are $\mathbf{H^b}$ and $\mathbf{H^d}$ respectively. In the ^{13}C-{^1H} NMR spectra, the ethene carbons are equivalent, as expected for fast rotation, giving one signal at δ 52.47 or 51.80 for (**4.34a**) and (**4.36a**) respectively, similar finding at δ 41.0 and 37.6 for $[(\eta^2\text{-}C_2H_4)(\eta^6\text{-}Me_6C_6)RuH(Ph_2PCH_2CH_2OMe)]$.[20]

The FAB mass spectra of (**4.34a**) and (**4.36a**) show molecular ions with maxima at *m/z* 518 and 530 respectively and fragment ions at *m/z* 490 and 502 respectively due to $[M\text{-}C_2H_4]^+$. Crystals of (**4.34a**) suitable for X-ray determination were obtained from dichloromethane/hexane. The structure confirms the coordination of ethene to the metal centre, and is shown in **Fig. (4.6)**, with selected bond distances and angles listed in **Table 4.5**.

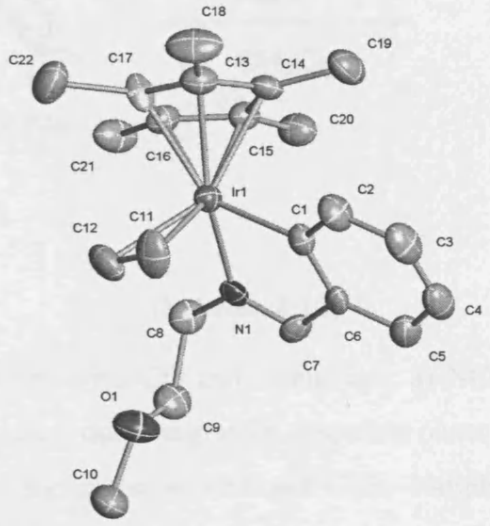

Fig. 4.6 Molecular structure of cation of (**4.34a**)

Table 4.5 Selected bond distances [Å] and bond angles [°] for (**4.34a**)

Bond distances/[Å]			
Ir(1)-C(1)	2.061(11)	Ir-C(Cp*)	2.201(5)
Ir (1)-N(1)	2.064(9)	Ir-C(Cp*)	2.202(5)
Ir (1)-C(11)	2.170(12)	Ir-C(Cp*)	2.223(5)
Ir (1)-C(12)	2.171(13)	Ir-C(Cp*)	2.261(5)
C(11)-C(12)	1.380(2)	Ir-C(Cp*)	2.265(5)
Bond angles/ [°]			
C(1)-Ir(1)-N(1)	77.60(4)	C(1)-Ir(1)-C(11)	79.60(4)
N(1)-Ir(1)-C(12)	83.60(5)		

The complex adopts a typical three legged piano stool structure with a pseudo-octahedral geometry about the metal. The Ir-N(1) and Ir-C(1) bond lengths [2.064(9) and 2.061(11) Å respectively] and the C(1)-Ir(1)-N(1) bond angle [77.60(4)°] are the same as those of the corresponding neutral chloride complex **(3.30a)** [2.036(3), 2.078(3) Å and 77.84(13)°, respectively]. This indicates that the geometry of the Ir(imine) Cp* fragment is relatively unperturbed by substitution of chloride by CH_2CH_2. The Ir-C(1) bond length is shorter than the Ir-C(ethene) bond lengths [2.170(12) and 2.171(13) Å].

Having found that imine cationic cyclometallated complexes react easily with ethene, the reaction of N,N pyrrole cationic complex **(4.26b)** with ethene was examined. In this case, no reaction occurred, and the ^1H NMR spectrum showed only the starting material.

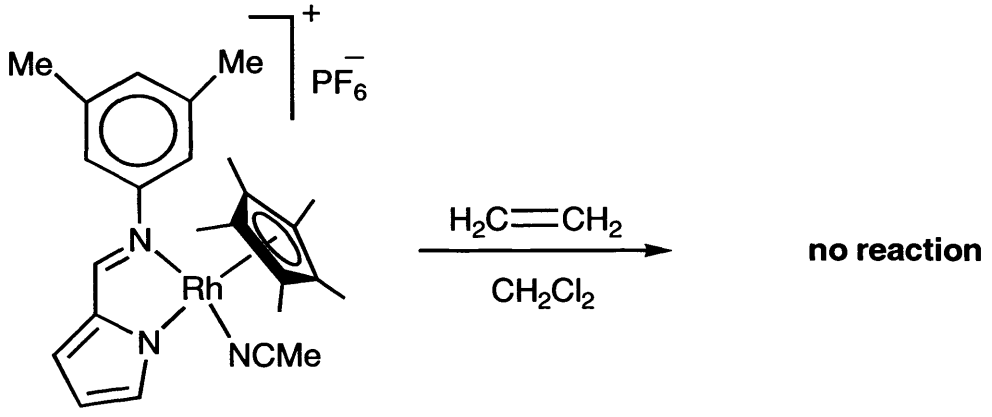

(4.26b)

(Scheme 4.20)

The conclusions from reactions with CO and ethene are: **a)** NCMe is easily substituted by CO or C_2H_4, however, in no cases does migratory insertion occur under the mild conditions examined. **b)** Epimerisation at the metal in CO and C_2H_4 complexes is slow on the NMR timescale, consistent with CO and C_2H_4 being stronger ligands than NCMe.

4.2.4 Reactions of half-sandwich cyclometallated complexes with alkynes

As mentioned previously, **(Section 4.1),** Pfeffer showed that arene ruthenium complex **(4.8)** will react with disubstituted alkynes to give isoquinolinium complexes. We have carried out a more substantial study of the reactions of half-sandwich cyclometallated complexes with alkynes varying the cyclometallated ligand, the M(ring) fragment and the alkyne, and the results are described below.

4.2.4a Reactions with PhC≡CPh

Reaction of the iridium oxazoline complex **(3.37a)** with PhC≡CPh was attempted first **(Scheme 4.21)**. In NCMe at room temperature, **(3.37a)** reacts slowly with PhC≡CPh in the presence of KPF_6. The reaction was monitored by ES mass spectrometry, a peak at *m/z* 502 [M-Cl] of starting material declines in intensity while a peak at m/z 679 [M-Cl+PhC≡CPh] increases. After 72 hours there was still evidence of starting material present and the reaction appeared to have stopped. This may be because the reaction proceeds by dissociation of chloride and after this there is a competition between PhC≡CPh and NCMe for the vacant site. As the reaction approaches completion the concentration of PhC≡CPh drops hence NCMe competes more effectively. To force the reaction to completion the crude material was evaporated and redissolved in CH_2Cl_2. After 24 hours stirring the reaction had gone to completion. At this stage the ^1H NMR spectrum showed all the starting material had disappeared and signals for another Cp*Ir complex were seen. The complex was characterised by ^1H and ^{13}C-{^1H} NMR spectroscopy, FAB mass spectrometry, IR, elemental analysis and X-ray crystallography.

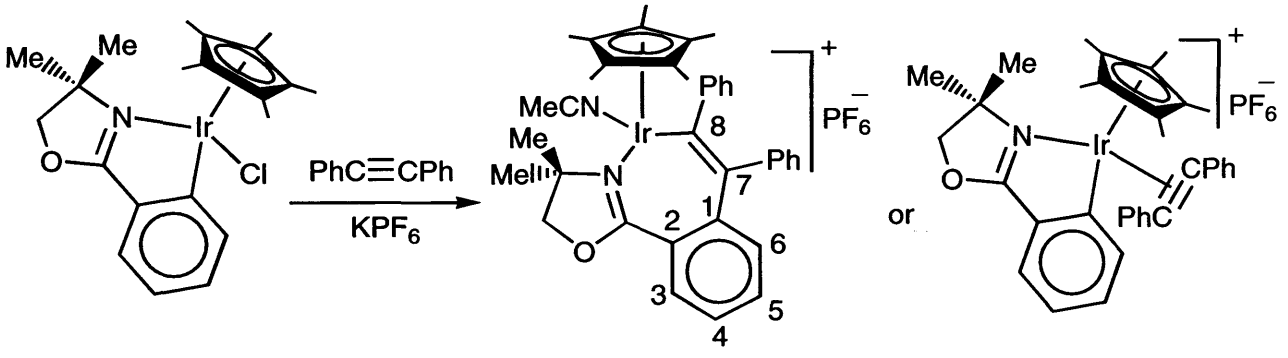

(3.37a) **(4.38a)** **(4.39a)**

(Scheme 4.21)

The ^1H NMR spectrum of the product shows a 1:1:1 ratio of the Cp*, the oxazoline ligand and PhC≡CPh. A singlet integrating to 3H at δ 2.00 is assigned to NCMe protons. This is very close to free NCMe, however, a peak of the same intensity is still observed if the sample is dried under vacuum for several hours. This is therefore assigned to coordinated NCMe, suggesting the product is the monoinsertion product **(4.38a)** since the simple substitution product **(4.39a)** does not contain NCMe. The upfield shift of 0.42 ppm of the NCMe signal compared with the NCMe complex **(4.25a)** is proposed to be due to a ring-current effect from the adjacent phenyl substituent of the alkyne (see X-ray structure of **4.38c** below). The Cp* signal is seen at δ 1.31, an upfield shift of 0.48 ppm compared to the NCMe complex **(4.25a)**. This may also be due to an aromatic ring-current but the structure suggests it may be from the original cyclometallated

phenyl rather than the alkyne substituents. Similar shifts have been observed for benzene bis(oxazoline) complexes, which have a similar 7-membered ring.[18] The CMe_2 group gives rise to two singlets at δ 1.31 and 1.37, the CH_2 protons are also inequivalent giving two mutually coupled doublets at δ 4.27 and 4.58. The inequivalence of the CH_2 protons and the methyls of the CMe_2 group is consistent with the chiral centre at the metal, and shows that epimerisation at the metal is slow on the NMR timescale.

The ^{13}C-{^1H} NMR spectrum shows the expected carbons for the monoinsertion product (**4.38a**). Thus, the NCMe carbons are observed at δ 2.35 and 124.80. Carbons (C^7) and (C^8) are inequivalent confirming insertion of the alkyne, the two carbons should be equivalent by rotation in (**4.39a**). (C^1) is observed at *ca.* δ 146, about 33 ppm upfield compared with the NCMe complex (**4.25a**). A large shift is consistent with insertion of alkyne into the M-C bond not the M-N bond, as found by Pfeffer.[11] The FAB mass spectrum of (**4.38a**) showed an ion at *m/z* 679 due to $[M\text{-}NCMe]^+$, confirming the presence of PhC≡CPh.

Ruthenium oxazoline complex (**4.38c**) was obtained from the reaction of cationic complex (**3.40c**) with PhC≡CPh in CH_2Cl_2 after 24 h stirring (**Scheme 4.22**). The ^1H NMR spectrum of the crude product showed more than one Ru(*p*-cymene) complex, therefore, the product was purified by filtering through silica. This gave one product (**4.38c**) which was characterised by ^1H and ^{13}C-{^1H} NMR spectroscopy, FAB mass spectrometry, IR spectroscopy, elemental analysis and X-ray crystallography.

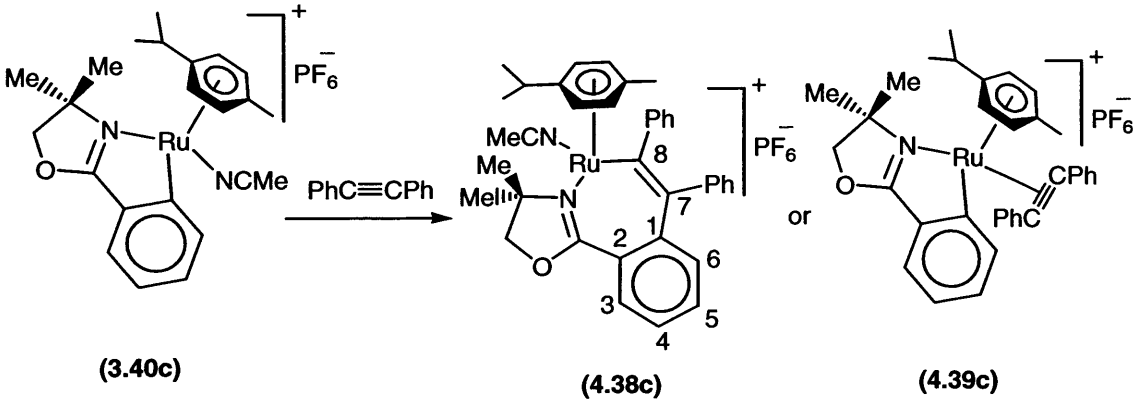

(3.40c) (4.38c) (4.39c)

(Scheme 4.22)

The ^1H NMR spectrum of (**4.38c**) shows a 1:1:1 ratio of the *p*-cymene, the oxazoline ligand and PhC≡CPh. As found in (**4.38a**), the NCMe protons are strongly shielded at δ 1.78, 0.43 ppm upfield from (**3.40c**), consistent with a ring current effect from the adjacent phenyl substituent

(see X-ray structure below). The four multiplets of the *p*-cymene are also shifted 0.5-0.8 ppm upfield from **(3.40c)** due to a ring-current of the phenyl of the oxazoline. The CMe_2 group gives rise to two singlets at δ 1.09 and 1.59 and the CH_2 protons are also inequivalent giving two mutually coupled doublets at δ 4.34 and 4.47. The inequivalence of the CH_2 protons, the methyls of the CMe_2 group and the *p*-cymene protons is consistent with the chiral centre at the metal, and shows that epimerisation at the metal is slow on the NMR timescale. The ^{13}C-{^1H} NMR spectrum shows NCMe carbons at δ 2.99 and 126.46, confirming the coordination of NCMe. The carbons (C^1) and (C^7) are observed at δ 145.92 and 148.88 (not necessarily in that order) and (C^8) at δ 171.46, the inequivalence of (C^7) and (C^8) confirms the insertion of the alkyne as for **(4.38a)** and carbon (C^1) is shifted, approximately 30 ppm upfield from **(3.40c)**, confirming the insertion of alkyne into the M-C bond not the M-N bond. The FAB mass spectrum showed an ion at *m/z* 588 due to $[M\text{-}NCMe]^+$, confirming the presence of PhC≡CPh.

Recrystallisation from dichloromethane/hexane gave X-ray quality crystals of **(4.38c)**. The crystal structure is shown in **Fig. 4.7**, with selected bond distances and angles in **Table 4.6**.

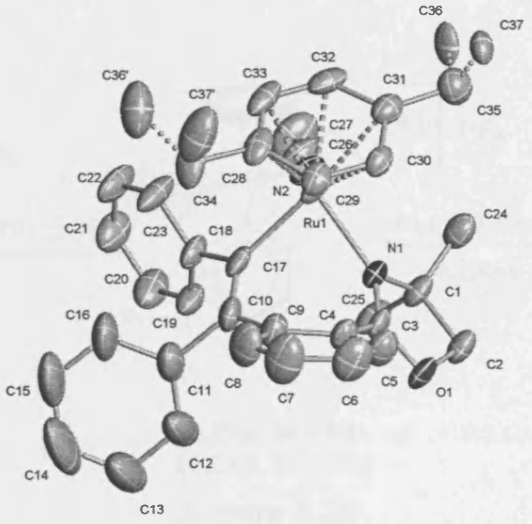

Fig. 4.7 Molecular structure cation of **(4.38c)**

Table 4.6 Selected bond distances [Å] and bond angles [°] for **(4.38c)**

Bond distances/[Å]			
Ru(1)-C(17)	2.095(4)	C(9)-C(10)	1.489(6)
Ru (1)-N(1)	2.123(3)	C(10)-C(17)	1.336(6)
Ru(1)-N(2)	2.053(3)		
Bond angles/ [°]			
C(17)-Ru(1)-N(2)	88.73(16)	C(17)-Ru(1)-N(1)	81.50(13)
N(1)-Ru(1)-N(2)	89.80(13)		

The complex adopts the expected pseudo-octahedral structure, and confirms that the alkyne has inserted into the M-C bond with formation of a seven membered ring. The C(17)-Ru(1)-N(1) chelate bite angle of the seven-membered ring [81.50(13)°] is larger than that [77.08(12) Å] in the five-membered ring of **(4.25a)**. The oxazoline ring is rotated out of the plane of the phenyl [C(4)-C(9)] (dihedral angle N(1)-C(3)-C(4)-C(9) = 52.8°), this angle is much larger than the corresponding angle (4.5°) in **(4.25a)**, presumably, this occurs as a consequence of the expansion in ring size. Similar tilting of the oxazoline ring is seen in benzene bisoxazoline complexes with a 7-membered ring.[18] The structure also shows that the NCMe lies in region of the ring current of the phenyl [C(18)-C(23)] and the *p*-cymene is tilted to lie over the ring [C(4)-C(9)]. These features account for the high field shifts observed in the ^{1}H NMR spectrum of **(4.38c)** (see above). Similar features are expected for **(4.38a)**.

Reactions of the cationic iridium and rhodium imine complexes **(4.21a)** and **(4.21b)** respectively with PhC≡CPh were also investigated. The reactions were carried out at room temperature in CH_2Cl_2 and were monitored by ES mass spectrometry and in each case only one peak was observed, at *m/z* 668 and 578 respectively corresponding to [M-NCMe+ PhC≡CPh] (M = **4.21a, b**).

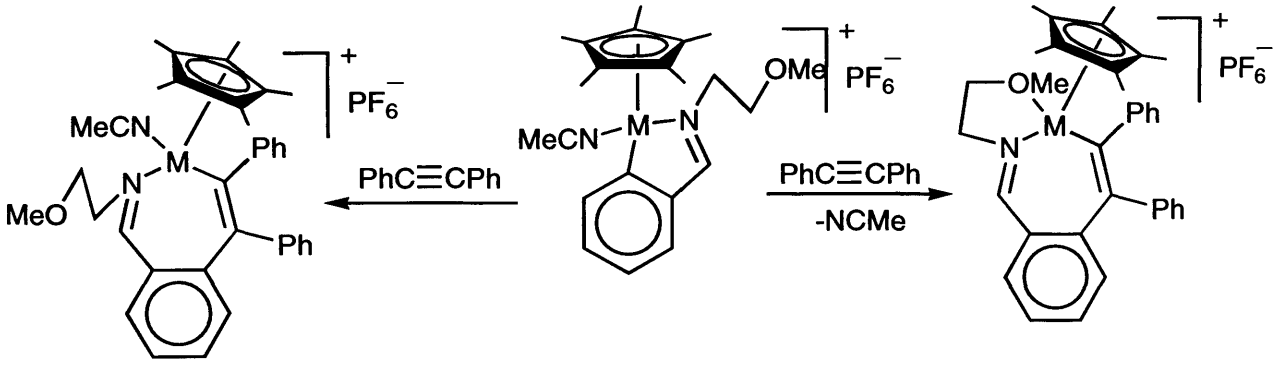

(4.41a, M = Ir)
(4.41b, M = Rh)

(4.21a, M = Ir)
(4.21b, M = Rh)

(4.40a, M = Ir)
(4.40b, M = Rh)

. **(Scheme 4.23)**

The ^{1}H NMR spectra of the products, each show a 1:1:1 ratio of the Cp*, the imine ligand and PhC≡CPh, but no peak due to NCMe suggesting that the products are not **(4.41a)** and **(4.41b)** as expected by analogy to the oxazoline reactions above. In each complex, the Cp* is observed, 0.35 ppm upfield from the starting cationic complex, at *ca.* δ 1.38 suggesting a ring-current effect of an alkyne-insertion product. The OMe signals are observed at δ 2.48 and 2.35, more than 0.86 ppm upfield from the starting materials. These large shifts are in the opposite direction to that expected for coordination of the OMe to the metal centre and are typical of ring-current effects. Coordination of the OMe places the methyl in the vicinity of one of the Ph

groups of the alkyne. Similar ring-current effects were seen on coordination of the OMe in $Pd(PPh_3)$ complexes of this imine **(2.53a, Scheme 2.31)**. The imine protons also show large shifts, 0.74 and 0.95 ppm downfield compared with **(4.21a)** and **(4.21b)** respectively, possibly a reflection of coordination of the OMe. In both cases, the NCH_2 and CH_2O protons are observed as inequivalent multiplets, consistent with the chiral centre at the metal, and demonstrate that epimerisation at the metal and decoordination of the oxygen is slow on the NMR timescale. The ^{13}C-$\{^1H\}$ NMR spectrum of **(4.40a)** shows the imine carbon at δ 170.84, and (C^1) is observed at 145, 18 ppm upfield from the **(4.1a)**. The carbons (C^7) and (C^8) are observed at δ 145 and 159, the inequivalence confirms the insertion of the alkyne. No ^{13}C-$\{^1H\}$ NMR spectrum was obtained for **(4.40b)**. The FAB mass spectra of **(4.40a)** and **(4.40b)** show molecular ions at *m/z* 668 and 578 respectively.

Careful recrystallisation of **(4.40a)** from dichloromethane/ether gave crystals suitable for X-ray diffraction. The X-ray structure is shown in **Fig. 4.8** with selected distances and angles in **Table 4.7**.

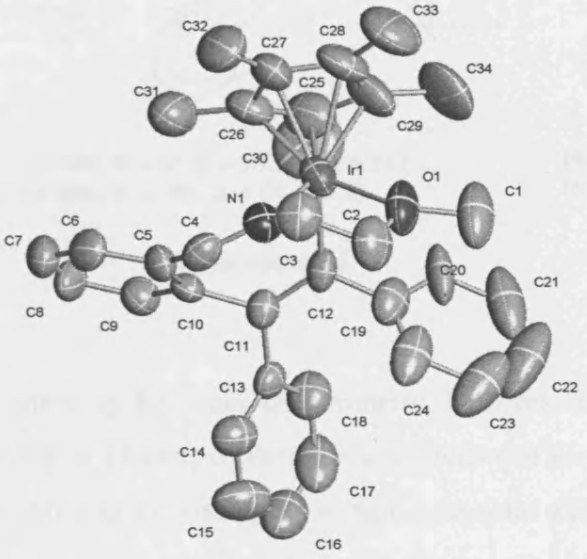

Fig. 4.8 Molecular structure of the cation of **(4.40a)**

Table 4.7 Selected bond distances [Å] and bond angles [°] for **(4.40a)**

Bond distances/[Å]			
Ir(1)-C(12)	2.018(7)	O(1)-C(2)	1.422(8)
Ir(1)-N(1)	2.062(7)	N(1)-C(3)	1.468(9)
Ir(1)-O(1)	2.274(5)	C(11)-C(12)	1.390(9)
C(10)-C(11)	1.491(8)	N(1)-C(4)	1.279(8)
Bond angles/ [°]			
C(12)-Ir(1)-N(1)	84.6(2)	C(12)-Ir(1)-O(1)	89.3(2)
N(1)-Ir(1)-O(1)	75.3(2)		

The complex adopts the expected pseudo-octahedral structure, and confirms that the insertion of the alkyne into the Ir-C bond has resulted in the formation of a seven-membered ring and coordination of the OMe has formed a five-membered ring. The C(12)-Ir(1)-N(1) chelate bite angle [84.6(2)°] is larger than those for the N(1)-Ir(1)-O(1) angle [75.3(2)°], which is expected because of the larger chelate ring size. The structure shows variations in the Ir-Cp* bond lengths; three short Ir-C bonds; which are approximately *trans* to the N(1) and O(1) and two longer ones *trans* to the carbon (C12).

Reaction of the phenyl-substituted imines **(4.23a)** and **(3.32b)** with PhC≡CPh was also tested since these did not have a pendant OMe group able to stabilise the insertion product. The expected products **(4.42)** are shown in **Scheme 4.24**.

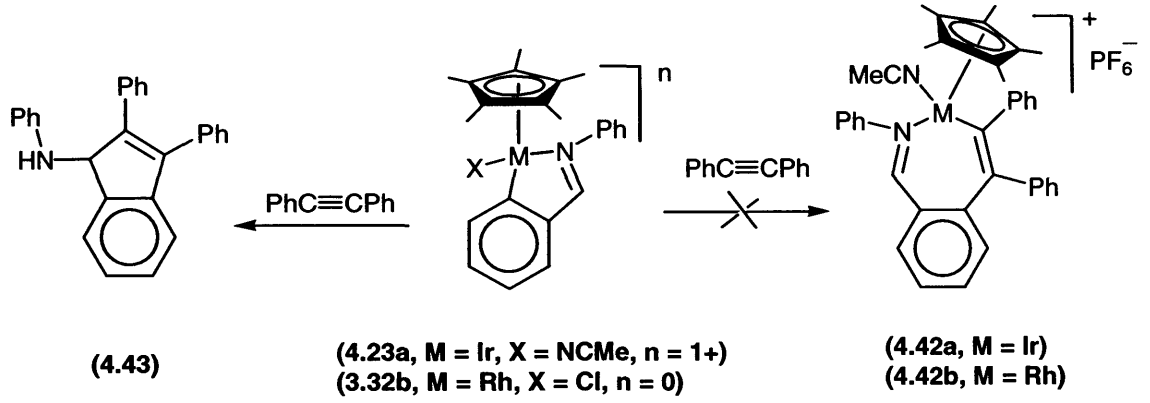

(4.43)

(4.23a, M = Ir, X = NCMe, n = 1+)
(3.32b, M = Rh, X = Cl, n = 0)

(4.42a, M = Ir)
(4.42b, M = Rh)

(Scheme 4.24)

The reactions were monitored by ES mass spectrometry, both reactions gave an ion at *m/z* 358 and in contrast to reactions of **(4.21a, b)** there was no evidence for the expected insertion products **(4.42a, b)**. The reaction was worked up by washing the solid with hexane to give a light brown hexane soluble fraction and a deep brown insoluble fraction, the latter was filtered though silica, however, no pure fraction could be isolated. Fortunately, crystallisation of the hexane soluble fraction gave crystals suitable for X-ray diffraction (see below) and this allowed identification of the compound as **(4.43)**. The ^{1}H NMR spectrum of **(4.43)** shows a broad peak integrating to 1H at δ 3.90 due to NH and a sharp singlet at δ 5.65 assigned to CH; multiplets integrating to 19H are observed in the aromatic region. The structure of **(4.43)** is shown in **Fig. 4.9** with selected bond distances.

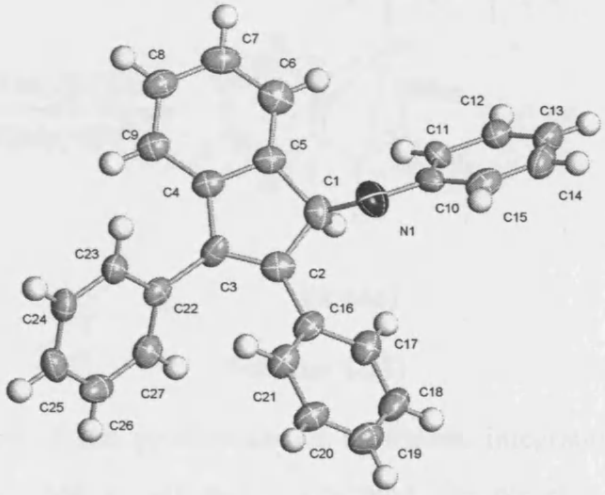

Fig. 4.9 Molecular structure of **(4.43)**

Table 4.8 Selected bond distances [Å] and bond angles [°] for **(4.43)**

Bond distances/[Å]			
C(1)-C(2)	1.518(5)	C(5)-C(1)	1.514(5)
C(1)-N(1)	1.428(4)	C(4)-C(5)	1.394(5)
C(2)-C(3)	1.355(5)	C(3)-C(4)	1.488(5)
Bond angles/ [°]			
C(1)-N(1)-C(10)	122.8(4)	N(1)-C(1)-C(2)	112.7(3)
N(1)-C(1)-C(5)	117.3(4)		

The structure shows a five-membered ring carbocyclic compound with an exocyclic amine. The C(1)-N(1) bond length [1.428(4) Å] is typical of a single bond showing the imine has been reduced to an amine. The product can be viewed as having formed by insertion of PhC≡CPh into the M-C bond of **(4.23a)** or **(3.32b)** and then ring closure from the new M-C to the imine carbon (*i.e* C-C bond formation) and protonation at the nitrogen. This is in contrast to ring closure to form isoquinolinium cations by reductive elimination and C-N bond formation as observed by Pfeffer[11] for an arene ruthenium cyclometallated amine **(Scheme 4.5)**. Therefore, reaction of Cp*Ir cyclometallated amine complex **(3.36a)** with PhC≡CPh was studied.

Complex **(3.36a)** was reacted with PhC≡CPh in NCMe in the presence of KPF_6. The reaction was monitored by ES mass spectrometry and was complete in 24 h. The long reaction time is probably a consequence of doing the reaction in NCMe as described earlier.

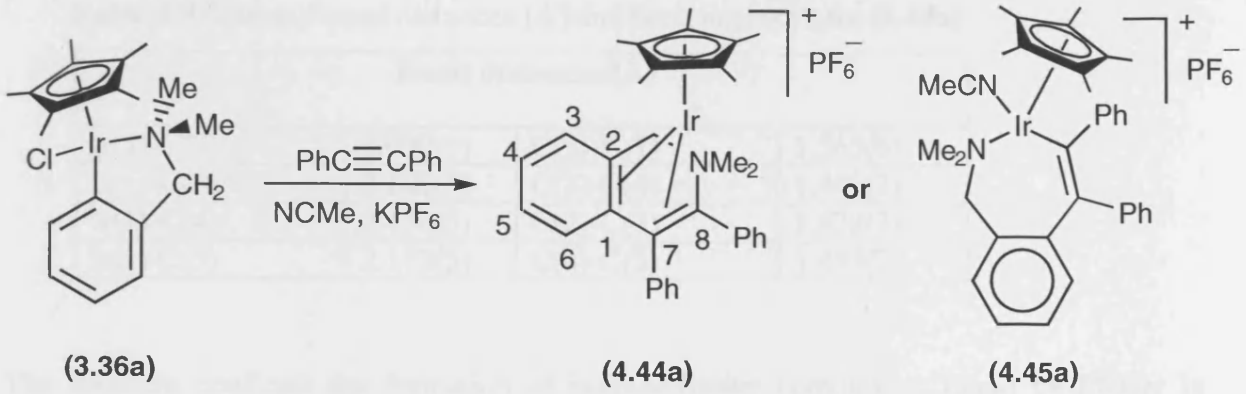

(3.36a) (4.44a) (4.45a)

(Scheme 4.25)

The ^{1}H NMR spectrum of the product shows multiplets integrating to 14 protons in the aromatic region (10H assigned to alkyne), confirming the presence of one equivalent of PhC≡CPh. The Cp* is seen at δ 1.28, 0.35 ppm upfield from the staring chloride complex, the extra shielding being consistent with insertion of PhC≡CPh as discussed earlier for **(4.38)**. The NMe_2 group gives rise to two sharp singlets at δ 2.81 and 3.20, with the benzyl protons being observed as mutually coupled doublets at δ 3.30 and 4.42. No peak was observed for NCMe, suggesting that reductive elimination had occurred to form isoquinolinium complex **(4.44a)**. Complex **(4.45a)** is presumably an intermediate. The ^{13}C-{^{1}H} NMR spectrum shows the expected number of signals for **(4.44a)** and no signals for NCMe again ruling out **(4.45a)**. There are four quaternary carbon signals at δ 140.99, 146.50, 148.11 and 153.71 due to (C^1), (C^2), (C^7) and (C^8) (not necessarily in that order). The FAB mass spectrum showed a molecular ion at *m/z* 639, interestingly, a fragment ion is also observed at *m/z* 312 due to the isoquinolinium unit. None of the other simple insertion products **(4.38)** and **(4.40)** show loss of the organic ligand in the mass spectrum. The structure of **(4.44a)** has been determined by X-ray crystallography **(Fig. 4.10)** and selected bond distances and angles are listed in **Table 4.9**.

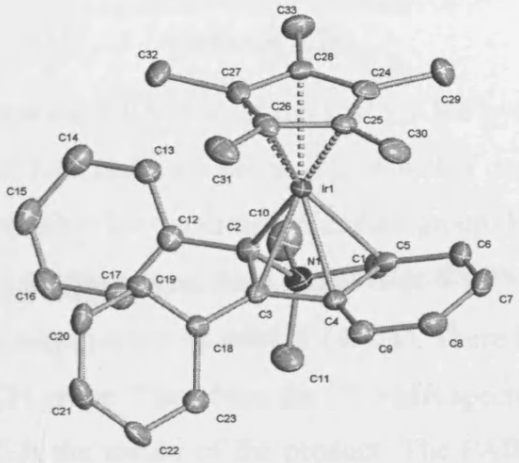

Fig. 4.10 Molecular structure of cation **(4.44a)**

Table 4.9 Selected bond distances [Å] and bond angles [°] for **(4.44a)**

Bond distances/[Å]			
Ir(1)-C(2)	2.090(5)	C(2)-N(1)	1.565(6)
Ir(1)-C(3)	2.106(5)	C(3)-C(4)	1.446(7)
Ir(1)-C(4)	2.170(5)	C(2)-C(3)	1.478(7)
Ir(1)-C(5)	2.173(5)	C(4)-C(5)	1.433(7)

The structure confirms the formation of isoquinolinium complex as found by Pfeffer in related arene ruthenium reactions[11] **(4.9, Scheme 4.4)**. The complex has a sandwich structure involving η^5-coordination of a Cp* ligand and η^4-coordination of a cationic heterocycle to a formally Ir(I) centre. The Ir-N(1) distance is 3.103(5) Å showing there is no bonding interaction between these atoms.

Reaction of the cyclometallated N-methyl pyrrole complex **(4.27a)** with PhC≡CPh in CH_2Cl_2 was also investigated **(Scheme 4.26)**. ^{1}H NMR spectrum of the crude product showed a mixture of species. Filtering the mixture through silica gave one pure product which was characterised by ^{1}H NMR spectroscopy, FAB mass spectrometry, IR, elemental analysis and X-ray crystallography.

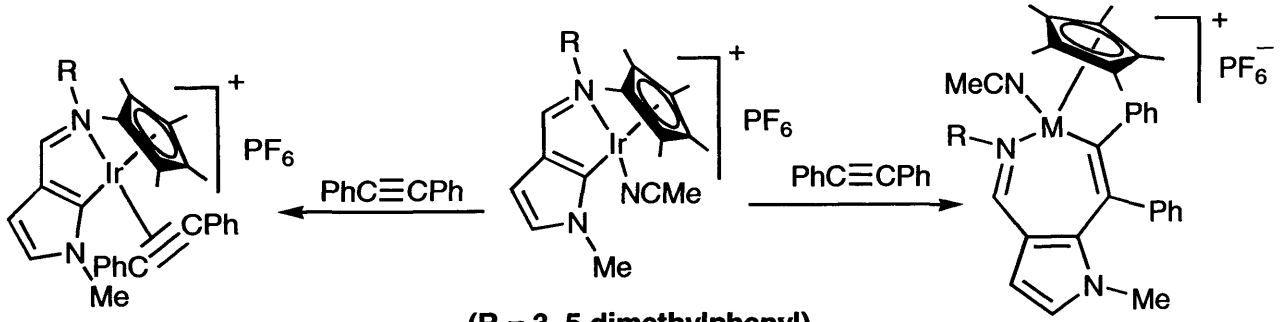

(Scheme 4.26)

The ^{1}H NMR spectrum shows a 1:1:1 ratio of the Cp*, N-Me pyrrole and PhC≡CPh. There are two doublets at δ 5.96 and 7.75 and a singlet at δ 3.84 which can be assigned to the N-Me pyrrole protons and two singlets (2:1) for the dimethyl aniline group. However, there is no longer any evidence for an imine proton, the lowest field signal is at δ 7.75, and there is no signal for coordinated NCMe, thus, the product is not **(4.46a)** or **(4.47a)**. There is an additional singlet at δ 5.85 which corresponds to a CH group. Therefore, the ^{1}H NMR spectrum shows addition of one PhC≡CPh but does not establish the nature of the product. The FAB mass spectrum showed a molecular ion at *m/z* 715, and a fragment ion at *m/z* 389 which corresponds to [N-Me

pyrrole+PhC≡CPh]. The observation of a purely organic fragment ion is similar to the isoquinolinium product **(4.44a)**. Hence, a monoinsertion product and formation of a heterocycle is likely but to establish the structure a X-ray diffraction study was carried out. The structure is shown in **Fig. 4.11** with selected bond distances and angles listed in **Table 4.10**.

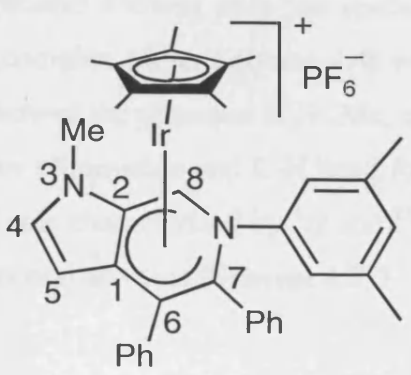

(4.48a)

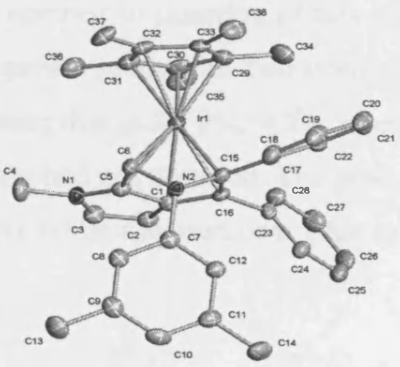

Fig. 4.11 Molecular structure of the cation of **(4.48a)**

Table 4.10 Selected bond distances [Å] and bond angles [°] for **(4.48a)**

Bond distances/[Å]			
Ir(1)-C(5)	2.252(3)	C(15)-N(2)	1.456(4)
Ir(1)-C(6)	2.121(3)	C(1)-C(5)	1.429(5)
Ir(1)-C(1)	2.287(3)	C(5)-C(6)	1.457(4)
Ir(1)-C(15)	2.171(3)	C(1)-C(16)	1.450(5)
Ir(1)-C(16)	2.215(3)	C(15)-C(16)	1.449(5)
C(6)-N(2)	1.457(4)		
Bond angles/ [°]			
C(1)-Ir(1)-C(5)	36.70(11)	C(5)-Ir(1)-C(6)	37.98(12)
C(15)-Ir(1)-C(16)	38.56(12)	C(1)-Ir(1)-C(16)	37.54(13)

The structure confirms the insertion of PhC≡CPh into the Ir-C bond but shows that C-N bond formation has also occurred to form a pyridinium ring which is η^5-bond to iridium(I). The bond lengths in the pyridinium ring range between 1.429(5) Å and 1.457(4) Å showing that there is some delocalisation around the ring.

The results described above show that PhC≡CPh can insert into the M-C bond of all the cyclometallated complexes. In the case of the oxazolines and alkyl imines these initial products are stable. The N-Ph-imine complexes undergo C-C bond formation and dissociation of the carbocyclic product. In the case of the cyclometallated amine **(3.36a)** and NMe pyrrole imine **(4.27a)**, alkyne insertion occurs followed by reductive elimination by C-N bond formation to

form **(4.44a)** and **(4.48a)** respectively and the resultant heterocycles remain coordinated to the metal as found previously for arene ruthenium complex **(4.8)**.[11]

4.2.4b Reactions with PhC≡CCO$_2$Et:

Reaction of the asymmetrically disubstituted alkyne PhC≡CCO$_2$Et with **(4.25a)** was attempted to investigate the regioselectivity of the insertion reaction. The ^{1}H NMR spectrum of the crude product showed only one species, in contrast to insertion of this alkyne in the arene ruthenium complex **(4.9e, Scheme 4.4)** which gave a mixture of two isomers.[11] The ^{1}H NMR spectrum showed the presence of NCMe, suggesting that as for PhC≡CPh, insertion had occurred but reductive elimination and C-N bond formation had not occurred. The product, either **(4.49a)** or **(4.49a`)** was characterised by ^{1}H and ^{13}C-{^{1}H} NMR spectroscopy, FAB mass spectrometry, IR and elemental analysis **(Scheme 4.27)**.

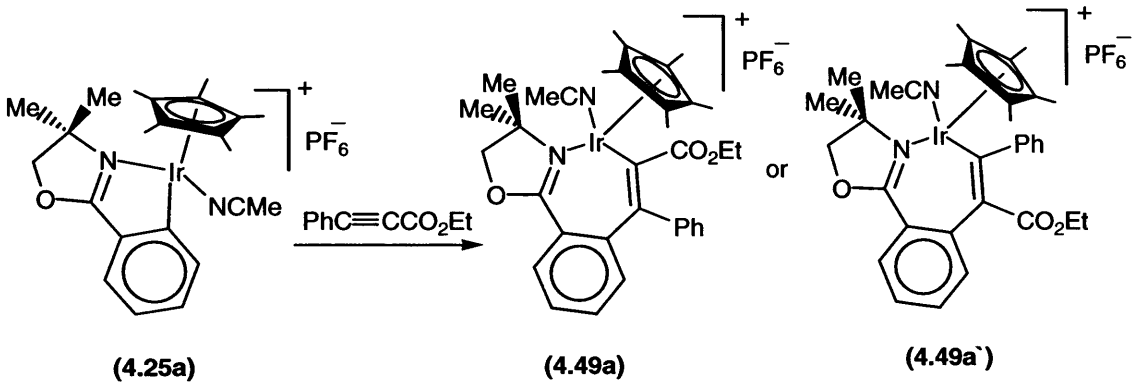

(4.25a) **(4.49a)** **(4.49a`)**

(Scheme 4.27)

The ^{1}H NMR spectrum shows a 1:1:1 ratio of the Cp*, the oxazoline and alkyne ligands. The NCMe protons are observed at δ 2.77, much lower field than that δ 2.00 in **(4.38a)** suggesting that it is not affected by a ring-current of an adjacent phenyl; suggesting the phenyl is on the carbon atom adjacent to the phenyl oxazoline *i.e.* isomer **(4.49a)**. The Cp* is observed at δ 1.41, 0.4 ppm upfield from the starting cationic complex, consistent with a ring-current effect from the originally cyclometallated phenyl. The CMe$_2$ group gives rise to two sharp singlets at δ 1.31 and 1.46, with the OCH$_2$ protons being observed as two doublets at δ 4.23 and 4.53; the inequivalence is consistent with epimerisation at the metal being slow on the NMR timescale. Two multiplets are observed at δ 1.38 and 3.79 assigned to the CO$_2$Et protons. The ^{13}C-{^{1}H} NMR spectrum shows the expected number of carbon signals. The FAB mass spectrum shows an ion at *m/z* 676 due to [M-NCMe]$^+$. The IR spectrum shows υ(C=N) at 1624 cm^{-1}, similar to that in the starting cationic complex with υ(C=O) at 1695 cm^{-1}, confirming the presence of PhC≡CCO$_2$Et. The spectroscopic data is consistent with isomer **(4.49a)** *i.e* the insertion occurs such that the carboxylate group is found on the carbon atom adjacent to the metal, with the

phenyl group being on the carbon atom adjacent to the phenyl oxazoline. This suggests that the CO_2Et has no steric interaction with the Cp*. The regioselectivity is similar to that found by Larock[21] and opposite to that observed by Pfeffer[11] and Bennett.[7]

4.2.4c Reactions with Monosubstituted alkynes HC≡CR (R = Ph, CO_2Et):

To further probe regioselectivity issues we investigated monosubstituted alkynes. Reaction of PhC≡CH with chloride complex (**3.37a**) in 1:1 ratio in NCMe in the presence of KPF_6 led to formation of a monoinsertion complex in 30% yield after 4 hours (method A). When the reaction was repeated using cationic NCMe complex (**4.25a**) as starting material in CH_2Cl_2, the same complex was isolated in 86% yield after 1 hour (method B) (**Scheme 4.28**). For both methods, ES mass spectrometry are showed only peak at *m/z* 604 due to $[M\text{-}NCMe+PhC{\equiv}CH]^+$ (M = **4.25a**) corresponding to monoinsertion of PhC≡CH. The ^1H NMR spectrum of the crude product showed only one isomer is present in the solution, and a peak for NCMe, suggesting that reductive elimination and C-N bond formation had not occurred. The product was characterised by ^1H and $^{13}C\text{-}\{^1H\}$ NMR spectroscopy, FAB mass spectrometry, IR, elemental analysis and X-ray crystallography.

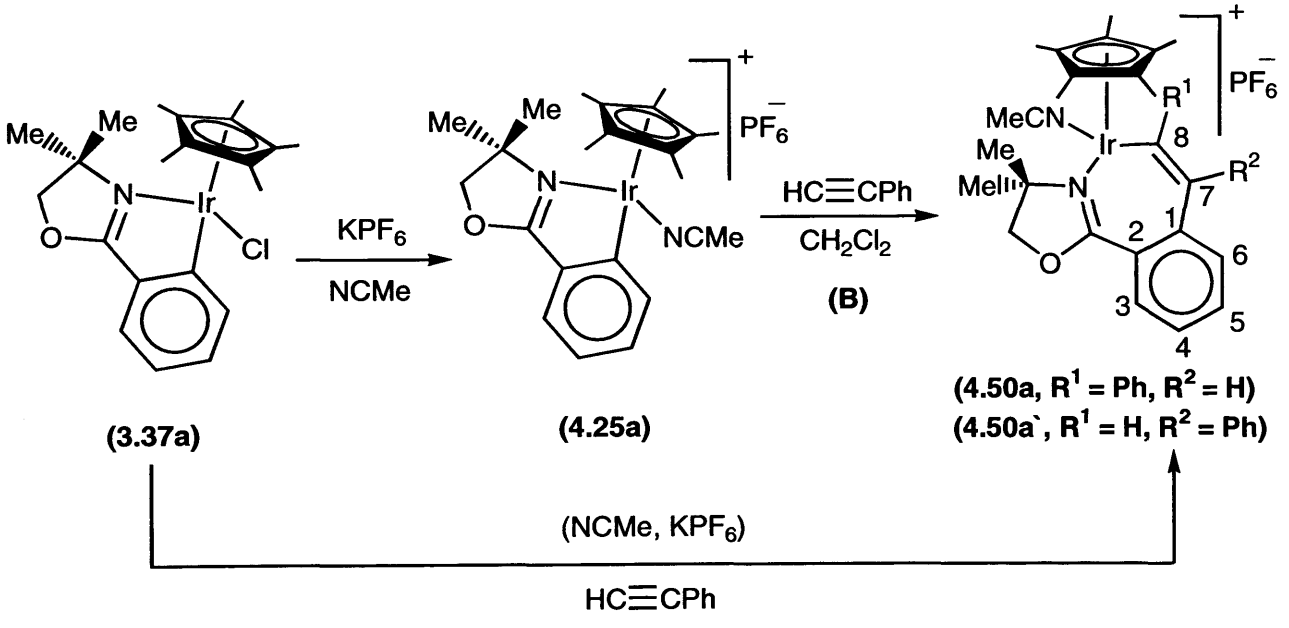

(Scheme 4.28)

The ^1H NMR spectrum of the product shows a 1:1:1 ratio of the Cp*, oxazoline and alkyne ligands. The Cp* signal is observed at δ 1.34, 0.46 ppm upfield from the starting chloride and cationic complexes, the high field shift due to a ring-current from the oxazolinyl phenyl as discussed previously for (**4.38a**). The signal for NCMe is also shielded at δ 1.99, 0.43 ppm

upfield from the starting cationic complex as found in **(4.38a)** and **(4.38c)**; this suggests that the phenyl of PhC≡CH is adjacent to iridium and the product is **(4.50a)** rather than **(4.50a`)** (confirmed by X-ray crystallography, see below). The CMe_2 group gives two singlets at δ 1.14 and 1.29 and the OCH_2 protons give rise to two mutually coupled doublets at δ 4.11 and 4.42. The inequivalence of the CH_2 protons, and of the methyls of the CMe_2 group is consistent with the chiral centre at the metal, and that epimerisation at the metal is slow on the NMR timescale. The ^{13}C-{^1H} NMR spectrum of **(4.50a)** shows the expected carbons. The NCMe carbons are observed at 2.67 and 121.84 with (C^7) at δ 132.11. The FAB mass spectrum of **(4.50a)** shows an ion at *m/z* 604 due to $[M\text{-}NCMe]^+$, confirming the presence of PhC≡CH.

The corresponding reaction was also attempted with the cationic cycloruthenated complex **(3.40c)** **(Scheme 4.29)**. The ^1H NMR spectrum of the crude product showed a mixture of products, filtering the mixture through silica gave one pure product.

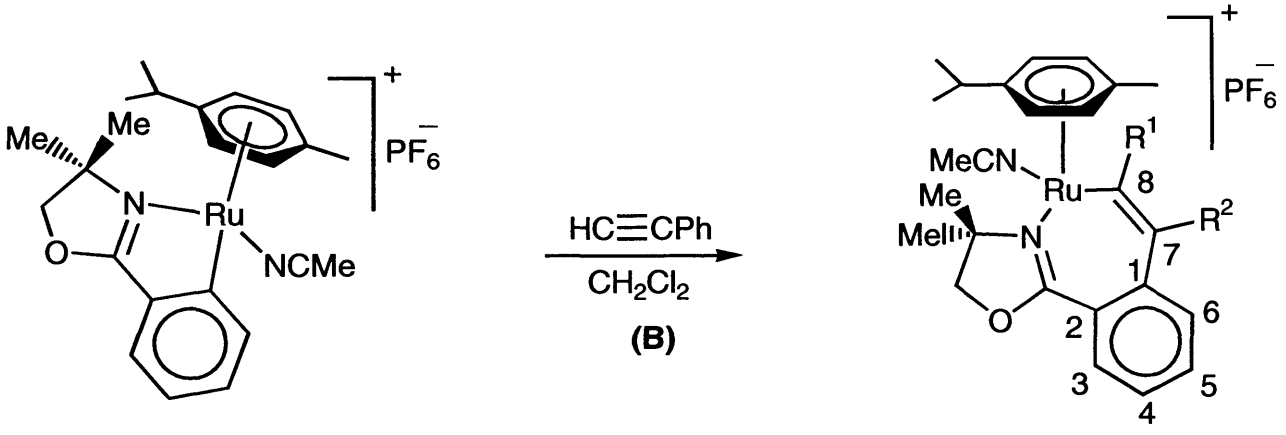

(3.40c)

(4.50c, R^1 = Ph, R^2 = H)
(4.50c`, R^1 = H, R^2 = Ph)

(Scheme 4.29)

The ^1H NMR spectrum of the product shows *p*-cymene signals as four multiplets at δ 4.39-5.41, *ca.* 0.6 ppm upfield from the starting cationic complex consistent with a ring-current from the oxazolinyl phenyl as found in **(4.50a)**. A signal for NCMe is observed at δ 1.85, 0.36 ppm upfield from the starting cationic complex, this suggests that the phenyl of alkyne is adjacent to ruthenium and the product is **(4.50c)** not **(4.50c`)** (this was confirmed by X-ray diffraction, see later). The alkyne proton (H^7) is observed at δ 7.12, this proton shift is assigned by noesy spectrum and found close to (H^6) confirming that the small group of alkyne is adjacent to the oxazolinyl phenyl ring. The CMe_2 group gave two singlets at δ 1.00 and 1.58 and the OCH_2 protons gave rise to two mutually coupled doublets at δ 4.32 and 4.35. The inequivalence of the CH_2 protons and of the methyls of the CMe_2 group and of the *p*-cymene protons is consistent

with the chiral centre at the metal, and shows that epimerisation at the metal is slow on the NMR timescale. The $^{13}C-\{^{1}H\}$ NMR spectrum of **(4.50c)** shows the expected carbons. NCMe carbons are observed at δ 3.05 and 124.01 with δ 132.32. The FAB mass spectrum of **(4.50c)** shows an ion at *m/z* 512 due to $[M-NCMe]^+$, confirming the presence of PhC≡CH.

Careful recrystallisation of **(4.50a)** and **(4.50c)** from dichloromethane/ether gave crystals suitable for X-ray diffraction. The X-ray structures are shown in **Figs. 4.12** and **4.13** with selected distances and angles in **Table 4.11**.

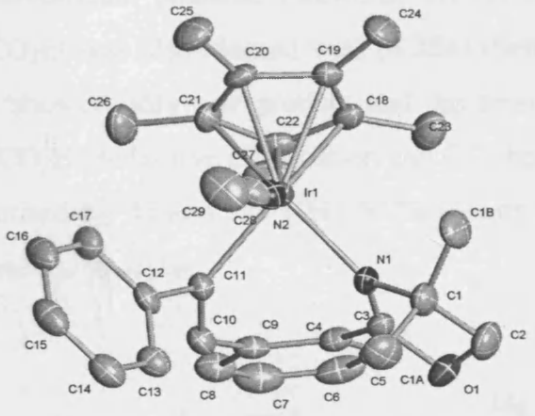

Fig. 4.12 Molecular structure of the cation of **(4.50a)**

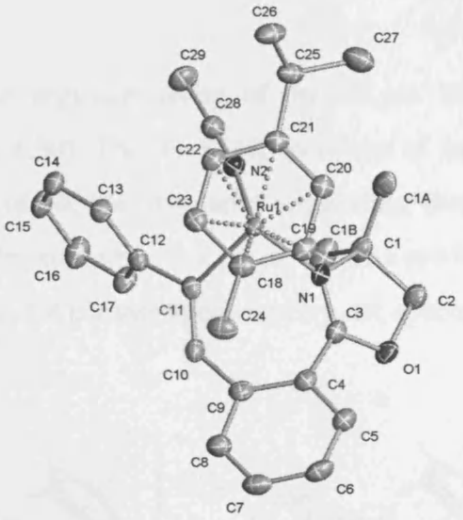

Fig. 4.13 Molecular structure of the cation of **(4.50c)**

Table 4.11 Selected bond distances [Å] and bond angles [°] for **(4.50a) and (4.50c)**

Bond distances/[Å]	**(4.50a)**	**(4.50c)**
M(1)-N(1)	2.095(4)	2.094(2)
M(1)-N(2)	2.058(6)	2.059(2)
M(1)-C(11)	2.079(5)	2.097(3)
C(9)-C(10)	1.459(8)	1.471(4)
C(10)-C(11)	1.331(8)	1.347(4)
Bond angles/ [°]		
N(1)-M(1)-C(11)	81.7(2)	83.49(10)
N(1)-M(1)-N(2)	86.3(2)	86.14(10)
N(2)-M(1)-C(11)	85.92(9)	86.53(7)

Each complex adopts the expected pseudo-octahedral structure, and shows that the alkyne has inserted into the M-C bond to form a seven-membered ring. The bond lengths and angles are similar in both complexes. The Ru-C bond length [2.097(3) Å] and the bite chelate angle N(1)-M(1)-C(11) [83.49(10)°] are similar to the PhC≡CPh insertion product **(4.38c)** [2.095(4) Å and

81.50(13)° respectively], though, the Ru-N(1) bond length [2.094 Å] is shorter than that [2.123(3) Å] in **(4.38c)**. As found in **(4.38c)**, in both **(4.50a, c)** the oxazoline is rotated out of the plane of the phenyl (C(4)-C(9) (dihedral angle N(1)-C(3)-C(4)-C(9) = 48.4° and 44.5° respectively). The structures confirm that the NCMe lies in region of the ring-current of the alkyne phenyl and the Cp* and *p*-cymene to lie over the oxazolinyl phenyl ring.

The insertion is highly regioselective (none of the other isomer is observed) with the smaller substituent (H) on the carbon atom adjacent to the phenyl oxazoline and the larger group (phenyl) being on the carbon atom adjacent to the metal. It is interesting to note that the regioselectivity of formation of **(4.50a)** and **(4.50c)** is similar to that found by Bennett[7] and opposite to that observed by Pfeffer[11] **(Scheme 4.4)**.

To investigate possible electronic effects on the regioselectivity of the alkyne insertion, $HC{\equiv}CCO_2Et$ was also reacted with **(4.25a)** **(Scheme 4.30)**. The ^1H NMR spectrum of the crude product showed only one product and the presence of NCMe, the latter suggesting that as for $PhC{\equiv}CCO_2Et$, reductive elimination and C-N bond formation had not occurred. The product was characterised by ^1H and ^{13}C-{^1H} NMR spectroscopy, FAB mass spectrometry, IR spectroscopy and elemental analysis.

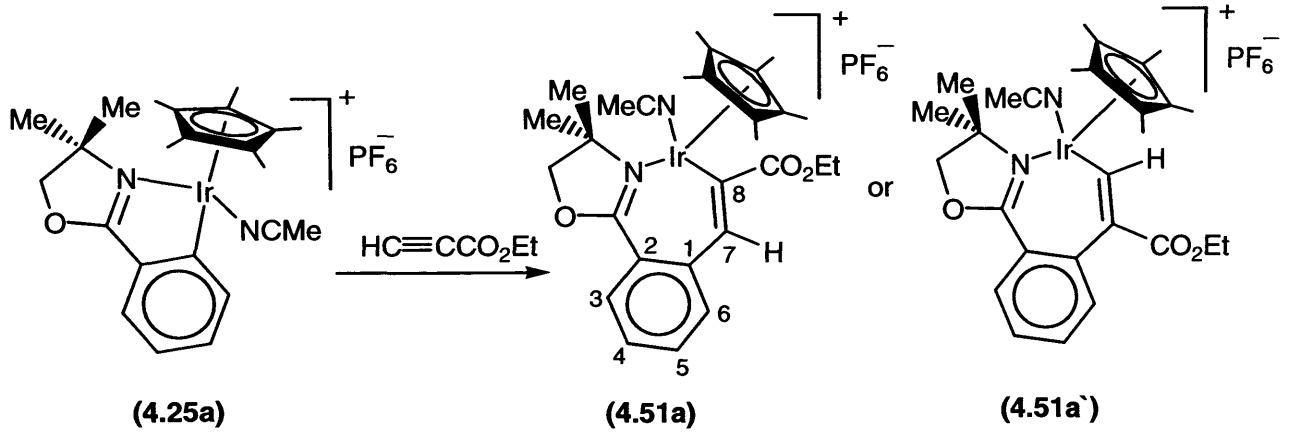

(4.25a) **(4.51a)** **(4.51a`)**

(Scheme 4.30)

The ^1H NMR spectrum shows a 1:1:1 ratio of the Cp*, the oxazoline and the alkyne and a signal for the NCMe protons is observed at δ 2.71. The Cp* is observed at δ 1.30, 0.5 ppm upfield from the starting cationic complex, consistent with a ring current effect from the phenyl. The CMe_2 group gives rise to two sharp singlets at δ 1.22 and 1.37, with the OCH_2 protons being observed as two doublets at δ 4.11 and 4.38; the inequivalence consistent with epimerisation at the metal being slow on the NMR timescale. Two multiplets at δ 1.27 and 4.11 are assigned to the CO_2Et protons and the alkyne proton (H^7) is observed as a singlet at δ 7.48. A Noesy

spectrum shows that (H^7) is adjacent to (H^6), confirming that the insertion occurs with the large group (CO_2Et) ending up on the carbon atom adjacent to the metal. The ^{13}C-{^1H} NMR spectrum of **(4.51a)** shows the expected number of carbon signals. The NCMe carbons are observed at δ 3.93 and 123.25 and (C^7) at δ 136.60. The FAB mass spectrum shows an ion at *m/z* 600 due to $[M\text{-}NCMe]^+$. The IR spectrum shows υ(C=N) at 1622 cm^{-1}, similar to that in the starting complex **(4.25a)** with υ(C=O) at 1682 cm^{-1}, confirming the presence of $HC{\equiv}CCO_2Et$. This regioselectivity is opposite to that observed by Pfeffer,[11] and similar to that found by Larock[21] and Bennett *et al.*[7]

As mentioned above, an isoquinolinium complex **(4.44a)** was isolated from the reaction of cyclometallated amine **(3.36a)** and PhC≡CPh. The corresponding complex was also reacted with PhC≡CH. and KPF_6 in NCMe. The ^1H NMR spectrum of the crude product showed the presence of more than two new species which could not be separated by chromatography or recrystallisation. Therefore, the reaction was repeated using cationic complex **(4.24a)** as starting material in $CDCl_3$ in an NMR tube. The reaction was complete in a matter of *ca* 5 min according to the ^1H NMR spectrum and only one Cp*Ir complex was present.

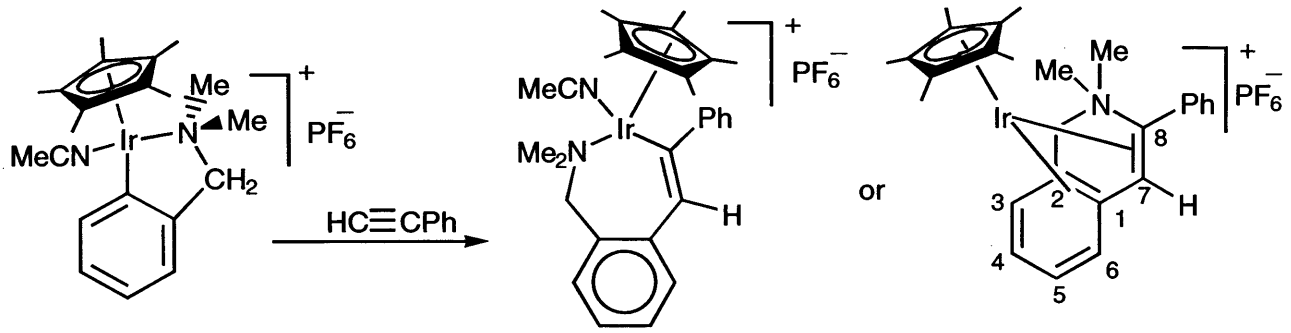

(4.24a) **(4.52a)** **(4.53a)**

(Scheme 4.31)

The ^1H NMR spectrum of product shows a Cp* signal at δ 1.52 and multiplets integrating to nine protons in the aromatic region, and no signal due to NCMe. The latter observation shows the product is not the simple insertion product **(4.52a)**. In addition, there are two singlet at δ 2.00 and 3.07 due to the NMe_2 and two (1H) doublets at δ 4.56 and 5.12 and a singlet at δ 4.60. The doublets are not significantly downfield from those (δ 3.30 and 4.42) in **(4.44a)** suggesting that the product is not **(4.53a)**. The ^{13}C-{^1H} NMR spectrum shows the expected number of signals for complex **(4.53a)**. However, there is no signal due to a CH_2 carbon. Rather there are three signals at δ 58.28 and 62.91 and 63.96 due to non-aromatic CH carbons.

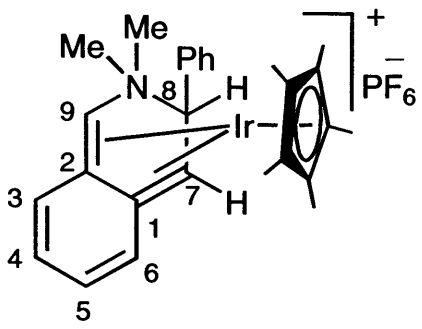

(4.54a)

The mass spectrum showed an ion at *m/z* 562 consistent with **(4.53a)**. Therefore, we propose that the complex is an isomer of **(4.53a)**, namely **(4.54a)** in which formally a 1,3-H shift has occurred transferring a hydrogen from the CH_2 to the CPh carbon. The reason why this should occur with PhC≡CH but not PhC≡CPh is not clear. A related process has been observed in palladium chemistry, conversion of **(4.55)** to **(4.56)** **(Scheme 4.32)**.[9]

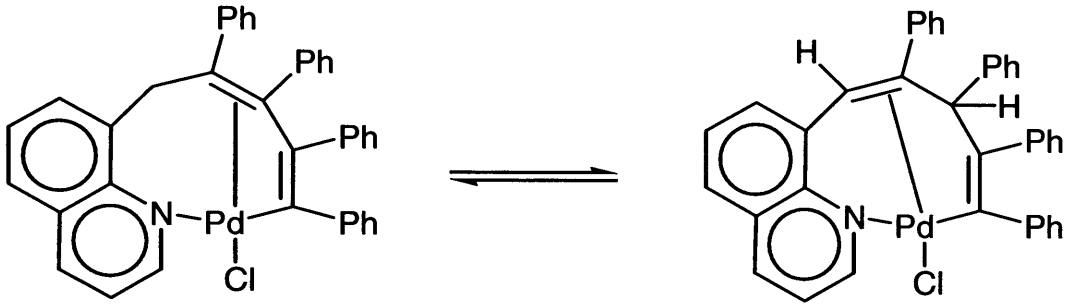

(4.55) **(4.56)**

(Scheme 4.32)

The reactions of imine complexes were also examined. Reaction of **(4.21a)** with PhC≡CH in 1:1 ratio in CH_2Cl_2 was monitored by ES mass spectrometry. After 4 hours two major ions at *m/z* 592 and 490 were seen assigned to [**4.21a**+ HC≡CPh-NCMe] and starting material [**4.21a**-NCMe]. After 7 hours a further peak was observed at m/z 694 equivalent to [**4.21a**+2(HC≡CPh)-NCMe]. Thus the reaction appears to give a mixture of mono insertion and diinsertion with the second insertion being at least as fast as the first one, so that it is not possible to get clean conversion to the initial product. Therefore, the reaction was repeated for 30 hours in the presence of two equivalent of PhC≡CH, and the ^{1}H NMR spectrum of the crude product showed only one species present in the solution. The expected product is shown in **Scheme 4.33**.

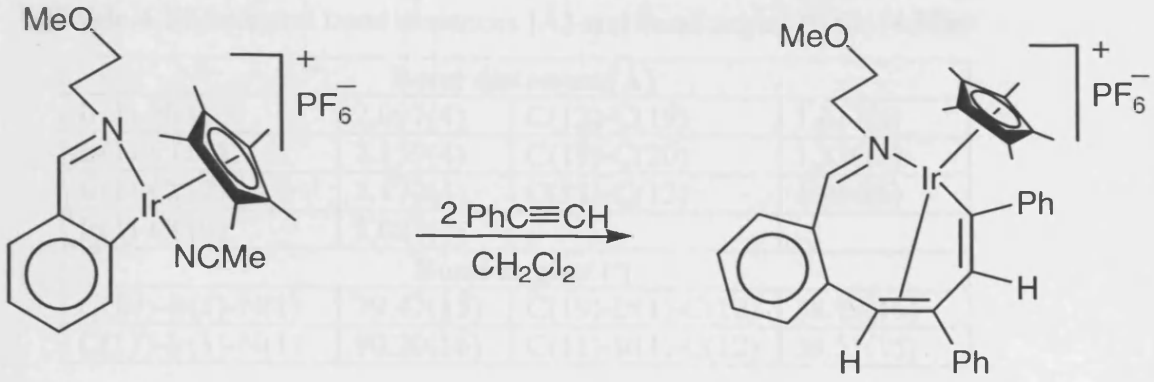

(4.21a) **(4.58a)**

(Scheme 4.33)

The ^{1}H NMR spectrum of the product shows a 1:1:2 ratio of the Cp*, oxazoline and alkyne ligands and no signal for NCMe is observed, consistent with the mass spectral data. The Cp* is observed at δ 1.69, similar to that δ 1.75 in **(4.21a)**, suggesting that there is no ring-current effect in this case. Two singlets due to the alkyne protons are observed at δ 6.06 and 6.72 for to (H^{7}) and (H^{10}) respectively. The NCH_2 protons give rise to two multiplets at δ 3.93 and 4.13; consistent with a chiral metal centre and slow empimerisation. The FAB mass spectrum showed an ion at *m/z* 694, confirming the presence of diinsertion of PhC≡CH. Hence, the spectroscopic data is not able to unambiguously identify the product. Fortunately, recrystallisation from dichloromethane/hexane gave X-ray quality crystals. The structure confirmed the novel insertion product **(4.57a)**. The ^{13}C-{^{1}H} NMR spectrum also shows (C^{7}) and (C^{10}) at δ 48.45 and 121.18 respectively. The crystal structure of this complex is shown in **Fig. 4.14**, with selected bond distances and angles in **Table 4.12**.

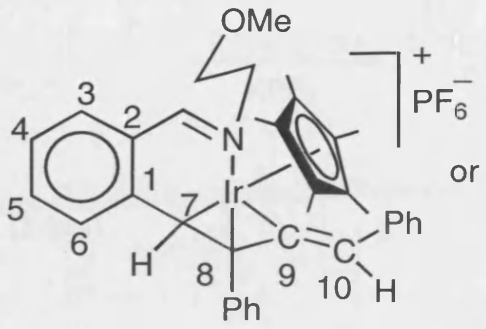

(4.57a)

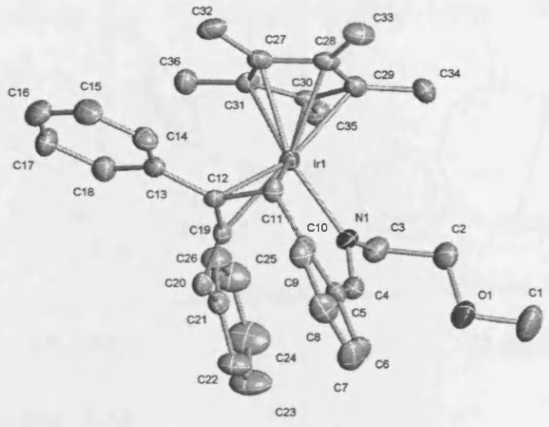

Fig. 4.14 Molecular structure of **(4.57a)**

Table 4.12 Selected bond distances [Å] and bond angles [°] for **(4.57a)**

Bond distances/[Å]			
Ir(1)-N(1)	2.097(4)	C(12)-C(19)	1.417(6)
Ir(1)-C(11)	2.159(4)	C(19)-C(20)	1.326(6)
Ir(1)-C(12)	2.172(4)	C(11)-C(12)	1.464(6)
Ir(1)-C(19)	2.087(4)		
Bond angles/ [°]			
C(19)-Ir(1)-N(1)	79.47(15)	C(19)-Ir(1)-C(12)	38.79(16)
C(11)-Ir(1)-N(1)	90.20(16)	C(11)-Ir(1)-C(12)	39.51(15)

The structure shows the expected η^5-Cp* and an eight-membered metallacycle formed by insertion of two molecules of PhC≡CH into the M-C bond of **(4.21a)**. The new ligand coordinates through the imine nitrogen and via three adjacent carbon atoms in a η^3-allyl type interaction. The bonding of the η^3-allyl is slightly asymmetric with the Ir-C(19) bond length [2.087(4) Å] being shorter than the bonds to C(11) and C(12) [2.159(4) and 2.172(4) Å respectively]. The allyl is oriented with the central carbon atom (12) and its phenyl substituent C(13)-C(18) pointing up towards the Cp*. The C(19)-C(20) [1.326(6) Å] is typical of a double bond and is much shorter than the C(11)-C(12) bond length [1.464(6) Å] which is now part of the η^3-allyl.

A similar reaction was attempted with the NPh-imine complex. Thus, **(3.32a)** reacted with PhC≡CH (1:2 ratio) in NCMe in the presence of KPF_6 for 7 hours then the NCMe was replaced by dichloromethane and stirred for 21 hours. The ^{1}H NMR spectrum of the crude product showed more than one Cp* signal, filtering the mixture through silica gave one pure product **(Scheme 3.34)**.

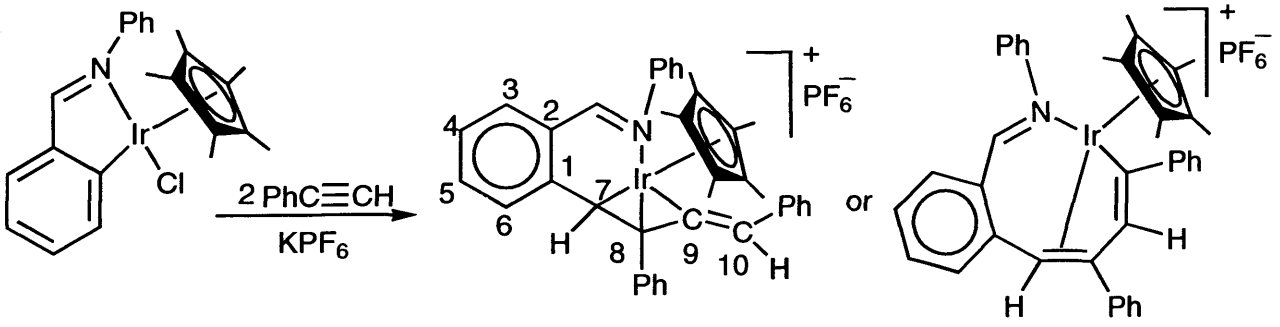

(3.32a) **(4.59a)** **(4.60a)**

(Scheme 3.34)

The ^{1}H NMR spectrum of the product shows a 1:1:2 ratio of the Cp*, oxazoline and alkyne ligands as expected for the formation of a diinsertion product. The Cp* is observed at δ 1.51,

similar to that, δ 1.47, in the starting chloride complex. Two singlets are observed at δ 5.20 and 6.72 assigned to (H^7) and (H^{10}) respectively. The FAB mass spectrum showed a molecular ion at *m/z* 712, confirming the presence of two molecules of PhC≡CH. The X-ray structure confirmed the product as **(4.59a)**, however, the result of the structure was not of sufficient quality to merit discussion of the bond lengths and angles.

Having observed diinsertion reactions with imines, reaction of the oxazoline complexes **(4.25a)** with two equivalent of PhC≡CH was attempted **(Scheme 4.35)**.

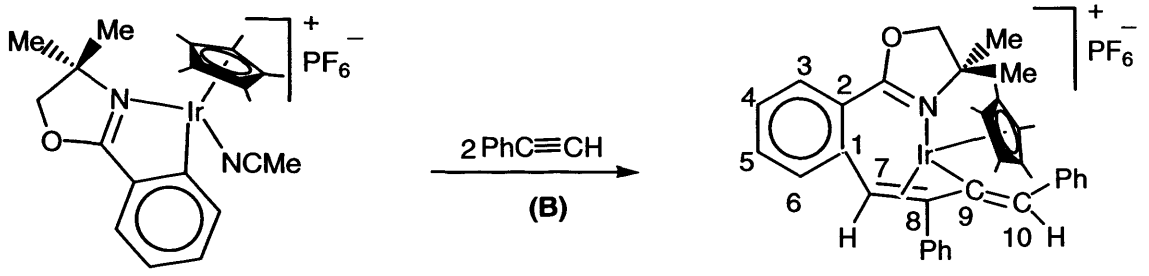

(4.5a) **(4.61a)**

(Scheme 4.35)

The ^1H NMR spectrum of the product shows a 1:1:2 ratio of the Cp*, oxazoline and alkyne ligands as expected for the formation of a diinsertion product. The Cp* signal is at δ 1.76, 0.42 ppm downfield compared with the monoinsertion complex **(4.50a)**, suggesting it is no longer influenced by a ring-current. Two singlets are observed at δ 4.68 and 6.41 due to the alkyne protons. The CMe_2 group gives two singlets at δ 1.18 and 1.37, and the OCH_2 protons give rise to two mutually coupled doublets at δ 2.94 and 4.18; the inequivalence is consistent with no epimerisation at the metal. The ^{13}C-{^1H} NMR spectrum shows carbons corresponding to the expected product (4.61a) with (C^7) and (C^{10}) observed at δ 48.58 and 119.84. The FAB mass spectrum **(4.61a)** showed a molecular ion at *m/z* 704, confirming the diinsertion of PhC≡CH. The IR spectrum shows υ(C=N) at 1604 cm^{-1}, similar to that in the starting cationic complex suggesting that the oxazoline is still coordinated.

The structure of **(4.61a)** has been determined by X-ray crystallography and is shown in **Fig. 4.15** and selected bond distances and angles are listed in **Table 4.13**. The structure is similar to that of **(4.57a)** with an eight-membered metallacycle formed by insertion of two molecules of PhC≡CH into the M-C bond of **(4.25a)**.

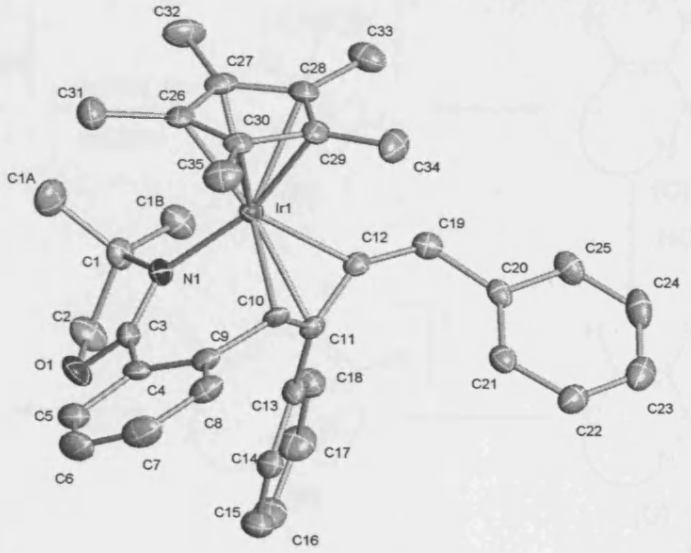

Fig. 4.15 Molecular structure of **(4.61a)**

Table 4.13 Selected bond distances [Å] and bond angles [°] for **(4.61a)**

Bond distances/[Å]			
Ir(1)-C(10)	2.150(4)	Ir(1)-C(12)	2.093(4)
Ir(1)-N(1)	2.093(4)	C(9)-C(10)	1.470(6)
Ir(1)-C(11)	2.241(4)	C(11)-C(12)	1.402(6)
Bond angles/ [°]			
C(10)-Ir(1)-N(1)	87.58(15)	C(10)-Ir(1)-C(11)	38.46(15)
C(12)-Ir(1)-N(1)	103.94(15)	C(11)-Ir(1)-C(12)	37.54(15)

The organic fragment is again bonded through a nitrogen and an η^3-allyl. However, the orientation of the η^3-allyl is different from that in **(4.57a)**. In **(4.61a)**, the central carbon atom of the allyl C(11) and its associated phenyl substituent (C(13)-C(18)) are oriented down, away from the Cp* ligand *ie.* opposite to that in **(4.67a)**. The η^3-allyl is again bonded asymmetrically with Ir-C(12) being the shortest bond.

Mechanistic considerations

The mechanism of formation of the diinsertion complexes can be rationalised by the pathways described in **Scheme 4.36**.

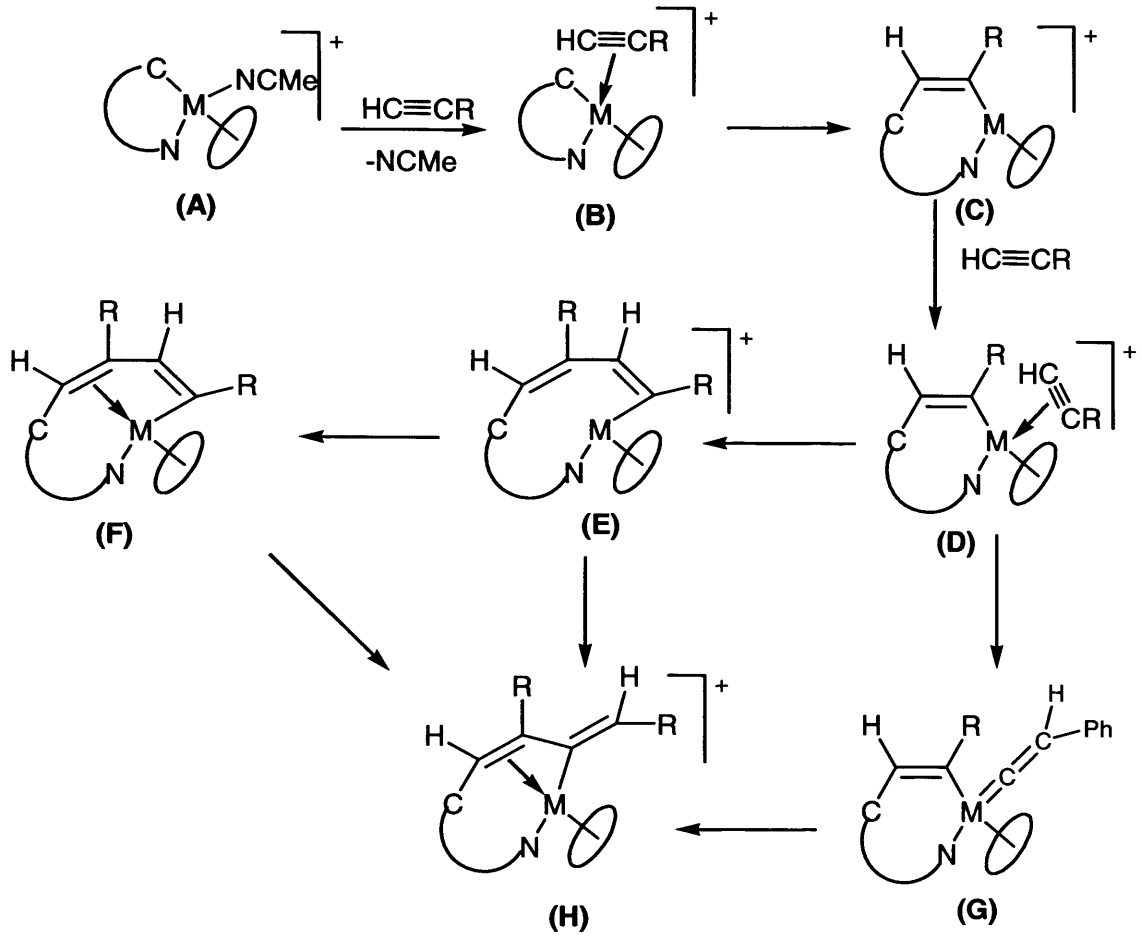

(Scheme 4.36)

Coordination of alkyne in NCMe forms **(B)** which undergoes insertion to 16-electron species **(C)**. In the absence of more alkyne this can recoordinate NCMe to form 18-electron species (C+NCMe) *e,g* complexes **(4.50a, c)**. In the presence of excess alkyne **(D)** could be formed. A second insertion could be expected to give 16e-electron species **(E)** which might be expected to give **(F)**. However, a 1,2 H-shift from **(F)** could give **(H)**. Alternatively, **(D)** could rearrange to a vinylidene **(G)**, then undergo insertion to give **(H)**. Complexes of type **(F)** have been isolated previously with palladium,[9] however, there are no previous examples of complexes of type **(H)**. This may be in part because there are very few reports of reactions with monosubstituted alkynes.

The main conclusions that can be inferred from this study of the insertion reactions of alkynes into the M-C bond of cyclometallated oxazolines, imines, amines and N-methyl pyrrole are as follows:

1. In CH_2Cl_2, the reaction of cationic NCMe complexes with alkynes is faster and gives better yields than the reaction with chloride complexes in NCMe.

2. In all cases, insertions of alkyne are into the M-C bond of the cyclometallated complexes not the M-N bond.
3. The products of the insertion reaction are dependent on the nature of the ligands on the metal centre, *e.g.* isoquinolinium complexes only form when amines are used consistent with previous results with Ru and Rh.
4. The reaction of unsymmetrical alkynes with imines, oxazolines and amine are highly regioselective.
5. No epimerisation could be observed on NMR timescale for all mono and diinsertion alkynes products.

4.3 Experimental

The spectroscopic techniques/instruments used were as described in Chapter Two. ^{1}H, ^{13}C and ^{31}P NMR spectra were obtained using a Bruker ARX250 or 300 MHz spectrometers, with $CDCl_3$ as solvent, unless otherwise stated.

General procedure for NCMe cationic reactions

KPF_6 was added to a solution of cyclometallated chloride complexes in acetonitrile (5-15 ml). The mixture was stirred for several hours, then filtered through Celite to remove excess KPF_6. The filtrate was evaporated to dryness and then washed with hexane to solidify the cyclometallated NCMe cationic products. The compounds could be recrystallised from dichloromethane/hexane.

Preparation of [Ir(NCMe){C_6H_4-2-C(H)=N(CH_2)$_2$OCH$_3$-$_K$*C*,*N*}Cp*][PF_6] (4.21a)

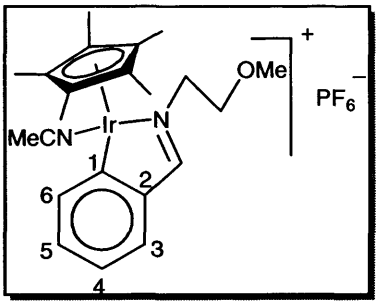

This was prepared from **(3.30a)** (70 mg, 0.13 mmol), KPF_6 (excess); after stirring overnight, **(4.21a)** was isolated as a brown precipitate (70 mg, 77.7%). Calc. for $C_{22}H_{30}N_2OIrPF_6$: C, 39.11, H, 4.48, N, 4.15. Found: C, 38.95, H, 4.69, N, 3.97%. ^{1}H NMR: δ 1.75 (s, 15H, Cp*), 2.36 (s, 3H, NCMe), 3.34 (s, 3H, OMe), 3.66 (m, 1H, C*H*HO), 3.84 (dt, 1H, *J* 10, 2.5, CH*H*O), 4.17 (m, 2H, NCH_2), 7.11 (t, 1H, *J* 7.5, H^4), 7.22 (dt, 1H, *J* 7.5, 1, H^5), 7.60 (d, 1H, *J* 7.5, H^3), 7.69 (d, 1H, *J* 7, H^6), 8.40 (s, 1H, HC=N). ^{13}C NMR: δ 3.71 (NC*Me*), 9.10 (C_5*Me*$_5$), 58.88 (OMe), 61.65 (CH_2O), 69.50 (NCH_2), 91.52 (*C*$_5$Me$_5$), 119.16 (N*C*Me), 123.87, 129.52, 132.69, 134.65 (C^3, C^4, C^5, C^6), 146.92 (C^2), 162.29 (C^1Ir), 179.28 (HC=N). MS (FAB): *m/z* 490 $[M\text{-}NCMe]^+$. IR: ν(C=N) 1606 cm^{-1}.

Preparation of [Rh(NCMe){C_6H_4-2-C(H)=N(CH_2)$_2$OMe-$_K$*C*,*N*}Cp*][PF_6] (4.21b)

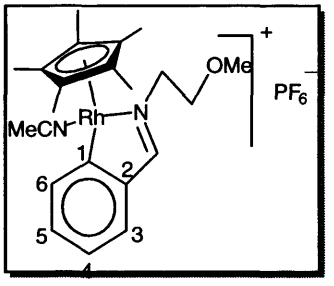

This was prepared from **(3.30b)** (134 mg, 0.31 mmol), KPF_6 (113 mg, 0.61 mmol); after stirring overnight, **(4.21b)** was isolated as a yellow solid (181 mg, 86%). Calc. for $C_{22}H_{30}N_2ORhPF_6$: C, 45.06, H, 5.16, N, 4.78. Found: C, 45.14, H, 5.21, N, 4.55%. ^{1}H NMR: δ 1.70 (s, 15H, Cp*), 2.23 (s, 3H, NCMe), 3.36 (s, 3H, OMe), 3.74 (m, 1H, C*H*H`O), 3.90 (dt, 1H, *J* 10, 3, CH*H*`O), 4.01 (m, 1H, NC*H*H`), 4.16 (m, 1H, NCH*H*`), 7.16 (dt, 1H, *J* 7.5, 1, H^4), 7.31 (dt, 1H, *J* 7.5, 1.5, H^5), 7.52 (dd, 1H, *J* 7.5, 1.5, H^3), 7.72 (d, 1H, *J* 7.5, H^6), 8.24 (d, 1H, J_{RhH} 4, HC= N). ^{13}C NMR: δ 3.54 (NCMe), 9.42 (C_5*Me*$_5$), 58.91 (OMe), 60.43 (CH_2O), 69.85 (NCH_2), 98.29 (d, J_{RhC} 7, *C*$_5$Me$_5$), 124.44, 129.43, 131.96, 135.51 (C^3, C^4, C^5,

C^6), 145.96 (C^2), 176.37 (HC= N), C^1Rh (not observed). MS (FAB): *m/z* 400 $[M\text{-}NCMe]^+$. IR: ν(C=N) 1614 cm^{-1}.

Preparation of [Ir(NCMe){C_6H_4-2-C(H)=N(CH_2)$_3$$OCH_3$-$_K$*C,N*}Cp*][$PF_6$] (4.22a)

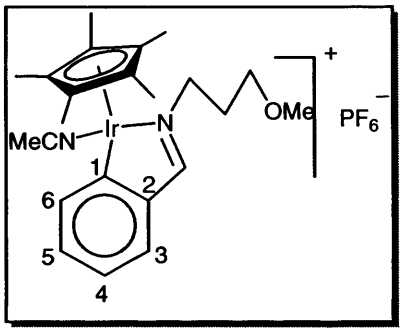

This was prepared from **(3.31a)** (70 mg, 0.13 mmol), KPF_6 (48 mg, 0.26 mmol); after stirring overnight, **(4.22a)** was isolated as a green precipitate (72 mg, 80%). Calc. for $C_{23}H_{32}IrN_2OPF_6$: C, 40.05, H, 4.68, N, 4.06. Found: C, 39.94, H, 4.53, N, 3.93%. ^{1}H NMR: δ 1.75 (s, 15H, Cp*), 1.84 (m, 1H, CH_2), 2.14 (m, 1H, CH_2), 2.37 (s, 3H, NCMe), 3.33 (s, 3H, OMe), 3.48 (m, 2H, CH_2O), 4.06 (m, 2H, NCH_2), 7.12 (t, 1H, *J* 7.5, H^4), 7.23 (t, 1H, *J* 7.5, H^5), 7.59 (d, 1H, *J* 7.5, H^3), 7.69 (d, 1H, *J* 7.5, H^6), 8.40 (s, 1H, HC=N). ^{13}C NMR: δ 3.65 (NC*Me*), 9.05 (C_5*Me*$_5$), 29.69 (CH_2), 58.91 (OMe), 60.15 (CH_2O), 69.32 (NCH_2), 91.55 (C_5Me_5), 119.59 (N*C*Me), 123.96, 129.39, 132.70, 134.64 (C^3, C^4, C^5, C^6), 146.79 (C^2), 162.12 (C^1Ir), 178.43 (HC=N); MS (FAB): *m/z* 502 $[M\text{-}NCMe\text{-}H]^+$. IR: ν(C=N) 1606 cm^{-1}.

Preparation of [Rh(NCMe){C_6H_4-2-C(H)=N(CH_2)$_3$OMe-$_K$*C,N*}Cp*][PF_6] (4.22b)

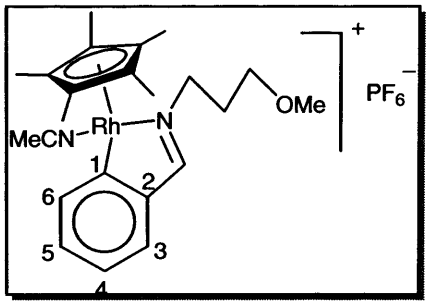

This was prepared from **(3.31b)** (120 mg, 0.27 mmol), KPF_6 (98 mg, 0.53 mmol); after stirring overnight, **(4.22b)** was isolated as a yellow solid (140 mg, 87.5%). Calc. for $C_{23}H_{32}N_2ORhPF_6$: C, 46.00, H, 5.33, N, 4.66. Found: C, 46.53, H, 5.52, N, 4.55%. ^{1}H NMR: δ 1.70 (s, 15H, Cp*), 1.85 (m, 1H, CH_2), 2.20 (m, 1H, CH_2), 2.20 (s, 3H, NCMe), 3.35 (s, 3H, OMe), 3.44 (m, 1H, C*H*H`O), 3.53 (m, 1H, CH*H*`O), 3.92 (m, 1H, NC*H*H`), 4.10 (m, 1H, NCH*H*`), 7.16 (dt, 1H, *J* 7.5, 1, H^4), 7.31 (dt, 1H, *J* 7.5, 1, H^5), 7.52 (dd, 1H, *J* 7.5, 1.5, H^3), 7.72 (d, 1H, *J* 7.5, H^6), 8.23 (d, 1H, J_{RhH} 4, HC= N). ^{13}C NMR: δ 3.47 (NC*Me*), 9.35 (C_5*Me*$_5$), 29.96 (CH_2), 58.78 (CH_2O), 58.93 (OMe), 69.36 (NCH_2), 98.30 (d, J_{RhC} 7, C_5Me_5), 123.65 (N*C*Me), 124.55, 129.34, 132.03, 135.53 (C^3, C^4, C^5, C^6), 145.76 (C^2), 175.52 (HC=N), C^1Rh (not observed). MS (FAB): *m/z* 414 $[M\text{-}NCMe]^+$. IR: ν(C=N) 1614 cm^{-1}.

Preparation of [Ir(NCMe){C_6H_4-2-C(H)=NPh-$_K$*C,N*}Cp*][PF_6] (4.23a)

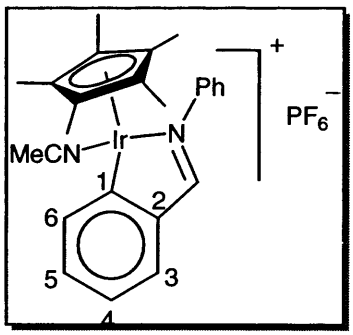

This was prepared from **(3.32a)** (130 mg, 0.24 mmol), KPF_6 (130 mg, 0.71 mmol); after stirring for 24 h, **(4.23a)** was isolated as an orange precipitate (120 mg, 72%). Calc. For $C_{25}H_{28}IrN_2PF_6$(1 equiv. CH_2Cl_2): C, 40.10, H, 3.85, N, 3.60. Found: C, 39.57, H, 3.10, N, 3.03%. ^{1}H NMR: δ 1.51 (s, 15H, Cp*), 2.49 (s, 3H, NCMe), 7.19 (dt,

1H, *J* 7.5, 1, H^4), 7.30 (dt, 1H, *J* 7.5, 1.5, H^5), 7.40 (m, 3H, Ph), 7.56 (m, 2H, Ph), 7.73 (dd, 1H, *J* 7.5, 1, H^3), 7.80 (d, 1H, *J* 7.5, H^6), 8.42 (s, 1H, HC=N). ^{13}C NMR: δ 3.72 (NC*Me*), 8.61 (C_5Me_5), 91.93 (C_5Me_5), 120.06 (NCMe), 122.31, 124.07, 128.58, 130.11, 130.82, 133.61, 135.00 (C^3, C^4, C^5, C^6 and Ph), 147.42 (C^2), 149.83 (Ph), 163.67 (C^1Ir), 178.13 (HC=N). MS (FAB): *m/z* 549 $[M]^+$, 508 $[M\text{-}NCMe]^+$. IR: ν(C=N) 1583 cm^{-1}.

Preparation of [Ir(NCMe){C_6H_4-2-CH_2NMe_2-$_K$*C,N*}Cp*][PF_6] (4.24a)

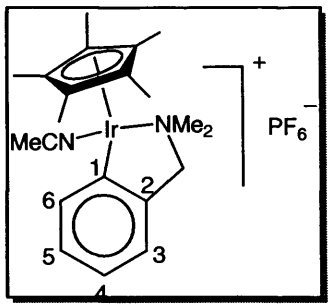

This was prepared from (**3.36a**) (150 mg, 0.30 mmol), KPF_6 (111 mg, 0.60 mmol); after stirring for 23 h, (**4.24a**) was isolated as a yellow precipitate (160 mg, 82%). Calc. for $C_{21}H_{30}N_2IrPF_6$: C, 38.94, H, 4.67, N, 4.33. Found: C, 39.15, H, 4.73, N, 4.36%. ^{1}H NMR: δ 1.67 (s, 15H, Cp*), 2.56 (s, 3H, NCMe), 2.91 (br, 6H, N*MeMe*`), 3.80 (s, 2H, NC*HH*`), 6.99 (dt, 1H, *J* 7, 1, H^4), 7.05 (dt, 1H, *J* 7, 2, H^5), 7.13 (dd, 1H, *J* 7, 1.5, H^3), 7.43 (dd, 1H, *J* 7, 1, H^6). ^{13}C NMR: δ 3.87 (NCMe), 9.25 (C_5Me_5), 53.66 (br, 2 × NMe), 76.39 (NCH_2), 90.90 (C_5Me_5), 120.37 (NCMe), 122.60, 124.00, 127.59, 134.94 (C^3, C^4, C^5, C^6), 146.99 (C^2), 149.54 (C^1Ir). MS (FAB): *m/z* 460 $[M\text{-}NCMe\text{-}H_2]^+$.

Preparation of [Ir(NCMe){C_6H_4-2-Me_2oxaz)-$_K$*C,N*}Cp*][PF_6] (4.25a)

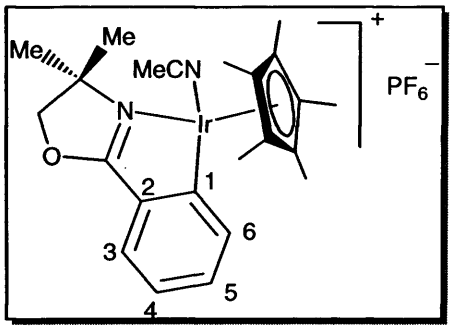

This was prepared from (**3.37a**) (70 mg, 0.13 mmol), KPF_6 (55 mg, 0.30 mmol); after stirring overnight, (**4.25a**) was isolated as a yellow precipitate (75 mg, 83.3%). Calc. for $C_{23}H_{30}IrN_2OPF_6$: C, 40.17, H, 4.40, N, 4.07. Found: C, 40.29, H, 4.37, N, 3.97%. ^{1}H NMR: δ 1.47 (br, 6H, 2x Me), 1.80 (s, 15H, Cp*), 2.42 (br, 3H, NCMe), 4.58 (s, 2H, CH_2), 7.15 (dt, 1H, *J* 7.5, 1, H^4), 7.33 (dt, 1H, *J* 7, 1.5, H^5), 7.48 (dd, 1H, *J* 7.5, 1.5, H^3), 7.75 (d, 1H, *J* 7.5, H^6). ^{13}C NMR: δ 3.45 (NCMe), 9.87 (C_5Me_5), 27.00 (Me), 28.27 (Me), 67.96 (CMe_2), 82.78 (OCH_2), 90.96 (C_5Me_5), 119.64 (NCMe), 123.74, 127.36, 133.38, 135.20 (C^3, C^4, C^5, C^6), 156.64 (NCO), 179.26(C^1Ir). MS (FAB): *m/z*. 502 $[M\text{-}NCMe]^+$. IR: ν(C=N) 1622 cm^{-1}.

Preparation of [Rh(NCMe){C_4H_3N-2-C(H)=N(3,5-$Me_2C_6H_3$)-$_K$N,N}(η-C_5Me_5)][PF_6] (4.26b)

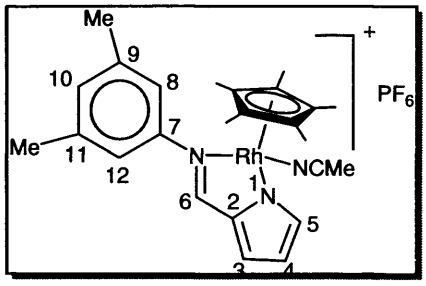

This was prepared from (**3.41b**) (70 mg, 0.15 mmol), KPF_6 (82 mg, 0.45 mmol); after stirring for 23 h, (**4.26b**) was isolated as a brown precipitate (75 mg, 82%). Calc. for $C_{25}H_{31}N_3RhPF_6$: C, 48.32, H, 5.03, N, 6.76. Found: C, 48.12, H, 4.98, N, 6.73%. ^{1}H NMR: δ 1.55 (s, 15H, Cp*), 2.29 (s, 3H,

NCMe), 2.41 (s, 6H, 2x Me), 6.43 (dd, 1H, *J* 4, 2, H^4), 6.88 (d, 1H, *J* 7.5, H^3), 6.90 (s, 2H, H^8, H^{12}), 6.96 (s, 1H, H^{10}), 7.33 (s, 1H, H^5), 7.75 (s, 1H, HC=N). ^{13}C NMR: δ 3.38 (NCMe), 8.91 (C_5Me_5), 21.41 (2x Me), 97.29(d, J_{RhC} 7.5, C_5Me_5), 114.79 (C^4), 119.64 (C^3), 120.66 (C^8, C^{12}), 122.93 (NCMe), 128.88 (C^{10}), 137.14 (C^5), 139.81 (C^9, C^{11}), 140.97 (C^2), 149.38 (C^7), 157.75 (N=CH). MS (FAB): *m/z* 435 $[M\text{-}NCMe]^+$. IR: ν(C=N) 1595 cm^{-1}.

Preparation of [Ru(NCMe){C_4H_3N-2-C(H)=N(3,5-$Me_2C_6H_3$)-$_K$N,N}(η-*p*-cymene)][PF_6] (4.26c)

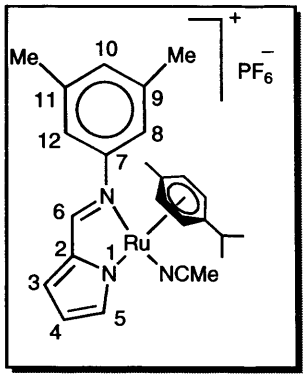

This was prepared from **(3.41c)** (100 mg, 0.21 mmol), KPF_6 (118 mg, 0.64 mmol); after stirring overnight, **(4.26c)** was isolated as a yellow precipitate (100 mg, 76%). Calc. for $C_{25}H_{30}N_3RuPF_6$: C,48.54, H, 4.89, N, 6.79. Found: C, 48.50, H, 4.71, N, 6.61%. ^{1}H NMR: δ 1.05 (d, 3H, *J* 7, CH*Me*Me`), 1.09 (d, 3H, *J* 7, CHMe*Me*`), 2.13 (s, 3H, Cy-*Me*), 2.33 (s, 3H, NCMe), 2.44 (s, 6H, 2x Me(Ar)), 2.56 (sept, 1H, *J* 7, C*H*MeMe`), 5.36 (d, 1H, *J* 6, Cy), 5.41 (d, 1H, *J* 6, Cy), 5.57 (d, 1H, *J* 6, Cy), 5.84 (d, 1H, *J* 6, Cy), 6.39 (dd, 1H, *J* 4, 1.5, H^4), 6.85 (d, 1H, *J* 4, H^3), 6.99 (s, 1H, H^{10}), 7.03 (s, 2H, H^8, H^{12}), 7.52 (s, 1H, H^5), 7.67 (s, 1H, HC=N). ^{13}C NMR: δ 3.72 (NCMe), 18.63 (*Me*C_6H_4), 21.43 (2x*Me*Ph), 21.98, 22.60 (2xMe (^{i}Pr)), 31.04 (CH (^{i}Pr)), 85.43, 85.64, 85.86, 86.89 (CH (C_6H_4 Cy)), 102.16, 104.70 (C(C_6H_4 Cy)), 115.07, 119.55, 135.70 (C^3,C^4, C^5), 120.30 (C^8, C^{12}), 124.34 (NCMe), 129.14 (C^{10}), 139.98 (C^9, C^{11}), 141.15(C^2), 153.16 (C^7), 157.93 (N=CH). MS (FAB): *m/z* 468 $[M\text{-}NCMe+Cl]^+$, 433 $[M\text{-}NCMe]^+$. IR: ν(C=N) 1590 cm^{-1}.

Preparation of [Ir(NCMe){C_4H_3N-3-CH_3-2-C(H)=N(3,5-$Me_2C_6H_3$)-kC,N}(η-C_5Me_5)][PF_6] (4.27a)

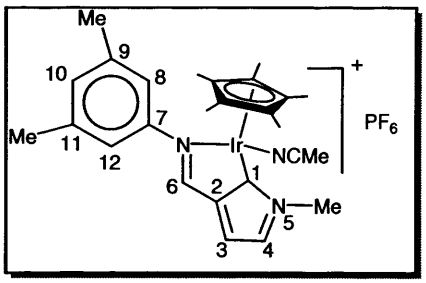

This was prepared from **(3.48a)** (70 mg, 0.12 mmol), KPF_6 (67 mg, 0.36 mmol); after stirring 22 hours, **(4.27a)** was isolated as an orange precipitate (70 mg, 80%). Calc. for $C_{26}H_{33}N_3IrPF_6$: C, 43.09, H, 4.59, N, 5.80. Found: C, 42.93, H, 4.67, N, 5.72%. ^{1}H NMR: δ 1.59 (s, 15H, Cp*), 2.39 (s, 6H, 2x Me), 2.50 (NCMe), 3.86 (s, 3H, NMe), 6.36 (d, 1H, *J* 2, H^5), 6.89 (m, 4H, H^4, H^8, H^{10}, H^{12}), 7.90 (s, 1H, HC=N). ^{13}C NMR: δ 3.93 (NCMe), 8.99 (C_5Me_5), 21.42 (2x Me), 35.14 (NMe) 90.97 (C_5Me_5), 113.43 (C^5), 119.40 (N*C*Me), 120.01 (C^8, C^{12}), 128.56 (C^{10}), 132.79 (C^4), 139.53 (C^9, C^{11}), 145.11 (C^2), 150.60 (C^7), 158.21 (N=CH), 150.93 (C^1). MS (FAB): *m/z* 539 $[M\text{-}NCMe]^+$. IR: ν(C=N) 1596 cm^{-1}.

General procedure for CO cationic reactions

CO gas was bubbled into a solution of the cationic cyclometallated NCMe complex in $CDCl_3$. The mixture was stirred for ½-1 h, then the sample analysed by NMR. The solution was evaporated to dryness to give the products. The compounds could be recrystallised from dichloromethane–hexane.

Preparation of [Ir(CO){C_6H_4-2-C(H)-N(CH_2)$_2$$OCH_3$-$\kappa C,N$}Cp*][$PF_6$] (4.28a)

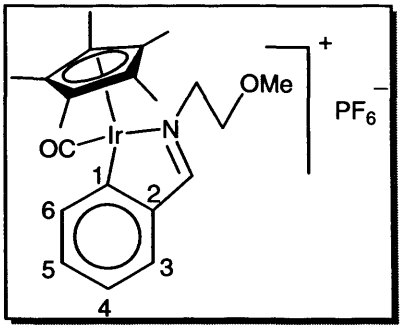

This was prepared from **(4.21a)** (40 mg, 0.06 mmol); after stirring for ½ h, **(4.28a)** was isolated as a yellow precipitate (34 mg, 85%). Calc. for $C_{21}H_{27}NO_2IrPF_6$: C, 38.06, H, 4.11, N, 2.11. Found: C, 38.14, H, 4.21, N, 1.99%. ^{1}H NMR: δ 1.97 (s, 15H, Cp*), 3.30 (s, 3H, OMe), 3.68 (m, 2H, CH_2O), 3.90 (m, 1H, NCH_2), 4.17 (m, 1H, NCH_2), 7.31 (m, 2H, H^4, H^5), 7.55 (d, 1H, *J* 7, H^3), 7.78 (d, 1H, *J* 6.5, H^6), 8.47 (s, 1H, HC=N). ^{13}C NMR: δ 9.20 (C_5Me_5), 58.70 (OMe), 62.34 (CH_2O), 69.92 (NCH_2), 101.61 (C_5Me_5), 125.97, 131.43, 133.38, 135.83 (C^3, C^4, C^5, C^6), 147.13 (C^2), 151.43 (C^1Ir), 164.47 (CO), 182.33 (HC=N). MS (FAB): *m/z* 518 $[M]^+$, 490 $[M-CO]^+$. IR: ν(C≡O) 2033 cm^{-1}.

Preparation of [Ir(CO){C_6H_4-2-C(H)-N(CH_2)$_3$$OCH_3$-$\kappa C,N$}Cp*][$PF_6$] (4.30a)

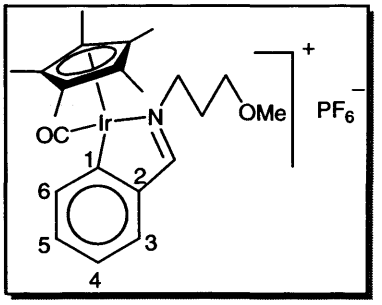

This was prepared from **(4.22a)** (40 mg, 0.06 mmol); after stirring for 1 h, **(4.30a)** was isolated as a yellow precipitate (36 mg, 92%). Calc. for $C_{22}H_{29}NO_2IrPF_6$: C, 39.05, H, 4.32, N, 2.07. Found: C, 39.14, H, 4.19, N, 2.14%. ^{1}H NMR: δ 1.80 (m, 1H, C*H*H`), 1.95 (s, 15, Cp*), 2.10 (m, 1H, CH*H*`), 3.28 (s, 3H, OMe), 3.40 (m, 2H, CH_2O), 3.85 (m, 1H, NC*H*H`), 4.08 (m, 1H, NCH*H*`), 7.31 (m, 2H, H^4, H^5), 7.56 (dd, 1H, *J* 7, 1.5, H^3), 7.80 (dd, 1H, *J* 7, 2, H^6), 8.55 (s, 1H, HC=N). ^{13}C NMR: δ 9.14 (C_5Me_5), 30.43 (CH_2), 58.91 (OMe), 60.85 (CH_2O), 68.87 (NCH_2), 101.79 (C_5Me_5), 126.07, 131.44, 133.39, 135.79 (C^3, C^4, C^5, C^6), 147.24 (C^2), 151.14 (C^1Ir), 164.78 (CO), 181.67 (HC=N). MS (FAB): *m/z* 532 $[M]^+$, 504 $[M-CO]^+$. IR: ν(C≡O) 2032cm^{-1}. ν(C=N) 1607 cm^{-1}.

Preparation of [Rh(CO){C_6H_4-2-C(H)-N(CH_2)$_3$$OCH_3$-$\kappa C,N$}Cp*][$PF_6$] (4.30b)

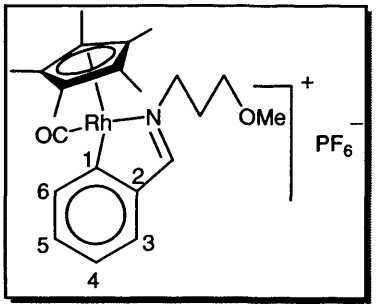

This was prepared from **(4.22b)** (43 mg, 0.07 mmol); after stirring for 1 h, **(4.30b)** was isolated as a red precipitate (35 mg, 83%). Calc. for $C_{22}H_{29}NO_2RhPF_6$(1 equiv. Of CH_2Cl_2): C, 41.07, H, 4.62, N, 2.08. Found: C, 41.04, H, 5.27, N, 2.38%. ^{1}H NMR: δ

1.78 (m, 1H, C*H*H`), 1.87 (s, 15, Cp*), 2.06 (m, 1H, CH*H*`), 3.28 (s, 3H, OMe), 3.41 (m, 2H, CH_2O), 3.90 (m, 2H, NCH_2), 7.28 (dt, 1H, J 7, 1, H^4), 7.39 (dt, 1H, J 7.5, 2, H^5), 7.53 (d, 1H, *J* 7.5, H^3), 7.71 (dd, 1H, *J* 7.5, 1.5, H^6), 8.35 (d, 1H, J_{RhH} 4, HC=N). ^{13}C NMR: δ 9.57 (C_5Me_5), 30.64 (CH_2), 58.90 (OMe), 59.22 (CH_2O), 69.17 (NCH_2), 106.30 (d, J_{RhC} 4, C_5Me_5), 126.36, 131.49, 132.97, 136.41 (C^3, C^4, C^5, C^6), 145.58 (C^2), 169.65 (d, J_{RhC} 28, C^1), 177.41 (N=CH), 185.40 (d, J_{RhC} 74, CO). MS (FAB): *m/z* 442 $[M]^+$, 414 $[M\text{-}CO]^+$. IR: ν(C≡O) 2060cm^{-1}. ν(C=N) 1612 cm^{-1}.

Preparation of [Ir(CO){C_6H_4-2-CH_2NMe_2-$_K$*C,N*}Cp*][PF_6] (4.32a)

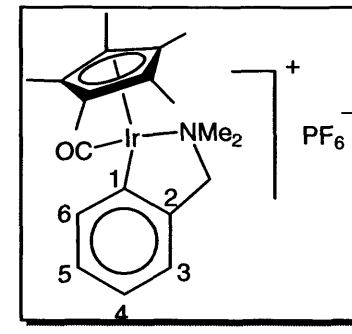

This was prepared from (**4.24a**) (35 mg, 0.05 mmol); after stirring for 1/2 h, (**4.32a**) was isolated as a yellow precipitate (33 mg, 96.2%). Calc. for $C_{20}H_{27}NOIrPF_6$: C, 37.85, H, 4.29, N, 2.21. Found: C, 37.64, H, 4.49, N, 2.17%. ^1H NMR: δ 1.92 (s, 15H, Cp*), 3.13 (s, 3H, N*Me*Me`), 3.21 (s, 3H, NMe*Me*`), 3.82 (d, 1H, *J* 14, NC*H*H`), 4.05 (d, 1H, *J* 14, NCH*H*`), 7.12 (m, 2H, H^4, H^5), 7.28 (m, 2H, H^3, H^6). ^{13}C NMR: δ 9.43 (C_5Me_5), 57.45 (N*Me*Me`), 61.07 (NMe*Me*`), 77.23 (NCH_2), 101.88 (C_5Me_5), 124.10, 126.24, 128.69, 136.53 (C^3, C^4, C^5, C^6), 138 (C^2), 146.28 (C^1), 170.04 (CO). MS (FAB): *m/z* 490 $[M]^+$. ν(C≡O) 2034cm^{-1}.

Preparation of [IrN(CO){C_6H_4-2-Me_2oxaz)-$_K$*C,N*}Cp*][PF_6] (4.33a)

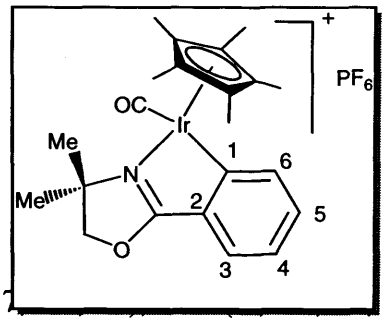

This was prepared from (**4.25a**) (42 mg, 0.62 mmol); after stirring for 1½ h, (**4.33a**) was isolated as a yellow precipitate (38 mg, 92.3.3%). Calc. for $C_{22}H_{27}IrN_2O_2PF_6$: C, 39.17, H, 4.03, N, 2.08. Found: C, 39.05, H, 3.96, N, 1.97%. ^1H NMR: δ 1.30 (s, 3H, Me), 1.50 (s, 3H, Me), 2.00 (s, 15H, Cp*), 4.20 (d, 1H, *J* 5, C*H*H`) 4.22 (d, 1H, *J* 5, CH*H*`), 7.30 (dt, 1H, *J* 7.5, 1, H^4), 7.43 (dt, 1H, *J* 7 H^6). ^{13}C NMR: δ 10.05 (C_5Me_5), 27.05 (Me), 27.85 (Me), 69.20 (CMe_2), 81.99 (OCH_2), 102.17 (C_5Me_5), 126.01, 129.12, 134.42, 136.27 (C^3, C^4, C^5, C^6), 144.76 (C^2), 165.52 (CO), 180.44 (C^1Ir). MS (FAB):*m/z*. 530 $[M]^+$, 502 $[M\text{-}CO]^+$. IR: ν(C≡O) 2042cm^{-1}. ν(C=N) 1614 cm^{-1}.

General procedure for ethylene reactions

Ethene (1 atm) was bubbled into a solution of cyclometallated NCMe complexes in CH_2Cl_2 for ½ h. The mixture was stirred for several hours. The solution was evaporated to dryness to give ethylene-containing cationic products. The compounds could be recrystallised from dichloromethane/hexane.

Preparation of [Ir(η^2-C_2H_4){C_6H_4-2-C(H)=N(CH_2)$_2$OCH_3-$_K$*C,N*}Cp*][PF_6] (4.34a)

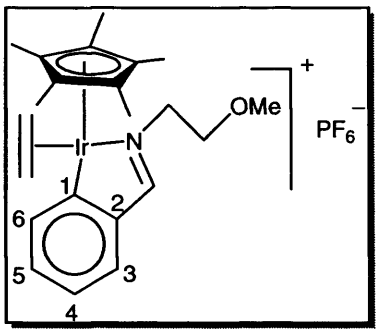

This was prepared from **(4.21a)** (60 mg, 0.11 mmol); after stirring overnight, **(4.34a)** was isolated as a brown precipitate (42 mg, 72.5%). Calc. for $C_{22}H_{31}NOIrPF_6$: C, 39.87, H, 4.72, N, 2.11. Found: C, 39.84, H, 4.62, N, 2.07%. ^{1}H NMR: δ 1.71 (s, 15H, Cp*), 3.03 (t, 2H, *J* 4.5, CH_2CH_2), 3.10 (t, 2H, *J* 4.5, CH_2CH_2), 3.34 (s, 3H, OMe), 3.77 (m, 2H, CH_2O), 4.15 (m, 2H, NCH_2), 7.14 (dt, 1H, *J* 7.5, 1, H^4), 7.17 (dt, 1H, *J* 7.5, 1.5, H^5), 7.52 (d, 1H, *J* 7.5, H^3), 7.65 (dd, 1H, *J* 7.5, 1.5, H^6), 8.32 (s, 1H, HC=N). ^{13}C NMR: δ 8.47 (C_5Me_5), 52.47 (CH_2CH_2), 58.94 (OMe), 62.33 (CH_2O), 70.21 (NCH_2), 100.07 (C_5Me_5), 124.64, 130.57, 132.11, 135.62 (C^3, C^4, C^5, C^6), 146.19 (C^2), 160.93 (C^1Ir), 178.71 (HC=N). MS (FAB): *m/z* 518 $[M]^+$, 490 $[M-CH_2CH_2]^+$. IR: ν(C=N) 1604 cm^{-1}.

Preparation of [Ir(η^2-C_2H_4){C_6H_4-2-C(H)=N(CH_2)$_3$OCH_3-$_K$*C,N*}Cp*][PF_6] (4.36a)

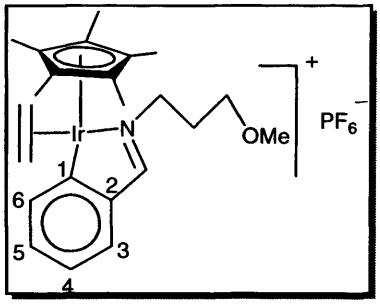

This was prepared from **(4.22a)** (70 mg, 0.10 mmol); after stirring overnight, **(4.36a)** was isolated as a brown precipitate (60 mg, 87%). Calc. for $C_{23}H_{33}NOIrPF_6$: C, 40.82, H, 4.92, N, 2.07. Found: C, 39.95, H, 3.87, N, 1.99%. ^{1}H NMR: δ 1.62 (s, 15H, Cp*), 2.11 (m, 2H, CH_2), 2.90 (t, 2H, *J* 4.5, CH_2CH_2), 2.98 (t, 2H, *J* 4.5, CH_2CH_2), 3.28 (s, 3H, OMe), 3.46 (m, 2H, CH_2O), 4.00 (m, 2H, NCH_2), 7.06 (dt, 1H, *J* 7.5, 1, H^4), 7.16 (dt, 1H, *J* 7.5, 1.5, H^5), 7.46 (d, 1H, *J* 7.5, H^3), 7.60 (dd, 1H, *J* 7.5, 1.5, H^6), 8.25 (s, 1H, HC=N). ^{13}C NMR: δ 8.49 (C_5Me_5), 30.62 (CH_2), 51.80 (CH_2CH_2), 58.93 (OMe), 60.43 (CH_2O), 69.33 (NCH_2), 100.21 (C_5Me_5), 124.74, 130.52, 132.13, 135.55 (C^3, C^4, C^5, C^6), 146.11 (C^2), 160.57 (C^1Ir), 177.82 (HC=N). MS (FAB): *m/z* 530 $[M]^+$, 502 $[M-CH_2CH_2]^+$. IR: ν(C=N) 1604 cm^{-1}.

General procedure for alkyne insertions

Insertion of alkyne into cyclometallated complexes can be synthesized by two methods:

Method **(A)** KPF_6 and appropriate alkyne were added to a solution of cyclometallated chloride complexes in acetonitrile (10-15 ml). The mixture was stirred or refluxed for several hours, then

filtered through Celite to remove excess KPF_6. The filtrate was evaporated to dryness and then washed with hexane to give the insertion complexes.

Method **(B)** the appropriate alkyne was added to a solution of the cyclometallated acetonitrile complexes in dichloromethane (1–20 ml). The mixture was stirred or refluxed for several hours. The solution was evaporated to dryness and then washed with hexane to give the insertion complexes. Some of these were usually pure at this stage but the compounds, which showed evidence for mixtures by ^1H NMR spectroscopy could be purified by washing through silica (DCM/NCMe). The compounds could be recrystallised from dichloromethane–hexane. Details of individual reactions are shown below.

Preparation of (4.38a)

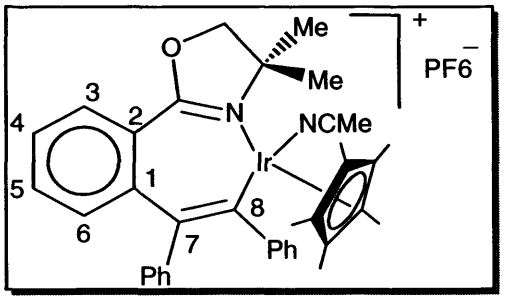

This was prepared by method **(A)**; PhC≡CPh (67 mg, 0.38 mmol), KPF_6 (103 mg, 0.56 mmol) were added to solution of **(3.37a)** (100 mg, 0.19 mmol) in acetonitrile; after stirring for 72 h, no insertion was observed by ESMS, then acetonitrile was replaced by dichloromethane. The solution was stirred for 24 h. **(4.38a)** was isolated as a yellow precipitate (122 mg, 76%). Calc. for $C_{37}H_{40}IrN_2OPF_6$: C, 51.32, H, 4.66, N, 3.24. Found: C, 51.12, H, 4.53, N, 3.31%. ^1H NMR: δ 1.31 (s, 3H, C*Me*Me`), 1.37 (s, 3H, CMe*Me*`), 1.41 (s, 15H, Cp*), 2.00 (s, 3H, NCMe), 4.27 (d, 1H, *J* 9, OC*H*H`), 4.58 (d, 1H, *J* 9, OCH*H*`), 6.30 (br, 1H, H^6), 6.76 (m, 4H, Ph), 6.99 (m, 5H, Ph), 7.24 (m, 2H, H^4, Ph), 7.31 (dt, 1H, *J* 7.5, 1.5, H^5), 7.72 (dd, 1H *J* 7.5, 1, H^3). ^{13}C NMR: δ 2.35 (NCMe), 8.74 (C_5Me_5), 24.64, 27.57 (2xMe), 72.31 (*C*MeMe`), 81.50 (CH_2), 91.66 (C_5Me_5), 124.80 (NCMe), 124.17, 125.32, 125.95, 127.52, 128.12, 131.72 132.40, 134.14 (Ar-H), 141.88 (C^2), 146.3, 147.91 (C^1, C^7), 151.38 (^iC, Ph of alkyne), 152.40 (C^8), 169.16 (CNO). MS (FAB): *m/z* 679 $[M\text{-NCMe}]^+$. IR: ν(C=N) 1624 cm^{-1}.

Preparation of (4.38c)

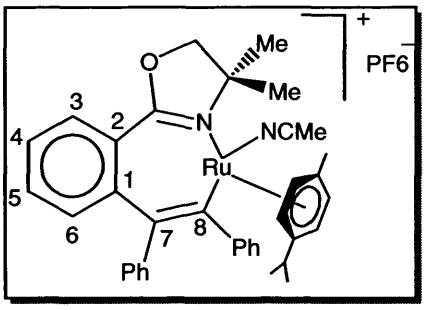

This was prepared by **method (B)**; PhC≡CPh (33 mg, 0.19 mmol) was added to solution of **(3.40c)** (100 mg, 0.17 mmol) in dichloromethane; after stirring for 24 h, **(4.38c)** was isolated and washed over silica (DCM/NCMe) to give a pure complex as a green precipitate (66 mg, 51%). Calc. for $C_{37}H_{39}RuN_2OPF_6$: C, 57.43, H, 5.08, N, 3.62. Found: C, 55.81, H, 4.67, N, 3.29%. ^1H NMR: δ 1.09 (s, 3H, oxz Me), 1.11 (d, 1H, *J* 7, CH*Me*Me`), 1.31 (d, 1H, *J* 7, CHMe*Me*`), 1.59 (s, 3H, oxz Me), 1.78 (s, 3H, NCMe), 2.27 (s, 3H, Me-Cy), 2.90 (sept, 1H *J* 7, C*H*MeMe`), 4.34 (d, 1H,

J 9, OC*H*H`), 4.35 (d, 1H, *J* 6, Cy), 4.47 (d, 1H, *J* 9, OCH*H*`), 4.54 (d, 1H, *J* 6, Cy), 5.10 (d, 1H, *J* 6, Cy), 5.65 (d, 1H, *J* 6, Cy), 6.18 (d, 1H, *J* 8, H^6), 6.73 (t, 1H, *J* 7.5, Ph), 6.83 (m, 3H, Ph), 6.96 (m, 3H, Ph), 7.14 (d, 1H, *J* 7.5, Ph), 7.31 (m, 3H, H^4, Ph), 7.38 (dt, 1H, *J* 7.5, 1.5, H^5), 7.62 (dd, 1H, *J* 7.5, 1, H^3). ^{13}C NMR: δ 2.99 (NCMe), 19.57 (Me-Cy), 22.74, 24.45 (CH*MeMe*`), 25.44, 28.28 (2xMe), 31.61 CH(^{i}Pr)), 71.08 (CMe_2), 81.57 (OCH_2), 80.32, 85.32, 88.09, 91.28 (CH(C_6H_4)), 109.46, 112.61 (C(C_6H_4), 126.46 (NCMe), 124.32, 125.57, 126.25, 127.80, 128.49, 131.80 132.02, 133.58, (Ar-H),141.87 (C^2), 145.92, 148.88 (C^1, C^7), 151.54 (^{i}C, Ph of alkyne), 168.64 (C^9), 171.46 (C^8). MS (FAB): *m/z* 588 $[M\text{-}NCMe]^+$. IR: ν(C=N) 1602 cm^{-1}.

Preparation of (4.40a)

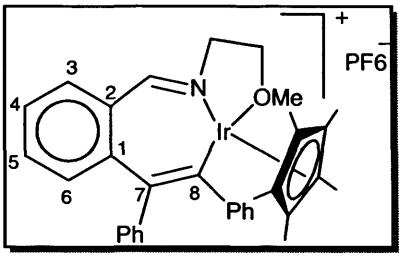

This was prepared by **method (B)**; PhC≡CPh (11 mg, 0.23 mmol) was added to solution of **(4.21a)** (40 mg, 0.06 mmol) in dichloromethane; after stirring for 30 h, **(4.40a)** was isolated as a yellow precipitate (105 mg, 85.5%). Calc. for $C_{34}H_{37}IrNOPF_6$: C, 50.24, H, 4.59, N, 1.72. Found: C, 50.00, H, 4.47, N, 1.64%. ^1H NMR: δ 1.39 (s, 15H, Cp*), 2.48 (s, 3H, OMe), 3.21 (m, 1H, C*H*H`O), 3.32 (m, 1H, CH*H*`O), 4.13 (m, 2H, NCH_2), 6.72 (m, 2H, Ph), 6.97 (m, 6H, H^4, H^5, Ph), 7.29 (m, 5H, H^6, Ph), 7.59 (m, 1H, H^3), 9.14 (s, 1H, HC=N). ^{13}C NMR: δ 9.04 (C_5Me_5), 61.53 (OMe), 65.51 (CH_2O), 73.14 (NCH_2), 89.18 (C^9), 99.07 (C_5Me_5), 125.45, 126.37, 127.52, 128.63, 131.37, 131.94, 132.26, 132.10, 134.13 (Ar-H), 141.86 (C^2), 144.65, 145.65 (C^1, C^7), 149.49 (^{i}C, Ph), 158.93 (C^8), 170.84 (HC=N). MS (FAB): *m/z* 668 $[M]^+$. IR: ν(C=N) 1595 cm^{-1}.

Preparation of (4.40b)

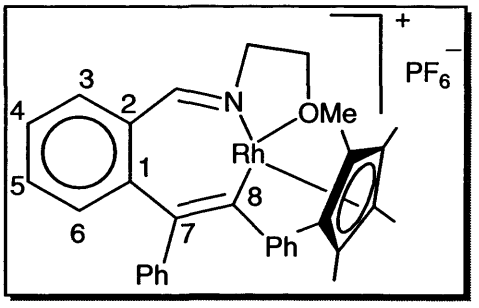

This was prepared by **method (B)** in an NMR tube; PhC≡CPh (5.2 mg, 0.03 mmol) was added to solution of **(4.21b)** (16 mg, 0.03 mmol) in $CDCl_3$; after stirring for 30 h, **(4.40b)** was isolated as a yellow precipitate (18 mg, 85%).. ^1H NMR: δ 1.36 (s, 15H, Cp*), 2.35 (s, 3H, OMe), 3.04 (m, 1H, C*H*H`O), 3.43 (m, 1H, CH*H*`O), 4.05 (m, 1H, NC*H*H`), 4.23 (m, 1H, NCH*H*`), 6.75 (m, 2H, Ph), 6.95 (m, 4H, H^4, H^5, Ph), 7.08 (m, 1H, Ph), 7.33 (m, 5H, H^6, Ph), 7.53 (m, 1H, Ph), 7.64 (m, 1H, H^3), 9.14 (d, 1H, *J* 3, HC=N). MS (FAB): *m/z* 578 $[M]^+$. IR: ν(C=N) 1596 cm^{-1}.

Reaction of (3.32a) and (4.21a) with PhC≡CPh

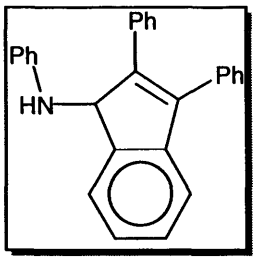

This was prepared by method **(A)** and **(B)**; **(A)** PhC≡CPh (23.7 mg, 0.13 mmol) was added to solution of **(3.32b)** (60 mg, 0.13 mmol) in dichloromethane; after stirring for 20 mins; $(ES)^+$ showed an ion at *m/z* 358. The solution was stirred for 8 h and then the solvent exchanged by NCMe and refluxed for 18 h. The solution was evaporated to dryness and washed with hexane to give a light brown hexane soluble and a deep brown insoluble fraction. The latter was washed through silica, however, no pure fraction could be isolated. **(4.43)** was then isolated from the hexane soluble fraction as an orange solid (24 mg, 50%). **(B)** Diphenylacetylene (51.4 mg, 0.29 mmol) was added to solution of **(4.21a)** (100 mg, 0.14 mmol) in dichloromethane; after refluxing for 20 mins, **(4.43)** was isolated as an orange solid (23 mg, 45%), Calc. for $C_{27}H_{21}N$: C, 90.21, H, 5.89, N, 3.90. Found: C, 90.03, H, 5.81, N, 3.80%. ^1H NMR: δ 3.90 (br, 1H NH), 5.65 (S, 1H, CH), 6.70-7.60 (19H, 4xPh). MS (FAB): *m/z* 358 $[M]^+$.

Preparation of (4.44a)

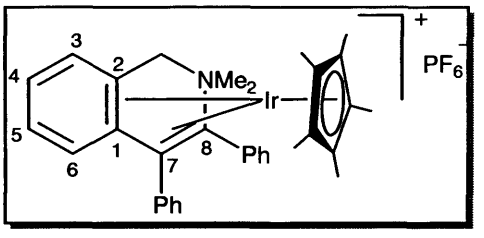

This was prepared by method **(A)**; PhC≡CPh (25 mg, 0.14 mmol), KPF_6 (52 mg, 0.28 mmol) were added to solution of **(3.36a)** (70 mg, 0.14 mmol) in acetonitrile; after stirring overnight, **(4.44a)** was isolated as a yellow precipitate (95 mg, 85%). Calc. for $C_{33}H_{37}IrNPF_6$(1 equiv. Of CH_2Cl_2): C, 46.95, H, 4.49, N, 1.61. Found: C, 46.56, H, 4.80, N, 1.64%. ^1H NMR(CD_3CN): δ 1.28 (s, 15H, Cp*), 2.81 (s, 3H, N*Me*Me`), 3.20 (s, 3H, NMe*Me*`), 3.30 (d, 1H, *J* 11, C*H*H`), 4.42 (d, 1H, *J* 11, CH*H*`), 6.90 (m, 6H, Ph), 6.98 (d, 1H, *J* 7, H^6), 7.00 (d, 1H, *J* 7.5, H^3), 7.10 (m, 4H, Ph), 7.22 (dt, 1H, *J* 7, 1, H^4), 7.32 (dt, 1H, *J* 7, 1, H^5). ^{13}C NMR: δ 7.83 (C_5Me_5), 57.29 (N*Me*Me`), 57.91 (NMe*Me*`), 69.38 (CH_2), 91.96 (C_5Me_5), 123.24, 124.55, 124.85, 126.13, 126.66, 126.80, 127.92, 130.03, 131.05, 131.59 (Ar-H), 140.99 (C^2), 146.50, 148.11 (C^1, C^7), 132.98, 152.32 (^iC, Ph of alkyne), 153.71 (C^8). MS (FAB): *m/z* 639 $[M]^+$. 312 [isoquinolinium].

Preparation of (4.48a)

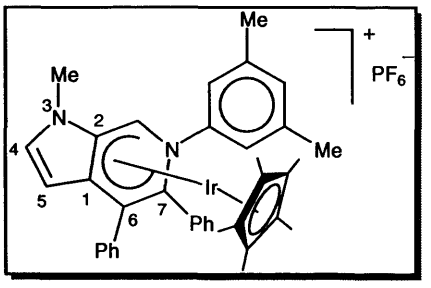

This was prepared by method **(B)**; PhC≡CPh (27 mg, 0.15 mmol) was added to solution of **(4.27a)** (100 mg, 0.14 mmol) in dichloromethane; after stirring for 3 h, **(4.48a)** was isolated and washed over silica (DCM/NCMe) to give a pure complex as a beige precipitate (50 mg, 42%). Calc. for $C_{38}H_{40}N_2IrPF_6$(1 equiv. Of $CHCl_3$): C, 47.73, H, 4.21, N, 2.85. Found: C, 47.63, H, 3.82, N, 2.31%. ^1H NMR: δ 1.59 (s, 15H, C_5Me_5), 2.15 (s, 6H, 2x Me), 3.84 (s, 3H, NMe), 5.85 (s, 1H, H^8). 5.96 (d, 1H, *J*

3.5, H^4), 6.24 (s, 2H, H^{10}, H^{14}), 6.41 (s, 1H, H^{12}), 7.19 (m, 5H, Ph), 7.61 (m, 5H, Ph), 7.75 (d, 1H, *J* 3.5, H^5). MS (FAB): *m/z* 715 $[M]^+$. 389 [N-Me pyrrole+PhC≡CPh].

Preparation of (4.49a)

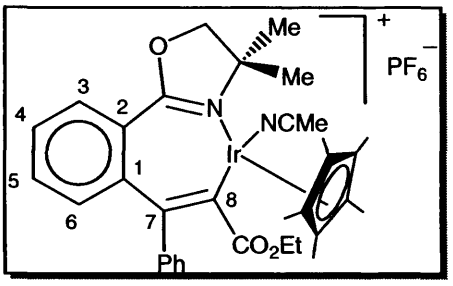

This was prepared by method **(B)**; $PhC{\equiv}CCO_2Et$ (21 mg, 0.12 mmol) was added to solution of **(4.25a)** (75 mg, 0.11 mmol) in dichloromethane; after stirring for 3 h, **(4.49a)** was isolated and washed over silica (DCM/NCMe) to give a pure complex as a beige precipitate (66 mg, 51%). Calc. for $C_{34}H_{40}IrN_2O_3PF_6$: C, 47.38, H, 4.68, N, 3.25. Found: C, 47.25, H, 4.63, N, 3.16%. ^{1}H NMR: δ 1.31 (s, 3H, C*Me*Me`), 1.38 (m, 3H, $CO_2CH_2CH_3$), 1.41 (s, 15H, Cp*), 1.46 (s, 3H, CMe*Me*`), 2.77 (s, 3H, NCMe), 3.79 (m, 2H, $CO_2CH_2CH_3$), 4.23 (d, 1H, *J* 9, OC*H*H`), 4.53 (d, 1H, *J* 9, OCH*H*`), 7.06 (m, 3H, Ph), 7.26 (m, 2H, H^4, H^6, Ph), 7.36 (m, 1H, H^5), 7.68 (dd, 1H, *J* 7.5, 1, H^3). ^{13}C NMR: δ 4.12 (NCMe), 8.53 (C_5Me_5), 14.15 ($CO_2CH_2CH_3$), 24.63, 27.24 (2xMe), 59.48 ($CO_2CH_2CH_3$), 72.79 (*C*MeMe`), 81.65 (OCH_2), 91.93 (C_5Me_5), 124.56 (NCMe), 126.67, 127.05, 128.22, 129.96 131.92, 132.52, 133.61 (Ar-H), 142.64 (C^8), 144.69 (C^1), 168.71 (CNO), (other quaternary carbons are not seen). MS (FAB): *m/z* 676 $[M\text{-NCMe}]^+$. IR: ν(C=N) 1624 cm^{-1}. ν(C=O) 1695 cm^{-1}.

Preparation of (4.50a)

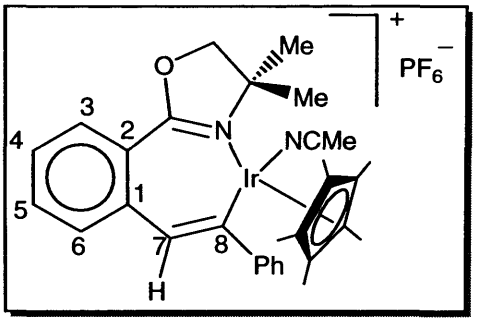

This was prepared by method **(A)** and method **(B)**; **(A)** PhC≡CH (18 mg, 0.18 mmol), KPF_6 (96 mg, 0.52 mmol) were added to solution of **(3.37a)** (93 mg, 0.17 mmol) in acetonitrile; after stirring for 4 h, **(4.50a)** was isolated as a yellow precipitate and washed over silica (DCM/NCMe) to give a pure complex (41 mg, 30%). **(B)** Phenylacetylene (11 mg, 0.11 mmol) was added to solution of **(4.25a)** (73 mg, 0.11 mmol) in dichloromethane; after stirring for 1 h, **(4.50a)** was isolated as a pale yellow precipitate (72 mg, 86%). Calc. for $C_{31}H_{36}IrN_2OPF_6$: C, 47.14, H, 4.59, N, 3.55. Found: C, 47.28, H, 4.37, N, 3.47%. ^{1}H NMR: δ 1.14 (s, 3H, C*Me*Me`), 1.29 (s, 3H, CMe*Me*`), 1.34 (s, 15H, Cp*), 1.99 (s, 3H, NCMe), 4.11 (d, 1H, *J* 9, OC*H*H`), 4.42 (d, 1H, *J* 9, OCH*H*`), 6.97 (m, 2H, Ph), 7.06 (m, 2H, H^7, Ph), 7.20 (m, 4H, H^4, H^6, Ph), 7.41 (dt, 1H, *J* 7.5, 1.5, H^5), 7.63 (dt, 1H *J* 8, 1.5, H^3). ^{13}C NMR: δ 2.67 (NCMe), 8.93 (C_5Me_5), 24.89, 27.33 (2xMe), 72.66 (CMeMe`), 81.08 (CH_2), 91.55 (C_5Me_5), 121.84 (NCMe), 122.97 (^{i}C, Ph), 125.82, 127.02, 125.82, 132.07, 132.11, 133.02 (Ar-H), 132.11 (C^7), 143.63 (C^1), 152.59 (^{i}C, Ph of alkyne), 155.68 (C^8), 169.00 (CNO). MS (FAB): *m/z* 602 $[M\text{-NCMe}]^+$. IR: ν(C=N) 1527 cm^{-1}.

Preparation of (4.50c)

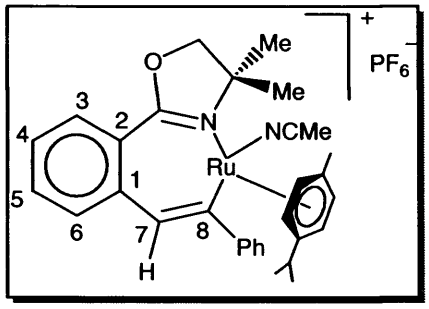

This was prepared by method **(B)**; PhC≡CH (33 mg, 0.33 mmol) was added to solution of **(3.40c)** (194 mg, 0.33 mmol) in dichloromethane; after stirring overnight, **(4.520c)** was isolated and washed over silica (DCM/NCMe) to give a pure complex as an orange precipitate (120 mg, 53%). Calc. for $C_{31}H_{35}RuN_2OPF_6$: C, 53.37, H, 5.06, N, 4.02. Found: C, 53.47, H, 5.01, N, 3.95%. ^{1}H NMR: δ 1.00 (s, 3H, oxz Me), 1.18 (d, 1H, *J* 7, CH*Me*Me`), 1.21 (d, 1H, *J* 7, CHMe*Me*`), 1.58 (s, 3H, oxz Me), 1.85 (s, 3H, NCMe), 2.06 (s, 3H, Me-Cy), 2.71 (sept, 1H *J* 7, C*H*MeM`), 4.32 (d, 1H, *J* 9, OC*H*H`), 4.35 (d, 1H, *J* 9, OCH*H*`), 4.39 (dd, 1H, *J* 6, 1, Cy), 5.03 (dd, 1H, *J* 6, 1, Cy), 5.35 (dd, 1H, *J* 6, 1, Cy), 5.41 (dd, 1H, *J* 6, 1, Cy), 7.12 (m, 4H, H^7, Ph), 7.29 (m, 4H, H^4, H^6, Ph), 7.50 (dt, 1H, *J* 7.5, 1.5, H^5), 7.68 (d, 1H, *J* 7.5, H^3). ^{13}C NMR: δ 3.05 (NCMe), 19.43 (Me-Cy), 22.73, 23.69 (CH*MeMe*`), 25.28, 27.63 (2xMe), 31.37 (CH(^{i}Pr)), 71.01 (CMe_2), 80.58 (CH_2), 82.00, 84.76, 87.84, 88.68 (CH(C_6H_4)), 108.07, 113.97 (C(C_6H_4), 124.01 (NCMe), 125.60, 125.90, 127.28, 128.05, 130.66 131.43, 132.08 (Ar-H), 132.32 (C^7), 143.72 (C^1), 152.48 (^{i}C, Ph of alkyne), 168.57 (CNO), 176.01 (C^8). MS (FAB): *m/z* 512 [M-NCMe]$^+$. IR: ν(C=N) 1635 cm^{-1}.

Preparation of (4.51a)

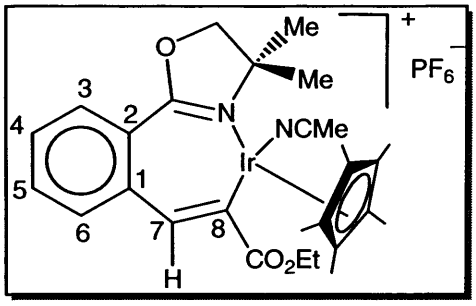

This was prepared by **method (B)**; $EtO_2CC{\equiv}CH$ (21 mg, 0.22 mmol) was added to solution of **(4.25a)** (75 mg, 0.11 mmol) in dichloromethane; after stirring for 3 h, **(4.51a)** was isolated as a pale yellow precipitate (70 mg, 82%). Calc. for $C_{28}H_{36}IrN_2O_3PF_6$: C, 42.80, H, 4.62, N, 3.57. Found: C, 42.70, H, 4.51, N, 3.56%. ^{1}H NMR: δ 1.22 (s, 3H, C*Me*Me`), 1.27 (m, 3H, $CO_2CH_2CH_3$), 1.30 (s, 15H, Cp*), 1.37 (s, 3H, CMe*Me*`), 2.71 (s, 3H, NCMe), 4.11 (m, 3H, $CO_2CH_2CH_3$, overlap, d, 1H, *J* 9, OC*H*H`), 4.38 (d, 1H, *J* 9, OCH*H*`), 7.22 (m, 2H, H^4, H_6), 7.45 (dt, 1H, *J* 7.5, 1.5, H^5), 7.48 (s, 1H, H^7), 7.62 (d, 1H, *J* 7.5, H^3). ^{13}C NMR: δ 3.93 (NCMe), 8.61 (C_5Me_5), 14.84 ($CO_2CH_2CH_3$), 24.81, 27.37 (2xMe), 60.52 ($CO_2CH_2CH_3$), 72.99 (CMeMe`), 81.14 (OCH_2), 91.67 (C_5Me_5), 123.25 (NCMe), 126.95, 131.82, 132.43, 133.09 (C^3, C^4, C^5, C^6), 136.60 (C^7), 141.65, 144.01 (C^1, C^8), 168.64 (CNO), 174.70 (CO_2). MS (FAB): *m/z* 600 [M-NCMe]$^+$. IR: ν(C=N) 1622 cm^{-1}. ν(C=O) 1682 cm^{-1}.

Preparation of (4.54a)

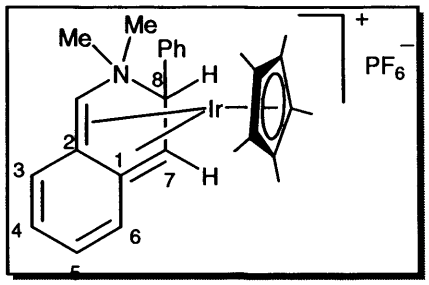

This was prepared by method (**A**) and method (**B**); (**A**) PhC≡CH (11 mg, 0.11 mmol), KPF_6 (56 mg, 0.30 mmol) were added to solution of (**3.36a**) (50 mg, 0.10 mmol) in acetonitrile; after stirring for 4 h, (**4.54a**) was isolated as a green precipitate and washed over silica (DCM/NCMe) to give a mixture products. (**B**) Phenylacetylene (2 mg, 0.02 mmol) was added to solution of (**4.24a**) (10 mg, 0.03 mmol) in $CDCl_3$; after shaking in an NMR tube for 5 mints, (**4.54a**) was isolated as a yellow precipitate (10 mg, 90%). Calc. for $C_{27}H_{33}IrNPF_6$(1 equiv. of $CHCl_3$): C, 40.62, H, 4.11, N, 1.69. Found: C, 42.19, H, 3.17, N, 1.61%. ^{1}H NMR: δ 1.52 (s, 15H, Cp*), 2.00 (s, 3H, N*Me*Me`), 3.07 (s, 3H, NMe*Me*`), 4.56 (d, 1H, *J* 12, H^8), 4.60 (s, 1H, H^9), 5.12 (d, 1H, *J* 12, H^7), 7.17-7.50 (m, 9H, H^3, H^4, H^5, H^6, Ph). ^{13}C NMR: δ 8.79 (C_5*Me*$_5$), 43.12 (N*Me*Me`), 57.50 (NMe*Me*`), 58.28 (C^7), 62.91 (N-CH), 63.96 (C^8), 99.95 (C_5Me$_5$), 127.42, 128.09, 128.96, 129.24, 129.58, 130.21 132.25 (Ar-H), 139.03 (^{i}C, Ph), 141.12 (C^1), 146.74 (C^2). MS (FAB): *m/z* 562 $[M]^+$.

Preparation of (4.57a)

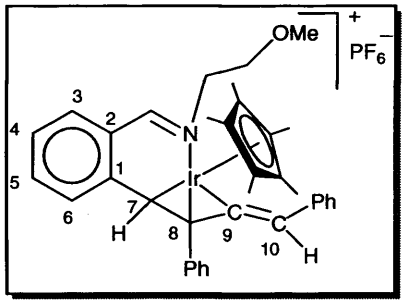

This was prepared by method (**B**); PhC≡CH (30 mg, 0.30 mmol) was added to solution of (**4.21a**) (100 mg, 0.15 mmol) in dichloromethane; after stirring for 30 h, (**4.57a**) was isolated as a yellow precipitate (105 mg, 85%). Calc. for $C_{36}H_{39}IrNOPF_6$: C, 51.54, H, 4.69, N, 1.67. Found: C, 51.22, H, 4.59, N, 1.59%. ^{1}H NMR: δ 1.69 (s, 15H, Cp*), 3.06 (m, 2H, CH_2O), 3.14 (s, 3H, OMe), 3.93 (m, 1H, NC*H*H`), 4.13 (m, 1H, NCH*H*`), 6.06 (s, 1H, H^7), 6.72 (s, 1H, H^{10}), 7.46 (m, 8H, H^4, H^5, (2xPh, H_m, H_p)), 7.73 (m, 5H, H^3, (2xPh, H_o)), 8.04 (d, 1H, *J* 8, H^6), 8.09 (s, 1H, HC=N). ^{13}C NMR: δ 9.05 (C_5*Me*$_5$), 48.45 (C^7), 58.65 (OMe), 70.72 (CH_2O), 71.73 (NCH_2), 80.18 (C^9), 99.07 (C_5Me$_5$), 121.18 (C^{10}), 127.57, 127.81,129.00, 129.30, 130.06, 130.23, 131.17, 135.53, 136.34 (Ar-H), 128.09, 129.20 (C^2, ^{i}C, Ph), 133.39, 135.18 (C^1, C^8), 150.17 (^{i}C, Ph of alkyne), 167.90 (HC=N). MS (FAB): *m/z* 694 $[M]^+$. IR: ν(C=N) 1615 cm^{-1}.

Preparation of (4.59a)

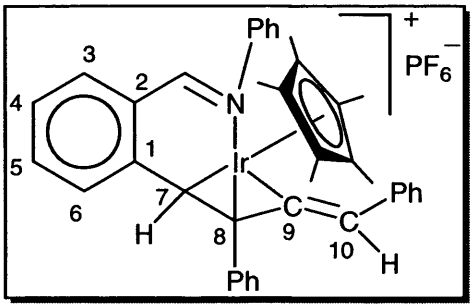

This was prepared by method (**A**); PhC≡CH (34 mg, 0.33 mmol), KPF_6 (76 mg, 0.41 mmol) were added to solution of (**3.32a**) (90 mg, 0.17 mmol) in NCMe; after stirring for 7 h, NCMe was replaced by dichloromethane and the solution stirred for 21 h. (**4.59a**) was isolated as a

red precipitate and washed over silica (DCM/NCMe) to give pure product (92 mg, 65%). Calc. for $C_{36}H_{37}IrNPF_6$: C, 54.66, H, 4.35, N, 1.63. Found: C, 54.51, H, 4.23, N, 1.53%. ^{1}H NMR (in MeOD): δ 1.51 (s, 15H, Cp*), 5.20 (s, 1H, H^7), 6.72 (s, 1H, H^{10}), 6.89 (m, 2H, 2xPh), 7.01 (m, 3H, H^4, 2xPh), 7.20 (m, 4H, H^6, 2xPh), 7.54 (m, 8H, Ph), 7.92 (dt, 1H, *J* 7.5, 1.5, H^5), 8.02 (d, 1H, *J* 7.5, H^3), 8.18 (s, 1H, HC=N). MS (FAB): *m/z* 712 $[M]^+$. IR: ν(C=N) 1615 cm^{-1}.

Preparation of (4.61a)

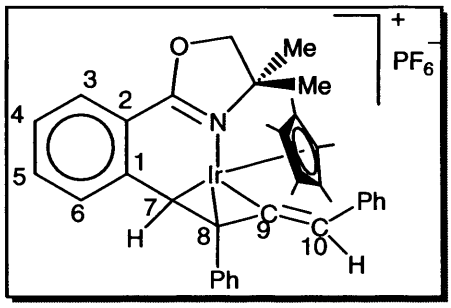

This was prepared by method **(A)** and method **(B)**; **(A)** PhC≡CH (13.3 mg, 0.13 mmol), KPF_6 (72 mg, 0.39 mmol) were added to solution of **(3.37a)** (70 mg, 0.13 mmol) in acetonitrile; after stirring for 4 h, the precipitate was washed over silica (DCM/NCMe) to give a pure product **(4.61a)** as an orange (28 mg, 25.2%). **(B)** Phenylacetylene (21.6 mg, 0.22 mmol) was added to solution of **(4.25a)** (73 mg, 0.11 mmol) in dichloromethane; after stirring for 2 h, **(4.61a)** was isolated as a brown precipitate (80 mg, 89%). ^{1}H NMR: δ 1.18 (s, 3H, C*Me*Me`), 1.37 (s, 3H, CMe*Me*`), 1.76 (s, 15H, Cp*), 2.94 (d, 1H, *J* 9, OC*H*H`), 4.18 (d, 1H, *J* 9, OCH*H*`), 4.68 (s, 1H, H^7), 6.41 (s, 1H, H^{10}), 7.02 (m, 3H, Ph), 7.13 (m, 3H, Ph), 7.34 (m, 2H, Ph), 7.40 (dt, 1H, *J* 6.5, 1.5, H^4), 7.50 (m, 2H, Ph), 7.55 (dd, 1H, *J* 7, 1, H^6), 7.77 (dt, 1H, *J* 7, 1.5, H^5), 7.83 (dd, 1H, *J* 7.5, 1, H^3). ^{13}C NMR: δ 9.50 (C_5Me_5), 25.99, 27.66 (2xMe), 48.58 (C^7), 71.01 (*C*MeMe`), 80.44 (OCH_2), 95.99 (C_5Me_5), 104.92 (C^9), 119.84 (C^{10}), 127.37, 127.47, 127.90, 128.51, 128.69, 131.65, 132.32 133.64 (Ar-H), 123.98, 125.38 (^iC, Ph), 133.75, 138.24 (C^1, C^8), 152.61 (^iC), 165.33 (CNO). MS (FAB): *m/z* 704 $[M]^+$. IR: ν(C=N) 1604 cm^{-1}.

Bibliography

1 A. D. Ryabov, *Synthesis*, 1985, 233.

2 H. Takahashi and J. Tsuji, *J. Organomet. Chem.*, 1967, **10**, 511.

3 J. M. Thompson and R. F. Heck, *J. Org. Chem.*, 1975, **40**, 2667.

4 V. Ritleng, J. P. Sutter, M. Pfeffer, and C. Sirlin, *Chem. Commun.*, 2000, 129.

5 I. R. Girling and D. A. Widdowson, *Tetrahedron Lett.*, 1982, **23**, 4281.

6 M. Pfeffer, *Pure Appl. Chem.*, 1992, **64**, 335.

7 M. A. Bennett, S. A. Macgregor, and E. Wenger, *Helv. Chim. Acta*, 2001, **84**, 3084.

8 F. Maassarani, M. Pfeffer, and G. Le Borgne, *Organometallics*, 1987, **6**, 2043.

9 F. Maassarani, M. Pfeffer, and G. Le Borgne, *Organometallics*, 1987, **6**, 2029.

10 W. Ferstl, I. K. Sakodinskaya, N. Beydoun-Sutter, G. Le Borgne, M. Pfeffer, and A. D. Ryabov, *Organometallics*, 1997, **16**, 411.

11 H. C. L. Abbenhuis, M. Pfeffer, J.-P. Sutter, A. de Cian, J. Fischer, H. L. Ji, and J. H. Nelson, *Organometallics*, 1993, **12**, 4464.

12 M. Pfeffer, *Recueil des Travaux Chimiques des Pays-Bas*, 1990, **109**, 567.

13 F. Maassarani, M. Pfeffer, and G. Le Borgne, *J. Chem. Soc. Chem. Commun*, 1987, 565.

14 F. Calderazzo, *Angew. Chem.*, 1977, **89**, 305.

15 E. J. Kuhlman and J. J. Alexander, *Coord. Chem. Rev.*, 1980, **33**, 195.

16 R. F. Heck, *J. Am. Chem. Soc.*, 1968, **90**, 313.

17 Y. Yamamoto, K. Sugawara, and X.-H. Han, *J. Chem. Soc., Dalton Trans.*, 2002, 195.

18 D. L. Davies, J. Fawcett, S. A. Garratt, and D. R. Russell, *Organometallics*, 2001, **20**, 3029.

19 S. Fernandez, M. Pfeffer, V. Ritleng, and C. Sirlin, *Organometallics*, 1999, **18**, 2390.

20 E. Lindner, S. Pautz, R. Fawzi, and M. Steimann, *Organometallics*, 1998, **17**, 3006.

21 R. C. Larock, E. K. Yum, and M. D. Refvik, *J. Org. Chem.*, 1998, **63**, 7652.

Additional Activities

I have participated/attended the postgraduate activities listed below.

APG - Postgraduate Training Activities, Lectures, Modules and Examinations

APG Training

Demonstration Training

18 / 9 / 01 Pre-Session Demonstrator Training

Induction

24 / 9 / 01 Departmental Induction

25 / 9 / 01 Introduction to Key Techniques and Equipment

26 / 9 / 01 Graduate School Induction

27 / 9 / 01 Faculty Induction

Information Skills

17 / 10 / 01 Information Skills for Chemists Session 1 - An Introduction to Chemical Information Databases

24 / 10 / 01 Information Skills for Chemists Session 2 – Advanced Searching in *Crossfire*

5 / 12 / 01 Developing a Personal Skills Portfolio – *Royal Society of Chemistry*

12 / 6 / 02 Advanced Scientific Writing for Chemists

12 / 6 / 02 Applications of *Endnote*

Module CH501

31 / 10 / 01 1D-NMR Spectroscopy

28 / 11 / 01 2D-NMR Spectroscopy

30 / 1 / 02 The *nOe* Effect

5 / 6 / 02 Presentation of NMR data

6 / 3 / 02 *Chemdraw*, *Molecular Modelling* and *Powerpoint*

Study, Writing and Presentation Skills

4 / 3 / 02 and 11 / 3 / 02 Study Skills - Effective Management, Reading and Note Making Skills

6 / 2 / 02 and 13 / 2 / 02 Writing Skills

1 / 5 / 02 Presentation Skills – Powerful Spoken and Poster Presentations

Career Skills

29 / 5 / 02 Developing Skills for a Future Career

Intellectual Property Rights

13 / 5 / 02 IPR, Patent Protection and Commercialisation

APG Undergraduate Modules Attended

Module CH316 : Catalysis

Module CH309 : Strategies of Organic Synthesis

Internal Seminars – External Speakers

1 / 10 / 01 *Royal Society of Chemistry Centenary Lecture*

Professor Kyriacos Nicolaou – Scripps Research Institute, California

'Enabling Technologies for Biology and Medicine Arising from Endeavours in Total Synthesis'

4 / 10 / 01 *Royal Society of Chemistry Lecture*

Dr Peter O'Brien – University of York

'Basic Instinct: New Synthetic Adventures with Chiral Bases'

10 / 10 / 01

Dr Didier Bourrissou – Universitié Paul Sabatier, Toulouse

'Stable Carbenes and Diradicals: New Stabilisation and Bonding Modes'

22 / 10 / 02 *Royal Society of Chemistry Student Chemical Society Lecture*

Dr Anthony Hooper – Institute of Arable Crops, Rothamstead

'Sex, Bugs and Rock and Roll: Identification and Synthesis of Semiochemicals and Exploitation of the Ecological Interactions they Regulate as an Approach to Pest Management'

14 / 11 / 01 *Royal Society of Chemistry Joseph Chatt Lecture*

Professor Vernon C. Gibson – Imperial College, London

'Designing Catalysts for Polymer Synthesis'

10 / 12 / 01 Dr Jonathan McMaster – University of Nottingham

'The Electronic Structure of the Active Sites of Molybdenzymes'

14 / 12 / 02 Professor Peter Flecker – Johannes Gutenberg University, Mainz

'Dissecting Intramolecular versus Intermolecular Protein Recognition'

28 / 1 / 02 Professor Judith Howard – University of Durham

'The Application of Very Low Temperature Crystallography to Chemical Problems'

11 / 2 / 02 Dr Robin Bedford – University of Exeter

'High Activity Catalysts for C-C Bond Formation'

25 / 2 / 02 Professor John Nixon – University of Sussex

'The New World of Phospha-Organometallic Chemistry'

4 / 3 / 02 Dr Holger Braunschweig – Imperial College, London

'Compounds with Novel Boron Containing Ligands: Transition Metal Complexes of Boron and [1] Bora – Metallocenophanes'

6 / 3 / 02 Dr Richard Shutt – ExxonMobil, Belgium

'Supercritical Phase Phenomena in Ethylene Polymerisation and Polymer Separation'

8 / 5 / 02 Dr Nick Long – Imperial College, London

'Ferrocene – Ligand Design'

20 / 5 / 02 Dr Martyn Coles – University of Sussex

'Anionic and Neutral Guanidine – based Ligands in Coordination Chemistry and Catalysis'

Internal Seminars and Literature Discussion Sessions – Internal Speakers Project Seminars

11 / 10 / 01 Christopher. J. Davies – PhD second year project outline

1 / 11 / 01 Sukhvinder K. Kandola, Toby Reeve and Samuel Suhard – PhD second year project outlines

29 / 10 / 01 MChem project outlines

8 / 11 / 01 Alice Hickman, R. K. Chaggar – PhD first year project outline

22 / 11 / 01 Jérémie D. Pelletier and **Omar Duaij** – PhD first year project outlines

3 / 12 / 01 Dr. G. A. Solan and Dr P. W. Dyer – Current Projects

6 / 12 / 01 Martin Hanton – PhD third year project outline

4 / 2 / 02 Alice Hickman, Jérémie D. Pelletier and Katie Sharpe – PhD first year projects

18 / 2 / 02 Andrew West, R. K. Chaggar and **Omar Duaij** – PhD first year projects

18 / 3 / 02 Dr. E. Raven and Dr. D. Davies – Current projects

19 / 3 / 02 MChem final presentations

Final Year PhD Presentations attended

27 / 5 / 02 Martin Hanton *(Unattended due to examination)*

17 / 6 / 02 Neesha Patel

24 / 6 / 02 Ben. Croxtall and James Sherrington

Literature Discussion Sessions

29 / 10 / 01 Speakers: M. Hanton and N. Patel, Chair: C. J. Davies

Questioners: B. Croxtall and J. Sherrington

5 / 11 / 02 Speakers: P. Griffith and D. Harding, Chair: M. Dix

Questioners: M. Giardiello and G. Barth

26 / 11 / 01 Speaker: G. Barth, Chair: M. Hanton

Questioners: P. Griffith and D. Harding

11 / 3 / 02 Speakers: T. Reeve, B. Croxtall and S. K. Kandola, Chair: N. Patel

Questioners: C. J. Davies, S. Suhard and M. Hanton

25 / 3 / 02 Speakers: C. J. Davies, S. Suhard and J. Sherrington, Chair: B. Croxtall

Questioners: S. K. Kandola, T. Reeve and N. Patel

24 / 4 / 02 Speakers: A. Hickman, A. West and J. D. Pelletier, Chair: N. Patel

Questioners: R. K. Chaggar, K. Sharp and **Omar Duaij**

13 / 5 / 02 Speakers: **Omar Duaij**, K. Sharp and R. K. Chaggar, Chair: S. K. Kandola

Questioners: A. Hickman and A. West

13 / 11 / 03 Speakers: Y. Champouret, R. K. Chaggar and **Omar Duaij**

11 / 12 / 03 Speakers: A. Gregory and E. A. Sabban

Symposia, Conferences and Poster Sessions Attended

1 / 7 / 02 – 2 / 7 / 02 ***Royal Society of Chemistry*** **– Coordination Chemistry Discussion Group Meeting**

Two Day Conference at The University of Loughborough

Poster Title: Cyclopalladated Imines Containing an O-Functionalised Tether Factors Controlling *Coordination Of the Oxygen*

PhD Second and Third year Seminars

Internal Seminars – External and Internal Speakers

21 / 10 / 02 Dr Paul Raithby – University of Bath

'Adventures in Organometallic Polymer Chemistry'

28 / 10 / 02 Dr Clive Metcalfe – University of Leicester

'Transition Metal Complexes and their Interaction with DNA'

18 / 11 / 02 Dr Mike Turner – University of Sheffield

'Synthesis of Conjugated Polymers for Polarised Electroluminescence and Polymer Electronics'

9 / 12 / 02 Prof. Todd Marder – University of Durham

'The Role of Transition Metal Boryl Complexes in Catalysed Borylations including Rhodium Catalysed C-H Bond Functionalisation'

17 / 2 / 03 Prof. V. McKee – University of Loughborough

'Manipulating Metal Arrays within Macrocycles'

10 / 3 / 03 Prof. Duncan Bruce – University of Exeter

'Metallomesogens by Design'

28 / 4 / 03 Prof. Kingsley Cavell – University of Cardiff

'Reactions of Heterocyclic Carbene Complexes: Important Ramifications for their Application in Catalysis'

30 / 5 / 03 Dr Carine Aubrey – University of Leicester

'Synthèse, Analyse Stucturale et Activité Biologique d'analogues Rigides d'un Antagoniste de l'octadecaneuropeptide (ODN)'

2 / 6 / 03 Dr Sarah Heath – University of Manchester

'Shedding Light on Biological Systems: the Development of Dinuclear Lanthanide Probes'

Inaugural Lecture

3 / 6 / 03 Prof. Jonathan Percy – Appointed as Professor of Chemistry at the University of Leicester

'Against Nature: Unnatural Products in the Service of Humanity'

9 / 6 / 03 Dr Alan Spivey – Imperial College, London

'Catalytic Asymmetric Acylation – Studies towards the Total Synthesis of Polyol Sesquiterpenes'

29 / 9 / 03 Dr Zoe Pikramenou – University of Birmingham

'Luminescent Supramolecular Architectures: from Shape to Function'

6 / 10 / 03 Dr Chris Richards – Queen Mary, University of London

'Palladium and Platinum Metallacycles for Organic Synthesis'

The Second Tim Norwood Memorial Lecture

8 / 10 / 03 Prof. Ian Campbell – University of Oxford

'NMR and Proteins'

20 / 10 / 03 Dr Sandie Dann – University of Loughborough

'Something Old, Something New Something Borrowed and Something Blue: Complex Oxides and Sulphides'

27 / 10 / 03 Dr Chris Hayes – University of Nottingham

'Natural and non-Natural Products: Total Synthesis and Biological Applications'

3 / 11 / 03 Prof. Helen Fielding – University College London

'Controlling Electrons and Molecules using Light'

17 / 11 / 03 Prof. Chris Binns – Department of Physics University of Leicester

'Building High-Performance Magnetic Materials by Assembling Nanoclusters'

1 / 12 / 03 Prof. Richard Winpenny – University of Manchester

'Synthetic Studies of Metal Wheels and other Cages'

8 / 12 / 03 Prof. Peter Hore – University of Oxford

'Bird Navigation: a Photochemical Magnetic Compass?'

19 / 1 / 04 Prof. Bill Levason – University of Southampton

'Recent Developments in the Chemistry of Antimony Ligands'

9 / 2 / 04 Dr Michael Whittlesey – University of Bath

'Stoichiometric and Catalytic Small Molecule Activation by Ruthenium N-Heterocyclic Carbene Complexes'

8 / 3 / 04 Dr Chris Kay – Free University of Berlin

'Applications of Electron Spin Resonance Spectroscopy to Biological Problems'

Royal Society of Chemistry – East Midlands Local Section sponsored seminar

15 / 3 / 04 Prof. David Schiffrin – University of Liverpool

'Connectivity of Functionalised Nanoparticles and their Arrays'

Royal Society of Chemistry – East Midlands Local Section

26 / 4 / 04 Dr Graham Sandford – University of Durham

'Polyfunctional Heterocycles and Macrocycles'

10 / 5 / 04 Dr Dominic Wright – University of Cambridge

''Cation and Anion Coordination using 'Torocyclic' Ligands''

7 / 6 / 04 Prof. Peter Scott – University of Warwick

'Catalysis with Chiral Metal Complexes'

Internal Seminars and Literature Discussion Sessions – Internal Speakers Project Seminars

24 / 10 / 02 Jérémie Pelletier and Alice Hickman (PhD project update)

31 / 10 / 02 MChem project introductions

7 / 11 / 02 MChem / MSc project introductions

14 / 11 / 02 Rajinder Kaur Chaggar and **Omar Al-Duaij** (PhD project update)

28 / 11 / 02 Yohan Champouret and Ishaq Dadhiwala (PhD project outlines)

5 / 12 / 02 Samuel Suhard and Sukvinder Kandola (PhD project update)

12 / 12 / 02 Christopher Davies and Toby Reeve (PhD project update)

25 / 3 / 03 Projects seminar

Yohan Champouret (1st year PhD), Jérémie Pelletier (2nd year PhD), Ishaq Dadhiwala (1st year PhD), Carly Anderson (MSc), **Omar Al-Duaij** (2nd year PhD), Rajinder Kaur Chaggar (2nd year PhD), Alice Hickman (2nd year PhD), Duncan Harding (1st year PhD), Andrew West (2nd year PhD), Nektaria Papadopalou (1st year PhD)

26 / 11 / 03 MChem Introductory Presentations

27 / 11 / 03 Projects Seminar 3rd Year PhD

Jérémie Pelletier and **Omar Al-Duaij**

4 / 12 / 03 Projects Seminar

Rajinder Kaur Chaggar (3rd year PhD) and Yohan Champouret (2nd year PhD)

11 / 12 / 03 MChem and 1st year PhD Projects Seminar

17 / 3 / 04 MChem Final Presentations

22 / 3 / 04 PhD 1st Year Projects Seminar

E. A. Sabban, R. Griffin, M. Gourlay, J. Bennett, B. Parmar, M. Giardiello and P. Villuendas

20 / 5 / 04 PhD 2nd Year Projects Seminar

Yohan Champouret, Nektaria Papadopalou and Duncan Harding

22 / 6 / 04 Final Year PhD Presentations

Rajinder Kaur Chaggar, Andrew West, **Omar Al-Duaij**, Jérémie Pelletier and Katie Sharp

Symposia, Conferences and Poster Sessions Attended

12 / 7 / 04 – 14 / 7 / 04 ***Royal Society of Chemistry*** **– Coordination Chemistry Discussion Group Meeting**

Two Day Conference at The University of Leicester

Poster Title: Cyclopalladated Imines Containing an O-Functionalised Tether Factors Controlling *Coordination Of the Oxygen*